CORA Cork Open Research Archive
Cartlann Taighde Oscailte Chorcaí

Title	Electrofuels in a circular economy
Authors	Rusmanis, Davis
Publication date	2023
Original Citation	Rusmanis, D. 2023. Electrofuels in a circular economy. PhD Thesis, University College Cork.
Type of publication	Doctoral thesis
Rights	© 2023, Davis Rusmanis. - https://creativecommons.org/licenses/by-nc-nd/4.0/
Download date	2026-11-15 14:02:33
Item downloaded from	https://hdl.handle.net/10468/15488



UCC
University College Cork, Ireland
Coláiste na hOllscoile Corcaigh

Ollscoil na hÉireann, Corcaigh

National University of Ireland, Cork



Electrofuels in a Circular Economy

Thesis presented by

Davis Rusmanis

BE Civil, Structural & Environmental Engineering

for the degree of

Doctor of Philosophy

University College Cork

School of Engineering and Architecture

Head of School:

Prof. Jorge Oliveira

Supervisors:

Prof. Jerry D. Murphy (Chair of Civil Engineering)

Dr. David M. Wall

2023

Table of contents

Declaration i
Acknowledgements ii
Abstract iv
Thesis output vi
Chapter 2 vi
Chapter 3 vi
Chapter 4 vi
Chapter 5 vi
Other contributions where I was not the primary author. vi
Nomenclature vii
1. Introduction 1
1.1. Electrofuels in a Circular Economy 1
1.2. The rationale for the thesis 3
1.3. Objectives 4
1.4. Outline and link between the chapters 4
Chapter 2: Literature review 5
Chapter 3: Design and Commission of a novel biological methanation system. 5
Chapter 4: Electrofuels in a circular economy: A systems approach towards net zero. 5
Chapter 5: Operation of a circular economy, energy, and environmental system at a wastewater treatment plant. 5
References 7
2. Biological Hydrogen Methanation Systems – An overview of design and efficiency 11
Graphical abstract 11
Abstract 12
Highlights 12
2.1 Introduction 13
2.1.1 Background 13
2.1.2 Anaerobic Digestion 13
2.1.3 Biological Hydrogen Methanation 14
2.2 Review of State of the Art 16
2.2.1 The Role of Hydrogen in Power to gas Systems 16
2.2.2 Microbiology of BHM and AD 18
2.2.3 Nutrients in BHM 22

2.2.4 Process Conditions 24
2.2.5 Biological Hydrogen Methanation systems: A comparison 25
2.2.6 Reactor Systems: A comparison 27
2.2.7 System key parameter comparison 41
2.2.8 Analysis of the relationship between key operational parameters 42
2.2.9 A full-scale demonstration plant 45
2.2.10 Conclusions 48
Acknowledgements 49
Conflict of Interest 49
List of references 50
3. Design and commission of a novel biological methanation system 56
3.1 Introduction 58
3.2 Design of the system 61
3.2.1 Simulated system by Voelklein *et al.* 61
3.2.2 Design of the cascading biomethanation rig 62
3.2.3 Manufacture of the cascading biomethanation rig 63
3.3 Commissioning of the system 67
3.3.1 Operation 67
3.3.2 Analytical methods 68
3.3.3 Performance vs previous study 69
3.4 Results and Discussion 71
3.4.1 Limitations and solutions 71
3.4.2 Discussion of data accuracy 76
3.5 Conclusion 79
Acknowledgements 79
List of References 80
4 Electrofuels in a circular economy: A systems approach towards net zero 82
4.1 Introduction 84
4.1.1 The role of electrofuels in reacing net-zero 84
4.1.2 Circular approach to electrofuel production 85
4.1.3 Aims and objectives 87
4.2 Methods 89
4.2.1 Potential to store surplus variable renewable energy as green hydrogen 89

4.2.2 Design of electrolyser for the industrial site 89
4.2.3 Potential end uses for the green hydrogen 91
4.2.4 Oxygen recovery in the wastewater aeration process 92
4.2.5 Carbon capture and utilisation through biological methanation 93
4.2.6 Integration of pyrolysis as a negative emissions technology 94
4.2.7 Emissions reduction by integrating anaerobic digestion with pyrolysis 95
4.3 Results and discussion 95
4.3.1 Wind resource potential from the industrial site 95
4.3.2 Electrolyser specifications for the industrial site 96
4.3.3 Hydrogen as a transport fuel 98
4.3.4 Oxygen recycling to the wastewater treatment process 99
4.3.5 Biomethanation and the potential for carbon capture 99
4.3.6 Co-locating electrolysers and biomethanation at municipal wastewater treatment plants 101
4.3.7 Emission reductions using anaerobic digestion and pyrolysis 102
4.3.8 The sustainability of the circular electrofuel production systems 104
4.3.9 Study limitations and future research 105
4.4 Conclusions 106
Acknowledgements 106
List of References 107
5 Operation of a circular economy, energy, and environmental system at a wastewater treatment plant 112
5.1 Introduction 114
5.1.1 The benefits of circular economy, energy, and environmental systems 114
5.1.2 Dispatch down of variable renewable electricity 115
5.1.3 Hydrogen production via electrolysis 117
5.1.4 Circular economy, energy, and environmental systems at wastewater treatment plants 117
5.1.5 Anaerobic Digestion at WWTPs 118
5.1.6 Biological hydrogen methanation 119
5.1.7 Aims and objectives 119
5.2 Methodology 120
5.2.1 Relationship between the size of a wind farm, dispatch down and the size of an electrolyser 120

5.2.2 Oxygen demand, sludge production and biogas produced 123
5.2.3 Biological hydrogen methanation 125
5.2.4 What emissions savings can be achieved at the wastewater treatment plant? 125
5.2.5 End-use of renewable gases in fuelling trucks 126
5.3 Discussion and Results 128
5.3.1 The relationship between the size of a wind farm, dispatch down and the size of an electrolyser 128
5.3.2 Relationship between electrolyser size and oxygen demand in an extended aeration basin. 133
5.3.3 The H_2 required to upgrade the digested sludge biogas to biomethane 136
5.3.4 Emissions savings achieved at the wastewater treatment plant 138
5.3.5 How many diesel trucks can be offset with the generated H_2 and CH_4? 139
5.3.6 Alternative configurations 142
5.3.7 Limitations of the research and recommendations for future research. 143
5.4 Conclusion 144
Acknowledgements 144
List of References 145
6. Conclusions and Recommendations 151
6.1. Conclusions 151
6.2. Recommendations 154
6.2.1. Recommendations for Industry 154
6.2.2. Recommendations for Policymakers 154
6.2.3. Recommendations for Communities 154
6.2.4. Recommendations for future research 155
Appendices 156
Chapter 2 - Supplementary data 157
Chapter 3 - Supplementary data 158
[SD 1] Supplementary Figures 158
[SD 3] A18CK038- KD-001 163
[SD 4] A18CK038- KD-002 164
[SD 5] A18CK038- KD-003 165
[SD 6] Methanation rig 166
[SD 6.1] Diffuser images 166
[SD 6.2] Manifold 168

[SD 6.3] General Arrangement Drawings 169
[SD 7] Flow totaliser conversion table 170
Chapter 4 - Supplementary data 171
Supplementary references 179
Chapter 5 - Supplementary data 180
Supplementary References 181
[SD 2] Standard Operating Procedure V3 182

Declaration

I, Davis Rusmanis hereby declare that this thesis is my work, and has not been submitted for another degree, either at University College Cork or elsewhere. Where other information sources were used, these have been referenced accordingly. I have read and understand the regulations of University College Cork concerning the consequences of plagiarism.

Signed: 

DAVIS RUSMANIS

Date: 05/04/2023

Acknowledgements

I have never been very eloquent in expressing gratitude; no matter how I've put things, it's been incomparable to the thanks I've felt for the people who've helped me get to where I am today. This time will be no different. I could not have gotten to where I am without my family, friends, supervisors, and everyone in between. I am who I am because of you.

Jerry, I still remember my final group meeting during my 1st-year internship with the biofuels group in 2015. You jokingly declared, "…You'll go back to college, get to 4th year and do your final year project with me, and then you'll come back and do a PhD with us...", funny how it all came to pass! Words cannot express the gratitude I have for the opportunity you have given me, for believing in me and for giving me this chapter of my life. The comradery you have fostered in the Biofuels/CEEES group throughout the years is nothing short of a family, for which I am eternally grateful to have been invited into.

To David, your supervision throughout the PhD and especially through EFACE has been invaluable. Thank you for having the patience and knowledge in guiding me along in my PhD. Here's to the circular economy, energy and environmental systems!

To Richie, the man who swooped in on the eleventh hour to save my bacon with the hydrogen rig. Without your help, it would not have been possible to dredge through the bureaucracy of it all, and I would not be here today without your help. If there ever was a saint of a man, it's you. Eternally grateful to have had the opportunity to work with you.

To my colleagues[a] (just another name for friends, really), who I have had the privilege of working with these past years; I have been inspired by your work ethic, friendliness, support and the knowledge you have shared with me throughout my time knowing you all. I could not have asked for a better community to surround myself with.

To my best friends, Paul, Gaby, and Adam, thanks for the COVID company, the philosophy talks, the unwavering support, and the friendship you have provided me with. Let's hope I can now find the time to go on a holiday with ye. Love ye!

To my pals, Simon, Sebastian, Clara, Yusuf, The UCC Archery Club family, and many more, thanks for not taking my flakiness and absence these past four years personally. You've been a wonderful bunch of friends to me.

And finally, my family, my brothers, and my parents, who raised and instilled the best of themselves in me, taught me to strive to better myself with each day, respect, and honour those around me, and instilled in me a healthy dose of stubbornness. The unwavering support in everything I've chosen to do and the sacrifices you made to make my life what it is today, I cannot ever repay.

"If you only do what you can do, you will never be more than you are now."

[a] Benteng, Xihui, Archishman, Richie, Nathan, Shane, Anga, Rajas, Yunfei, Xue, Daniel, Aoife, Richen, Chen, Markus, Paritosh, Enrique, Ketan, Tara, Aoife, and so many more.

Dedicated to

Rita Plotniece

Mom

And

In loving memory

Egils Rusmanis
Dad

Abstract

With the global shift away from traditional dispatchable fossil hydrocarbon fuels, the requirement for energy storage is of increasing importance. Renewable electricity generation is predominately in the form of variable renewable electricity, produced by wind and solar technologies. Intermittent production of electricity leads to an inevitable mismatch in supply and demand between the grid and the consumers. This can lead to periods of surplus power generation – and subsequent dispatch down – during low demand; conversely it can also lead to energy shortages during periods when there is insufficient power generation to match high demand which can lead to grid blackouts. Due to the difficulty in storing significant quantities of electricity via the grid, or batteries, sustainable alternative methods of energy storage must be devised.

In recent years, electrofuels have become a centre-stage topic due to the opportunity to store electricity as low-carbon energy vectors which can be utilised where electrification may not be ideal, such as the hard-to-abate sectors of haulage, shipping, agriculture, and industry (iron, steel and chemicals). Further, the generation of these electrofuels could be carried out using electricity which would otherwise be lost, during times of excess production, and low grid demand. Combining technologies such as electrolysers (capable of producing hydrogen and oxygen) and biomethanation (which can combine carbon dioxide with hydrogen to form biomethane), offer a green alternative to fossil natural gas, and can use the existing gas grid as both a distribution system and a sustainable energy storage method.

Based on the literature review and previous research, the initial thesis work focused on the design and commission of a prototype three-phase cascading biomethanation system. The fabricated prototype used diffusers as the agitation method and was deemed to be at a technology readiness level (TRL) of 4. The system was designed based on the results of a previously simulated system published by this research group (Voelklein et al., 2019); the results from this study were of similar performance to the previous model. The commissioning process produced carbon conversion rates between 72% and 97% across 3 reactors which can operate in parallel or series. A methane evolution rate of 2.9 L $CH_4/L_{VR}/d$ was achieved at medium flow rates. Increasing the flow rates resulted in substantial drops in the conversion efficiency of the system. This limitation was mooted as likely due to the low bubble column height of the system. The design of the system was limited by the dimensions of the system, which were associated with health and safety concerns of the University.

Assessing the integration of biomethanation technology into the wider energy, and environment sector, an initial small-scale case study of a circular economy system was carried out, based on local industry. Using a dataset from two local wind turbines to assess available surplus electricity, a small 122 kW electrolyser was proposed to be of a suitable size for the local site. This electrolyser would generate enough by-product oxygen to supply 8.9% of the oxygen demand of the aeration process for the local wastewater treatment plant of approximately 65,000 population equivalent. The product hydrogen could be used directly as a transport fuel, or convert 40% of the CO_2 generated by the

anaerobic digesters at the wastewater treatment plant into biomethane. This system could reduce the wastewater treatment plant emissions by 3.6% due to the reduced aeration requirement (pumping oxygen instead of air would reduce electricity usage). Should an appropriately sized electrolyser be used, up to a 40% reduction in emissions and energy use could be achieved. However, the small scale of the system was identified as a major barrier to the application of the technology, with the levelised cost of hydrogen evaluated at €8.92/kg H_2 (or 27c/kWh). This resulting high cost cannot justify the implementation of a small-scale system to capture intermittent curtailed electricity as initially proposed.

Expanding the circular economy system is possible with a carbon-negative emission pathway integrating pyrolysis technology to generate biochar. Anaerobic digesters and pyrolysis systems could potentially reduce greenhouse gas emissions by 42.7 kt CO_2 through biomethane production from substrates within a 10km radius and through biochar production from digestate. When considering the sustainability considerations set by the latest version of the EU Renewable Energy Directive, electrofuels may only be certified as a renewable energy supply by affecting a 70% emission saving when compared to the current fossil hydrocarbon fuels. Additionally, the Directive does not allow for emission saving associated with carbon capture and reuse within the biological methanation system despite the added capture and use of otherwise curtailed electricity.

Assessing a large-scale circular economy system, once again co-locating electrolysers with anaerobic digesters and biomethanation systems on new or existing large wastewater treatment plants can offer significant benefits. To supply a 10 MW electrolyser operating at an 80% operating capacity, a wind farm of 144MW size (18 x 8 MW turbines) operating at 57 % capacity would be necessary, with an assumed 10% curtailment scenario, reflective of the Irish grid dispatch down of the recent years. The 10 MW electrolyser could supply oxygen for a wastewater treatment plant of 426,000 population equivalent, reducing the plant emissions (and power demand) by 40% when compared to traditional gaseous air aeration. The produced wastewater sludge can be digested to produce biogas. The CO_2 component of biogas can be converted to methane using a biomethanation system, requiring 22% of the electrolyser-produced hydrogen. This would result in the capture of 16 ktCO_2e per annum while producing enough electrofuels to offset 390 diesel trucks with 94 compressed biomethane trucks and 296 compressed hydrogen trucks.

Thesis output

Chapters published as papers or currently under review in peer-reviewed journals for which I am the primary author.

Chapter 2

D. Rusmanis, R. O'Shea, D. M. Wall, and J. D. Murphy,
"**Biological hydrogen methanation systems–an overview of design and efficiency,**" Bioengineered. Vol. 10, p. 604–34, 2019.

Chapter 3

D. Rusmanis, B. Wu, R. O'Shea, D. M. Wall, J. D. Murphy, **"Design and Commission of a novel biological methanation system," (To be confirmed)**

Chapter 4

D. Rusmanis, Y. Yang, A. Long, N. Gray, K. C. Martins, S. Óg Ó Loideáin, R. Lin, X. Kang, D. Óg Cusack, J. G. Carton, R. Monaghan, J. D. Murphy, D. M. Wall, **"Electrofuels in a circular economy: A systems approach towards net zero,"** Energy Convers Manag. 2023

Chapter 5

D. Rusmanis, Y. Yang, R. Lin, D. M. Wall, and J. D. Murphy, **"Operation of a circular economy, energy, and environmental system at a wastewater treatment plant,"** Adv. Appl. Energy. 2022 Dec 1;8:100109

Other contributions where I was not the primary author.

M. A. Voelklein, **D. Rusmanis**, and J. D. Murphy, "**Biological methanation: Strategies for in-situ and ex-situ upgrading in anaerobic digestion**," Appl. Energy, vol. 235, pp. 1061–1071, Feb. 2019.

Nomenclature

Abbreviation	Definition	Abbreviation	Definition
/a	*Per annum*	**PE**	*Population equivalent*
AD	*Anaerobic Digestion*	**PEM**	*Proton exchange membrane*
AEC	*Alkaline electrolysis cell*	**PICV**	*Pressure indicator control valve*
AGI	*Above ground installation*	**PS**	*Primary sludge*
ATEX	*Hazardous and explosive atmosphere*	**PSV**	*Pressure safety valve*
BHM	*Biological hydrogen methanation*	**REDII**	*Renewable Energy Directive recast*
BOD	*Biological oxygen demand*	**SBR**	*Sequential batch reactor*
CBG	*Compressed biomethane gas*	**SMR**	*Steam methane reforming*
CCU	*Carbon capture and utilisation*	**SMY**	*Specific methane yield*
CH_4	*Methane*	**SNSP**	*System non-synchronous penetration*
CHG	*Compressed hydrogen gas*	**SOEC**	*Solid oxide electrolysis cells*
CO_2	*Carbon dioxide*	**TRL**	*Technology readiness level*
Cp	*Capacity factor*	**TS**	*Total solids*
Cp_{WT}	*Wind turbine operating capacity factor*	**TSS**	*Total suspended solids*
CSO	*Central statistics office*	**TT**	*Tube trailer*
EU	*European Union*	**VRE**	*Variable renewable electricity*
FC	*Fuel cell*	**VS**	*Volatile solids*
GC	*Gas chromatograph*	**VS/TS**	*Volatile solids to total solids ratio*
GHG	*Greenhouse gas*	**W**	*Watts*
H_2	*Hydrogen*	**WAS**	*Waste activated sludge*
HGV	*Heavy goods vehicle*	**WS**	*Wind speed*
HHV	*Higher heating value*	**WT**	*Wind turbine*
LCOE	*Levelised cost of energy*	**WWTP**	*Wastewater treatment plant*
LCOH	*Levelised cost of hydrogen*		
LHV	*Lower heating value*		
LNG	*Liquefied natural gas*		
MER	*Methane evolution rate*		
NETs	*Negative emission technologies*		
O_2	*Oxygen*		
P&ID	*Process and Instrumentation diagram*		

1. Introduction

The introductory section of this thesis outlines the overarching concept of electrofuels in a circular, cascading economy. The first chapter of the thesis discusses the current state-of-the-art, without an in-depth analysis, providing a rationale for the work carried out in this thesis.

1.1. Electrofuels in a Circular Economy

With Ireland being a member of the UN Climate Change Conference (COP), it has aligned itself with the other world governments in leading global climate research groups and Non-Governmental Organisations (NGOs). During the latest Paris Agreement, a consensus on the necessity to limit the global temperature rise to below 1.5°C was agreed upon [1]. Subsequently, the European Union (EU) Green deal members are in search of pathways to attain climate neutrality by 2050 through promotion of circular economies and by reducing the reliance on Russian fossil hydrocarbons through diversification of energy sources [2]. Addittionally, this green deal seeks to increase the share of renewable energy sources to at least 32% of the final energy consumption by 2030, including for wind, solar and biomass energy. The deal also seeks to achieve a 32.5% energy efficiency in 2030, compared to the current projections of the national energy usage [2].

On a national level, the Irish government is also set to reduce its overall greenhouse emissions by over 51% by 2030 and to achieve carbon neutrality by 2050. Coupled with ambitions to increase the share of renewable electricity to 80% by 2030 through installed solar panels, and onshore and offshore wind, the country needs to revise its energy consumption and production. This need for revision is compounded by the set target of 34.1% overall Renewable Energy Share (RES-Overall) by 2030, as set out by the National Energy and Climate Plan (NECP). As per the “RePowerEU” plan this is likely to increase to 45% in RES-Overall [3]. This will be particularly important for the decarbonisation of the transport and agriculture sectors.

While the government wishes to achieve these targets, the country’s greenhouse gas emissions paint a complex picture. 59% of the country’s emissions are energy related, and the non-energy emissions are dominated by the agriculture sector (Figure 1.1). These emissions originate from the livestock methane emissions, nitrous oxide from the chemical fertilisers, and poor manure management strategies. The current solutions presented to the public are wind and solar for green electricity, and electric vehicles for clean transportation. However, these solutions either foster further challenges, or do not sufficiently address the issues. Passenger cars account for only half of the transport emissions, the rest being dominated by light and heavy haulage vehicles [3].

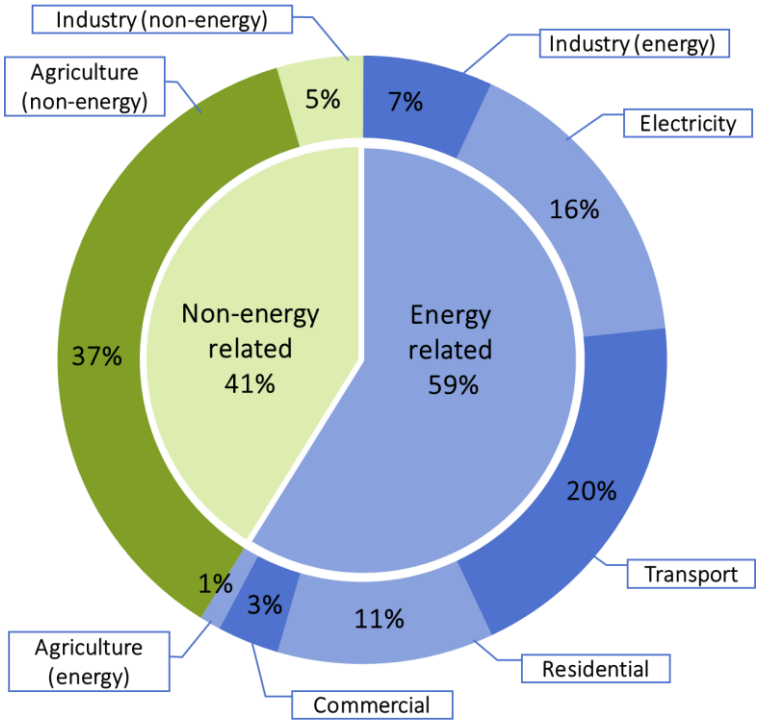


Figure 1.1: A breakdown of the greenhouse emissions across the sectors for the country of Ireland for the year 2018.

Transport and heat are responsible for approximately 70% of Ireland's primary energy use (not depicted in Figure 1.1), and can be more problematic to decarbonise than electricity [3]. The transport sector consists of several hard-to-abate sub-sectors, such as heavy transport, shipping, and aviation. Industrial heat is also challenging. To achieve the above mentioned emission targets, it is necessary to reimagine existing systems to enable energy recycling and increase the efficiency of existing infrastructure.

In Ireland, a notable issue is the isolated nature of the Island's energy infrastructure. The increased generation of electricity through variable renewable electricity (VRE) sources (namely wind and solar), has resulted in growing losses due to a mismatch in the supply and demand of electricity, called dispatch-down [4]. In 2020, the dispatch-down of wind electricity was nearly 12% of total generated electricity; this dropped to 7.4% in 2021 [5]. However, dispatch down is expected to increase with higher VRE production capacities. With the Irish wind capacity currently at 5.6 GW, and with the government committing resources to increase solar generation to 5.5 GW and offshore wind generation to 7 GW by 2030, the dispatch-down is expected to grow along with the increased VRE in the energy market [3],[6]. Consequently, this loss of electricity will result in lower turbine efficiencies, higher costs per unit of energy and reduced overall profitability of offshore wind farms [7]. The capture of this otherwise lost energy creates an opportunity for the production and storage of green alternative hydrocarbon fuels, such as Hydrogen (H_2), CH_4, and methanol (CH_3OH). This issue is further explored in chapters 4 and 5 of the thesis.

Hydrogen is often portrayed as a fuel of the future, primarily due to its appealing properties, like its energy density (120.2 MJ/kg), being almost 2.5 times that of natural gas (48.6 MJ/kg), while also having no emissions upon combustion, other than water. To

generate this H_2, traditionally steam methane reformation (SMR) was used to split fossil natural gas, releasing H_2, carbon monoxide, and a small amount of CO_2. This form of H_2 production is termed 'grey hydrogen'. Due to the associated CO_2 emissions (without carbon capture and storage) this method is undesirable [8]. As such, a sustainable 'green hydrogen' method of production is necessary to justify an energy transition to H_2.

Electrolysers are growing in popularity, using electricity and pure water to generate H_2 and by-product oxygen (O_2). In recent years, proton exchange membranes (PEM) have been poised as the technology of choice, due to its higher efficiency over the current technology [9]. However, while the electrolysers and the product H_2 are a green pathway for H_2 production, it relies heavily on the source of electricity. With the current efficiency losses and fossil heavy grid electricity, poorly managed electrolysers are at risk of producing more emission-intense H_2 than the grey H_2 pathway. Thus, a green pathway for H_2 can be established through integration with wind turbines. Converting some of the produced electricity to hydrogen can avoid the potential dispatch-down of electricity and reduce the use of more carbon intensive grid electricity. Current gas grids cannot handle high concentrations of H_2 gas and are prone to leaking hydrogen [10],[11]. Thus, the H_2 can be compressed and stored on-site for use as a transport fuel in heavy goods vehicles (HGVs) or combined with CO_2 via biological methanation before injection into the existing gas grid as a low-carbon alternative to fossil methane. This would alleviate the emissions associated with the transport sub-sectors. These issues related to hydrogen are further investigated in chapter 4 of the thesis.

The electrolyser produced by-product O_2 is likely to be vented to the atmosphere. To promote a circular economy, energy and environment system, wastewater treatment plants may have beneficial use of O_2. Comprising of mature and established technologies, these plants handle wastewater from municipalities and industries alike. Their primary function is to treat the sewage of the local regions, separating the biomass from the liquid, and treating the liquid to a regulation standard before reintroduction into the environment [12]. The treatment of wastewater takes place in the form of microbial treatment and aeration. Compressors diffuse large quantities of air in the water, creating aerobic zones for microbes to break down wastewater. With system lifespans of up to 50 years, the technology can range from traditional open-air oxidation ditches with settling tanks, to modern sequential batch reactors. This variety in technology and long operation life means that a range of system efficiencies are present in the wastewater treatment sector. This issue is more significant when assessing the literature, which reveals that the water sector accounts for 1.3% of global GHG emissions [13],[14]. The author proposes that in this system-of-systems model, local wastewater treatment plants (WWTPs) could greatly benefit using O_2-enriched air, or pure O_2 aeration processes. The literature suggests a potential 5.5-fold reduction in aeration demand, and subsequently, up to a 40% reduction in the total emissions, power consumption and operation costs of the WWTP through the reduced electricity use and purchase [15]. Details of the O_2 use in a circular economy are delved into in chapter 5 of the thesis [16].

When considering the disposal of sludge waste in WWTPs, it can comprise up to 50-70% of the total cost of the sewage treatment process [17],[18]. Anaerobic digestion has become increasingly common in the industry for the reduction of biomass sludge into gaseous biogas, which mainly consists of 50-70% CH_4 and 30-50% CO_2. Multiple WWTPs around Ireland have co-located anaerobic digesters (AD) with WWTPs to recoup some of the costs by generating CH_4 to heat and power the plants. In Austria, the majority of WWTPs designed to handle a population equivalent of over 20,000 persons have integrated AD systems [19]. Sludge pretreatment technology has shown to significantly benefit the treatment process, with improved biogas yields, reduced water and solids content, could poise the technology to improve the economical viability of the system [16],[20].

The co-location of an electrolyser at a WWTP with an AD system creates symbiosis across the electricity and water sectors. To integrate the gas sector, the authors propose the use of biological methanation technology to further marry the systems together. Biological methanation systems use *Methanothermobacter* archaea, which consume CO_2 and H_2, releasing CH_4, some water and a small amount of energy. In research, biomethanation systems have traditionally been adapted from the anaerobic digestion process, with in-situ and ex-situ systems predominantly fashioned after continually stirred tank reactor (CSTR) systems, reflected in a majority of research investigating the performance of said systems [21]. Recent literature has shown the biomethanation processes limited by the dissolution of the H_2 gas into the substrate medium [22]. More innovative biomethanation systems have been investigated, and the authors have undertaken research in designing and commissioning a methanation system using a novel diffusion-based mixing and H_2 dissolution (See chapters 2 and 3). CO_2 has a multitude of uses, ranging from use in laboratories, hospitals, slaughterhouses, meat packaging, carbonation of beer and soft drinks. While all valid uses, the author has chosen to focus on the use of CO_2 within the energy sector, with a view of the energy sector generating significant CO_2 emissions [23]. The re-introduction of CO_2 in the energy production thus exemplifies the circular economy aspect of the produced electrofuels, allowing for recycling of the otherwise released emissions. The use of CO_2 and Carbon monoxide (CO) in the Fischer-Tropsch process for green liquid hydrocarbon fuels is also a topic that is currently discussed across literature, generating green fuels for the shipping and aviation sectors [24]. It is possible to include other such uses of CO_2 in the circular economy, but the authors excluded the alternatives in order to keep the overarching story focused on the energy sector as much as possible.

From a policy viewpoint, this thesis discusses some of the problems associated with the rationalisation of emissions savings by the existing Directives (recast Renewable Energy Directive [REDII]), which can downplay or ignore associated process emissions savings. This is discussed in detail in Chapter 4. The author believes this can be counter-productive due to the rationale of the Directive, as exemplified by Ireland's reduced renewable energy supply in electricity (RES-E) for the years 2020-2021;this dropped by 2.6%, to 36.4% under REDII. Half of the reduction was attributed to the exclusion of some biomass with the shift from the REDI to REDII methodology, while the remaining reduction was due to the lower renewable electricity generation, due to the lower wind speeds experienced in 2021. The discrepancy across methodologies is even more evident in the renewable energy share in

transport (RES-T) which reduced from 9.9% to 4.3% due to the revised methodology [3]. This is primarily due to the changes in the weightings used in the calculation of RES-T, specifically, the renewable electricity on the road and rail, as well as the biofuels [3]. Within the confines of this thesis, the argument is also made for the absence of methodology for the calculation of emission savings by the capture of otherwise curtailed electricity.

1.2. The rationale for the thesis

With an evolving energy grid, the necessity for the capture and storage of surplus electricity in energy-dense storage methods will become a growing requirement. Based on the national and international ambitions for a sustainable future, the author proposes a system of systems, serving as a potential solution for both energy and non-energy related emissions. The system-of-systems is capable of integrating the previously independent sectors of water, electricity, and gas. Interconnecting wastewater treatment plants (WWTPs), onshore or offshore wind turbines, and novel biological methanation technologies, along with existing anaerobic digestion (AD) plants (typically near municipal WWTPs), can open alternative green hydrocarbon pathways to the existing fossil hydrocarbons, such as biomethane (CH_4) or methanol (CH_3OH).

Additionally, these technologies can supply alternative energy storage methods, prolonging the utility of existing infrastructure, and increasing the efficiency of wind turbines through the capture of otherwise curtailed (or constrained) electricity.

1.3. Objectives

The objectives of this thesis have evolved throughout its lifecycle, adapting to the literature and global events. The primary objective has been to develop and promote the use of biomethanation technology, and provide a scenario in which this novel technology can integrate into a circular economy, cascading energy and environment system.

The primary objectives are:

- Design and commission a novel biomethanation system at a higher TRL than previous work within the research group.
- Investigate a potential local scenario in which the proposed circular economy, energy and environment system may feasibly operate.
- Assess the operation feasibility of a large-scale circular economy system.
- Determine the potential benefits and savings to the sectors, due to the implemented circular economy system.

Detailed objectives from chapters 2 to 5 can be summarised as:

- Assess the state-of-the-art of biomethanation technologies in literature and identify potential gaps.
- Design and commission a previously simulated reactor system, thus, creating a prototype of a cascading three-phase biomethanation system.

- Investigate the relationship across wind farms, dispatch down, electrolysers, wastewater treatment plants, anaerobic digestion plants, and biomethanation systems.
- Assess the potential emission savings achieved with the integrated systems at wastewater treatment plants.
- Investigate potential negative carbon emission pathways in the proposed circular economy system.

1.4. Outline and link between the chapters

The thesis comprises 6 chapters, with supplementary data and references located at the end of each associated chapter. The chapters follow the layout of the typical academic publication structure, known as PhD by publication. The published (or under peer review) journal articles may be assessed independently or as part of the whole thesis.

Chapter 1 serves as the introduction to the thesis, providing an overview of the global and national policies, and the industry. It identifies the main objectives of the thesis. Chapter 2 provides a literature review of state-of-the-art biomethanation technologies and discusses the theory of coupling the technologies. The purpose of the technology is to facilitate the integration of the electricity and the gas grids. Chapter 3 is a novel study on the design and commission of a novel biomethanation system, facilitating the conversion of hydrogen and carbon dioxide gases to biomethane gas. The study primarily focuses on the design, manufacture, and safety of the designed system. Chapters 4 and 5 are published novel research articles. The chapters investigate the feasibility of the thesis proposed system-of-systems. An energy balance for the system is conducted and a small scale system is investigated. A large scale system is also investigated in chapter 5, depicting an ideal case scenario for the idea. Chapter 6 is a synthesis of the thesis, with conclusions and recommendations on current and future research. Chapters 3 to 5 appear as published manuscripts, bar a few grammatical or minor modifications to reduce repetition, and abbreviations to improve the reading experience. Each chapter builds upon the previous, expanding on the concept of biomethanation on its role in the industry, before assessment as an assay of systems working synergistically. A bibliography is provided at the end of each chapter for the reader.

Chapter 2: Literature review

As the rise in variable renewable electricity production presents a new global challenge in energy storage, biological methanation can facilitate wind and solar energy production through the storage of otherwise curtailed or constrained electricity in the form of gaseous biomethane. Biological methanation in the circular economy involves reacting hydrogen with carbon dioxide to produce methane ($4H_2 + CO_2 = CH_4 + 2H_2$). In the circular economy context, this can typically increase the methane output of the biogas systems by up to 70%. In this literature review, multiple biological hydrogen methanation (BHM) systems are compiled and compared in key parameters such as methane evolution rate and retention time. Increased retention times were suggested to be related to less efficient systems as longer gas residence in reactors meant slower upgrading times. A significant

lack of information on gas-liquid transfer co-efficient was identified, along with a scarcity of diffusion-based methanation systems.

Chapter 3: Design and Commission of a novel biological methanation system.

As chapter 2 investigates the ability of biomethanation technology to produce clean green gas, chapter 3 investigated the design, fabrication and commissioning of this technology, in an effort to advance the technology readiness level. The chapter built upon the literature review and previous research, which the student was a co-author on. The previous study simulated a cascading, three-stage reactor system, utilising diffusion-based mixing and gas dissolution to achieve grid-quality biomethane. This chapter followed the designed and fabrication process of the novel biomethanation system. Constructed to a high-quality standard, under restraints of the university health and safety system, the chapter reviews the process, the initial performance of the system, and the revisions necessary to further advance the prototype reactors.

Chapter 4: Electrofuels in a circular economy: A systems approach towards net zero.

Building upon the concept of electrofuels in a circular economy, the author carries out a case study in the locality to integrate the independent sectors of water, gas and electricity by the development of existing wastewater treatment plants into an energy hub. This is carried out by situating an electrolyser, anaerobic digester and a biomethanation system at the plant. The paper primarily investigates the viability of small-scale energy hubs, which would be determined by the available variable renewable electricity in the locality, such as onshore turbines or solar panels. The chapter also investigates opportunities for the production of carbon-negative fuels through the incorporation of pyrolysis technology. According to the recast EU Renewable Energy Directive, it was also apparent that the current methodology does not accommodate for emission savings through the capture of otherwise curtailed electricity. From the authors perspective, this warrants revision to the existing methodology.

Chapter 5: Operation of a circular economy, energy, and environmental system at a wastewater treatment plant.

This chapter investigated the scaling of circular economy systems, and the availability of electricity when assessing dispatch down from wind turbines. This also followed on from the previous study, by looking at a large-scale system, particularly a 10 MW electrolyser co-located at a large wastewater treatment plant of approx. 430,000 population equivalent size. The downstream resource assessment of wastewater sludge, by-product oxygen use, hydrogen, carbon dioxide and biomethane, and the final end-use of the electrofuels was assessed in use for decarbonising hard-to-abate sectors.

References

[1] IPCC. Climate Change 2021: The Physical Science Basis [Internet]. Vol. AR. 2021 Jun. Available from: https://www.ipcc.ch/report/ar6/wg1/downloads/report/IPCC_AR6_WGI_Full_Report.pdf

[2] European Commission. The European Green Deal. Eur Comm [Internet]. 2019;53(9):24. Available from: https://eur-lex.europa.eu/legal-content/EN/TXT/PDF/?uri=CELEX:52019DC0640&from=EN

[3] SEAI. Energy in Ireland 2022 [Internet]. 2022. Available from: https://www.seai.ie/publications/Energy-in-Ireland-2020.pdf

[4] EirGrid and SONI. Annual Renewable Energy Constraint and Curtailment Report 2020 [Internet]. 2021 [cited 2021 May 26]. Available from: https://www.soni.ltd.uk/media/documents/Annual-Renewable-Constraint-and-Curtailment-Report-2020-V1.0.pdf

[5] EirGrid and SONI. Annual Renewable Energy Constraint and Curtailment Report 2021. 2022;(August):1–28. Available from: http://www.soni.ltd.uk/media/documents/Operations/Annual Renewable Constraint and Curtailment Report 2014.pdf

[6] Department of Communications, Climate Action and Environment G of I. Climate Action Plan 2019: to Tackle Climate Breakdown [Internet]. 2019. Available from: https://www.dccae.gov.ie/en-ie/climate-action/topics/climate-action-plan/Pages/climate-action.aspx

[7] McDonagh S, Ahmed S, Desmond C, Murphy JD. Hydrogen from offshore wind: Investor perspective on the profitability of a hybrid system including for curtailment. Appl Energy [Internet]. 2020 May 1 [cited 2020 Apr 7];265:114732. Available from: https://linkinghub.elsevier.com/retrieve/pii/S0306261920302440

[8] IEA. The Future of Hydrogen [Internet]. The Future of Hydrogen. OECD; 2019. Available from: https://www.oecd-ilibrary.org/energy/the-future-of-hydrogen_1e0514c4-en

[9] Schmidt O, Gambhir A, Staffell I, Hawkes A, Nelson J, Few S. Future cost and performance of water electrolysis: An expert elicitation study. Int J Hydrogen Energy [Internet]. 2017 Dec 28 [cited 2021 Feb 26];42(52):30470–92. Available from: https://linkinghub.elsevier.com/retrieve/pii/S0360319917339435

[10] ONEY F, VEZIROLU T, DULGER Z. Evaluation of pipeline transportation of hydrogen and natural gas mixtures. Int J Hydrogen Energy [Internet]. 1994 Oct;19(10):813–22. Available from: https://linkinghub.elsevier.com/retrieve/pii/0360319994901988

[11] Svensson M. Biomethane standards: Gas quality standardisation of biomethane, going from national to international. In Brussels; 2014. Available from: www.socalgas.com/documents/business/Rule30_BiomethaneGuidance.pdf

[12] Environmental Protection Agency. Primary, Secondary and Tertiary Treatment. Waste Water Treatment Manuals. 1997. 27–28 p.

[13] Hannah Ritchie. Sector by sector: where do global greenhouse gas emissions come from? [Internet]. Our World In Data. 2020. Available from: https://ourworldindata.org/ghg-emissions-by-sector#licence

[14] International Energy Agency. IEA: World Energy Outlook 2018 [Internet]. IEA. 2018 [cited 2021 Mar 24]. Available from: https://www.iea.org/reports/world-energy-outlook-2018

[15] Mohammadpour H, Cord-Ruwisch R, Pivrikas A, Ho G. Utilisation of oxygen from water electrolysis – Assessment for wastewater treatment and aquaculture. Chem Eng Sci. 2021 Dec 31;246:117008.

[16] Sun C, Xia A, Fu Q, Huang Y, Lin R, Murphy JD. Effects of pre-treatment and biological acidification on fermentative hydrogen and methane co-production. Energy Convers Manag [Internet]. 2019 Apr 1 [cited 2019 Feb 27];185:431–41. Available from: https://www.sciencedirect.com/science/article/pii/S0196890419301943?dgcid=coauthor

[17] Andreoli C V, von Sperling M, Fernandes F. Sludge Treatment and Disposal. Water Intell Online [Internet]. 2015 Dec 30;6:9781780402130–9781780402130. Available from: https://library.oapen.org/bitstream/id/2cfbc8d9-8306-4c26-8b13-27e213a14f26/640145.pdf

[18] Potdukhe RM, Sahu N, Kapley A, Kumar R. Co-digestion of waste activated sludge and agricultural straw waste for enhanced biogas production. Bioresour Technol Reports. 2021 Sep 1;15:100769.

[19] Shen Y, Linville JL, Urgun-Demirtas M, Mintz MM, Snyder SW. An overview of biogas production and utilization at full-scale wastewater treatment plants (WWTPs) in the United States: Challenges and opportunities towards energy-neutral WWTPs. Renew Sustain Energy Rev [Internet]. 2015;50:346–62. Available from: http://dx.doi.org/10.1016/j.rser.2015.04.129

[20] Li C, Wang X, Zhang G, Li J, Li Z, Yu G, et al. A process combining hydrothermal pretreatment, anaerobic digestion and pyrolysis for sewage sludge dewatering and co-production of biogas and biochar: Pilot-scale verification. Bioresour Technol. 2018 Apr 1;254:187–93.

[21] Rusmanis D, O'Shea R, Wall DM, Murphy JD. Biological hydrogen methanation systems–an overview of design and efficiency [Internet]. Vol. 10, Bioengineered. 2019 [cited 2020 Jan 29]. p. 604–34. Available from: https://www.tandfonline.com/doi/full/10.1080/21655979.2019.1684607

[22] Voelklein MA, Rusmanis D, Murphy JD. Biological methanation: Strategies for in-situ and ex-situ upgrading in anaerobic digestion. Appl Energy [Internet]. 2019 Feb;235:1061–71. Available from: https://linkinghub.elsevier.com/retrieve/pii/S0306261918317124

[23] IEA Bioenergy. Production of food grade sustainable CO2 from a large biogas facility-GO'CO2 at The Korskro Biogas Plant, Denmark. 2020;(Figure 1):1–4.

[24] Gray N, McDonagh S, O'Shea R, Smyth B, Murphy JD. Decarbonising ships, planes

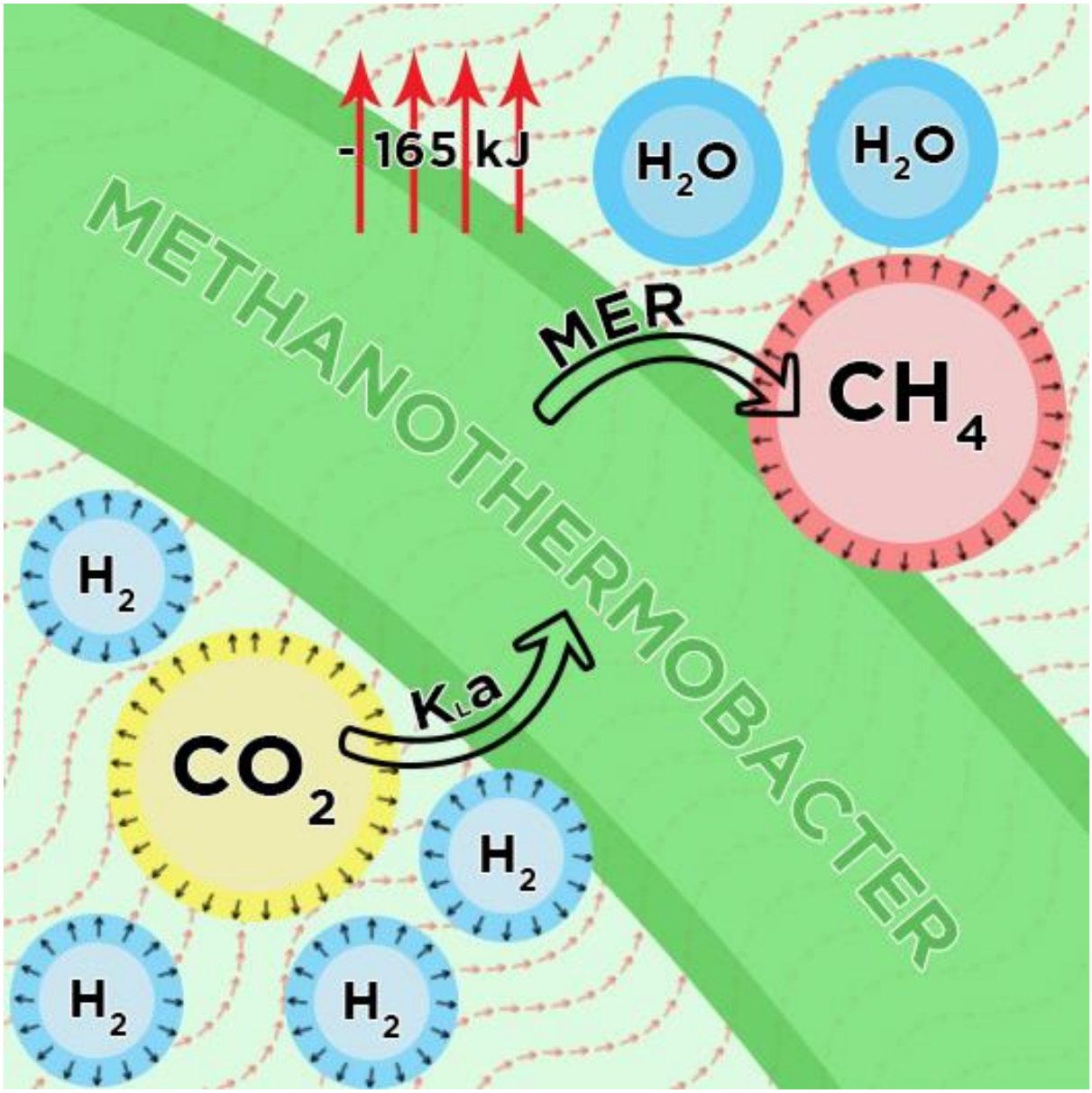
and trucks: An analysis of suitable low-carbon fuels for the maritime, aviation and haulage sectors. Adv Appl Energy. 2021 Feb 23;1:100008.

2. Biological Hydrogen Methanation Systems – An overview of design and efficiency

Davis Rusmanis[1,2], Richard O'Shea[1,2,*], David M. Wall[1,2], Jerry D. Murphy[1,2]

1. MaREI Centre, Environmental Research Institute, University College Cork, Ireland.
2. Civil, Structural and Environmental Engineering, School of Engineering and Architecture, University College Cork, Cork, Ireland

Graphical abstract



Abstract

The rise in intermittent renewable electricity production presents a global requirement for energy storage. Biological hydrogen methanation (BHM) facilitates wind and solar energy through the storage of otherwise curtailed or constrained electricity in the form of the gaseous energy vector biomethane. Biological methanation in the circular economy involves the reaction of hydrogen - produced during electrolysis - with carbon dioxide in biogas to produce methane ($4H_2 + CO_2 = CH_4 + 2H_2O$), typically increasing the methane output of the biogas system by 70%. In this paper, several BHM systems were researched, and a compilation of such systems was synthesised, facilitating a comparison of key parameters such as methane evolution rate (MER) and retention time. Increased retention times were suggested to be related to less efficient systems with long travel paths for gases through reactors. A significant lack of information on gas-liquid transfer co-efficient was identified.

Highlights

Novel technologies are essential for optimal biomethanation.

Retention time is a poor indication of biomethanation system efficiency.

Bubble diffusion in biomethanation presents a gap in the state of the art.

Reactor gas-liquid transfer data is scarce, showing gaps in the state of the art.

2.1 Introduction

2.1.1 Background

As part of the COP21 Paris Agreement, many countries have agreed on action to reduce greenhouse gas (GHG) emissions and meet reduction targets to limit global temperature rise below 2°C. It is often misconstrued that electricity can effect a silver bullet solution for decarbonising energy with emphasis put on solar and wind energy devices. Of issue with renewable electricity is the variable intermittent nature of electricity production (from wind and solar), the temporal mismatch with variable energy demand (night and day, summer and winter), and differences in energy vectors used in each energy sector (solid, gaseous and liquid fuels for the production of electricity, heat and transport). Fossil fuel systems have been optimised over hundreds of years and will be difficult to fully displace in a short period. Fossil fuel systems are dispatchable, easy to store, have high energy density and are cheap. Renewable energy systems are at various stages of maturity and to replace the full extent of fossil fuel systems we must overcome challenges in unpredictability, storage, and cost. Wind and solar systems are the most developed renewable energy systems and recently have become price comparative with fossil fuel-generated electricity, but intermittency and storage are still of issue. The energy transition will involve innovative integrated design, generating dispatchable decarbonised electricity, heat and transport fuel, including solid, liquid and gaseous vectors. Hydrogen (H_2) generated from curtailed/constrained solar/wind energy during times of low demand/excess generation can serve as both a means of conversion to renewable gaseous fuel and as a storage mechanism through “Power-To-Gas” concepts [1]. In the energy transition utilising the natural gas infrastructure of many developed economies, biomethanation involves a circular economy integration of organic waste treatment using anaerobic digestion (AD), coupled with H_2 production from intermittent renewable electricity. Natural gas may be substituted with biomethane and renewable gaseous fuel from non-biological sources (i.e. renewable electricity).

2.1.2 Anaerobic Digestion

Many EU countries are unlikely to meet their 2020 renewable energy share (RES) targets which range from 10% RES (in Malta), to as high as 49% RES (in Sweden). In the case of Ireland, 16% of all energy must be sourced from renewables by 2020, however, as of 2017, overall RES was just 10.6% [2]. Conversion of wastes to biomethane using AD can reduce GHG production (from fugitive methane emissions) and increase RES in the form of green gas, reducing the current shortfall in EU targets [3]. Significant resources of biomass including livestock manures and slurries, as well as terrestrial biomass from non-food cellulosic material may be utilised in AD systems. AD can reduce GHG emissions by replacing open slurry storage (with significant fugitive methane emissions) with a concurrent generation of low carbon (even GHG-negative) energy in the form of biogas, and digestate as a valuable bio-fertiliser [4]. The uptake of AD within International Energy Agency (IEA) Bioenergy countries is significant in Germany, the UK, France, and Switzerland [5],[6]. Countries such as Estonia, Ireland and Norway have a huge potential for growth in the

resource of biogas. Biogas primarily consists of methane (CH_4) (50-70%v/v) and CO_2 (30-50%v/v) [7]. To produce biomethane, CO_2 is removed from the biogas. The energy content of biomethane is of the order of 35 MJ/m_{STP}^3, slightly lower than that of natural gas (39 MJ/m_{STP}^3) [8]. The use of biomethane is however becoming more prevalent as depicted in the latest IEA Bioenergy reports, with rapid growth in biomethane production in The UK, France and Denmark [5], [9]. Biogas upgrading can be considered an energy-intensive process, traditional biogas upgrading technologies have an energy demand ranging from 0.05 kWh_e/Nm^3 to 0.76 kWh_e/Nm^3 raw biogas [7], [10].

2.1.3 Biological Hydrogen Methanation

More recently, biological hydrogen methanation (BHM) has been investigated as a means of upgrading biogas [7], [11]. The process involves the Sabatier reaction, utilising a carbon source (CO_2) and H_2 to generate CH_4 (Equation 2.1).

$$4H_2 + CO_2 \rightarrow CH_4 + 2H_2O\ \Delta G^0 = -165\ kJ/mol \qquad \text{Equation 2.1}$$

The BHM process utilises this reaction, catalysed by specific archaea of the *Methanothermobacter* genus, capable of converting H_2 and CO_2 to CH_4 with water as a by-product. This biological method of CO_2 conversion could potentially eliminate the traditional energy-intensive CO_2 separation processes in AD whilst allowing for the potential doubling of the CH_4 yield (depending on biogas composition). In turn, CH_4 could be directly injected into the natural gas grid if grid quality specifications are met.

BHM is a means of capturing CO_2 in biogas that would have been emitted to the atmosphere and converting it to an extra quantity of renewable fuel; this is termed gaseous fuel from a non-biological origin in the recast Renewable Energy Directive (RED II) [12]. As such the system can be more sustainable than biogas by itself if the hydrogen is sourced from renewable electricity that would have been curtailed or constrained [13]. In terms of economics, the BHM system can displace conventional biogas upgrading such as water scrubbing. Thus the net cost of the system is the cost of BHM less the saved costs of not installing traditional biogas upgrading. Also, the cost per unit of the produced gas is reduced as typically 70% extra gas is produced so the investment is divided between 70% more units of energy [11].

The BHM process is capable of being carried out both within an anaerobic digester system known as in-situ or in a separate, adjacent reactor known as ex-situ [7], [14]. In-situ biomethanation takes place within the anaerobic digester. H_2 gas is introduced typically through mixing or diffusion, to maximise the contact area with hydrogenotrophic methanogenic archaea, which produce CH_4 from CO_2 and H_2. Standard anaerobic digestion of feedstock also occurs within the reactor, providing nutrients, contained within the digested substrates, and also CO_2, needed by various microbes through acetogenesis, methanogenesis and methanation (Figure 2.1).

Ex-situ methanation takes place in a separate external reactor, typically tailored to suit the hydrogenotrophic methanogens. Specific nutrient media is supplied to the microbial

consortium, under a controlled environment. Gaseous reagent supply is also maintained to ensure optimal growth conditions and product concentrations. Gas purification remains to ensure grid quality gases and usually includes drying of gas to remove water vapour. (Figure 2.2).

BHM can be an energy-intensive process due to the processes which are required for effective H_2 solubilisation to allow H_2 uptake by archaea, such as intense mixing from impellers, compressors and recirculation of gas and liquids. This results in higher parasitic energy demands for the upgrading process. The literature suggests that agitation as a method of H_2 solubilisation in liquid is suitable for BHM [15]–[17]. However, agitation constitutes a large energy demand for these BHM systems. This is further compounded by the requirement for continuous operation, i.e. minimum power consumption of the plant can be assumed to be the power demand of the mixing component at the idle stage. At a large scale, the use of high-rate agitation to promote H_2 solubilisation may be justified, but a low-energy demand alternative would be far more beneficial.

This paper aims to review the current literature on BHM systems with regards to system performance, and H_2 solubilisation methods used in literature, and to determine the gaps in the state of the art with regards to BHM. This paper will also seek to use a short case study to see how biological methanation compares with traditional upgrading technologies.

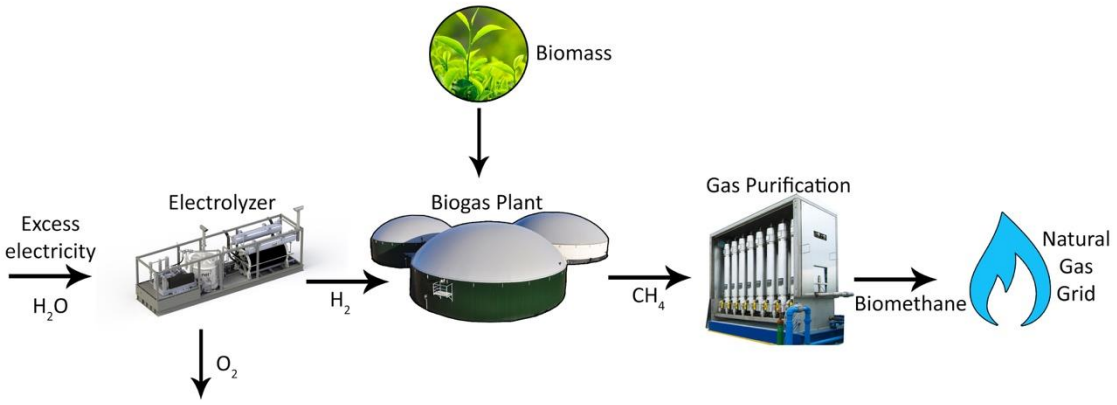


Figure 2.1: In-situ biological H_2 methanation schematic.

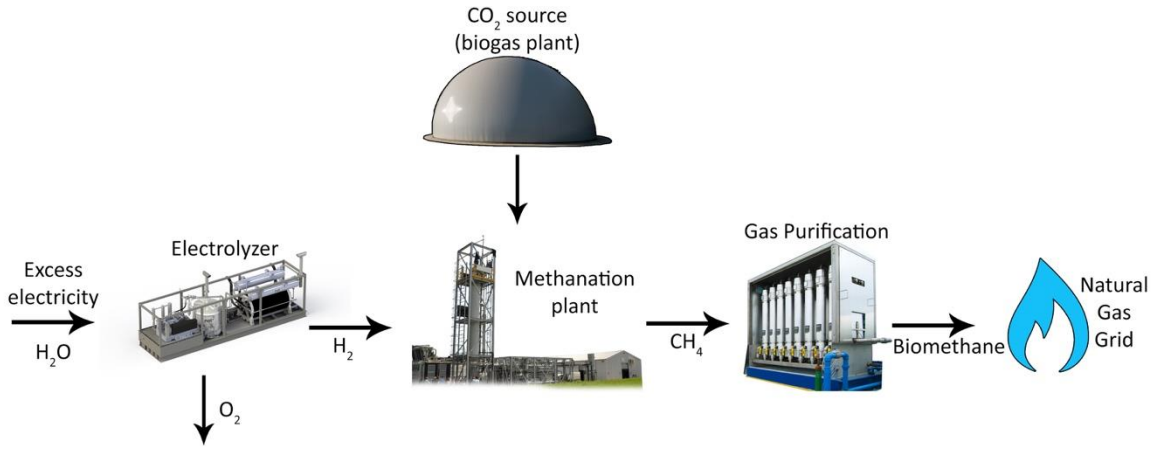


Figure 2.2: Ex-situ biological H_2 methanation schematic.

2.2 Review of State of the Art

The following section investigates the key operational parameters in biomethanation including the interplay between gases, microbiology, nutrient supply, reactor environmental conditions, and methane evolution rates (MER). Multiple reactor configurations described in the literature are studied and compared to assess performance across systems.

2.2.1 The Role of Hydrogen in Power to gas Systems

Hydrogen gas can be generated through electrolysis which is currently the only large-scale viable method for H_2 production that does not require fossil fuels, unlike the reformation of natural gas [18]. Hydrogen has been seen as a viable fuel for future energy systems as storage technologies become mature and more economically viable. Currently, the natural gas grid is not suitable for storing large H_2 volumes (or conveying high percentages of hydrogen in natural gas) as most pipelines would not be of a specification to prevent leakage. Small concentrations of H_2 are allowed to be injected into the existing gas grid infrastructure in some countries [19]. However, H_2 concentrations in gas grids are heavily regulated. In Europe, the maximum allowable H_2 concentrations vary from 0.1% to 10% by volume and vary by country [20], [21], as shown in Table 2.1.

Table 2.1: List of hydrogen limits allowed in the Natural Gas Grid per country.

Country	maximum H_2 content in HP gas pipeline	
	% volume/molar percent	% Mass
Czech Republic [a]	0	0
Ireland [a]	0.1	0.013
UK [a]	0.1	0.013
Belgium [a]	0.1	0.013
Sweden [a]	0.5	0.063
Holland [a]	0.5	0.063
Austria [a]	4	0.524
Switzerland [a]	4	0.524
France [a]	6	0.802
Germany [a]	10	1.396
Case 1 [b]	2	0.256
Case 2 [b]	5	0.661
Case 3 [b]	10	1.396

[a] Adapted from M. Svensson [21].
[b] Cases were proposed by Altfeld and Pinchbeck [22].
Case 1 – If a CNG filling station is connected.
Case 2 – If no filling station, gas turbine or gas engines with H_2 specification < 5% connected.
Case 3 – If no filling station, gas turbine or gas engines with H_2 specification < 10% connected.

Historically, carbon steel, stainless steel, cast iron and nickel steel have been used to transport H_2, but are not considered suitable for high-pressure H_2 transmission [23]. Furthermore, at elevated temperatures and pressures, H_2 attacks mild steel and other high-strength steels, causing decarburisation and embrittlement when in contact for extended periods, particularly with high-purity H_2 [20], [23]. As high-quality steel is required to facilitate the conveyance and storage of H_2, a large investment is required for a H_2 economy. Studies suggest that the optimum diameter for a transportation pipeline for 100% H_2 is 0.88m, while for 100% natural gas, it is 0.54m [20]. Therefore, for a H_2 pipeline with a wall thickness of 10mm, 1.6 times the volume of steel would be required as compared to a natural gas pipeline.

Typically, where H_2 is produced through electrolysis, it is compressed to high pressures, 200 - 300 bar for storage in gas cylinders; and up to 800 bar for use in transportation [24]. For grid injection, costs may be lower due to gas undergoing direct compression to a grid-level pressure. Compression is also an issue when using H_2, owing to its low density (0.09 kg/m^3). Transporting H_2 through pipes requires a larger diameter pipe or more compression power as compared to CH_4 to achieve the same energy throughput at the same operational pressure, with calculations showing that per kilometre of a pipeline, the energy demand of H_2 is significantly higher than that of CH_4 (see Box S1 in supplementary data) [20]. Previous

studies have stated that the cost of a large-scale transmission grid for H_2 is approximately 1.5-1.8 times that of natural gas/CH_4 [20], [25].

When raw biogas from AD is upgraded to biomethane, it can be injected into the existing natural gas grid infrastructure or compressed into Liquefied Natural Gas (LNG). The existing natural gas grid provides a means of energy storage for biomethane. As such, it is viewed as a solution to the anticipated energy storage issues that may arise in countries such as Denmark who intend to fully transition away from fossil fuels and be based solely on renewables by 2050 [26], [27].

While H_2 may be more efficient in energy density per unit mass, it is four times less dense in volume compared to CH_4. The issues associated with the construction of H_2 gas networks, including material requirements and other complications relating to density may not justify the large-scale shift to a H_2 gas grid when an existing natural gas grid may be used for biomethane. However, in some instances, localised city micro-gas grids are being built for H_2 such as in the UK [3].

Issues relating to the transportation of H_2 could be mitigated by using H_2 in BHM coupled with AD. While some studies have attempted in-situ upgrading, albeit at lower efficiencies, ex-situ is more developed. Removal of CO_2 from the raw biogas by upgrading to biomethane can almost double CH_4 yields (if biogas is 50% CO_2 and 100% efficiency is achieved). The extra energy obtained in the form of methane far exceeds the parasitic energy input in upgrading the gas. In essence, this is a fuel produced from biogenic CO_2, sometimes termed gaseous fuel from non-biological origin, which is considered an advanced transport fuel within the recast Renewable Energy Directive (RED II recast) [12].

Hydrogen may be generated from intermittent wind and solar energy that could otherwise have been curtailed or constrained and used as an energy source or used in conjunction with AD plants to upgrade raw biogas to a grid-quality biomethane gas (95% CH_4) [13]. As such, the CH_4 produced would allow for efficient, cost-effective energy storage of surplus/constrained electricity in the form of green gas in the natural gas grid. Integration of H_2 has the potential for the development of circular economy systems, integration of intermittent renewable energy production and elevating the biomethane resource whilst greening the gas grid and using existing infrastructure.

2.2.2 Microbiology of BHM and AD

The Methanothermobacter genus is responsible for the biological upgrading process. To date, eight main species of this genus have been officially identified in previous literature as functional methanogens [28]–[32]. Table 2.2 lists some of the properties of Methanothermobacters. Studies on Methanobrevibacters (mesophilic archaea), are limited and do not discuss BHM applications. There could be merit in researching mesophilic methanogenic archaea for BHM applications if these archaea are capable of matching the production and doubling rates of Methanothermobacters, the lowered environmental temperature at mesophilic conditions would result in increased hydrogen solubility.

Table 2.2: Archaeal data on Methanothermobacters.

Methanothermobacter	Opt. Temp. °C	Opt. pH	Chemical addition g/l	Specific Growth rate /h	Doubling time h	Size µm x µm	Reference
Crinale	65	6.9	0.025 NaCl 0.8-20 NaCl	3.6	0.193	0.3 x 5	[28]
Defluvii	60	7	0.025 Na2S 30 NaCl	0.462	1.5	0.42 x 6	[30]
Thermoflexum	55	8.1	0.05 Na2S 0.002 Na2WO4	0.198	3.5	0.4 x 20	[29], [30]
Wolfeii	60	7.25	10 NaCl	0.185	3.75	0.4 x 2.5	[33]
Tenebrarum	70	7.3	2.5 NaCl	0.058	12	0.5 x 10.5	[31]
Marburgensis	65	7.2	0.5 NaCl	0.1	0.288	0.6 x 6	[34], [35]
Thermoautotrophicus	67	7.4		0.231	3	0.6 x 7	[36]
Thermophilus	57	7.6	15 NaCl			0.36 x 6.5	[37]

Where values were missing from the literature, highlighted results (**bold**, *italic* and underlined) are calculated using the formula for the specific growth rate of microbes: $\mu = \ln(N_2/N_1)/ (t_2 - t_1)$; where μ is the specific growth rate, and N_1 and N_2 are the biomass at time 1 (t_1) and time 2 (t_2), respectively.

A summary of the biological processes which occur in the anaerobic environments of AD and BHM is illustrated in Figure 2.3. There are two key stages required for a BHM system to function. The first is the formation of CH_4 and CO_2 from the feedstock through processes known as acetogenesis and acetotrophic methanogenesis; which are responsible for the biogas production cycle in AD. The second stage involves the production of CH_4 via H_2 upgrading (hydrogenotrophic methanogenesis, referred to as hydrogenotrophic methanation for the BHM stage). Both processes require a specific environment to be maintained, with a pH in the range of 6.2-8.5 and a temperature range of 35-40°C (mesophilic), or 55-65°C (thermophilic) [38],[39].

The difference in the reactor environment for the two stages (AD and BHM) lies in the presence of H_2 in the reactor. If an in-situ system is used and H2 is introduced to the AD reactor, the increase in hydrogen partial pressure can lead to inhibition of volatile fatty acid (VFAs such as propionate and butyrate) degradation and the potential breakdown of the system (if not micro-managed) as acetogenesis requires very low H_2 partial pressures [40], [41]. This would require an in-situ system to convert close to 100% of the H_2 injected, as lower conversion would theoretically lead to the build-up of unconverted H_2 creating looping inhibition cycles, leading to reactor failure (Figure 2.4).

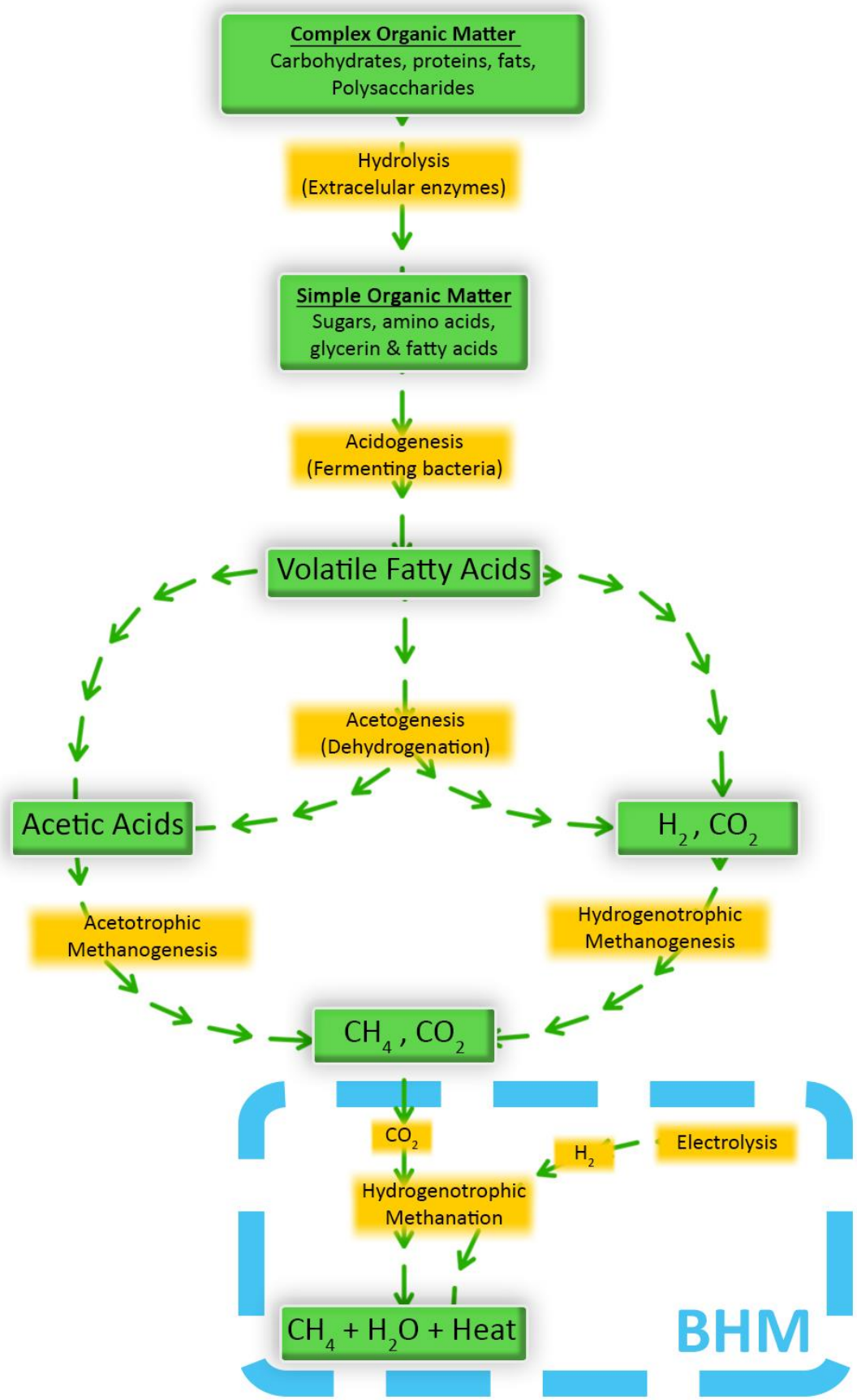


Figure 2.3: CH_4 formation through anaerobic digestion and biological hydrogen methanation.

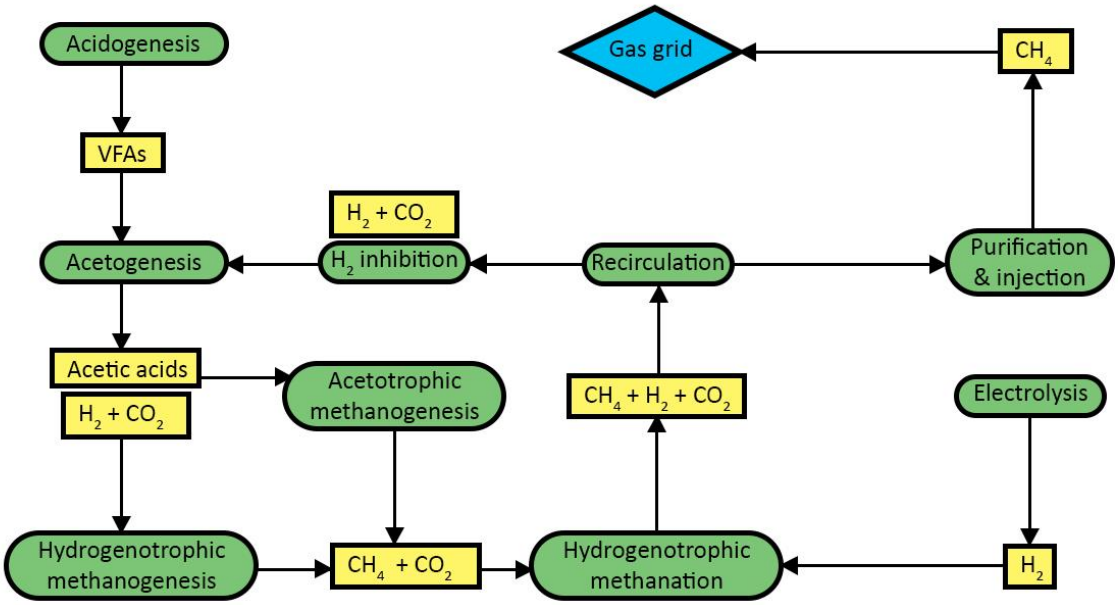


Figure 2.4: In-situ methanation failure process flow diagram.

Due to differences in the required environment for acetogenesis, acetotrophic methanogenesis and hydrogenotrophic methanation, the viability of efficient in-situ systems with high Methane Evolution Rates (MER) and purity is more challenging than for ex-situ systems. While in-situ systems would reduce the need for additional construction in an AD plant, the fundamental restriction of hydrogen partial pressures within the reactor space can theoretically lead to reactor failure. However, experiments by G. Luo and I. Angelidaki (including for hollow fibre membranes) at a small scale have been able to produce and upgrade biogas to a grid-level quality at a lab scale with in-situ upgrading [17], [42]. The experiment consisted of a 1L reactor volume, with 4 hours retention time, 1.5 barG pressure, and a second 1L reactor volume with a 0.75 barG pressure and agitation at 150rpm, respectively. Large-scale studies have yet to be published that depict a stable, functioning in-situ system. Thus, ex-situ systems maintaining a separate environment between acetotrophic methanogens and the biological hydrogen methanation processes are recommended by the authors; this ex-situ process allows separate conditions to be maintained, optimising both processes and minimising the risk of reactor failure.

Microbes that undertake methanogenesis respire anaerobically, utilising oxidised carbon such as CO_2 as an electron acceptor. Methanogens are found commonly in anaerobic environments which do not contain many oxygen sources, such as O_2 or NO_3^-. When combining AD and biological hydrogen methanation, it is important to optimise the bioreactor to enable the desired genus to thrive and deter unwanted archaea from multiplying. Concerning sources of carbon in a BHM system, studies have shown that with a larger build-up of microbial biomass, a higher fraction of CO_2 is used by microbes due to the need for a carbon source. Burkhardt *et al.* noted that a molar ratio for H_2 to CO_2 of 3.76: 1

gave a higher quality gas in terms of methane content [43]. This resulted in a reduction of available carbon sources, which could result in excess hydrogen. As such, the stoichiometric ratio (H_2:CO_2) is reduced to 3.76:1. While this is elucidated by Burkhardt *et al.*, further studies are required to investigate the relationship between biomass density and the molar ratio of gases [43].

2.2.3 Nutrients in BHM

For archaea to thrive within an environment, a unique mixture of nutrients is necessary to provide key trace elements for replication. Nutrient media relating to BHM varies substantially, depending on the specific cultures and archaea species involved in H_2 upgrading. To achieve high upgrading rates, an optimum nutrient feed is required to ensure no limitation from nutrient and elemental deficiencies. Table 2.3 shows the variation in nutrient media supplied to microbes found in the literature. This variation can be attributed to the limitation of chemical availability and the complexity of nutrient media. Using the "BacDive" Strain identifier for *Methanothermobacter* suggests an industrial growth culture medium of Methanobacterium growth media 141 and 119 as depicted in Table 2.4. The difference between literature and industry is evident in the variety of elements and concentrations recommended by the industry. As with AD, the addition of trace elements and nutrients also proves to be of great benefit to BHM [44]. Such additions allow for higher culture densities to thrive and thus boost the overall performance of the reactor significantly, by reducing microbial doubling time and thus increasing the microbial population. In ex-situ BHM, nutrient supply becomes a necessity due to the lack of solid feed addition. Excluding H_2 and CO_2 (or raw biogas) fed to ex-situ systems, nothing else is introduced into the reactor, and as such, there is a need for an external nutrient supply. Studies have been carried out on methanogenic microbiology, investigating the effect of elements on the methanogens, Wolfe *et al.* specified that sulphur is necessary for biosynthetic reactions and maintenance of low redox potential [36], [45]. Guneratnam *et al.* showed that *M. wolfeii* was dominant in thermophilic ex-situ biological hydrogen methanation and suggested, as supported by Winter *et al.*, that the microbes would benefit from the addition of tungsten (W)(8ηM) [32], [46]. The presence of tungsten in literature is found in one paper by Schill *et al.* [47]. The industrial nutrient media offered by DSMZ, in Table 4 contains tungsten as a constituent of the trace element solution in 0.40mg Na_2WO_4 x $2H_2O$. Observing the elemental composition of nutrient solutions used in BHM, the elements provided to the microbial population are not very different from those required for AD.

Archaea growth is heavily reliant on nutrient availability and the supply of gaseous feed, determined by the volumetric gas-liquid mass transfer coefficient (k_La) [48]. As such, the gas should also be treated as an essential growth component for archaea. The higher the accessibility of nutrients and gas to microbes, the more populous the reactor and the more efficient the system could be in improving methane yields. Microbial environmental conditions are closely related to the k_La factor which defines the consumable H_2 availability within the liquid [15], [49].

Table 2.3: Growth media of methanogenic archaea in literature.

Schill N. *et al.* (1996) [47]		Jean-Paul Peillex *et al.* (1988) [49]		Nishimura *et al.* (1991) [15]		M. Voelklein *et al.*(2019) [11]		L. Rachbauer *et al.* (2016) [50]	
(g/L[a])		(g/L)		(g/L dist. H_2O)		(g/L dist. H_2O)		(g/L)	
Na_2SeO_3	1.73×10^{-4}					Na_2SeO_3	5×10^{-3}	Na_2SeO_3	1.26×10^{-4}
Na2W04	2.94×10^{-3}								
NaCl	58.4×10^{-0}	NaCl	40×10^{0}	NaCl	6.1×10^{-1}	NaCl	6.1×10^{-1}	NaCl	300.0×10^{-3}
NH_4Cl	6.419×10^{0}	NH_4Cl	2.5×10^{-1}	NH_4Cl	1×10^{0}	NH_4Cl	1×10^{0}	NH_4Cl	300.0×10^{-3}
Nitrilotriacetic acid (NTA)	2.29×10^{-1}								
$MgCl_2.7H_2O$	2.21×10^{-1}	$MgCl_2 .2H_2O$	2.75×10^{0}					$MgCl_2 \times 6H_2O$	100.0×10^{-3}
KH_2PO_4	1.361×10^{0}	KH_2PO_4	3×10^{-1}	KH_2PO_4	3×10^{-1}	KH_2PO_4	3×10^{-1}	KH_2PO_4	408.0×10^{-3}
$CoCl_2$	3.25×10^{-4}					$CoCl_2 \times 6H_2O$	5×10^{-3}	$CoCl_2 \times 6H_2O$	1.0×10^{-3}
Na_2MoO_4	5.15×10^{-4}								
$NiCl_2$	6.48×10^{-4}							$NiCl_2 \times 6H_2O$	3×10^{-4}
$FeSO_4.7H_2O$	5.56×10^{-2}								
		$Fe(NH_4)_2(SO_4)_2$	2×10^{-3}	$(NH_4)_2SO_4$	3×10^{-1}	$(NH_4)_2SO_4$	3×10^{-1}		
		KCl	3.4×10^{-1}						
		$CaCl_2 .2H_2O$	1.4×10^{-1}					$CaCl_2 \times 2H_2O$	110.0×10^{-3}
		$MgSO_4 .7H_2O$	3.45×10^{0}	$MgSO_4.7H_20$	1.6×10^{-1}	$MgSO_4.7H_20$	1.6×10^{-1}		
				Resazurin	1×10^{-3}				
								$Na_2S \times 9H_2O$	360.3×10^{-3}
				$CaCl_2.2H_20$	8×10^{-3}				
				$FeSO_4.7H_2O$	3×10^{-3}				
		K_2HPO_4	3×10^{-1}						
		$NaHCO_3$	5×10^{0}					Na_2HPO_4	426.0×10^{-3}
		Trace minerals soln.	10×10^{0}						
		Vitamins solution	10×10^{0}						
		Yeast extract	2×10^{0}						
		Trypticase	2×10^{0}						
								conc. HCl	1.0×10^{-3}
								H_3BO_3	5×10^{-5}
								$ZnCl_2$	7×10^{-5}
								$CuCl_2 \times 2H_2O$	5×10^{-5}
								$MnCl_2 \times 4H_2O$	2.0×10^{-3}
						$H_{24}Mo_7N_6O_{24} \times 4H_2O$	5×10^{-3}	$(NH_4)_6Mo_7O_{24} \times 4H_2O$	1×10^{-5}
								$AlCl_3 \times 6H_2O$	9×10^{-5}
								EDTA (Disodium salt)	1.0×10^{-3}
						$FeCL_3 \times 6H_2O$	5×10^{-5}	$FeCl_2 X 4H_2O$	2.0×10^{-3}
						$Cl_2Ni \times 6H_2O$	5×10^{-3}		

[a] Assumed per Litre of water as not specified by the author. Originally in mM/µM.

Table 2.4: DSMZ nutrient media for the Methanothermobacter genus (141. for Defluvii and thermoflexus) (119. for Crinale, Marburgensis, Tenebrarum, Thermoautotrophicus, Thermophilus, wolfeii)

141. METHANOGENIUM MEDIUM (/L dist. H_2O)			119. METHANOBACTERIUM MEDIUM (/L dist. H_2O)		
KCl	3.40×10^{-1}	g	KH_2PO_4	5.38×10^{-1}	g
$MgCl_2 \times 6\ H_2O$	4.00×10^{0}	g			
$MgSO_4 \times 7\ H_2O$	3.45×10^{0}	g	$MgSO_4 \times 7\ H_2O$	4.30×10^{-1}	g
NH_4Cl	2.50×10^{-1}	g	NH_4Cl	4.30×10^{-1}	g
$CaCl_2 \times 2\ H_2O$	1.40×10^{-1}	g	CaCl2 x 2 H_2O	5.38×10^{-2}	g
K_2HPO_4	1.40×10^{-1}	g			
NaCl	1.80×10^{1}	g	NaCl	4.30×10^{-1}	g
Trace element solution	1.00×10^{1}	ml	Trace element solution SL-10	1.08×10^{0}	ml
$Fe(NH_4)_2(SO_4)_2 \times 6\ H_2O$ solution	2.00×10^{0}	ml			
Na-acetate	1.00×10^{0}	g	Na-acetate	1.08×10^{0}	g
Yeast extract (OXOID)	2.00×10^{0}	g	Yeast extract (OXOID)	1.08×10^{0}	g
Trypticase peptone (BD BBL)	2.00×10^{0}	g			
Na-resazurin solution (0.1% w/v)	5.00×10^{-1}	ml	Na-resazurin solution (0.1% w/v)	5.38×10^{-1}	ml
$NaHCO_3$	5.00×10^{0}	g	$NaHCO_3$	4.30×10^{0}	g
Vitamin solution	1.00×10^{1}	ml			
L-Cysteine-HCl x H_2O	5.00×10^{-1}	g	L-Cysteine-HCl x H_2O	5.38×10^{-1}	g
$Na_2S \times 9\ H_2O$	5.00×10^{-1}	g	$Na_2S \times 9\ H_2O$	5.38×10^{-1}	g
			Fatty acid mixture	2.15×10^{1}	ml
			Na-formate	2.15×10^{0}	g
			Sludge fluid	5.38×10^{1}	ml
			$FeSO_4 \times 7\ H_2O$ solution (0.1% w/v in 0.1 N H_2SO4)	2.15×10^{0}	ml
			KH_2PO_4	5.38×10^{-1}	g

2.2.4 Process Conditions

2.2.4.1 Pressure

Pressure plays a key role in the increase of methanation levels [51]. The higher the molecular volume of gases such as H_2 in a fixed volume the higher the gas solubility. The greater the number of H_2 molecules interacting with the gas-liquid interface the greater the interphase contact. As stated by Henry, water under pressure of one, two or more atmospheres, absorbs a quantity of two, three or more volumes of gas that are absorbed under normal atmospheric pressure [52].

Increased pressure gives better gas diffusion rates due to an elevated concentration gradient across the gas and liquid phases. Hydrogenotrophic methanogenic archaea are resistant to extreme pressures of over 100 atmospheres and exhibit improved growth and methanogenesis rates at higher pressures [53]. Many studies have managed to optimise the archaeal growth and activity within systems but are restricted by the gas to liquid transfer

limitations. Most commonly, pressure is increased to mitigate this issue, allowing higher gas-liquid mass transfer rates, with minimal alteration to systems.

2.2.4.2 Temperature

Many studies on the effect of temperature (mesophilic and thermophilic) on archaea in AD can be found in the literature [39], [54], [55]. The effect of temperature relates to two important aspects of biological methanation: the archaea growth rate and dissolution temperature dependence. To achieve optimum temperatures for thermophilic Methanothermobacters, temperature ranges of 55-65°C (35-40°C for mesophilic archaea) are required as outlined in Table 2.2. The temperature dependence of mass transfer flowrate into the liquid is also seen in Equation 2.2 through Henry's law constant for H_2. As stated by Henry, under isothermal and isobaric conditions, water takes up the same volume of gas [52]. Most studies examining the temperature effects on anaerobic microbes showed that as the operational temperature is lowered, the maximum specific growth rates of archaea and substrate uptake rate decrease [56]. Temperature variations alter the physical and chemical characteristics of reactor liquors such as viscosity. The solubility of gases also increases with lower temperatures, giving higher diffusivity levels for CH_4, CO_2 and H_2 at lower temperatures. This would also mean higher CO_2 diffusion and result in lower pH, whereas in the case of biomethanation, the dissolution of H_2 leads to a pH increase [57]. Diffusivity and temperature can be correlated as per Equation 2.2;

$$\frac{D_L \mu}{T} = Constant \qquad \text{Equation 2.2}$$

Where D_L is the diffusivity of the solute at infinite dilution (cm^2/s), μ is the viscosity of the solution, and T is the absolute temperature (K). Diffusivity, temperature and solution viscosity affect one another, also affecting the k_La variable. This means that k_La is unique for each reactor setup and is highly sensitive to the environment created for BHM. This is further discussed in Section 2.2.5.1.

2.2.5 Biological Hydrogen Methanation systems: A comparison

A comparison of the different types of systems used for BHM is presented. Various systems are compared using available key performance metrics. Calculations of these performance metrics are defined in the following sub-sections.

2.2.5.1 Key Operational Parameters – k_La – Volumetric gas-liquid mass transfer coefficient

The theory of interphase mass transfer in biological processes is well-defined, however, the application of these theories has mainly focused on oxygen transfer in the aerobic processes of wastewater treatment. In an anaerobic process, multiple gases are produced and consumed, rendering standard estimation methods challenging and/or unreliable. The volumetric gas-liquid mass transfer coefficient (k_La)(also referred to as the absorption coefficient) is frequently mentioned throughout BHM literature, but k_La is rarely obtained from experimental reactors [58],[59]. While this data is scarce in the literature, it is crucial in allowing for the determination of the efficiency of a reactor system, and cross-system performance comparisons. k_La indicates the system's ability to diffuse specific gases into a

liquid. Relying on multiple parameters, k_La is unique for a given reactor configuration and operating conditions.

The gas-liquid mass transfer rate is widely acknowledged as being the key to elevating the H_2 upgrading rate through mixing and other forms of dissolution. Equation 2.3 describes the gas-liquid mass transfer rate relationship.

$$r_t = 22.4\ k_L a\left(H_{2g} - H_{2l}\right) \quad \text{Equation 2.3}$$

Where; r_t *(L/L/h)* is the gas-liquid transfer rate; *22.4* is the molar volume; k_La *(/h)* is the gas transfer coefficient; H_{2g} (mol/L) is the H_2 concentration in the gas phase; H_{2l} (mol/L) is the H_2 concentration in the liquid phase.

Within this, k_La is a key coefficient, comprised of two other coefficients [60]:

k_L: The "film" coefficient, a function of the nature of the gas and the physiochemical properties of the liquid phase (m/h) [61].

a: The specific area of the interface per unit volume of liquid in the reactor (/m).

While carrying out experiments, it is key to determine k_La for H_2, CO_2 and CH_4; H_2 being the most important due to the necessity of the gas for biological methanation, and its inherent poor solubility. This data is scarce in the literature, but some studies have investigated similar concepts [15], [49], [59], [62].

k_La can be adjusted by changing parameters such as mixing speed, gas recirculation and H_2 diffusion devices [17],[42], [62],[63]. To accurately approximate k_La and the resulting mass transfer rates, the factor relies on specific experimental data being collected. The most complex data to collect is the mass transfer of H_2 from the gas to the liquid phase ($\dot{m}_{H2,\ G\ ->\ L}$). Often studies have omitted the collection of this data due to complex procedures in its determination. Work by Díaz *et al.* described the acquisition and presentation of the k_La value [59], [62]. Older sources for k_La include works by Peillex *et al.* that presented a large set of values, which were attributed to the high mixing speeds of Straight Edge and Rushton Impellers, at rates of 300-1200rpm [49], [64]. Research by Nishimura *et al.*, also elucidated the importance of k_La, being directly proportional to the gas produced, as well as the dependence of archaeal growth on the transfer of H_2 gas to the liquid phase [65].

2.2.5.2 Key Operational Parameters – Retention Time

Retention time, also known as residence time relates to the amount of time a gas spends within the system. The lower the retention time, the more compact a system is achieved due to the shorter travel path of gases within the reactor system. Numerous papers have not presented actual retention time data. As per Voelklein *et al.*, Equation 2.4 was used to estimate the values based on available literature data [11]. The equation utilises the averaging of volumes of gas entering and leaving the reactor system. This includes flows for CO_2, H_2 and CH_4. The equation deviates noticeably with retention times extending 50 h when compared to literature-stated values. As a result, care must be taken when working with estimated retention times.

$$RT = \frac{V_R}{(F_{gas\ in} + F_{gas\ out})/2}$$ Equation 2.4

Where:

RT is the retention time (unit time); V_R is the reactor volume (L); $F_{gas,\ out}$ is the volumetric flowrate of gases leaving the reactor (L/unit time); $F_{gas,\ in}$ is the volumetric flowrate of gases entering the reactor (L/ unit time).

2.2.5.3 Key Operational Parameters – MER

Methane evolution rate (MER) is a crucial and simple method in calculating system performance. This data relates the volume of methane produced by a unit volume of a working reactor. MER is presented in much of the literature. Some papers have also presented values such as gas throughput, which allows for the calculation of MER. Where this was the case, manipulation of Equation 2.5 was required.

$$MER = \frac{F_{CH_4,out} - F_{CH_4,in}}{V_R}$$ Equation 2.5

Where: MER is the methane evolution rate (L/L_{vr}/day); $F_{CH4,\ out}$ is the volumetric CH_4 flowrate leaving the reactor (L/day); $F_{CH4,\ in}$ is the volumetric CH_4 flowrate entering the reactor (L/day); V_R is the reactor volume (L)

2.2.6 Reactor Systems: A comparison

2.2.6.1 Continuously Stirred Tank Reactors (CSTRs)

CSTRs are the most common type of reactor used in AD, consisting of a cylindrical reactor space. As per the name, the reactors are continuously stirred by a set of impellers or by recirculation of reactor contents which keep the reactor content homogeneous and in motion. Agitation-oriented diffusion has proven to be amongst the most effective ways to enable hydrogenotrophic methanogenic archaea to come in contact with H_2 [15], [26], [35], [64]. MER ranges from experimental data of 0.86 L CH_4/L_{vr}/day, up to industry-ready 800 L CH_4/L_{vr}/day at grid injection purity (>95% CH_4 v/v) can be found across literature and industry (Table 2.5). Gas retention and interface area are maximised through the reduction of bubble diameter, usually achieved through intensive mixing. CSTRs prove to be the most effective in doing this when exceeding 1200 rpm. However, at such high speeds, high energy consumption can lead to a negative energy balance.

Reduction of bubble diameter is achieved when bubbles break apart due to surface tension forces of the bubble interface being overcome by a higher power density. CSTR systems depend on high impeller rotational speeds to increase gas diffusivity. While this is an effective method of increasing the volumetric gas-liquid mass transfer coefficient (k_La), the energy demand of impeller agitation, such as Rushton impellers, results in significant energy consumption by the system, often rendering the process inefficient [62]. An issue that arises with the Rushton Impellers is they are effective only in the vertical column they occupy. Scale-up would require reactor systems to have a large height-to-width ratio. This was elucidated by Savvas *et al.*, where a 2L reactor with a Rushton impeller at 1200rpm had a parasitic energy demand of 7% [66]. Scaling up of the 2L reactor to 5L showed a 90%

parasitic energy demand of the total energy generated. Due to the turbulent nature of stirring gas-liquid contactors, power usage by the impellers is obtained using Equation 2.6.

$$P = P_0 \, \rho N^3 D^5 \qquad \text{Equation 2.6}$$

Where: P_0 is the power number, depending on the structural characteristic of the mixing system (geometry); ρ is the fluid density; N is the angular velocity of the impeller; D is the diameter of the impeller.

Increasing the reactor radius results in a significant increase in mixing power consumption (parasitic energy demand) as the impeller power consumption increases proportionally to the diameter raised to the power of 5, as evident in Equation 2.6. This shows the importance of the geometry of impellers also playing a crucial role in reactor performance.

The effect of high shear force exertion due to the impeller has also been raised. Such shear forces form when liquids move at different velocities. Due to the nature of impellers, the velocity by the impeller tip will be larger than that near the centre. While no clear inhibitions can be deduced as of yet, cell damage may be a possibility due to high shear forces. Cases have shown syntrophic interaction across groups to be limited by shear forces in CSTRs [67]. Some studies have exhibited upper limits for mixing speeds, where biogas production declines [68]. A comparison of the performance indicators of CSTR reactors used in BHM systems is shown in Table 2.5. Only a few reactor configurations achieve a grid injection-level gas quality. These systems are either achieving this by sacrificing higher MER for high gas purity, such as Luo and Angelidaki while also utilising extended retention times for the purity of gas [69]. Other reactors such as those by Peillex *et al.*, or “Electrochaea GmbH” achieve high purity by using high mixing rates, elevated pressures and pure strain archaea cultures [26],[49].

Table 2.5: Comparison of CSTR BHM throughout literature.

type	Reactor Configuration	pH	H_2	CO_2	H_2/CO_2 Ratio	CH_4 out	Pressure	Temp.	Reactor Vol.	MER	Retention Time	k_La	Method of k_La Increase	Rate of mixing		Gas recirculation	Enriched Culture	Archaeal strain	Unit normalised to	Author
	(in/ex-situ)		(L/L_{vr}/min)	(L/L_{vr}/min)		(%)	(BarG)	(°C)	(L)	(L CH_4 /L_{vr}/day)	h	/h		(L/min)	(rpm)	(L/min)	(y/n)		(STP/NTP/NA)	
CSTR	Ex-situ	6.8	0.30	0.08	4 : 1	2	0	60	16	33.3	0.051		Agitator	-	1000	0	Yes	M. Thermoautotrophicus	STP	[16]
CSTR	Ex-situ	6.85	0.23	0.06	4 : 1	65	0.75	65	10	75.3	0.090		Agitator	-	1500	0	Yes	M. Marburgensis	STP	[35]
CSTR	Ex-situ	6.85	0.34	0.09	4 : 1	58	0.75	65	10	107.5	0.059		Agitator	-	1500	0	Yes	M. Marburgensis	STP	[35]
CSTR	Ex-situ	6.85	0.58	0.14	4 : 1	22	0.75	65	10	123.6	0.030		Agitator	-	1500	0	Yes	M. Marburgensis	STP	[35]
CSTR	Ex-situ	6.85	1.40	0.35	4 : 1	30	5	65	10	344.1	0.013		Agitator	-	1500	0	Yes	M. Marburgensis	STP	[35]
CSTR	Ex-situ	6.85	0.40	0.10	4 : 1	80	5	65	10	137.1	0.054		Agitator	-	1500	0	Yes	M. Marburgensis	STP	[35]
CSTR	Ex-situ	-	0.89	0.22	4 : 1	99	8.5	62.5	3750	800	0.050		Agitator	-	N/A	0	Yes	Patented Strain		[26], [70], [71]
CSTR	In-situ	7.8	0.0013	0.0003	4 : 1	94	1.5	55	1	0.5	8	7	Agitator	-	500	0	Yes	-	STP	[69]
CSTR	In-situ	7.8	0.0025	0.0006	4 : 1	95	1.5	55	1	0.9	4	11	Agitator	-	500	0	Yes	-	STP	[69]
CSTR	In-situ	7.8	0.01	0.0013	4 : 1	90	1.5	55	1	1.6	2	20	Agitator	-	500	0	Yes	-	STP	[69]
CSTR	In-situ	7.8	0.01	0.0013	4 : 1	94	1.5	55	1	1.6	2	21	Agitator	-	800	0	Yes	-	STP	[69]
CSTR	In-situ	7.8	0.01	0.0025	4 : 1	91	1.5	55	1	3.2	1	40	Agitator	-	800	0	Yes	-	STP	[69]
CSTR	Ex-situ	7.4	1.60	0.40	4 : 1	18	0	65	1	300.0	0.011		Agitator	-	1300	0	No	M. Thermoautotrophicus	N/A	[15]
CSTR	Ex-situ	7.4	1.60	0.40	4 : 1	9	0	65	1	194.4	0.010		Agitator	-	1300	0	No	M. Thermoautotrophicus	N/A	[15]
CSTR	Ex-situ	6.85	0.03	0.01	4 : 1	85	0	60	3.5	9.9	0.760		Agitator	-	700	0	Yes	M. Thermoautotrophicus	N/A	[72]
CSTR	Ex-situ	6.85	0.06	0.014	4 : 1	64	0	60	3.5	18.5	0.364		Agitator	-	700	0	Yes	M. Thermoautotrophicus	N/A	[72]
CSTR	Ex-situ	6.85	0.11	0.03	4 : 1	49	0	60	3.5	34.0	0.174		Agitator	-	700	0	Yes	M. Thermoautotrophicus	N/A	[72]
CSTR	Ex-situ	6.85	0.23	0.06	4 : 1	22	0	60	3.5	47.9	0.076		Agitator	-	700	0	Yes	M. Thermoautotrophicus	N/A	[72]
CSTR	Ex-situ	6.85	0.46	0.11	4 : 1	6	0	60	3.5	40.4	0.032		Agitator	-	700	0	Yes	M. Thermoautotrophicus	N/A	[72]
CSTR	Ex-situ	6.85	0.17	0.04	4 : 1	42	0.2	60	3	46.9	0.116		Agitator	-	700	0	Yes	M. Thermoautotrophicus	N/A	[72]
CSTR	Ex-situ	7.35	0.33	0.08	4 : 1	17	0.2	60	3	61.2	0.050		Agitator	-	700	0	Yes	M. Thermoautotrophicus	N/A	[72]
CSTR	Ex-situ	7.35	0.67	0.17	4 : 1	7	0.2	60	3	65.7	0.022		Agitator	-	700	0	Yes	M. Thermoautotrophicus	N/A	[72]
CSTR	Ex-situ	7.35	0.13	0.03	4 : 1	45	0.2	60	3	38.6	0.147		Agitator	-	700	0	Yes	M. Thermoautotrophicus	N/A	[72]
CSTR	Ex-situ	6.85	0.27	0.07	4 : 1	18	0.2	60	3	50.4	0.063		Agitator	-	700	0	Yes	M. Thermoautotrophicus	N/A	[72]
CSTR	Ex-situ	6.85	0.53	0.13	4 : 1	5	0.2	60	3	38.4	0.027		Agitator	-	700	0	Yes	M. Thermoautotrophicus	N/A	[72]
CSTR	Ex-situ	6.85	0.07	0.02	4 : 1	74	0.2	60	3	16.1	0.131		Agitator	-	700	0	Yes	M. Thermoautotrophicus	N/A	[72]
CSTR	Ex-situ	6.85	0.13	0.03	4 : 1	63	0.2	60	3	32.7	0.089		Agitator	-	700	0	Yes	M. Thermoautotrophicus	N/A	[72]
CSTR	Ex-situ	6.85	0.53	0.13	4 : 1	13	0.2	60	3	26.4	0.024		Agitator	-	700	0	Yes	M. Thermoautotrophicus	N/A	[72]
CSTR	Ex-situ	7.4	4	1	4 : 1	4	1	65	1	233.3	0.004		Agitator	-	1300	0	Yes	KN-15	STP	[65]
CSTR	Ex-situ	7.4	4	1	4 : 1	9	2	65	1	460.2	0.004		Agitator	-	1300	0	Yes	KN-15	STP	[65]
CSTR	Ex-situ	7.4	4	1	4 : 1	15	3	65	1	688.1	0.004		Agitator	-	1300	0	Yes	KN-15	STP	[65]
CSTR	Ex-situ	6.8	0.52	0.13	4 : 1	42	0	65	1.5	146.7	0.037	1200	Rushton Impeller	-	320	0	Yes	M. Thermoautotrophicus	N/A	[49]
CSTR	Ex-situ	6.8	0.64	0.16	4 : 1	52	0	65	1.5	194.5	0.031	1450	Straight blade	-	320	0	Yes	M. Thermoautotrophicus	N/A	[49]
CSTR	Ex-situ	6.8	1.92	0.48	4 : 1	44	0	65	1.5	551.0	0.010	3550	Straight blade	-	660	0	Yes	M. Thermoautotrophicus	N/A	[49]
CSTR	Ex-situ	6.8	0.54	0.13	4 : 1	24	0	65	1.5	118.1	0.033	1100	Rushton Impeller	-	660	0	Yes	M. Thermoautotrophicus	N/A	[49]
CSTR	Ex-situ	6.8	1.36	0.34	4 : 1	32	0	65	1.5	334.0	0.013	3250	Rushton Impeller	-	1015	0	Yes	M. Thermoautotrophicus	N/A	[49]
CSTR	Ex-situ	6.8	1.68	0.42	4 : 1	40	0	65	1.5	465.3	0.011	3750	Straight blade	-	1015	0	Yes	M. Thermoautotrophicus	N/A	[49]
CSTR	Ex-situ	6.8	0.83	0.21	4 : 1	35	0	65	1.5	219.2	0.023		Straight blade	-	400	0	Yes	M. Thermoautotrophicus	N/A	[49]
CSTR	Ex-situ	6.8	0.83	0.21	4 : 1	76	0	65	1.5	229.0	0.023		Rushton Impeller	-	300	0	Yes	M. Thermoautotrophicus	N/A	[49]
CSTR	Ex-situ	6.8	0.83	0.21	4 : 1	43	0	65	1.5	229.2	0.023		Straight blade	-	490	0	Yes	M. Thermoautotrophicus	N/A	[49]
CSTR	Ex-situ	6.8	0.83	0.21	4 : 1	83	0	65	1.5	249.9	0.024		Rushton Impeller	-	660	0	Yes	M. Thermoautotrophicus	N/A	[49]
CSTR	Ex-situ	6.8	0.83	0.21	4 : 1	52	0	65	1.5	250.4	0.024		Straight blade	-	660	0	Yes	M. Thermoautotrophicus	N/A	[49]
CSTR	Ex-situ	6.8	0.83	0.21	4 : 1	90	0	65	1.5	270.1	0.025		Rushton Impeller	-	900	0	Yes	M. Thermoautotrophicus	N/A	[49]
CSTR	Ex-situ	6.8	0.83	0.21	4 : 1	61	0	65	1.5	271.2	0.025		Straight blade	-	850	0	Yes	M. Thermoautotrophicus	N/A	[49]
CSTR	Ex-situ	6.8	0.83	0.21	4 : 1	97	0	65	1.5	289.8	0.026		Rushton Impeller	-	1200	0	Yes	M. Thermoautotrophicus	N/A	[49]

- Retention time values presented in papers are noted (**Bold**, underlined and *italic*), but where missing, retention time according to Voelklein *et al.*[11] calculated to allow comparison.

2.2.6.2 Diffusion Based Reactors

Diffusion as a phenomenon has been studied extensively, with research moving to micro (ø40-600µm) and nano-bubble (ø500 nm) production at viable levels [61], [73], [74]. These studies outline some of the common issues that must be overcome to achieve this scale of gas diffusion. When looking closer at the bubbles on an individual level, the interface of a bubble is governed by the Young-Laplace Law. The research found on diffusion-based reactors is limited, especially with respect to the determination of optimal diffusion rates. Few papers have studied this method of H_2 solubilisation. To the authors' knowledge, no research has focused on the bubble dynamics of H_2 or CO_2 in an AD or BHM setting. Voelklein *et al.* and Bassani *et al.* are the only papers found to study plate diffuser equipment to any appreciable degree, but microbubble diffusion per se was not achieved [11], [60]. An MER range of 1.05 - 9.1 L CH_4/L_{vr}/day was achieved, but the CH_4 purity was below 95%. Voelklein *et al.* were able to achieve a grid injection purity in terms of CH_4 content but this required a 24-hour batch duration [11]. Luo and Angelidaki achieved an MER of approximately 1.4L/L_{vr}/day and estimated the k_La value, presenting a very low range of 6-16 /h [75]. This is not comparable to other literature, such as that presented by Peillex *et al.* which reached up to 3750 /h [49]. A comparison of the performance indicators of diffusion-based reactors used in BHM systems is shown in Table 2.6.

Currently, it is difficult to portray diffusion as a competitive alternative as these methods are still in their infancy. In theory, the use of microbubble diffusers could be effective in providing a large interference area between gas and archaea, without the need for packing or high energy-demanding mixing, but further experiments need to be undertaken to verify this hypothesis.

Diffusion relies on the quality and type of diffuser used. This determines the dissolution of H_2 into the liquid. When nano-scale bubbles are formed, they exhibit unique properties when compared to standard bubbles. Nano-bubbles are capable of staying suspended in a liquid, remaining in agitation through Brownian motion for extended periods (days), and disappearing due to diffusion of the gaseous content [76]. There are some complications with this however as generation of these nano-bubble types may require considerable energy demand if systems are not optimised properly. Several companies have developed devices which are capable of creating micro bubbles, with the gas flow rates being adequate for research purposes. The current proposed concepts in the industry are:

1. The Swirl-type liquid flow method uses a specially designed chamber, utilising liquids rotating in a whirlpool manner to a narrower outlet [77]. Control of this method is regulated by the supply of gaseous flow rates to the chamber. Patents by H. Ohnari state that the invention is capable of generating micro-bubbles with diameters no larger than 20 µm on an industrial scale [78].
2. The high-pressure dissolution method uses an elaborate system set-up, increasing pressures and temperatures, followed by pressure decreases to stimulate gaseous diffusion into a liquid solute [79].

3. Venturi methods are now commercially available devices, utilising the shearing of bubbles through the circulation of water in a Venturi meter-like flow device. These devices have been studied in depth and bubble diameters are varied by restraining the supply rate of the gas, resulting in a trade-off of gaseous flow rate to bubble diameter.
4. The supersonic vibration method has been a long-established method for increased rates of gaseous dissolution in liquids [80]. Using designs based on a Galton whistle for air vibrations and a 'Langevin sandwich' – comprising of currents passed through special quartz slabs, allowing for sending out ultrasonic vibrations into liquid media.
5. Ultrafine pore diffusion methods utilise specially designed membranes or diffusion devices, utilising nano pore materials (no greater than 1 μm diameter) which are used to pass gas through, generating nanobubbles. These devices can range from ceramic diffusers and hollow fibre membranes to more unique and carbon-based diffusion devices [61], [74], [77].

The different methods of diffusion are used for a variety of services such as aquaponics, sterilization, cleaning, environmental purification, wastewater treatment, and paper manufacture. However, the idea of applying nano-bubble technology for H_2 dissolution, and BHM, to the best of the authors' knowledge, has not been studied. This means a significant gap in the state of the art for BHM is open to investigation as is the viability of nano-bubble diffusion in a BHM environment. Since the system is in its infancy, the reactor topology can be varied to suit the nature of the diffusion method used. This can be carried out by a bubble column-type reactor, or an entirely new concept unique to the method. In literature, a basic, modified CSTR was used, where the stirring mechanism was replaced by a ceramic gas diffuser, covering the base of the reactor. Figure 2.5 was adapted from Voelklein *et al.* [11].

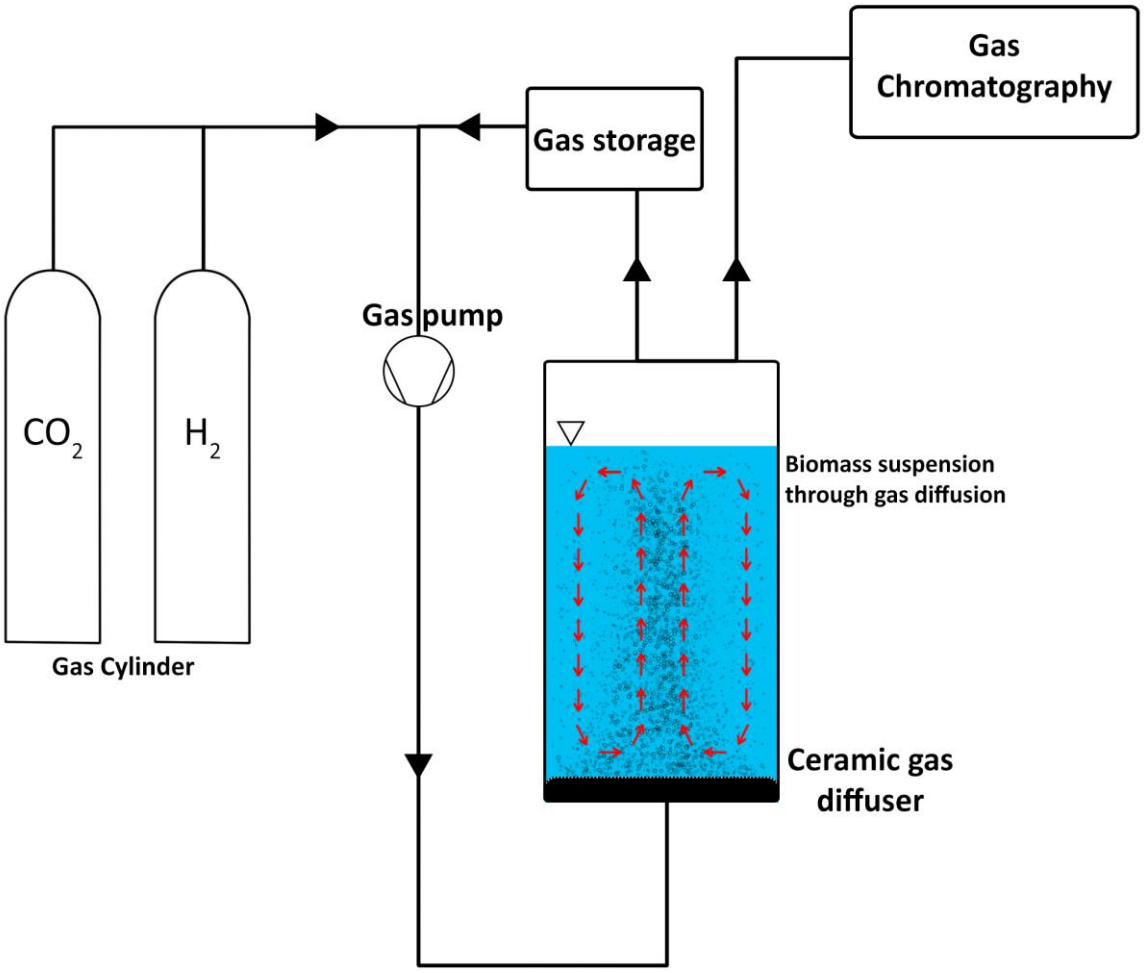


Figure 2.5: Modified CSTR with a ceramic diffuser base.

Other reactor system layouts using diffusion in BHM applications are possible and should be assessed in further work.

Table 2.6: Comparison of diffusion BHM throughout literature.

type	Reactor Config. (in/ex-situ)	pH	H_2 (L/L_{vr}/min)	CO_2 (L/L_{vr}/min)	H_2/CO_2 Ratio	$CH_{4\ out}$ (%)	Pressure (BarG)	Temp. (°C)	Reactor Vol. (L)	MER (L CH_4 /L_{vr}/day)	Retention Time h	k_La /h	Method of k_La Increase	Rate of mixing (L/min)	Rate of mixing (rpm)	Gas recirculation (L/min)	Enriched Culture (y/n)	Archaeal strain	Unit normalised to (STP/NTP/NA)	Author
CSTR	In-situ	7.93	0.0037	0.0009	4 : 1	6	0.2	55	9.5	0.3	24		Fish stone	4	-	4	No	-	STP	[11]
CSTR	Ex-situ	8.2	0.0038	0.0011	3.4 : 1	85	0.2	55	9.5	0.9	1.63		Ceramic Diffuser	4	-	4	No	-	STP	[11]
CSTR	Ex-situ	8.5	0.0051	0.0013	4 : 1	92	0.2	55	9.5	1.7	24		Ceramic Diffuser	4	-	4	No	-	STP	[11]
CSTR	Ex-situ	8.1	0.0095	0.0024	3.9 : 1	61	0.2	55	9.5	1.7	1.14		Ceramic Diffuser	4	-	4	No	-	STP	[11]
CSTR	In-situ	7.97	0.0035	0.0009	4 : 1	32	0.2	55	9.5	1.8	24		Fish stone	4	-	4	No	-	STP	[11]
CSTR	In-situ	8.37	0.0037	0.0009	4 : 1	60	0.2	55	9.5	2.5	24		Fish stone	4	-	4	No	-	STP	[11]
CSTR	Ex-situ	8.1	0.0102	0.0026	4 : 1	49	0.2	55	9.5	2.9	1.99		Ceramic Diffuser	4	-	4	No	-	STP	[11]
CSTR	In-situ	8.5	0.0107	0.0027	4 : 1	96	0.2	55	9.5	3.7	24		Ceramic Diffuser	4	-	4	No	-	STP	[11]
CSTR	Ex-situ	8.2	0.0351	0.0088	4 : 1	23	0.2	55	9.5	5.1	0.41		Ceramic Diffuser	4	-	4	No	-	STP	[11]
CSTR	Ex-situ	7.1	0.0327	0.0082	4 : 1	32	0.2	55	9.5	8.2	0.57		Ceramic Diffuser	4	-	4	No	-	STP	[11]
CSTR	Ex-situ	7.4	0.0509	0.0127	4 : 1	15	0.2	55	9.5	9.1	0.33		Ceramic Diffuser	4	-	4	No	-	STP	[11]
CSTR	In-situ	7.74	0.0022	0.0006	4 : 1	53	0	55	1	1.4	14.42	6.62	Column Diffuser	-	150	0	No	-	STP	[75]
CSTR	In-situ	7.84	0.0012	0.0003	4 : 1	68	0	55	1	1.2	92.37	11.78	Column Diffuser	-	300	0	No	-	STP	[75]
CSTR	In-situ	7.89	0.0021	0.0006	4 : 1	75	0	55	1	1.2	12.11	16.05	Ceramic Diffuser	-	150	0	No	-	STP	[75]

- Retention time values presented in papers are noted (**Bold**, <u>underlined</u> and *italic*), but where missing, retention time according to Voelklein *et al.*[11] calculated to allow comparison.

2.2.6.3 Fixed Film Bioreactors

Fixed film bioreactors are set up where the microbial populations adhere to a packing material within the reactor such that the maximum surface area is achieved. The purpose of this is to force the maximum interference of liquid and gas. Gas is diffused from the reactor bottom and passed through the packing fixed film layer (Figure 2.6). Liquids are recirculated and injected in the bottom of the reactor and are allowed to percolate upwards through the packing film with the aid of the influent gas stream, providing nutrients to the archaea. In some cases, both liquid and gas are recirculated, requiring a liquid/gas separation at a point before pumping [66]. A comparison of fixed film BHM reactors in varied stages of development is shown in Table 2.7.

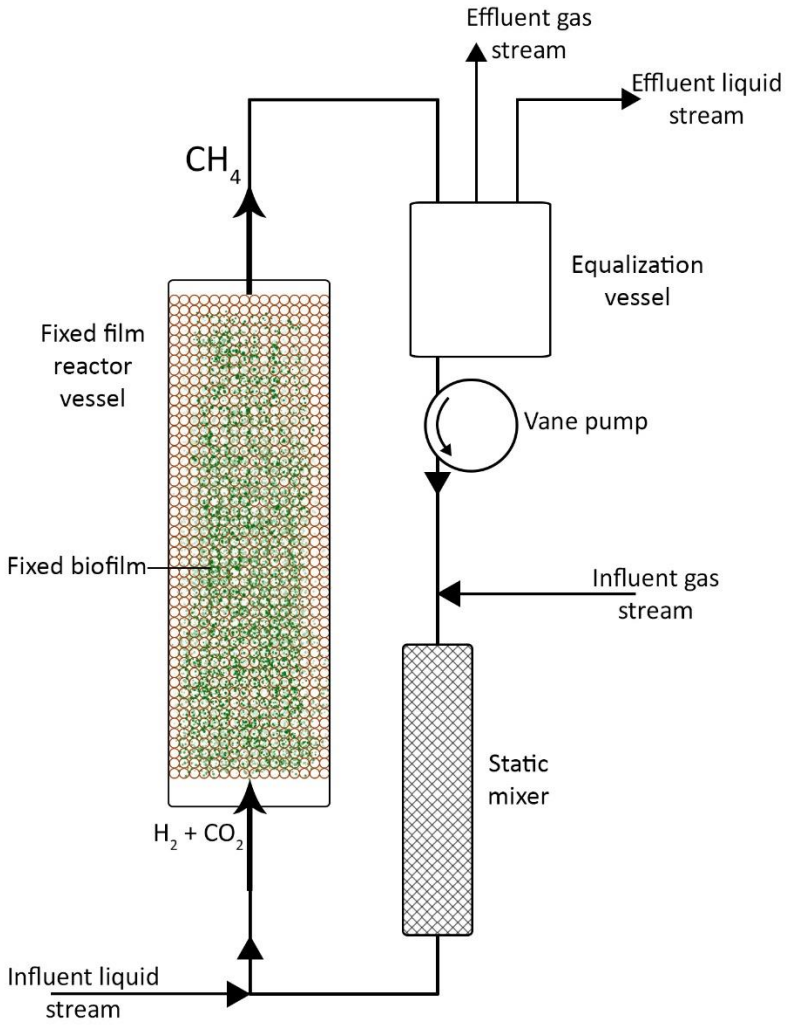


Figure 2.6: Fixed film/Anaerobic Filter and Soil packed reactor layout.

Work by Bassani *et al.* compares the performance of two reactors, one with in-situ BHM and another acting as a control AD reactor [60]. The reactor with in-situ methanation had a lower CH_4 concentration in outlet gas, owing to the presence of unconverted H_2. This is a common issue across the literature as the dissolution of H_2 is the bottleneck for high H_2 conversion rates. Bassani *et al.* highlight a reactor with 'rashig' rings with a CH_4 outlet percentage of 40.4%, where the control AD presents 60.6% [60]. However, the MER rates, of the in-situ and control AD were 1.528 L/L_{vr}/day and 1.350 L/L_{vr}/day, respectively. This highlights the problem encountered by many existing systems, the use of BHM results in the reduction in CH_4 purity leaving the reactor, but the MER is larger than the standard AD process.

This trade-off can be observed in Burkhardt *et al.*, where an 88L reactor system achieved 98-100% CH_4 purity, at a lower MER than that of Bassani *et al.*, 1.2-1.5 L/L_{vr}/day[43], [60]. It is important to observe that the residence time reported by Burkhardt is significantly longer. This also applies to the work by Alitalo *et al.* who depict the reactor's inability to convert the H_2 gas even at large batch retention times of 144 hours [81]. This could be due to a lack of enriched nutrient supply, or lack of pure strain culture use, making high rate methanation difficult to achieve.

Table 2.7: Comparison of Fixed Film reactors in BHM throughout literature.

type	Reactor Configuration (in/ex-situ)	pH	H_2 (L/L_{vr}/min)	CO_2 (L/L_{vr}/min)	H_2/CO_2 Ratio	$CH_{4\ out}$ (%)	Pressure (BarG)	Temp. (°C)	Reactor Vol. (L)	MER (L CH_4 /L_{vr}/day)	Retention Time h	k_La /h	Method of k_La Increase	Rate of mixing (L/min)	(rpm)	Gas recirculation (L/min)	Enriched Culture (y/n)	Archaeal strain	Unit normalised to (STP/NTP/NA)	Author
Biofilm	Ex-situ	-	0.0833	0.0208	4 : 1	90	0	37	0.75	30	0.27		Fixed Film Biomethanation	-	-	0	Yes	-	STP	[66]
Biofilm	Ex-situ	-	0.1278	0.0319	4 : 1	50	0	37	0.75	40	0.16		Fixed Film Biomethanation	-	-	0	Yes	-	STP	[66]
Biofilm	Ex-situ	-	0.0794	0.0199	4 : 1	75	0	37	0.75	27	0.27		Fixed Film Biomethanation	-	-	0	Yes	-	STP	[66]
Biofilm	Ex-situ	-	0.0578	0.0144	4 : 1	97	0	37	0.75	20	0.37		Fixed Film Biomethanation	-	-	0	Yes	-	STP	[66]
UASB	In-situ	8.18	0.0057	0.0014	4 : 1	40	0	55	1.4	1.5	2.82		Rashig Rings	-	-	0	No	-	STP	[60]
UASB	In-situ	8.38	0.0058	0.0015	4 : 1	45	0	55	1.4	1.5	2.76		Rashig Rings	-	-	0	No	-	STP	[60]
UASB	In-situ	8.24	0.0057	0.0014	4 : 1	52	0	55	1.4	1.5	2.83		Ceramic Sponge	-	-	0	No	-	STP	[60]
UASB	In-situ	7.83	0.0054	0.0014	4 : 1	66	0	55	1.4	2.1	3.60		Ceramic Sponge	-	-	0.006	No	-	STP	[60]
UASB	In-situ	7.93	0.0055	0.0014	4 : 1	66	0	55	1.4	1.8	3.18		Ceramic Sponge	-	-	0.006	No	-	STP	[60]
UASB	In-situ	7.9	0.0055	0.0014	4 : 1	68	0	55	1.4	1.8	3.38		Serial Chambers	-	-	0.006	No	-	STP	[60]
UASB	In-situ	7.92	0.0055	0.0014	4 : 1	81	0	55	1.4	1.8	3.29		Single chamber column	-	-	0.004	No	-	STP	[60]
TBR	Ex-situ	7.3	0.0034	0.0008	4 : 1	98-100	0	37	88	1.2	4		Trickle bed/ Packing	-	-	0	Yes	-	STP	[43]
TBR	Ex-situ	7.3	0.0042	0.0010	4 : 1	98	0	37	88	1.5	4		Trickle bed/ Packing	-	-	0	Yes	-	STP	[43]
TBR	Ex-situ	7.5	0.0038	0.0009	4.4 : 1	59	0	37	7.54	1.1	2.9		Packing & liquid spraying	-	-	0	Yes	-	STP	[50]
TBR	Ex-situ	7.5	0.0040	0.0006	6.8 : 1	98	0	37	7.54	0.9	3		Packing & liquid spraying	-	-	0	Yes	-	STP	[50]
TBR	Ex-situ	7.5	0.0038	0.0005	7.1 : 1	97	0	37	7.54	0.8	3.2		Packing & liquid spraying	-	-	0	Yes	-	STP	[50]
AF	Ex-situ	7.4	0.0215	0.0052	4 : 1	15	0	55	0.5	6.7	0.96		Cristobalite PQ10 + Recirculation	0.3	-	0.3	Yes	-	STP	[82]
AF	Ex-situ	6.6	0.0347	0.0087	4 : 1	16	0	65	0.083	127.2	-		Fixed bed reactor	-	-	0	Yes	M. Thermo-autotrophicus	N/A	[83]
AF	Ex-situ	6.6	0.0427	0.0107	4 : 1	58	0	65	0.136	122.7	-		Fixed bed reactor	-	-	0	Yes	M. Thermo-autotrophicus	N/A	[83]
AF	Ex-situ	6.8	0.0138	0.0035	4 : 1	46	0	55	4	4.0	144		Solid packing	-	-	0	No	-	N/A	[81]
AF	Ex-situ	6.9	0.0076	0.0019	4 : 1	26	0	55	4	1.7	144		Solid packing	-	-	0	No	-	N/A	[81]
AF	Ex-situ	6.9	0.0049	0.0012	4 : 1	87	0	55	4	1.7	144		Solid packing	-	-	0	No	-	N/A	[81]

- Retention time values presented in papers are noted (**Bold**, underlined and *italic*), but where missing, retention time according to Voelklein *et al.*[11] calculated to allow comparison.

2.2.6.4 Minimal Liquid Bioreactor

A novel system is presented by Savvas *et al.*, depicted in Figure 2.7 (adapted from Savvas *et al.*) [66]. A hose-like reactor was set up, packed internally, creating a high surface area where archaea lined the path of the gases throughout the length of the hose reactor. The reactor was first aligned vertically (Figure 2.7 rotated 90°) with alternating columns of liquid and gas pockets, due to the rise and fall of coils. The complex travel path allowed for alternating stages of gas-liquid transfer. This allows for a plentiful supply of nutrients to the archaea during the rise (liquid) phase, while a large interface of gas-to-archaea during the descending loop phase. The reactor consists of a 7-metre pipe, in a six-loop configuration, with packing wheels throughout. The reactor was later orientated horizontally, drained of liquid and operated with gas recirculation (Figure 2.7), with pulse (10ml/min) liquid addition for moisture and nutrient provision for the biofilm. The small diameter (13mm) of the reactor allowed the liquid to adhere to the inner surface of the reactor through surface tension forces, allowing for a uniform nutrient dispersal to archaea. The reactor was operated at four different gas loading rates, with a maximum gas throughput of 230 (L/L_{VR}/day) with 50% CH_4 and an MER of 40(L/L_{VR}/day), the highest rate achieved by a fixed film biomethanation system of this scale. As the experimental setup is part of a fixed film system, the data for the experiment are included in Table 2.7. The performance of this system is noteworthy, with MER ranges of 20-39 L CH_4/L_{vr}/day at 98-50% purity respectively. A larger scale operation of this test is required as the experimental reactor volume measured only 0.75L.

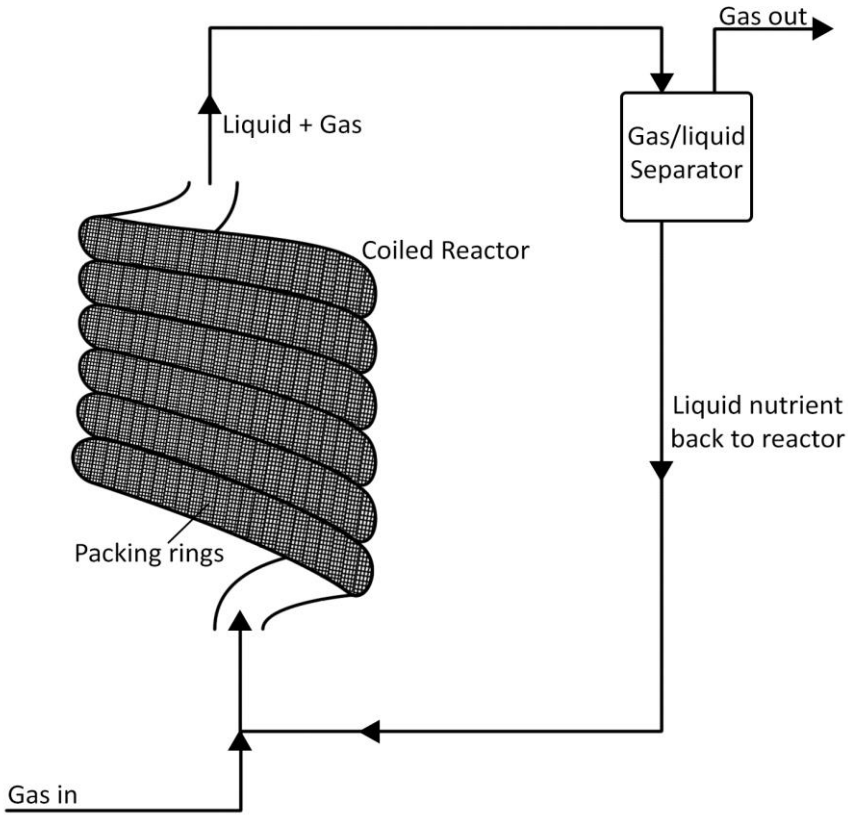


Figure 2.7: A novel BHM system using a tubular reactor setup of narrow diameter pipe and packed fixed biofilm.

2.2.6.5 Soil-based fixed film reactors.

Work conducted by Alitalo *et al.* utilised two solid-state bioreactors configured in series for the BHM of H_2 and CO_2 in a fixed bed reactor [81]. The reactor consisted of a polypropylene pipe with a 75mm diameter and 500mm height, with an effective volume of 4L across both reactors. The bottom 10cm of the reactor was comprised of pebble stones while the remainder was filled with solid support comprised of vermiculite, perlite, wood ash, hydrated cobalt sulfate and hydrated nickel chloride. The specific surface area was 37.44m^2/g. A maximum MER rate of 6.35 L CH_4/L_{vr}/day at a residence time of 144h was achieved. In comparison, Burkhardt *et al.* achieved 1.2 L CH_4/L_{vr}/day at a residence of 4h with a reactor area of 305m^2/m^3, reaching 20% of MER at 3% of the retention time achieved by Alitalo *et al.* [43], [81]. While these reactors did not produce large volumes of CH_4, the use of aerated soil is an interesting and novel alternative to custom, plastic packing. However, an issue with this type of packing may arise due to the settling of soil, formation of paths of least resistance and dead volume. As a result, modern packing may be a more suited option to promote gas dissolution and archaeal distribution.

Jee *et al.* documented a reactor packed with granular diatomaceous earth clay as a granular support material of varied sizes [83]. Tests were carried out with numerous particle sizes, where 2-3mm particle size proved the most productive as a packing material. The diatomaceous earth clay led to a consistent MER of approximately 127 L/L_{vr}/day at 15.5% CH_4 at the outlet. The same clay at 5-6mm diameter facilitates an MER of under 90 L/L_{vr}/day. Using the better-performing packing, the reactor height and volume were increased and operation resumed; methane production peaked at 58% CH_4 purity and an MER of 122.7 L/L_{vr}/day. The purity of the gas however steadily decreased over 160 hours to a low value of 34% CH_4 at the outlet. Jee *et al.* hypothesized the steady decline in gas purity was due to the channelling of substrate flows by the surplus cell biomass, decreasing the interference area between gas and archaea [83]. The paper reports such high MER rates due to the inclusion of microbial strains, enriched culture medium and increased surface area, maximising gas-to-archaea interference. While these results are impressive, the volumes of the reactors were small, at approximately 0.083L and 0.136L. As such, scaling up may yield different results. Due to soil properties, paths of least resistance may form, thus rendering the majority of the soil bed an essentially dead volume. An interesting alteration to this reactor is the injection of gas at the top of the reactor, forcing the gases to be pushed down through the fixed film and exit through the bottom. Traditional systems typically function in the opposite direction. Such a method is possible due to the reactor being primarily soil packed, allowing for gases to pass through the soil packing, as the liquid is not predominant within the reactor space as in traditional systems.

2.2.6.6 Hollow Fibre Reactors (HFR)

Membrane bioreactors are based on specially designed ceramic membranes, typically referred to as hollow fibre membranes. An example of such a system is shown in Figure 2.8 (adapted from Díaz *et al.*) [62]. These provide a barrier between the reactor liquor and gas supply. The fibre membrane comprises many fibres, from which gas is forced through small pores, diffusing straight into the surrounding liquid. This process relies on the porosity of the fibre membranes. Designs range from hydrophilic to hydrophobic, which represent a wide variety of hollow fibre materials. Hydrophilic fibres require the membranes to undergo a process called wetting, with membranes absorbing water into the pores. This process ensures no gas bubbles are present in the membrane before commissioning [84]. While hollow fibre membranes provide instantaneous gas-to-liquid mass transfer, the flow rates of the system are limited due to the porosity and relatively small surface area of these membranes. There are several merits that this system offers; high purity of exit gas, compactness and easier automation [85]. Disadvantages vary from high capital and operation costs from membrane fouling, relating to the build-up of biofilm on the membrane over the system lifespan, decreasing the operational efficiency of the system. A study by Díaz *et al.* demonstrated the utilisation of this system, with significant results achieved [62]. The system produced a MER of 7 L CH_4/L_{vr}/day at 95% H_2 utilisation with a 1h retention time. A noteworthy result was the lack of a biomass film found on the membrane of the module as compared to previous studies. This occurrence is attributed to the high recirculation rates of gas. Other literature setups involving HFR presented yields of 40-50 L CH_4/L_{vr}/day at 25-14% CH_4 purity respectively. A comparison of HFR used in BHM is shown in Table 2.8. Once again, the trade-off between purity and MER is evident as higher throughputs allow for higher MER rates but lower the purity of the exiting gas.

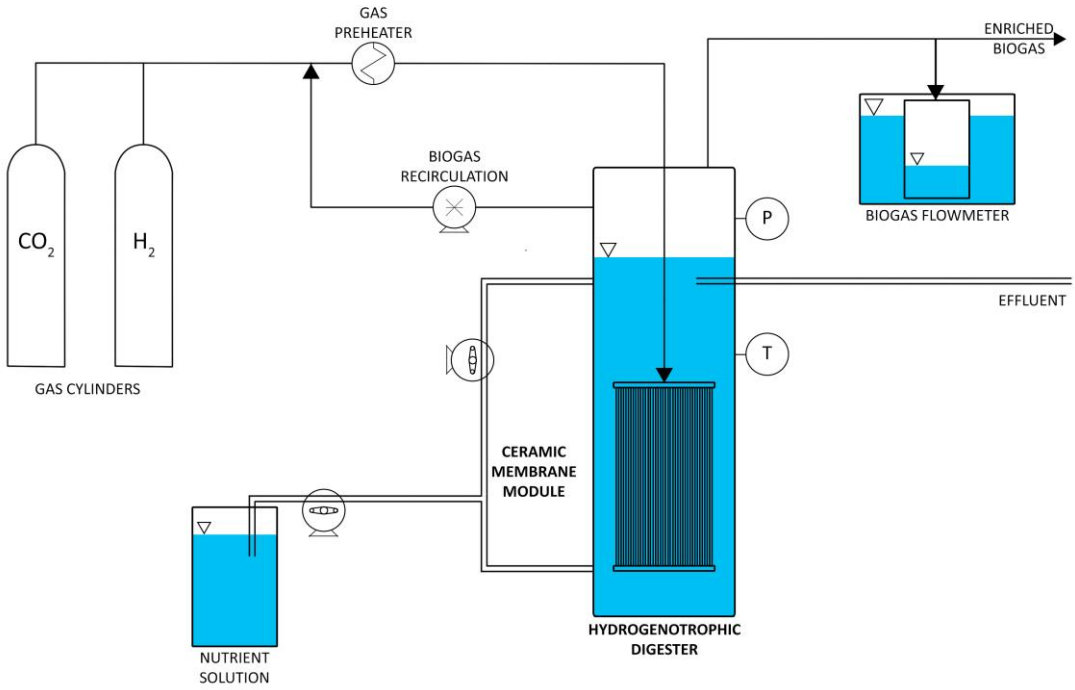


Figure 2.8: Diagram of a membrane bio-reactor experimental set-up.

Table 2.8: Comparison of Hollow membrane reactors in BHM throughout literature.

Type	Reactor Configuration	pH	H_2	CO_2	H_2/CO_2 Ratio	CH_4 out	Pressure	Temp.	Reactor Vol.	MER	Retention Time	k_La	Method of k_La Increase	Rate of mixing		Gas recirculation	Enriched Culture	Archaeal strain	Unit normalised to	Author
	(in/ex-situ)		(L/L_{vr}/min)	(L/L_{vr}/min)		(%)	(BarG)	(°C)	(L)	(L CH_4 /L_{vr}/day)	h	/h		(L/min)	(rpm)	(L/min)	(y/n)			
HFM R	Ex-situ	7.2	0.0070	0.0018	4 : 1	84	0	55	31	2.0	2.80	30	HFM + Recirculation	-	-	0.07	No	-	STP	[62]
HFM R	Ex-situ	7.2	0.0140	0.0035	4 : 1	75	0	55	31	3.8	1.37	155	HFM + Recirculation	-	-	1.12	No	-	STP	[62]
HFM R	Ex-situ	7.2	0.0210	0.0052	4 : 1	68	0	55	31	5.7	0.91	180	HFM + Recirculation	-	-	1.12	No	-	STP	[62]
HFM R	Ex-situ	7.2	0.0210	0.0052	4 : 1	79	0	55	31	6.9	1.01	240	HFM + Recirculation	-	-	1.67	No	-	STP	[62]
HFM R	Ex-situ	7.2	0.0314	0.0078	4 : 1	65	0	55	31	9.5	0.64	420	HFM + Recirculation	-	-	3.35	No	-	STP	[62]
HFM R	Ex-situ	7.2	0.0174	0.0044	4 : 1	82	0	55	31	5.8	1.21	205	HFM + Recirculation	-	-	1.51	No	-	STP	[62]
HFM R	Ex-situ	7.2	0.0279	0.0070	4 : 1	78	0	55	31	8.8	0.74	430	HFM + Recirculation	-	-	3.35	No	-	STP	[62]
HFM R	Ex-situ	7	0.0187	0.0047	4 : 1	25	0	65	0.104	40.3	-		HFM	-	-	0	Yes	M. Thermo-autotrophicus	N/A	[86]
HFM R	Ex-situ	7	0.0320	0.0080	4 : 1	14	0	65	0.104	50.7	-		HFM	-	-	0	Yes	M. Thermo-autotrophicus	N/A	[86]
MBR	Ex-situ	7.4	0.0069	0.0017	4 : 1	79	0	55	60	2.4	3.10	77	Ceramic tubular membrane	-	-	8	No	-	STP	[59]
MBR	Ex-situ	7.4	0.0139	0.0035	4 : 1	55	0	55	60	4.3	1.46	87	Ceramic tubular membrane	-	-	8	No	-	STP	[59]
MBR	Ex-situ	7.4	0.0139	0.0035	4 : 1	79	0	55	60	4.8	1.55	166	Ceramic tubular membrane	-	-	12.3	No	-	STP	[59]
MBR	Ex-situ	7.4	0.0208	0.0052	4 : 1	79	0	55	60	7.1	1.03	268	Ceramic tubular membrane	-	-	12.3	No	-	STP	[59]
HFM R	In-situ	7.61	0.0006	0.0003	4 : 1	78	0.32	55	1	0.9	585.37		Magnetic stirrer	-	150	0	No	-	STP	[75]
HFM R	In-situ	7.9	0.0010	0.0003	4 : 1	90	0.56	55	1	0.9	45.89		Magnetic stirrer	-	150	0	No	-	STP	[75]
HFM R	In-situ	8.31	0.0012	0.0003	4 : 1	96	0.75	55	1	0.9	28.74		Magnetic stirrer	-	150	0	No	-	STP	[75]

- Retention time values presented in papers are noted (**Bold**, underlined and *italic*), but where missing, retention time according to Voelklein *et al.*[11] calculated to allow comparison.

2.2.7 System key parameter comparison

As discussed, systems throughout the literature vary substantially in the capability to achieve a high MER and high purity output gas. The following subsections compare these systems to show the development of each of the technologies, as well as the current state of the art.

2.2.7.1 Comparison of methane evolution rate across reactor systems

Across the systems investigated, MER is a parameter that is shown to vary significantly. Concerning Figure 2.9, the use of CSTRs generates significantly higher MER than the other reactor systems, however, there is a substantial variation in the MER values achieved in the literature. Additionally, it is important to take into account the early development stage of the technologies. From the observation of data in Table 2.5 - Table 2.8, in the presence of microbial strains such as Methanothermobacter thermoautotrophicus the resulting methane production rates are substantially higher. The CSTR technology is the predominant system for the assessment of pure strain cultures. This highlights that even minor improvements to the different BHM systems can cause significant jumps in efficiency as illustrated by the MER. The use of pure cultures is usually omitted due to the additional complications this causes in laboratory-scale experiments.

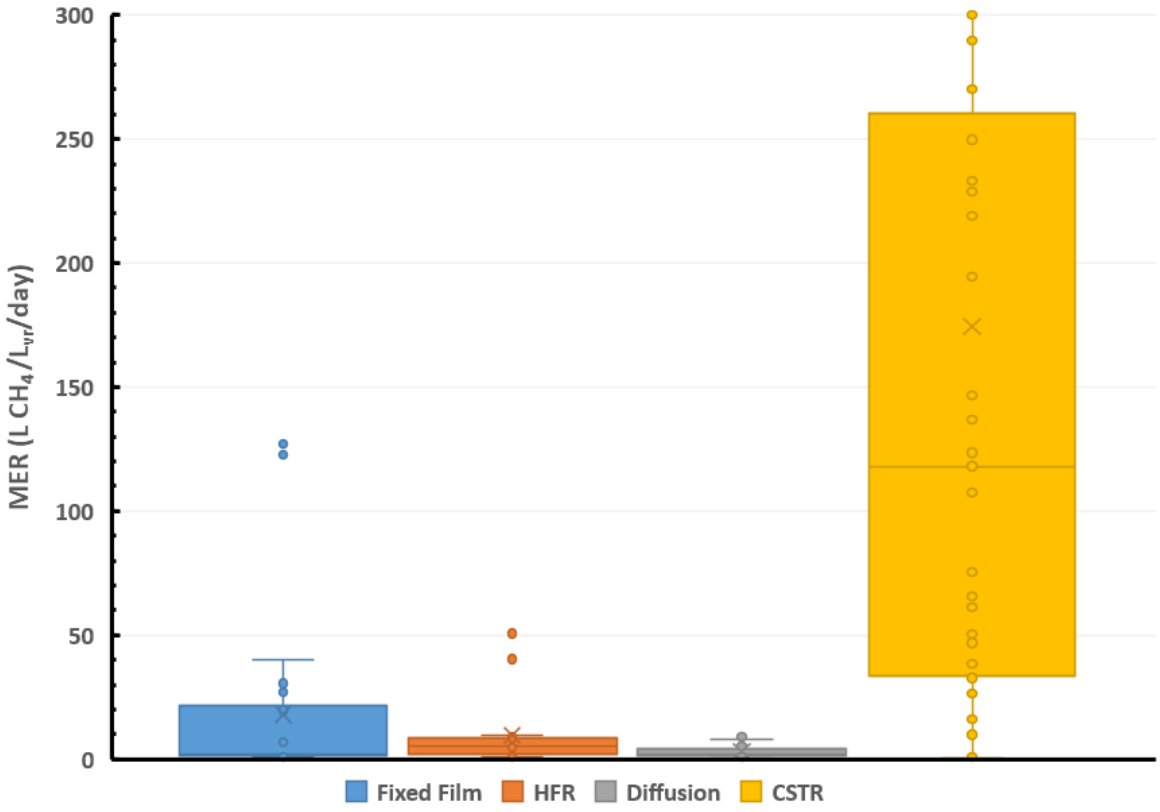


Figure 2.9: Comparison of MER across reactor systems.

2.2.7.2 Comparison of retention time across reactor systems

Figure 2.10 highlights the variations in retention time across reactor systems. Low retention times in BHM systems are indicative of a higher reactor efficiency, suggesting shorter travel paths and, as such, more compact and potentially cheaper systems resulting in more cost-effective renewable gas production. Recirculation is a simple method to prolong these travel paths within a compact system but can also be an indication of the lower performance of a reactor system and earlier development stage. Diffusion-based systems are found to have the highest retention times of the different BHM systems assessed. There was however a significant variation in the retention times. CSTR-based BHM systems typically had the lowest retention times. This highlights the performance of CSTR reactors, and also the more mature state of this reactor system when compared to others assessed.

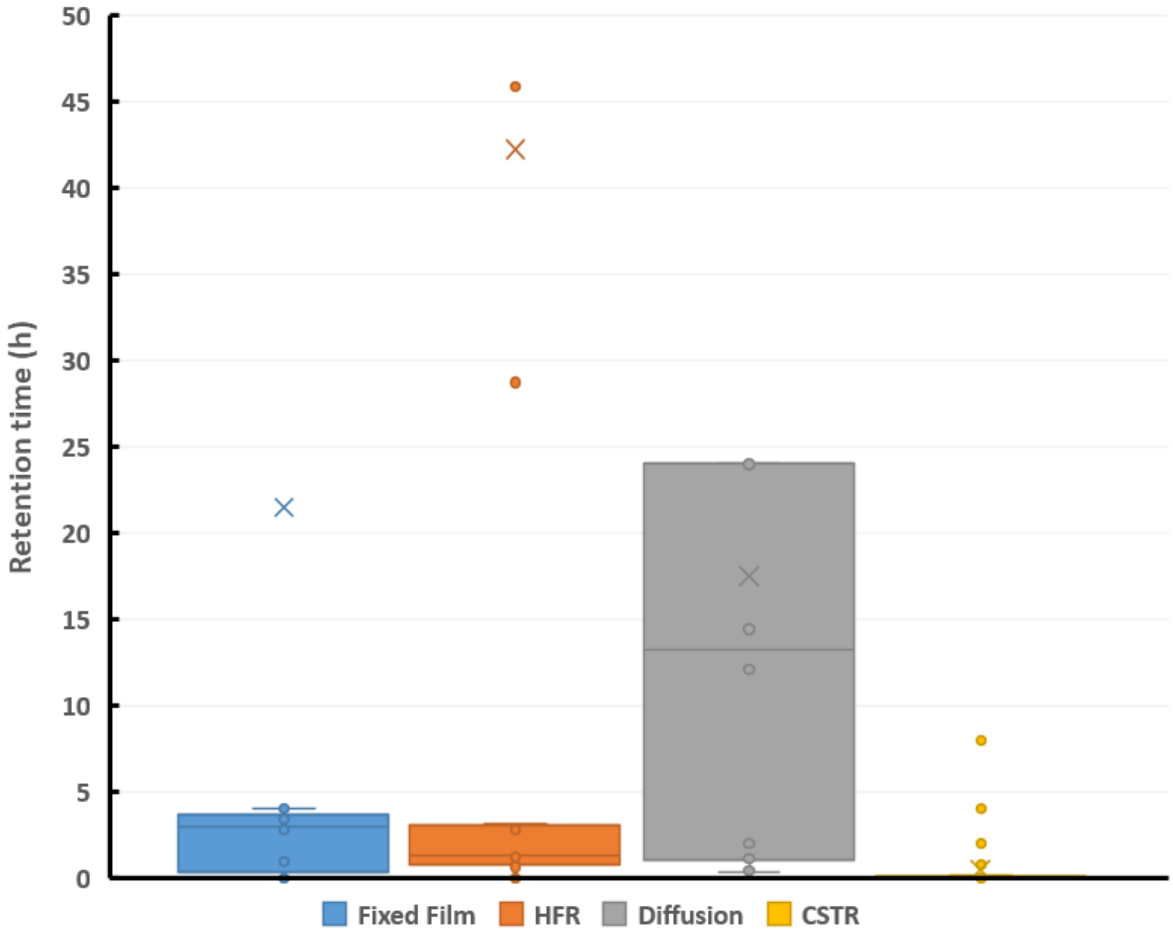


Figure 2.10: Comparison of retention time across reactor systems.

2.2.8 Analysis of the relationship between key operational parameters

As indicated in the analysis and comparisons, a cross-system appraisal is difficult at an experimental level. This is mainly due to the various technology development stages. Most research has focused on the use of CSTRs for BHM since this is the most mature reactor technology, and also the simplest. As a result, a more system-by-system comparison should be carried out across reactor set-ups, irrespective of the system implemented. The following sections seek to compare several parameters collated from the literature.

2.2.8.1 Relationship between retention time and methane evolution rate.

From an analysis of the data compilation in Table 2.5 - Table 2.8, a relationship was sought between methane evolution rate and retention time in the BHM reactors. Upon plotting the data, the relationship, as documented in Figure 2.11 was found. Instead of the expected increase in MER with a longer retention time, the opposite appeared to occur. The authors believe that this is an indication of the system's inefficiency at high retention time, in which gas requires longer residence times to be converted in the reactor system. This relationship suggests that smaller more efficient reactor systems will result in the generation of more cost-effective green gas.

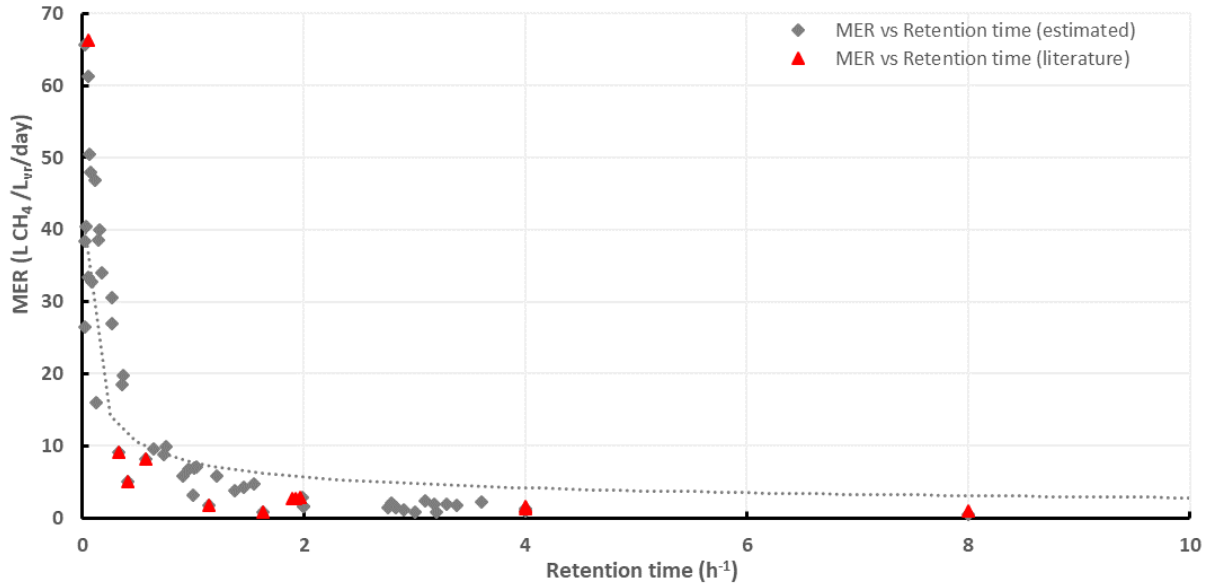


Figure 2.11: Relationship between MER and retention times.

2.2.8.2 Relationship between CH_4 concentration and methane evolution rate

Analysis of the data in Table 2.5-Table 2.8 reveals a weak relationship (Figure 2.12) between CH_4 concentration and MER, a concept supported by Lecker *et al.* [14]. While the relationship is weak, the earlier discussion of higher MER levels resulting in lower CH_4 percentages in the outlet gas supports the existence of this relationship. A conclusion can be made that lower MERs tend to yield higher purity exiting gas. Few studies have been able to maximise the values of these two variables. At a full demonstration scale, “Electrochaea GmbH” was capable of elevating the levels of both of these values, likely due to the refining of the full-scale methanation system, with the use of pure cultures, high agitation rates, high gas throughputs, low retention times and high pressures [26]. Optimal systems with ideal configurations require complex maintenance as imbalances and oversight may lead to reactor contamination and sub-optimal production rates.

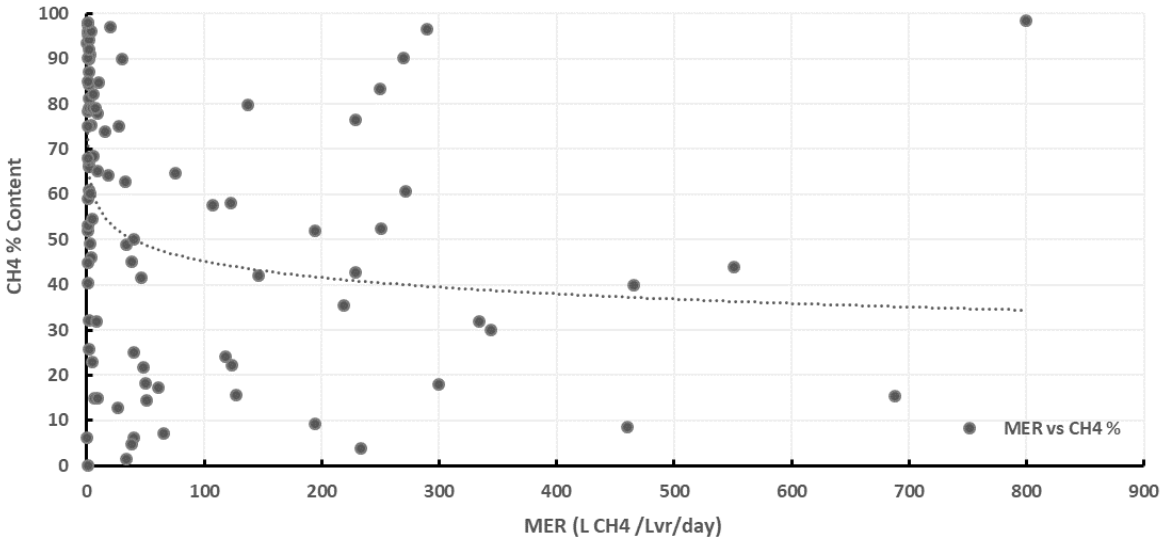


Figure 2.12: Relationship between MER and CH_4 percentage content.

2.2.8.3 Relationship between methane evolution rate and volumetric gas-liquid mass transfer coefficient k_La.

Using available data in the literature on k_La and MER, an exercise was carried out to observe any relationship between the two parameters. The literature data compiled in Table 2.9 allowed for the production of Figure 2.13. A cursory examination shows that there is a relationship between MER and k_La, as expected. Increased MER coincided with increased k_La values. However as outlined previously, data on exact k_La measurement is limited, more data and laboratory research are required to elucidate the exact significance and nature of this relationship.

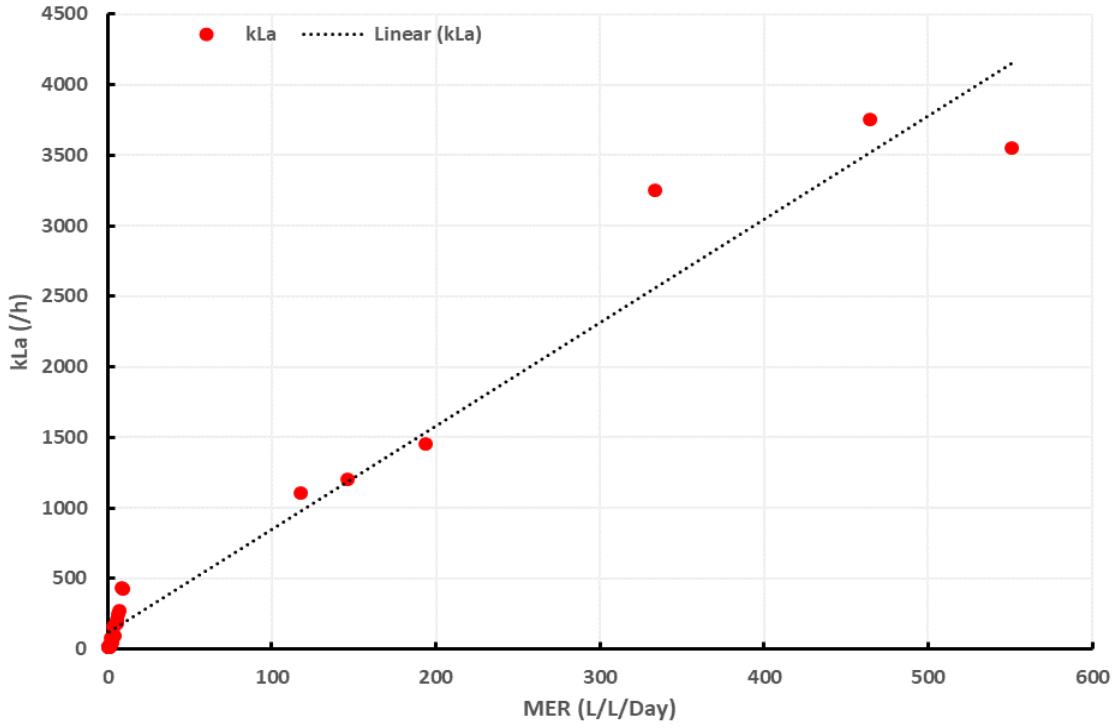


Figure 2.13: Comparison of MER vs k_La data in the literature.

Table 2.9: MER vs k_La comparison.

MER (L CH_4 /L_{vr}/day)	k_La /h	Author
465.3	3750	[49]
551.0	3550	[49]
334.0	3250	[49]
194.5	1450	[49]
146.7	1200	[49]
118.1	1100	[49]
8.8	430	[62]
9.5	420	[62]
7.1	268	[59]
6.9	240	[62]
5.8	205	[62]
5.7	180	[62]
4.8	166	[59]
3.8	155	[62]
4.3	87	[59]
2.4	77	[59]
3.2	39.9	[69]
2.0	30	[62]
1.6	20.5	[69]
1.6	19.9	[69]
1.2	16.1	[75]
1.2	11.8	[75]
0.9	11.4	[69]
0.5	6.8	[69]
1.429	6.62	[75]

2.2.9 A full-scale demonstration plant

To the author's knowledge, “Electrochaea GmbH” is the first full-scale methanation plant. It operates at a full load capacity of 1.502 MW (raw biogas case) in Copenhagen, Denmark. Personal communication with the company and conference presentations indicate MER values of 800 L CH_4/L_{vr}/day, at 99% CH_4 content and estimated gas residence times of 3 minutes [71]. The plant is heated only up to 50°C and the exothermic reaction of archaea brings the reactor temperature up to 60°C. The state-of-the-art plant yields 0.126 MWh_{th} thermal energy (counter-flow heat exchanger) generated from the bioreactor process, 0.544 MWh_{th} in the form of upgraded CO_2 and H_2, and 0.832 MWh_{th} in the form of injected methane contained in the raw biogas. The additional yield equates to a methane yield increase of over 65%. The report proposed scenarios for souring CO_2; purchasing raw biogas (CO_2/CH_4 mixture) from a nearby plant during operational hours, or, using CO_2 obtained from scrubbing raw biogas and injecting it into the upgrading plant along with H_2 for

upgrading. Hydrogen is sourced from an electrolyser on-site which operates during periods of excess electrical energy, capitalising on the availability of 'waste' electricity, based on Denmark's high renewable energy access in the form of wind. This allows for the electrical energy to be stored in gaseous form in the gas grid. Oxygen is also produced in the electrolyser, however, due to the intermittent generation and relatively low financial value of O_2, it is determined that the capture and use of the O_2 is not profitable. However, consideration was made to use the O_2 in the aeration of the nearby wastewater treatment facility. The BHM reactor is designed as a 9m tall CSTR with a 0.72m ID (estimated), with four impellers, mixing at a rapid speed, and gas injection of H_2 and CO_2 at the bottom of the tank. A plant layout schematic is depicted in Figure 2.14. The shear forces exerted by the impellers cause a breakup of bubbles, and subsequent impellers along the height of the reactor ensure the maintenance of small bubble sizes. The reactor operates at 60-65°C and 4-9 bar pressure. Due to the height of the reactor, pressure on the bottom will be 1 barG higher than the top. Industry examples suggest the agitation requires a 1.6 $W/L_{reactor}$, and with an estimated total reactor volume of 3750L, this equates to 5.70kW for CSTR agitation. This matches closely with the industry technical reports [26], [70], [71]. In terms of energy demand, Electrochaea (approximately 0.32 kWh/ Nm^3 raw biogas) is similar to traditional gas purification systems whose energy demand can range significantly (Water scrubber: 0.25-0.3 kWh/Nm^3; Chemical scrubber: 0.05 – 0.15 kWh/Nm^3; Membrane separation: 0.18 – 0.2 kWh/Nm^3; Pressure Swing Absorption 0.23-0.30 kWh/Nm^3; Cryogenic upgrading; 0.76 kWh/Nm^3; Organic physical scrubber: 0.2 – 0.3 kWh/Nm^3).

Biologically, a patented, isolated strain of Methanothermobacter Thermoautotrophicus UC 120910 is used in pure culture. When gases are injected, they undergo screening to ensure no contaminants are brought into the main reactor. Nutrient media is periodically injected. The environment has a pH range of 7-8 and an Oxidation-Reduction Potential (ORP) of 600mV, corresponding to a 0 coliform count per 100ml of water. A Life Cycle Analysis (LCA) baseline performance shows a 75% CO_2 emission reduction compared to fossil fuel-derived natural gas [26]. The reactor is capable of producing grid-quality gas, at pressures greater than 6 barG. The only additional step for grid injection is the removal of water vapour through drying.

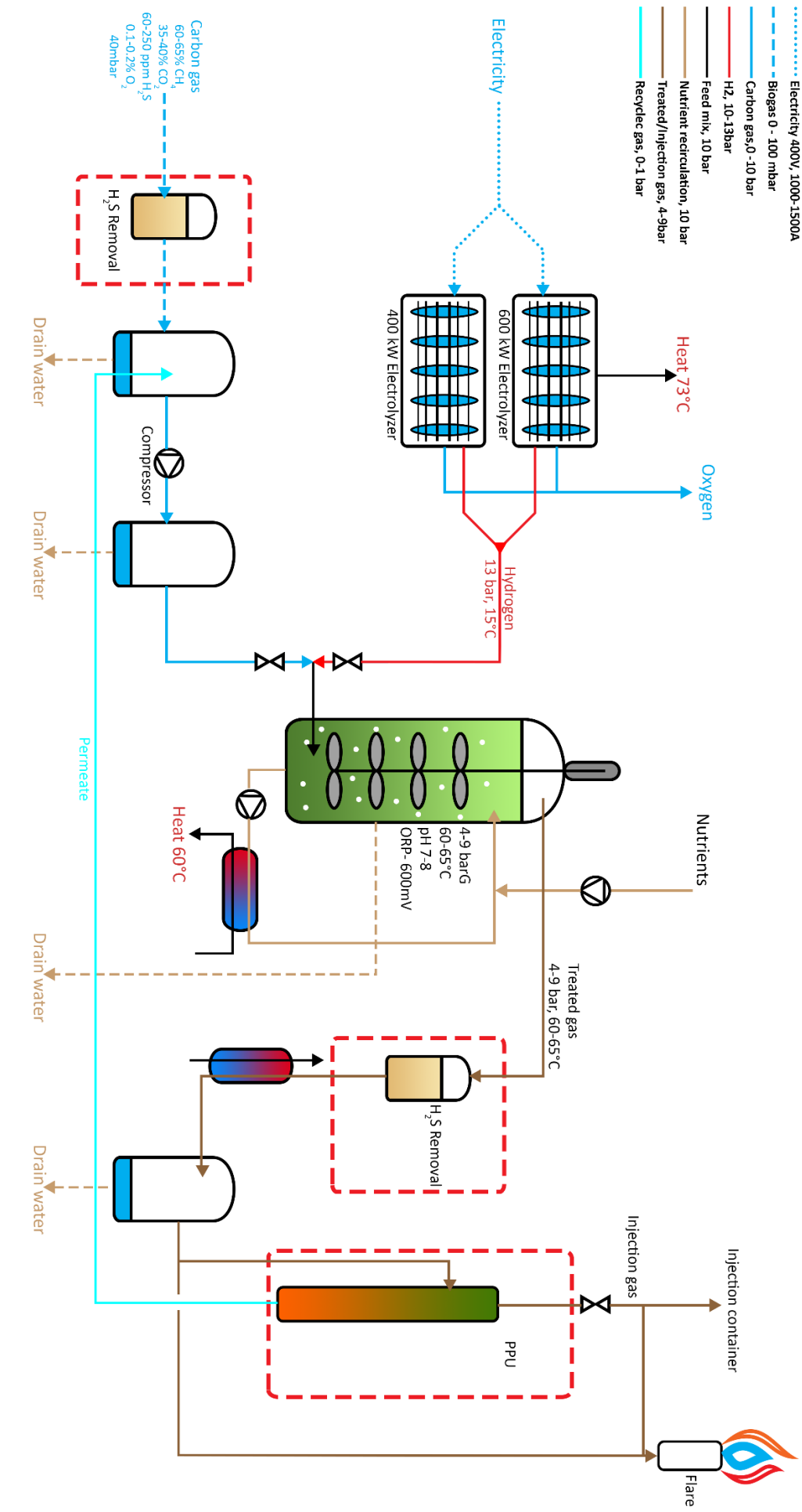


Figure 2.14: Electrochaea plant schematic adapted from the plant technical report [26].

2.2.10 Conclusions

The energy transition will raise dilemmas to challenge future energy systems. One major challenge is energy storage and the matching of energy production with energy demand. Another is, difficult to decarbonise sectors such as haulage. The circular economy combination of hydrogen produced via electrolysis of curtailed/constrained electricity, biogas production from the digestion of organic waste upgraded to gas grid specification through the reaction of biogas and the aforementioned hydrogen provides a decentralised form of energy storage and an energy vector for haulage.

The BHM systems reviewed have challenges. In-situ systems need to prevent complicated inhibition pathways due to hydrogen partial pressures. To produce a financially sustainable green gas ex-situ methanation system, optimisation of methane evolution rate through maximisation of gas transfer rates, while optimising methane content in the produced gas is required. The retention time was viewed as a method of elevating MER rates by extending the travel path of a unit of gas through the upgrading system. While this is a valid option for research, long retention times of gases imply an inefficient system producing expensive green gas. As such, prolonged retention times indicate low efficiency of BHM systems.

The ex-situ technology is at a low technology readiness level. Some literature demonstrates high MER values and high volumetric gas throughput utilising high-rate mixing and agitation (1500rpm), yet the percentage of CH_4 in the outlet gas remains low (15.50%) [15]. The energy demand of high-rate mixing can be substantial [15], [70]. CSTRs appear to be the reactor system most capable of achieving elevated MER. However, this is not indicative of the reactor configuration but rather of system optimisation (such as patented strains of pure culture) that has been carried out with CSTR reactors. As such, novel systems can currently be portrayed as less successful but may have strong benefits in future energy systems if fully optimised. Indeed, it is suggested by the authors that lower MER in recent publications indicate that optimisation has been delayed, as novel reactor systems are studied.

There are evident gaps in the state of the art concerning system efficiency and optimisation. This review has identified that a significant gap may be in the use of diffusion-based technology for H_2 dissolution. More work is required to ascertain where diffusion fits in the bigger picture of BHM. In addition, the lack of research into the solubilisation of H_2 leaves extensive gaps in the state of the art in BHM relating to H_2 diffusion through micro and nano-pore diffusers. Research of the smallest possible bubble diameters achievable in reactor liquors is open to exploration. This would require an investigation of liquor viscosity, shear forces, particulate presence, and chemical effects; and if viable, the application of the learned knowledge on an experimental ex-situ methanation reactor would provide a novel research opportunity. Finally, the development of a method of evaluation of k_La would allow for a more time-efficient method of evaluating k_La, a key reactor performance parameter when compared to laboratory procedures. This may allow for a better comparison between reactor configurations when coupled with MER and retention time.

Acknowledgements

This work was supported by Science Foundation Ireland (SFI) through the MaREI Centre for Energy, Climate and Marine Grant Number 12/RC/2302_P2 and 16/SP/3829 with industrial funding from Gas Networks Ireland through the Green Gas Innovation group. Dr Richard O'Shea recognises the industrial co-funding from Irish Distillers Pernod Ricard.

Conflict of Interest

The authors report no conflict of interest.

List of references

[1] B. Bensmann, R. Hanke-Rauschenbach, I. K. Peña Arias, and K. Sundmacher, "Energetic evaluation of high pressure PEM electrolyzer systems for intermediate storage of renewable energies," *Electrochim. Acta*, vol. 110, pp. 570–580, Nov. 2013.

[2] Sustainable Energy Authority of Ireland (SEAI), "Renewable energy in Ireland 2019 report," 2019.

[3] D. M. Wall, M. Dumont, and J. D. (Ed. . Murphy, *Green gas - Facilitating a future green gas grid through the production of renewable gas*, vol. 2, no. IEA Bioenergy Task 37. 2018.

[4] J. Liebetrau, T. Reinelt, A. Agostini, B. Linke, and J. D. Murphy, *Methane emissions from biogas plants Methods for measurement, results and effect on greenhouse gas balance of electricity produced*, vol. 2. IEA Bioenergy Task 37, 2017, p. 12.

[5] Members of IEA Bioenergy Task 37, *Country report summaries*. 2017.

[6] Energiforsk, "Biogas upgrading - Technical review," Energiforsk, 2016.

[7] I. Angelidaki *et al.*, "Biogas upgrading and utilization: Current status and perspectives," *Biotechnology Advances*, vol. 36, no. 2. Elsevier, pp. 452–466, 01-Mar-2018.

[8] Q. Sun, H. Li, J. Yan, L. Liu, Z. Yu, and X. Yu, "Selection of appropriate biogas upgrading technology-a review of biogas cleaning, upgrading and utilisation," *Renew. Sustain. Energy Rev.*, vol. 51, pp. 521–532, Nov. 2015.

[9] IEA, "Plant Lists - IEA Bioenergy Task 37," *IEA Bioenergy Task 37*, 2014. [Online]. Available: http://www.iea-biogas.net/plant-list.html.

[10] Svenskt Gastekniskt CenterAB, "Biogas upgrading: Review of commercial technologies (SGC Report 270/2013)," 2013.

[11] M. A. Voelklein, D. Rusmanis, and J. D. Murphy, "Biological methanation: Strategies for in-situ and ex-situ upgrading in anaerobic digestion," *Appl. Energy*, vol. 235, pp. 1061–1071, Feb. 2019.

[12] European Parliament, "Directive (EU) 2018/2001 Of The European Parliament and of the council on the promotion of the use of energy from renewable resources (recast)," 2018.

[13] S. McDonagh, R. O'Shea, D. M. Wall, J. P. Deane, and J. D. Murphy, "Modelling of a power-to-gas system to predict the levelised cost of energy of an advanced renewable gaseous transport fuel," *Appl. Energy*, vol. 215, no. January 2018, pp. 444–456, 2018.

[14] B. Lecker, L. Illi, A. Lemmer, and H. Oechsner, "Biological hydrogen methanation – A review," *Bioresour. Technol.*, vol. 245, no. August, pp. 1220–1228, 2017.

[15] N. Nishimura, S. Kitaura, A. Mimura, and Y. Takahara, "Growth of thermophilic methanogen KN-15 on H2-CO2 under batch and continuous conditions," *J. Ferment. Bioeng.*, vol. 72, no. 4, pp. 280–284, Jan. 1991.

[16] E. Gerhard, B. M. Butsch, I. W. Marison, and U. Von Stockar, "Improved growth and methane production conditions for Methanobacterium thermoautotrophicum," *Appl. Microbiol. Biotechnol.*, vol. 40, no. 2–3, pp. 432–437, Nov. 1993.

[17] G. Luo, S. Johansson, K. Boe, L. Xie, Q. Zhou, and I. Angelidaki, "Simultaneous hydrogen utilization and in situ biogas upgrading in an anaerobic reactor," *Biotechnol. Bioeng.*, vol. 109, no. 4, pp. 1088–1094, Apr. 2012.

[18] E. Zoulias, E. Varkaraki, N. Lymberopoulos, C. N. Christodoulou, and G. N. Karagiorgis, *A review on water electrolysis*, vol. 4, no. 2. Elsevier, 1979.

[19] Jacques de Bucy, “The potential of power-to-gas,” 2016.

[20] F. ONEY, T. VEZIROLU, and Z. DULGER, “Evaluation of pipeline transportation of hydrogen and natural gas mixtures,” *Int. J. Hydrogen Energy*, vol. 19, no. 10, pp. 813–822, Oct. 1994.

[21] M. Svensson, “Biomethane standards: Gas quality standardisation of biomethane, going from national to international.,” 2014.

[22] K. Altfeld and D. Pinchbeck, “Admissible hydrogen concentrations in natural gas systems,” *Gas Energy*, vol. March/2013, pp. 1–16, 2013.

[23] EIGA - European Industrial Gases Association, *Hydrogen transportation pipelines*. Brussels: European Industrial Gases Association, 2004.

[24] J. D. Murphy and T. Thamsiriroj, “What will fuel transport systems of the future?,” *Mater. Today*, vol. 14, no. 11, pp. 518–524, Nov. 2011.

[25] T. Nejat Veziroglu, S. A. Sherif, and F. Barbir, “Hydrogen energy solutions,” in *Environmental Solutions*, F. J. Agardy and N. L. Nemerow, Eds. Elsevier, 2005, pp. 143–180.

[26] E. Strasse, “Power-to-Gas via Biological Catalysis (P2G-Biocat),” 2014.

[27] Danish Government, “The Danish Climate Policy Plan,” *Minist. Clim. Energy Build.*, vol. 1, no. August, p. 61, 2013.

[28] L. Cheng, L. Dai, X. Li, H. Zhang, and Y. Lu, “Isolation and characterization of Methanothermobacter crinale sp. nov., a novel hydrogenotrophic methanogen from the Shengli oil field,” *Appl. Environ. Microbiol.*, vol. 77, no. 15, pp. 5212–5219, Aug. 2011.

[29] A. Wasserfallen, J. Nolling, P. Pfister, J. Reeve, and E. Conway de Macario, “Phylogenetic analysis of 18 thermophilic Methanobacterium isolates supports the proposals to create a new genus, Methanothermobacter gen. nov., and to reclassify several isolates in three species, Methanothermobacter thermautotrophicus comb. nov., Methano,” *Int. J. Syst. Evol. Microbiol.*, vol. 50, no. 1, pp. 43–53, Jan. 2000.

[30] S. V Kotelnikova, A. Y. Obraztsova, G. M. Gongadze, and K. S. Laurinavichius, “Methanobacterium thermoflexum sp . nov . and Methanobacterium defluvii sp . nov ., Thermophilic Rod-Shaped Methanogens Isolated from Anaerobic Digestor Sludge,” *Syst. Appl. Microbiol.*, vol. 16, no. 3, pp. 427–435, 1993.

[31] K. Nakamura *et al.*, “Methanothermobacter tenebrarum sp. nov., a hydrogenotrophic, thermophilic methanogen isolated from gas-associated formation water of a natural gas field,” *Int. J. Syst. Evol. Microbiol.*, vol. 63, no. Pt 2, pp. 715–722, Feb. 2013.

[32] A. J. Guneratnam *et al.*, “Study of the performance of a thermophilic biological methanation system,” *Bioresour. Technol.*, vol. 225, pp. 308–315, Feb. 2017.

[33] J. Winter, C. Lerp, H.-P. Zabel, F. X. Wildenauer, H. König, and F. Schindler, “Methanobacterium wolfei, sp. nov., a New Tungsten-Requiring, Thermophilic, Autotrophic Methanogen,” *Syst. Appl. Microbiol.*, vol. 5, no. 4, pp. 457–466, Dec. 1984.

[34] S. Rittmann, A. Seifert, and C. Herwig, “Quantitative analysis of media dilution rate effects on Methanothermobacter marburgensis grown in continuous culture on H2 and CO2,” *Biomass and Bioenergy*, vol. 36, pp. 293–301, Jan. 2012.

[35] A. H. Seifert, S. Rittmann, and C. Herwig, “Analysis of process related factors to increase volumetric productivity and quality of biomethane with Methanothermobacter marburgensis,” *Appl. Energy*, vol. 132, pp. 155–162, Nov. 2014.

[36] J. G. Zeikus and R. S. Wolfe, “Methanobacterium thermoautotrophicus sp. n., an anaerobic, autotrophic, extreme thermophile,” *J. Bacteriol.*, vol. 109, no. 2, pp. 707–713, 1972.

[37] J. Zabranska and D. Pokorna, “Bioconversion of carbon dioxide to methane using hydrogen and hydrogenotrophic methanogens,” *Biotechnol. Adv.*, vol. 36, no. 3, pp. 707–720, May 2018.

[38] A. M. Orozco, A. S. Nizami, J. D. Murphy, and E. Groom, “Optimizing the thermophilic hydrolysis of grass silage in a two-phase anaerobic digestion system,” *Bioresour. Technol.*, vol. 143, pp. 117–125, Sep. 2013.

[39] M. A. Voelklein, D. Rusmanis, and J. D. Murphy, “Increased loading rates and specific methane yields facilitated by digesting grass silage at thermophilic rather than mesophilic temperatures,” *Bioresour. Technol.*, vol. 216, pp. 486–493, 2016.

[40] S. Fukuzaki, N. Nishio, M. Shobayashi, and S. Nagai, “Inhibition of the fermentation of propionate to methane by hydrogen, acetate, and propionate.,” *Appl. Environ. Microbiol.*, vol. 56, no. 3, pp. 719–23, Mar. 1990.

[41] V. Siriwongrungson, R. J. Zeng, and I. Angelidaki, “Homoacetogenesis as the alternative pathway for H2 sink during thermophilic anaerobic degradation of butyrate under suppressed methanogenesis,” *Water Res.*, vol. 41, no. 18, pp. 4204–4210, Oct. 2007.

[42] G. Luo and I. Angelidaki, “Hollow fiber membrane based H2 diffusion for efficient in situ biogas upgrading in an anaerobic reactor,” *Appl. Microbiol. Biotechnol.*, vol. 97, no. 8, pp. 3739–3744, Apr. 2013.

[43] M. Burkhardt, T. Koschack, and G. Busch, “Biocatalytic methanation of hydrogen and carbon dioxide in an anaerobic three-phase system,” *Bioresour. Technol.*, vol. 178, pp. 330–333, Feb. 2015.

[44] M. A. Voelklein, R. O’ Shea, A. Jacob, and J. D. Murphy, “Role of trace elements in single and two-stage digestion of food waste at high organic loading rates,” *Energy*, vol. 121, pp. 185–192, Feb. 2017.

[45] J. G. Ferry, “Biochemistry of Methanogenesis,” *Crit. Rev. Biochem. Mol. Biol.*, vol. 27, no. 6, pp. 473–503, Jan. 1992.

[46] J. Winter, C. Lerp, H.-P. Zabel, F. X. Wildenauer, H. König, and F. Schindler, “Methanobacterium wolfei, sp. nov., a new tungsten-requiring, thermophilic, autotrophic methanogen,” *Syst. Appl. Microbiol.*, vol. 5, no. 4, pp. 457–466, Dec. 1984.

[47] N. Schill, W. M. van Gulik, D. Voisard, and U. von Stockar, “Continuous cultures limited by a gaseous substrate: Development of a simple, unstructured mathematical model and experimental verification with Methanobacterium thermoautotrophicum,” *Biotechnol. Bioeng.*, vol. 51, no. 6, pp. 645–658, Mar. 2000.

[48] L. Daniels, N. Belay, and Biswarup Mukhopadahyay, “Considerations for the use and large-scale growth of methanogenic bacteria,” in *Proceedings of the 6th Symposium on Biotechnology in Fuels and Chemicals. Biotechnology and Bioengineering no. 14.*, 1984, pp. 199–213.

[49] J.-P. Peillex, M.-L. Fardeau, R. Boussand, J.-M. Navarro, and J.-P. Belaich, “Growth of

Methanococcus thermolithotrophicus in batch and continuous culture on H2 and CO2: influence of agitation," *Appl. Microbiol. Biotechnol.*, vol. 29, no. 6, pp. 560–564, Dec. 1988.

[50] L. Rachbauer, G. Voitl, G. Bochmann, and W. Fuchs, "Biological biogas upgrading capacity of a hydrogenotrophic community in a trickle-bed reactor," *Appl. Energy*, vol. 180, pp. 483–490, Oct. 2016.

[51] T. Ullrich, J. Lindner, K. Bär, F. Mörs, F. Graf, and A. Lemmer, "Influence of operating pressure on the biological hydrogen methanation in trickle-bed reactors," *Bioresour. Technol.*, vol. 247, pp. 7–13, Jan. 2018.

[52] William Henry, "III. Experiments on the quantity of gases absorbed by water, at different temperatures, and under different pressures," *Philos. Trans. R. Soc. London*, vol. 93, no. 1803, pp. 29–274, Jan. 1803.

[53] G. Bernhardt, R. Jaenicke, H. Ludemann, and K. Stetter, "High pressure enhances the growth rate of the thermophilic Archaebacterium Methanococcus thermolithotrophicus without extending its temperature range," vol. 54, no. 5, pp. 1258–1261, 1988.

[54] I. Bassani, P. G. Kougias, L. Treu, and I. Angelidaki, "Biogas upgrading via hydrogenotrophic methanogenesis in two-stage continuous stirred tank reactors at mesophilic and thermophilic conditions," *Environ. Sci. Technol.*, vol. 49, no. 20, pp. 12585–12593, Oct. 2015.

[55] M. M. Kale and K. S. Singh, "Comparison of a mesophilic and thermophilic novel sludge-bed anaerobic membrane bioreactor treating prehydrolysis liquor from a dissolving pulp mill," *J. Environ. Eng.*, vol. 142, no. 7, p. 04016030, Jul. 2016.

[56] K. S. Singh, T. Viraraghavan, S. Karthikeyan, and D. E. Caldwell, "Low temperature start-up of UASB reactors for municipal wastewater treatment," in *Proc. 8th Intl. Conf. on Anaerobic Digestion*, 1997, pp. 192–195.

[57] G. Lettinga, "Challenge of psychrophilic anaerobic wastewater treatment," *Trends Biotechnol.*, vol. 19, no. 9, pp. 363–370, Sep. 2001.

[58] C. M. Cooper, G. A. Fernstrom, and S. A. Miller, "Performance of agitated gas-liquid contactors," *Ind. Eng. Chem.*, vol. 36, no. 6, pp. 504–509, Jun. 1944.

[59] N. Alfaro, M. Fdz-Polanco, F. Fdz-Polanco, and I. Díaz, "Evaluation of process performance, energy consumption and microbiota characterization in a ceramic membrane bioreactor for ex-situ biomethanation of H2 and CO2," *Bioresour. Technol.*, vol. 258, pp. 142–150, Jun. 2018.

[60] I. Bassani, P. G. Kougias, and I. Angelidaki, "In-situ biogas upgrading in thermophilic granular UASB reactor: key factors affecting the hydrogen mass transfer rate," *Bioresour. Technol.*, vol. 221, pp. 485–491, 2016.

[61] V. Tesař, "Microbubble generation by fluidics. Part II: Bubble formation mechanism," *Inst. Thermomechanics v.v.i., Acad. Sci. Czech Republic, Prague Abstr.*, vol. 1, pp. 1–25, 2012.

[62] I. Díaz, C. Pérez, N. Alfaro, and F. Fdz-Polanco, "A feasibility study on the bioconversion of CO2 and H2 to biomethane by gas sparging through polymeric membranes," *Bioresour. Technol.*, vol. 185, pp. 246–253, Jun. 2015.

[63] S. R. Guiot, R. Cimpoia, and G. Carayon, "Potential of wastewater-treating anaerobic granules for biomethanation of synthesis gas," *Environ. Sci. Technol.*, vol. 45, no. 5, pp. 2006–2012, Mar. 2011.

[64] J.-P. Peillex, M.-L. Fardeau, and J.-P. Belaich, "Growth of methanobacterium thermoautotrophicum on H2□CO2: High CH4 productivities in continuous culture," *Biomass*,

vol. 21, no. 4, pp. 315–321, Jan. 1990.

[65] N. Nishimura, S. Kitaura, A. Mimura, and Y. Takahara, “Cultivation of thermophilic methanogen KN-15 on H2-CO2 under pressurized conditions,” *J. Ferment. Bioeng.*, vol. 73, no. 6, pp. 477–480, Jan. 1992.

[66] S. Savvas, J. Donnelly, T. Patterson, Z. S. Chong, and S. R. Esteves, “Biological methanation of CO2 in a novel biofilm plug-flow reactor: A high rate and low parasitic energy process,” *Appl. Energy*, vol. 202, pp. 238–247, Sep. 2017.

[67] R. A. Hoffmann, M. L. Garcia, M. Veskivar, K. Karim, M. H. Al-Dahhan, and L. T. Angenent, “Effect of shear on performance and microbial ecology of continuously stirred anaerobic digesters treating animal manure,” *Biotechnol. Bioeng.*, vol. 100, no. 1, pp. 38–48, May 2008.

[68] C. Carliell-Marquet, R. Sindall, and J. Bridgeman, “Effect of mixing speed on lab-scale anaerobic digester stability and biogas production (short paper and poster),” 2013, no. June.

[69] G. Luo and I. Angelidaki, “Integrated biogas upgrading and hydrogen utilization in an anaerobic reactor containing enriched hydrogenotrophic methanogenic culture,” *Biotechnol. Bioeng.*, vol. 109, no. 11, pp. 2729–2736, Nov. 2012.

[70] N. Energy, “Power-to-gas via biological catalysis WP9 : Development of value maximizing strategy,” 2014.

[71] D. Hafenbradl, “Industrial scale biological methanation - Learnings and insights,” in *Power2gas Conference*, 2018, no. October.

[72] M. R. Martin, J. J. Fornero, R. Stark, L. Mets, and L. T. Angenent, “A single-culture bioprocess of methanothermobacter thermautotrophicus to upgrade digester biogas by CO2-to-CH4 conversion with H2,” *Archaea*, vol. 2013, Oct. 2013.

[73] S. Yoon, J. T. Chung, and Y. T. Kang, “The particle hydrodynamic effect on the mass transfer in a buoyant CO2-bubble through the experimental and computational studies,” *Int. J. Heat Mass Transf.*, vol. 73, pp. 399–409, Jun. 2014.

[74] V. Tesař, “Microbubble generation by fluidics. Part I: Development of the oscillator,” *Inst. Thermomechanics*, pp. 1–13, 2012.

[75] G. Luo and I. Angelidaki, “Co-digestion of manure and whey for in situ biogas upgrading by the addition of H2: process performance and microbial insights,” *Appl. Microbiol. Biotechnol.*, vol. 97, no. 3, pp. 1373–1381, Feb. 2013.

[76] C. Wu, K. Nesset, J. Masliyah, and Z. Xu, “Generation and characterization of submicron size bubbles,” *Adv. Colloid Interface Sci.*, vol. 179–182, pp. 123–132, Nov. 2012.

[77] W. S. Russel and B. Scholten, “Compositions containing nano-bubbles in a liquid carrier,” 2017.

[78] H. Ohnari, “Swirling fine-bubble generator,” 2002.

[79] M. Jamialahmadi, M. Emadi, and H. Müller-Steinhagen, “Diffusion coefficients of methane in liquid hydrocarbons at high pressure and temperature,” *J. Pet. Sci. Eng.*, vol. 53, no. 1–2, pp. 47–60, Aug. 2006.

[80] E. G. Richardson, “Supersonic vibrations and their applications,” *J. R. Soc. Arts*, vol. 95, no. 4734, pp. 90–105, 1947.

[81] A. Alitalo, M. Niskanen, and E. Aura, “Biocatalytic methanation of hydrogen and carbon

dioxide in a fixed bed bioreactor," *Bioresour. Technol.*, vol. 196, pp. 600–605, 2015.

[82] E. C. Bugante, Y. Shimomura, T. Tanaka, M. Taniguchi, and S. Oi, "Methane production from hydrogen and carbon dioxide and monoxide in a column bioreactor of thermophilic methanogens by gas recirculation," *J. Ferment. Bioeng.*, vol. 67, no. 6, pp. 419–421, Jan. 1989.

[83] H. S. Jee, N. Nishio, and S. Nagai, "Continuous CH4 Production from H2 and CO2 by Methanobacterium thermoautotrophicum in a fixed-bed reactor," *J. Ferment. Technol.*, vol. 66, no. 2, pp. 235–238, Jan. 1988.

[84] J. J. Orgill, H. K. Atiyeh, M. Devarapalli, J. R. Phillips, R. S. Lewis, and R. L. Huhnke, "A comparison of mass transfer coefficients between trickle-bed, hollow fiber membrane and stirred tank reactors," *Bioresour. Technol.*, vol. 133, pp. 340–346, Apr. 2013.

[85] S. K. Khanal, B. Giri, S. Nitayavardhana, and V. Gadhamshetty, *10 - Anaerobic Bioreactors/Digesters: Design and Development*. Elsevier B.V., 2017.

[86] H. S. Jee, N. Nishio, and S. Nagai, "CH4 production from H2 and CO2 by Methanobacterium thermoautotrophicum cells fixed on hollow fibers," *Biotechnol. Lett.*, vol. 10, no. 4, pp. 243–248, Apr. 1988.

3. Design and commission of a novel biological methanation system

Rusmanis, Davis[1,2], Wu, Benteng[1,2], O'Shea, Richard[1,2], Wall, David M.[1,2], Murphy, Jerry D.[1,2,*]

1. MaREI Centre, Environmental Research Institute, University College Cork, Ireland.
2. Civil, Structural and Environmental Engineering, School of Engineering and Architecture, University College Cork, Cork, Ireland.

Graphical Abstract



Abstract

This design study investigated a novel reactor design for the biological methanation of hydrogen and carbon dioxide in a three-stage cascading diffusion reactor design. Based on previously simulated experiments, associated with a small lab-scale reactor, a working prototype was designed and fabricated. The study advanced the design to a technology readiness level (TRL) of 4 with the fabrication of this consecutive three-reactor design prototype. The thermophilic system was shown to be capable of reaching a similar performance as the previous models based on the assessment of a small-scale lab reactor. This work documents the design and commissioning rather than the biological optimisation of the process. During the first stage, at a flow rate of 34.7 litres of hydrogen per litre volume of reactor per day (L $H_2/L_{vr}/d$) and 9.4 L $CO_2/L_{vr}/d$ carbon conversion rates of 72%, 91% and 97% were achieved, in the cascading reactors 1,2 and 3, respectively. This equated to an average methane evolution rate of 2.9 $LCH_4/L_{vr}/d$. Higher flow rates were tested, but this resulted in a significant drop in the conversion efficiency. For safety, the system was housed in a walk-in fume hood, resulting in significant space restrictions, leading to a limitation of the actual bubble column height. This imposed a limitation on the current design. During operation, several issues were identified in the system, from oversized components to unforeseen anomalies in the design. The authors have proposed solutions to allow for the advancement of the system to a TRL of 5 and higher.

Highlights

A novel diffusion-based biological methanation system was designed and fabricated.

The system was capable of matching and exceeding a previously simulated system.

The system achieved 95% CO_2 conversion through continuous cascade operation.

System dimension was identified as a major limitation at TRL 4.

Keywords

Biological methanation; Bubble column; Design and commission; Hydrogen; Biomethane; Carbon capture.

3.1 Introduction

The global climate crisis is a daunting challenge for humanity. Carbon budgets set by the IPCC and the targets imposed by the recast European Renewable Energy Directive create opportunities for disruptive technologies to produce clean alternative fuels and capture carbon from the atmosphere [1], [2],[3]. Challenges on energy systems associated with intermittent renewable energies (wind and solar) include a mismatch in the availability of variable renewable electricity and variable energy demand [4]. Liquid hydrocarbon fossil fuels are energy-dense, dispatchable, and easy to store. They provide dispatchable energy and once phased out, will pose challenges to the decarbonised energy system, if sustainable green alternatives are not put in place. Due to the ongoing war in Ukraine, Europe has been particularly sensitive to rapidly increasing energy prices and has experienced anxiety in terms of grid instability. Weaning systems off fossil hydrocarbon fuels and adapting them to renewable sources of energy requires novel and innovative solutions. While departing from fossil fuels is essential for decarbonisation, the existing energy networks are ill-equipped to adapt to 100% variable and intermittent renewable energy sources without relying on fossil hydrocarbon backup generators [5]. It is essential to develop renewable hydrocarbon fuels (gaseous and liquid) such as gaseous biomethane (CH_4) and liquefied renewable methanol (CH_3OH) to displace natural gas and diesel in the existing systems and to provide dispatchable energy. Research assessing the feasibility of producing renewable hydrocarbons or electrofuels to displace fossil fuels is documented in the literature and has shown promising results [6], [7], [8].

Green hydrogen (H_2) generated from curtailed and/or constrained electricity can serve as a means of alleviating issues associated with intermittent renewable electricity. This is possible by the H_2 acting as a form of energy storage, with a typical conversion efficiency of 60-70% [9], [10]. Green H_2 can be produced through electrolysis by splitting water into the constituent H_2 and O_2 gases. The green H_2 can be used further in the Sabatier reaction, combining H_2 and carbon dioxide (CO_2) to form methane (CH_4), the basic hydrocarbon (Equation 3.1). When combined with the by-product CO_2 from anaerobic digestion or industries in the food and beverage sector or cement manufacture, the CO_2 can be captured and reused to make fuel.

$$4H_2 + CO_2 \rightarrow CH_4 + 2H_2O \qquad \Delta G_0 = -165\ kJ/mol \qquad \text{Equation 3.1}$$

Traditional anaerobic digestion systems implement chemical or water scrubbing technologies to remove the CO_2 from the biogas. These technologies can be energy-intensive [11]. Biological methanation is a novel technology, involving the capture and conversion of CO_2 into CH_4 through the addition of H_2 in a bioreactor, using relatively low power consumption. The subsequent conversion of otherwise waste CO_2 into CH_4 from processes such as cement manufacture and anaerobic digestion creates pathways towards carbon neutrality. This conversion also increases the CH_4 yields (over biogas systems) by 50-70% when the technologies are coupled [12], [13]. Traditionally, anaerobic digestion plants have used water or chemical scrubbing technology to remove the by-product CO_2 from biogas, thereby increasing the calorific value of the product gas [14]. Installing biological

methanation systems may be beneficial due to the cost offset of traditional chemical and water scrubbers, and increased CH_4 yields (due to the conversion of CO_2 to CH_4 [11]). Previous studies by the authors have shown the benefits of coupling biological methanation with anaerobic digestion and electrolyser technologies in establishing energy hubs at existing wastewater treatment plants. In doing so, integrating the previously independent sectors of water, electricity and gas [7]. Studies throughout the literature have proposed novel designs of biological methanation systems, producing successful and efficient systems through optimisation of the gas/liquid interface for optimal methanogenic archaea performance [15]. Gas interface refers to the amount of time and surface area made available to archaea to undergo methanogenesis. This can involve fine bubble diffusion for the increased surface area; increased column height; high agitation to reduce the bubble velocity; high pressure; or packing to slow down bubbles and increase archaea growth area. While such systems can provide insight into the design process, the scale-up, and the maintenance of such novel design systems, are yet to be fully documented in the literature.

Similarly, a previous study by Voelklein *et al.* simulated a novel three-stage cascading reactor system [16]. The study used a single reactor to simulate the cascading effect. By passing H_2 and CO_2 (and later CH_4) through the reactors to upgrade to CH_4, a portion of the gas was upgraded. This composition was analysed and synthesised as the inlet composition, simulating the gas entering a second reactor. This was done twice after the initial gas injection, to simulate a three-reactor system. The technology readiness level (TRL) of this technology according to the previous study was assessed to be at TRL 3, as the experimental function and proof-of-concept was established in the simulated performance. A literature review carried out by the authors identified a gap in the state of the art of bubble column upgrading technology, with few biological methanation technologies presenting on this technology [11]. With the knowledge gained from these earlier studies, the authors designed and fabricated a novel cascading bubble column biological methanation system to advance the TRL to level 4. This required the fabrication, verification and testing of the prototype in a lab environment (Figure 3.1) [17].

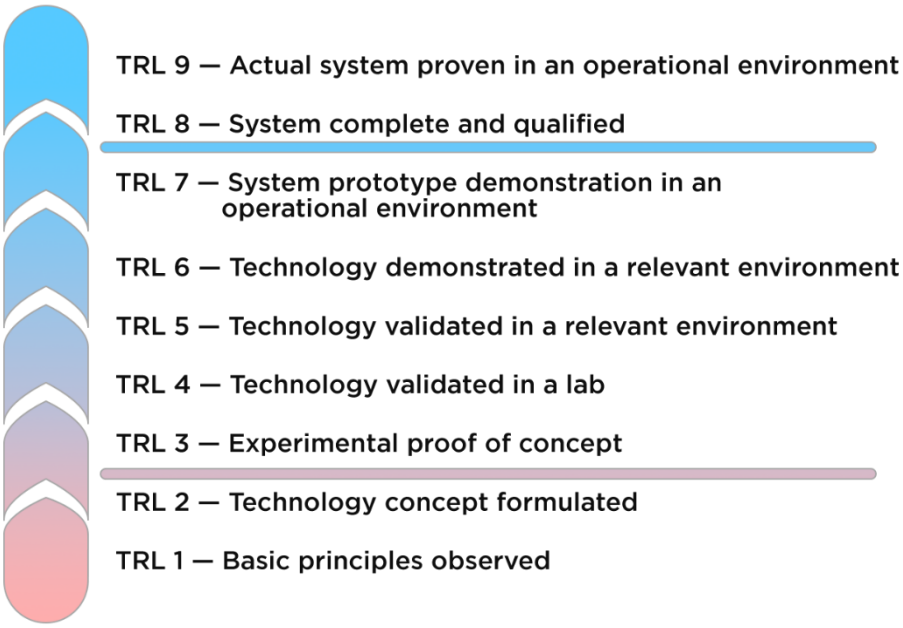


Figure 3.1: Technology readiness levels adapted from Horizon 2021-22 work programme [17].

The innovation of this engineering study is the design and commission of a cascading bubble column biological methanation technology. To match the previously simulated performance of a study by Voelklein *et al.*, this study will be compared to the previous, simulated study [16]. The parameters of evolution rate, retention time, gas conversion efficiency and gas throughput will act as performance indicators. The design aims to increase the system flow rate and operational pressure while reducing the gaseous retention time. This work is an engineering exercise, with the ambition of informing the reader of the processes for commissioning and design. The study does not seek to optimise the biological process of the system. The presented findings aim to inform future research focusing on the design and operation of the cascading bubble column biological methanation technology.

The key questions asked in this paper are as follows:

- Can the design and commission of the cascading bubble column biological methanation system be considered successful, and can the technology readiness level be improved?
- Is the system capable of exceeding the performance of the previously simulated system by Voelklein *et al.*, based on a single reactor and a series of experiments with calibrated gases [16]?
- Is the system capable of achieving grid quality and composition of biomethane suitable for injection into the natural gas grid?
- What alterations are required to advance the technology readiness level of the system?

3.2 Design of the system

3.2.1 Simulated system by Voelklein *et al.*

The initial design of the system relies on the model set out by the research team in a previous study [16]. This research by Voelklein *et al.* simulated an in-series three reactor system using a single reactor and a series of gas compositions to achieve the results in Figure 3.2.

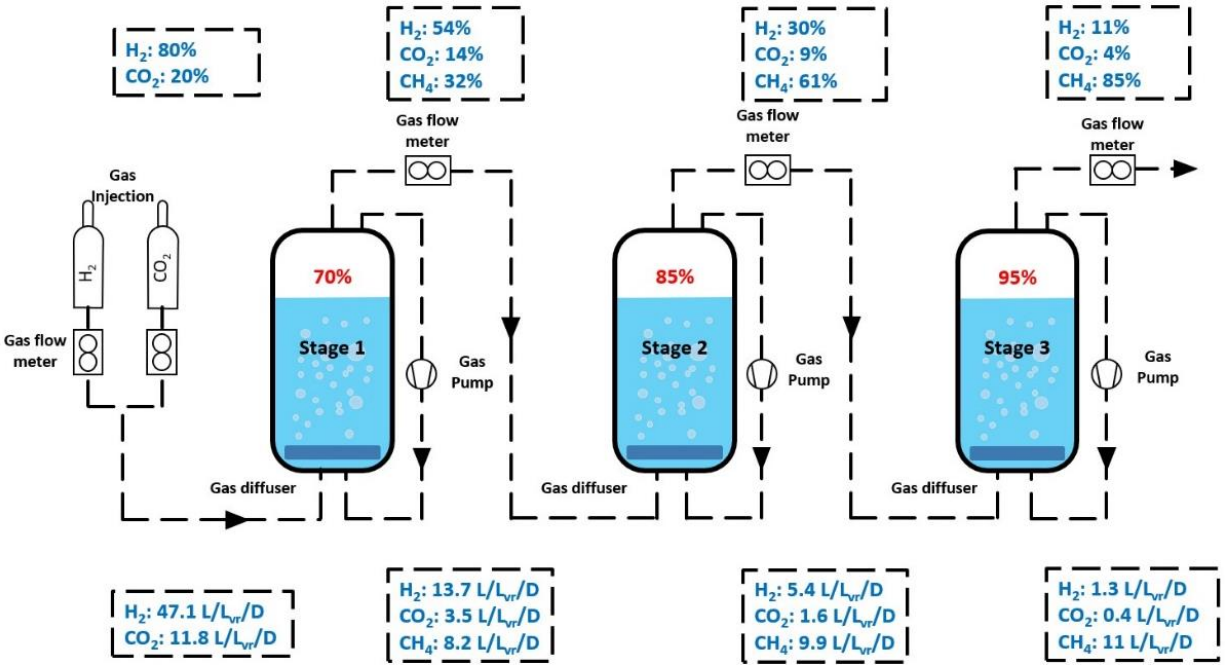


Figure 3.2: The simulated three-stage cascading biomethanation rig, adapted from Voelklein et al. [16]. L/L_{vr}/D refers to 'litres per litre-volume-reactor per day'.

The reactor held a total liquor volume of 9.5 L, with approximately 10.6 L of total chamber volume (corresponding to 0.54 m liquid column height). The initial inlet gas composition was at a stoichiometric ratio of 4:1 (H_2:CO_2), as per the Sabatier reaction (Equation 3.1). The gas composition exiting the reactor was collected and analysed using gas chromatography. The measured exiting gas composition was synthesised and reintroduced into the reactor. The resultant exit gas from this second reactor was analysed, synthesised, and reintroduced into the third reactor, simulating a cascading three-stage upgrading system. The system produced the gas composition results illustrated in Figure 3.2, with the model achieving a peak of 95% CO_2 conversion efficiency after reactor 3. Table 3.1 summarises the performance of the simulated system. These performance indicators will serve as the benchmarks for this paper's reactor design.

Table 3.1: Simulated reactor performance of M. Voelklein et al. (M.V.) [16].

		M.V. $R1_{in}$	M.V. $R2_{in}$	M.V. $R3_{in}$	M.V. $R3_{out}$
Gas Retention Time	h	-	0.57	1.13	1.62
Reactor vol.	L	-	10.6	10.6	10.6
Working vol.	L	-	9.5	9.5	9.5
Bubble column height	m	-	0.54	0.54	0.54
Chamber height	m	-	0.6	0.6	0.6
Chamber ID	m	-	0.15	0.15	0.15
Gas inflow					
H_2:CO_2 ratio		4.0	3.9	3.4	3.3
H_2	%	80.0%	53.9%	32.0%	10.2%
CO_2,	%	20.0%	13.8%	9.5%	3.1%
CH_4	%	0%	32%	59%	87%
H_2	$L/L_{vr}/d$	47.1	13.7	5.4	1.3
CO_2	$L/L_{vr}/d$	11.8	3.5	1.6	0.4
CH_4	$L/L_{vr}/d$	0.0	8.2	9.9	11.0
MER	$L/L_{vr}/d$	-	8.20	1.70	1.10
MER_{AVG}	$L/L_{vr}/d$	-	N/A*	N/A*	0.39
Gas conversion					
H_2	%	-	70.9%	88.5%	97.2%
CO_2	%	-	70.3%	86.4%	96.6%

Note: M.V. $R2_{in}$ and M.V. $R3_{in}$ are also the exit flow rates/gas compositions for M.V. R1 and M.V.R2, as seen in Figure 3.2. MER is the methane evolution rate; ID is the reactor's internal diameter.
**- MER_{AVG} refers to the average methane evolution rate when considering the three cascading reactors as one reactor. i.e., 11 $LCH_4/L/D$ divided by 9.5L * 3 = 0.39 $LCH_4/L/D$.*

3.2.2 Design of the cascading biomethanation rig

Based on the previous research by Voelklein *et al.* in this research team, the authors redesigned and adapted the biological methanation system at a larger scale, implementing three actual reactors working simultaneously [16]. To enable a modular system operation, multiple gas circulation routes were necessary to implement. Strict health and safety policies necessitated close consultation with the University health and safety engineers, an engineering consultancy, and an engineering fabrication company. The resulting system had to be in strict accordance with the hazardous operation safety standards required for the use of H_2 (and CH_4) in the University laboratory workspace. Through numerous brainstorming sessions with the above parties, potential design considerations, process issues and safety concerns were discussed and analysed. Consideration was given to the foaming of reactor liquid; a build-up of condensate in the gas lines; pressure drops; and hydrogen leaks. In a collaborative process, time was spent attempting to eliminate design flaws within the confines of the more critical health and safety environment. The safety documentation included: gas certification; factory acceptance tests; pressure test

certifications; certificates of conformity; Hazardous operation studies (HAZOP); ATEX certification (for control of explosive atmospheres); Process and instrumentation Diagrams (P&ID); hazardous area classification reports; and other certifications. All of this has been documented in the supplementary data. For safety, it was agreed to have the rig housed within a custom floor-mounted walk-in fume hood.

3.2.3 Manufacture of the cascading biomethanation rig

The methanation system consists of a three-stage reactor system, interconnected with gas lines that can be isolated, allowing for various modes of operation. A simplified P&ID is depicted in Figure 3.3 (Adapted from supplementary data "[SD 4] A18CK038 KD-002" and "[SD 5] A18CK038 KD-003"). This section discusses the multiple specialised components comprising the rig.

Mixing manifold: The external mixing manifold is connected to individual supply lines for CH_4, H_2, CO_2 and N_2. Each gas line has an upstream pressure of 5 barG, with manually operated rotameters controlling the flow. These lines merge into a manifold mixing tank, ensuring the mixing of gases before entering the system. Parker A-Lok manual valves control the manifold supply and system delivery lines (Figure 3.3). The "Krohne" inlet flow rotameters have a varied operation range: H_2 flow rates of 4.1 to 39.0 NL/h (litres per hour at standard temperature and pressure); CO_2 flow rates of 0.9 to 9.0 NL/h; and CH_4 flow rates of 1.7 to 17.0 NL/h. The N_2 supply is controlled via a simple pressure indication and control valve (PICV), to render the internal system environment inert (See supplementary data "[SD 1] Supplementary figures, Figure S3.1").

Piping: The 316L high-grade stainless-steel piping manufacture and the certified x-ray weld scan conducted ensured the absence of leaks from the pipeline joints during the manufacture and assembly processes.

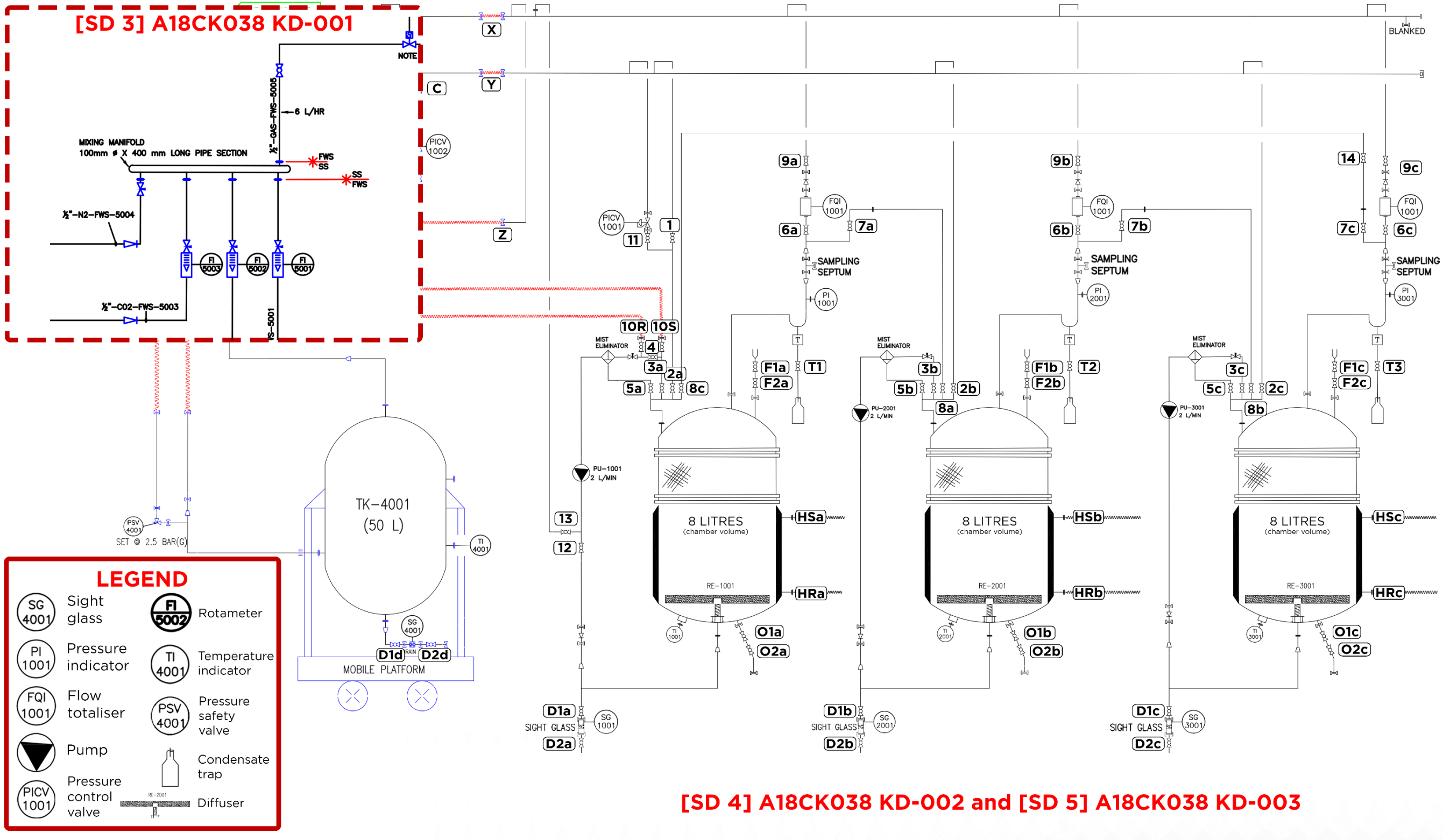


Figure 3.3: The simplified P&ID diagram of the biomethanation system, adapted from "[SD 4] A18CK038 KD-002" and "[SD 5] A18CK038 KD-003. Labelled valves are denoted for reference in the Standard Operating Procedure, on which information may be found in supplementary data ("[SD2] Standard Operating Procedure V3").

Reactor chamber: The individual reactor chamber vessels are identical in design and are made of 316L stainless steel, with ANSI 150 flanged connections. The reactor comprises the lower steel basin, housing the custom diffuser plate ("B" in Figure 3.4) and the liquid take-off valve (C). The upper sight glass section is made of borosilicate glass, allowing for observation of the reactor during operation. The flat top flange, holding the feed-in valves, sealing the reactor and gas recirculation/outlet lines. Between the components, a PTFE gasket ensures a gas-tight seal at the flange face under compression. A double rubber O-rings between the flange and the borosilicate glass seals the interface between the glass and the steel. The chamber has a 150 mm internal diameter (ID), with an approximate height of 450 mm (~370mm max column height). The installed pressure safety valves (PSV) are set to 2.5 barG, to prevent excess pressure build-up should the outlet gas flow be restricted at any point in the system (See supplementary figures "[SD 1], Figure S3.2").

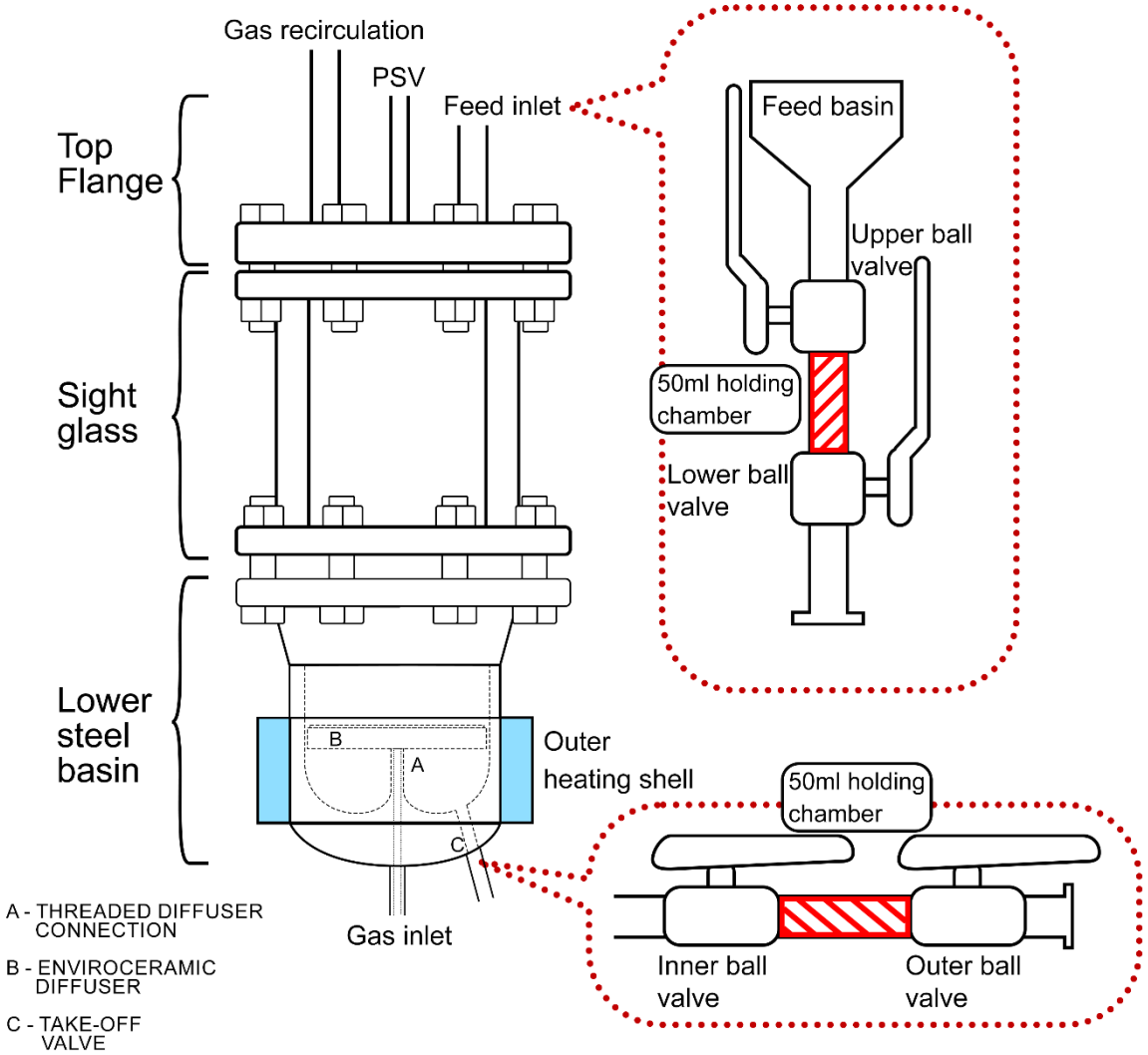


Figure 3.4: Profile of a methanation reactor chamber, where (A) is the threaded diffuser connection, (B) is the "Enviroceramic" diffuser and (C) is the liquid take-off line. PSV – Pressure safety valve.

Diffuser: The "Enviroceramic" diffusers provide approx. 140 cm^2 diffuser area and can handle a maximum flow rate of 9 NL/min (540 NL/h). These are traditionally used for aquaculture and wastewater treatment. The diffusers were chosen for their ability to produce sub-millimetre bubbles. In this study, the bubbles had a larger size variation primarily due to the use of the anaerobic digestor liquor as the diffusion media (See supplementary data [SD 6.1] for documentation).

Microbial culture: Initially a pure culture of *Methanothermobacter,* capable of converting H_2 and CO_2 to methane (CH_4) was selected due to the microbe capabilities for elevated gas upgrading rates. A pure culture sample from the microbe culture provider "DSMZ" was purchased based on increased performance using a pure culture compared to a mixed anaerobic culture [11]. The use of the pure culture would necessitate smaller reactor volumes, compared with the use of mixed cultures. However, the pure culture was postponed in this experiment due to complications in the early stages of the reactor operation. Instead, a methanogen-rich liquor was harvested from a thermophilic laboratory anaerobic digester processing grass silage. The liquor was sieved via a 150 µm mesh to remove particulates, leaving solely the liquor component to be added to the biological methanation rig. The resulting inoculum had a total solids (TS) content of 1.49% (15.80 g/L), a volatile solids (VS) content of 0.87% (9.24 g/L) and an initial pH of 7.40. Over time, with H_2 and CO_2 gases feeding in, the inoculum is dominated by the hydrogenotrophic methanogenic archaea.

Feed inlet/outlet: To allow for the addition of nutrients and the reintroduction of recirculated liquor during the rig operation, an airlock system was implemented for the feed inlet, comprising of two ball valves and a built-in funnel. This allows for the introduction of liquids into the system, without the risk of air entering the system or the working gases escaping from the system. The mechanism maintains a safe reactor environment and access to the reactor during operation (Figure 3.4).
In a similar fashion to the inlet, the outlet has an airlock system comprising two ball valves ('C' in Figure 3.4), allowing for the isolation of the liquor from the reactor vessel and sampling during pressurised operation.

Pump: Each reactor is equipped with a "KNF N630 EX" ATEX membrane diaphragm pump. With an operating range of 0.12 – 5 bar (abs.) [Design pressure 2.5 barG], an operating temperature of 5 to 55 °C, and a maximum flow of 35 L/min. The pump is sized to handle any present, and future, flows required within the research. Each pump is also equipped with a water separator module at the pump inlet, minimising the risk of liquids entering the pump head.

Flow totalisers: "Krohne DK37/M8E" electronic flow totalisers were chosen for the flow measurement, with an operational range of 19 to 160 NL/h; this is calibrated for CO_2. To calculate the flow rate of the other gases, a conversion table was provided by the supplier to estimate the flow of individual gases (See supplementary data "[SD 7] Flow totaliser conversion table").

Low pressure-reducing valve: This PICV is used exclusively for the batch operation of the system. The valve ("Wölpper GmbH" ZM-R15/25F) ensures that the system does not become negatively pressurised. This is at risk of occurring in the rigid vessel system under batch operation, when H_2 and CO_2 react, reducing the volume of gases by up to 80% (Equation 3.1) (See supplementary data "[SD 5] A18CK038-KD-003").

Gas sampling: "QUALTRU" membrane sampling ports were installed downstream of each reactor allowing for easy gas sampling using a 100 µl gastight syringe. Initially, a 50 ml gastight syringe was used to sample the gas to ensure a representative gas volume. However, multiple tests showed no difference in the gas quantification analysis between the two volume samples when analysed through gas chromatography.

Fume hood: A custom "ESCO Frontier floor mounted" walk-in fume hood was chosen (max. 1.6m height, 2.3m width, 0.9m depth). Fitted with an independent air extraction system, the fume hood ensured the safe containment of the methanation rig. "Helio DTEX detectors" for CO_2, N_2, CH_4 and H_2 were installed within the fume hood. Additional external gas detectors installed in the main laboratory environment maximised the detection of fugitive gases. If elevated levels of gases were detected, solenoid valves will terminate the supply of gas and power to the methanation system. This is to limiting the risk of conflagration or gas emissions into the main laboratory atmosphere. Due to the necessity of an ATEX environment within the fume hood and the space restrictions in place, a custom access port through the side of the fume hood accommodated an external heating system.

Heating system: The reactors have an isolated outer shell, capable of circulating water allowing for suitable control of the reactor chamber temperature. The heating system is located outside of the fume hood for health and safety reasons, connected by "Hosetech" Blovast flexible heat-resistant pipes through a custom access port built into the fume hood. To maintain a constant temperature, a "JULABO CD" immersion circulator and a custom temperature controller unit heated and circulated water through the reactor's outer shell.

Mist eliminator: "SMC AM 850" mist eliminators located upstream of the pumps minimised the risk of moisture entering the pumps and accumulating in the system's low points. A return line for moisture drainage back into the reactor chamber ensures minimal liquid evaporation from the chambers.

3.3 Commissioning of the system

3.3.1 Operation

Compliance with the health and safety standards set out by the University process was incorporated in the operation manuals outlining the Standard Operating Procedure (SOP), ensuring minimal risk. The produced SOP served as a strict guideline for any present and future researchers seeking to operate the system. For safety reasons, two researchers must operate and crosscheck the operation steps at all times, minimising the risk of hydrogen leaks or a dangerous reactor system arrangement. The reactors in this study operated for two months to ensure correct functionality and no gas leaks. The subsequent data acquisition stage lasted approximately another two months, during which the reactors were

operated at three different flow rates (referred to as stages). Data acquisition was carried out three to four times a week. This was limited by the health and safety procedure, requiring the system to be shut off during the weekend. Thus, the system would be restarted on a Monday, whereby data could be collected Tuesday through Friday, should no system issues arise.

3.3.2 Analytical methods

The analysis of TS and VS was carried out in triplicate, according to the methods of previous studies [18]. The pH monitoring was carried out with a standard pH meter (METTLER TOLEDO, Switzerland) to maintain a stable microbial environment. Due to complications with the outlet flow meters, compromises were made in the reactor performance assessment. To evaluate the gas loading at the inlets and outlets of the reactors, gas sampling was primarily carried out using a 100 µl gas syringe and analysis was carried out using a gas chromatograph (GC) (Agilent 7890B, USA). The gas volume measurement was completed in triplicate using a 100ml gas syringe, a 3-way stopcock and an empty foil gas bag. The gas bag filling rates and the measured gas compositions were used to estimate the flow rates, as defined in Equation 3.2.

$$Q_{flow} = \frac{L_1 + L_2}{2} * \frac{12}{1000} * \%_{GC} * \left(\frac{273.15}{T_{amb} + 273.15}\right) * \left(\frac{101.325}{\Delta P_{amb} + 101.325}\right) * \frac{24}{V_R} \quad \text{Equation 3.2}$$

Where; Q_{flow} is the measured flowrate ($L/L_{VR}/d$), L_1 and L_2 are the two 5-minute measurements (ml/5min), ‘12’ is the factor for 5-minute intervals in an hour, ‘1000’ adjusts for the ml/L, $\%_{GC}$ is the percentage of individual gas (H_2, CO_2, CH_4) the calculation being repeated for each gas composition estimation (%). T_{amb} is the ambient temperature of the room, adjusting for the temperature and pressure of the room (°C), ‘101.325’ refers to the atmospheric pressure at standard temperature and pressure (Kpa), ΔP_{amb} is the change in ambient pressure from the standard temperature and pressure (Kpa), ‘24’ is the number of hours in a day to convert the value to L/d, and V_R is the volume of the reactor to evaluate the loading rate on a per litre basis ($L/L_{VR}/d$).

The output gas datasets presented were normalised to standard temperature and pressure as per Equation 3.2 (273.15 K, 1 atm) [16]. To measure the methane evolution rate, Equation 3.3 was used.

$$MER = \frac{Q_{CH_{4,\text{out}}} - Q_{CH_{4,\text{in}}}}{V_R} \quad \text{Equation 3.3}$$

Where MER is the methane evolution rate ($L\ CH_4/L_{VR}/d$), Q_{CH4in} is the flowrate of CH_4 into the system ($L\ CH_4/L_{VR}/d$), Q_{CH4out} is the flowrate of CH_4 out of the system ($L\ CH_4/L_{VR}/d$), and V_r is the reactor volume (L).

To measure the retention time of the gas within each reactor (RT), Equation 3.4 was adapted from Voelklein *et al.* [16].

$$RT = \frac{V_R}{(Q_{tot,in} + Q_{tot,out})/\ 2}$$ Equation 3.4

Where, $Q_{tot,in}$ is the sum flow into the reactor (L/h); $Q_{tot,out}$ is the sum flow out of the reactor (L/h); and V_R is the total volume of the reactor (L).

To estimate the conversion efficiency of the system, the authors desired to evaluate the system based on the H_2 conversion efficiency, instead of CO_2. However, due to difficulties in maintaining a stoichiometric ratio of 4:1 for the gas inflow, the authors decided to follow the previous work of Voelklein *et al.* and assess the system on CO_2 conversion instead [16]. This was carried out using Equation 3.5.

$$X_{CO2} = \frac{\%_{CH4}}{\%_{CO2} + \%_{CH4}}$$ Equation 3.5

Where X_{CO2} is the carbon conversion efficiency, $\%_{CH4}$ is the outlet methane composition and $\%_{CO2}$ is the outlet carbon dioxide composition. This assesses the percentage of carbon converted into methane gas.

3.3.3 Performance vs previous study

The work carried out by Voelklein *et al.*, based on the reactor CO_2 conversion, achieved a total conversion efficiency of 70%, 85% and 95% in reactors 1 (VR1), 2 (VR2), and 3 (VR3), at respective inlet gas flow rates of 47.1 L $H_2/L_{vr}/d$ and 11.8 L $CO_2/L_{vr}/d$. Comparing our system to the simulated performance of Voelklein, during stage 1 (on day 13), reactor 1 (R1) matched the conversion rates of VR1, achieving 72% of the total conversion. Reactors 2 (R2) and 3 (R3) achieved 91% and 97% conversion, respectively (Figure 3.5A), albeit at a lower average flow rate of 34.7 L $H_2/L_{vr}/d$ and 9.4 L $CO_2/L_{vr}/d$; this equates to a methane evolution rate of 2.9 $L/L_{vr}/d$ (Figure 3.5B and Table 3.2).

As the system appeared to be capable of handling the gas throughput, on day 20, the second stage (S2) of the system operation commenced. Gas throughputs were increased to 51.3 L $H_2/L_{vr}/d$ and 11.5 L $CO_2/L_{vr}/d$. Due to the H_2 and CO_2 rotameter sensitivity and manual operation, the H_2: CO_2 gas volume ratio changed from 3.7:1 to 4.3:1. The conversion rates decreased across the three reactors, to 22%, 59% and 79% in reactors R1, R2, and R3, respectively. This is likely due to the higher gas throughput and the low liquid column height, resulting in a shorter contact period between the gas and the liquid media (Table 3.2). While underperforming, the system behaved expectedly. The individual gas composition readings for each reactor and detailed reactor stage summaries can be found in the supplementary data ("[SD 1] Supplementary figures", Figure S3.3 and Tables S3.1-3.3).

Table 3.2: System comparison of the current study to that of Voelklein et al. [16]. S1, S2, and S3 refer to stages 1-3 of this study, where flow rates were varied to investigate performance.

Study		Voelklein *et al.*	Stage 1	Stage 2	Stage 3
H_2	$L/L_{vr}/d$	47.1	34.7	51.4	34.9
CO_2	$L/L_{vr}/d$	11.8	9.4	11.8	9.7
H : C		4.0	3.7	4.3	3.6
MER R1	$L/L_{vr}/d$	8.2	6.3	3.1	4.5
MER R2	$L/L_{vr}/d$	1.7	2.1	4.0	2.9
MER R3	$L/L_{vr}/d$	0.85	0.3	3.2	0.2
MER avg.	$L/L_{vr}/d$	3.6	2.9	3.4	2.5
GRT	h	3.34	0.79	1.78	2.58
Chamber ID	m	0.15	0.15	0.15	0.15
Chamber height	m	0.6	0.43	0.43	0.43
Total vol.	L	10.5	8	8	8
Working vol.	L	9.5	6	6	6
Bubble column height	m	0.54	0.29	0.29	0.29

Note: MER – Methane evolution rate, ID – Internal diameter, GRT – Gas retention time through all three reactors. Note that the bubble column height refers to a single reactor bubble column height.

The estimated bubble column height is lower than that of the previous research. Voelklein *et al.* had a reactor volume of 9.5L with an internal diameter of 0.15 m, corresponding to approx. 0.54 m column height. This systems bubble column height is approximately 0.29 m. This is due to a 5 L (excluding the 1L volume below the diffuser) volume, equating to a total column height difference of 0.78 m across the three reactors, almost half the contact distance (0.87 m over three reactors) versus Voelklein *et al.* (1.62 m over three reactors) [16].

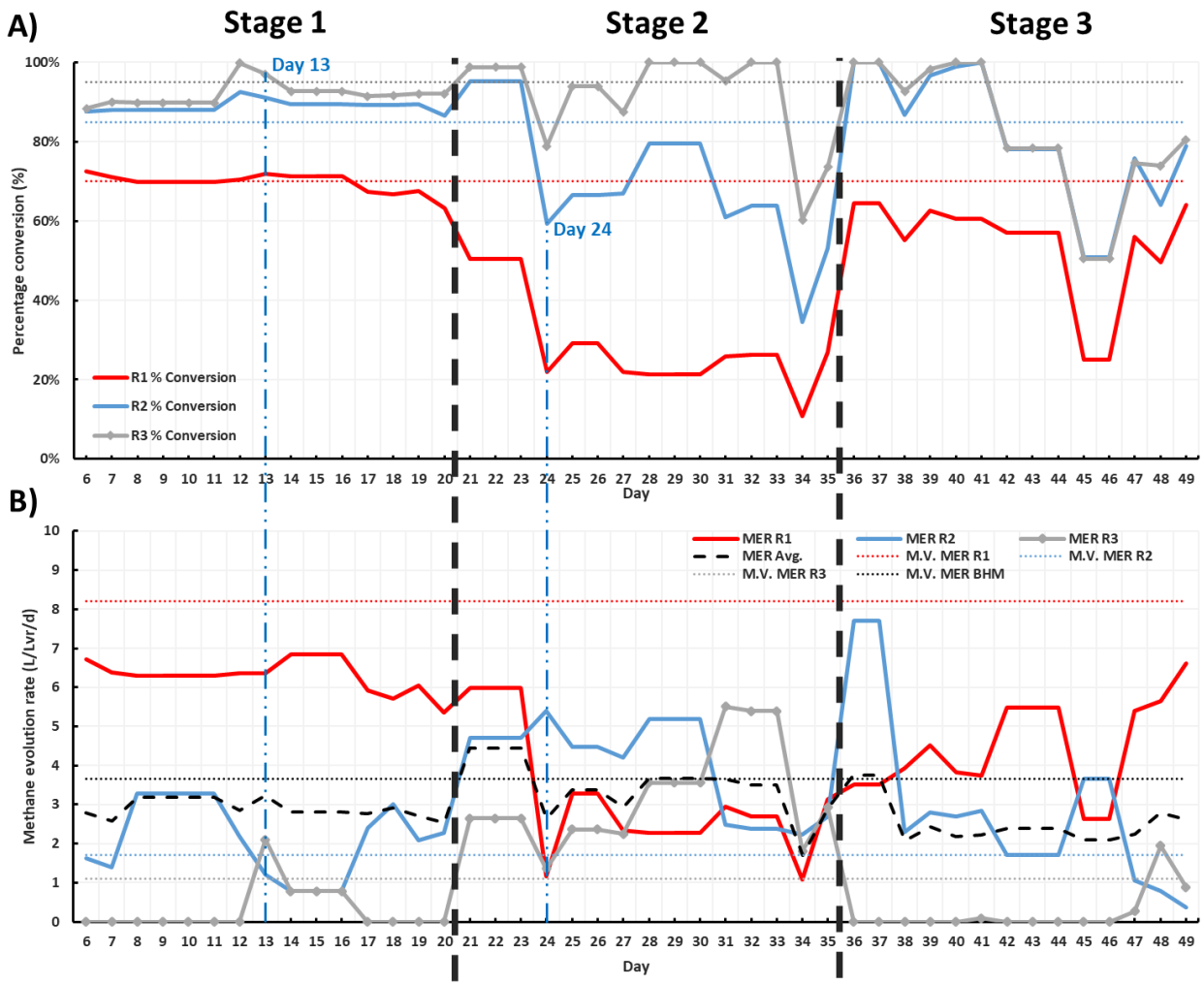


Figure 3.5: A) Percentage conversion of CO_2 in reactors 1 (red), 2 (blue) and 3 (grey). B) Methane Evolution Rates (MER); Dotted lines of respective colours indicate the peak performance of the simulated cascading system by Voelklein et al., the black dotted line denotes the average MER of the system, and the vertical dashed lines represent that change of flowrate from stages 1-3, as per Table 3.1 [16]. Days 13 and 24 are highlighted, indicating the data discussed earlier.

3.4 Results and Discussion

3.4.1 Limitations and solutions

Health and safety considerations were paramount and had a precedent over the research flexibility. This resulted in space, size, pressure, and volume restrictions for the system. The high-quality manufacture of the rig (meeting the ASTM A269 316L SS manufacture standards) and the complex nature of the prototype system resulted in restrictions. This limited its functionality, running counter to a fully flexible research and demonstration ethos, whereby it was desirable to increase the TRL. As a result, unforeseen issues were encountered post-manufacture, as discussed below.

Space limitations: The necessity for the rig to be housed in the fume-hood resulted in significant space restrictions. Coupled with the additional piping to accommodate a multitude of operations, the system necessitated installing a total of 58 Parker A-Lok manual valves. Due to minimal clearance, there is little room for future design changes, which may

require significant reconsideration of piping to accommodate any alterations. This has manifested in the low reactor volume and low bubble column height of the system.

The authors recommend a manual valve to be installed as per “Rev. 1” in Figure 3.6, to ensure a one-way flow of gas, which would be especially crucial during low flow rate operation. It is also advised that future revisions of the system eliminate space restrictions. This is to maximise the allowable bubble column height during the design phase, and ensure the maximum contact time for the working gases and the microbial fauna. This is noted as “Rev. 4” in Figure 3.6.

Microbial culture: The use of pure culture *Methanothermobacter* microbes, would suit laboratory scale experiments, due to the increased upgrading rates and overall better performance. The anaerobic environment of the system allows only for anaerobic microbes to grow. The continuous diffusion of H_2 and CO_2 promotes an environment for the hydrogenotrophic methanogens.

The authors recommend future experiments to be run using pure culture *Methanothermobacters*, after the system has been field tested, ensuring lasting operation, and maintaining the health of the microbes.

Flow totalisers: During the commissioning process, it was found that the outlet flow totalisers had been oversized. Initial design specifications necessitated the system to be capable of operating under pressure. The selected Krohne DK37/M8E (K 015) totaliser requires an operating pressure loss to be at least five times the pressure loss for gases (95 mbar pressure loss for the installed flow totaliser). This means that low gas flow rates would be difficult to measure if a pressure differential of 95 mbar cannot be achieved. This issue is especially important in a three-reactor *parallel* operation scenario.

The authors recommend replacing the flow totalisers with ones of a lower operational range. In addition, the use of a water displacement drum for measurement of the volume would be beneficial for accurate readings, should totalisers not be suitable, or flow verification be required. This revision is denoted as “Rev. 2” in Figure 3.6.

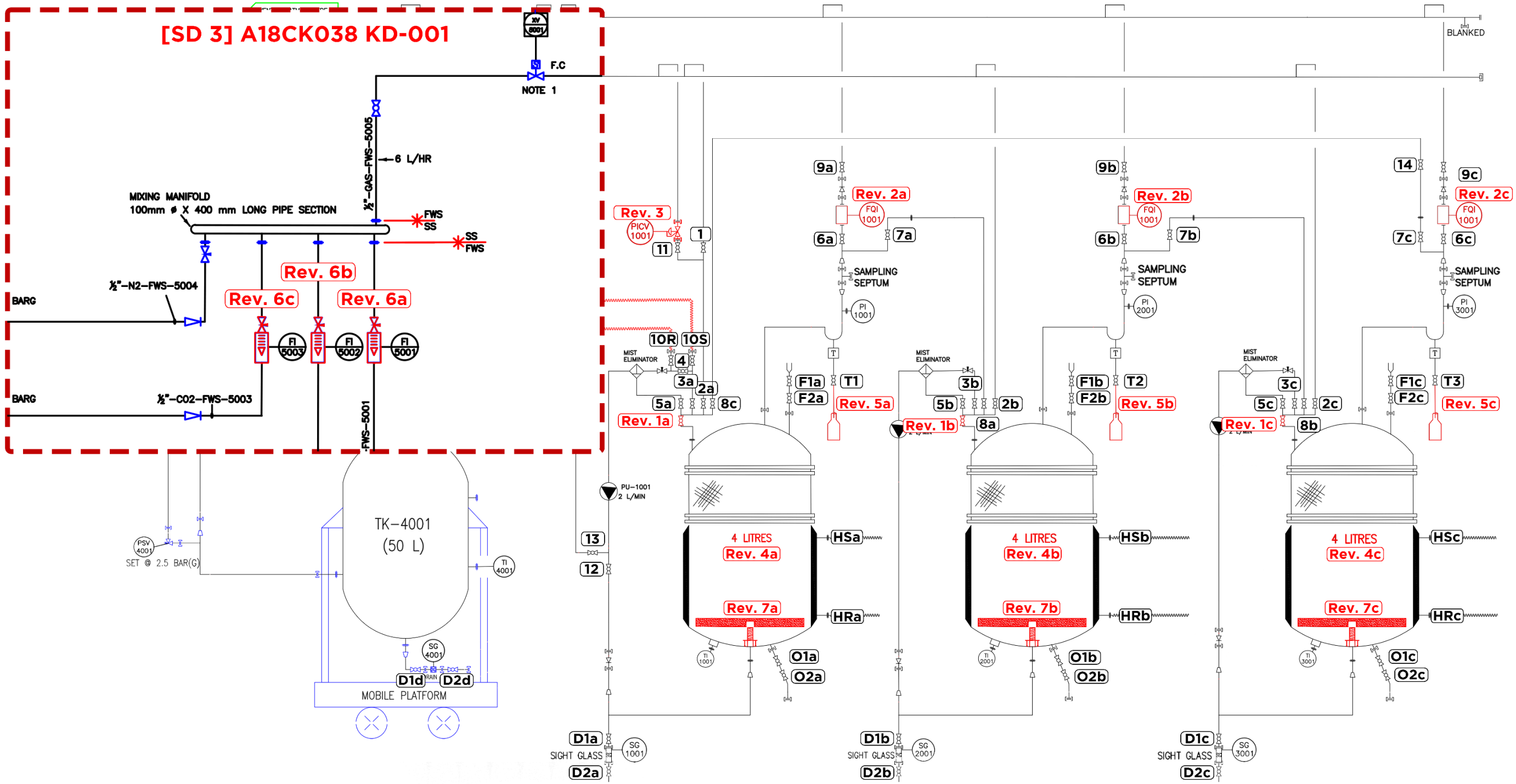


Figure 3.6: Edited P&ID of the proposed revisions to the biological methanation system

Low pressure-reducing valve: During the commissioning process, a leak was discovered on the PICV. Despite the fact that it was not in use and isolated from the system by an immediate downstream valve, a nozzle (Figure 3.7) appears to have been capable of leaking gas out into the fume hood, regardless of the flow rate. This was unprecedented and with no ability to isolate the PICV, the component was removed, and the line blanked. The associated PICV documentation does not show the leaking component ("B)" in Figure 3.7), nor were they found on general arrangement drawings. Figure 3.7 shows the absent components from the manual and the general arrangement drawings (See supplementary data "[SD 6.3] General arrangement drawings" and "[SD6.4] Manual valves"). The proposed revision is denoted as "Rev. 3" in Figure 3.6.

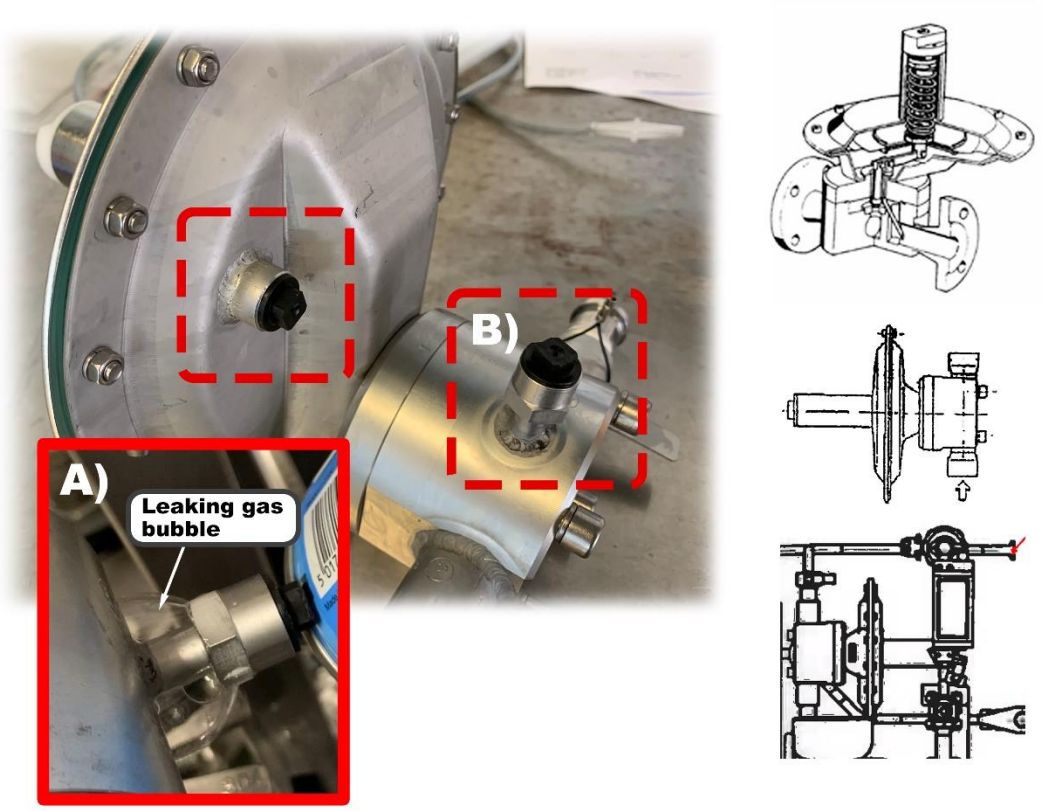


Figure 3.7: a) Image of leaking "nozzle" on the pressure indication and control valve. A bubble has formed by the use of a leak detector spray to reveal the leak. b) The leaking 'nozzle' is absent from the manual and general arrangement drawings.

Foaming: By using a standard liquor mix, the system encountered substantial foaming of the reactor liquor. During the early commissioning stage, and post-weekend start-up, the injection of H_2 into the reactors led to foaming; this is suggested to be associated with the dormancy of the methanogens over periods. Due to the small headspace, allowing the foaming to subside naturally was implausible. Instead, a low dosage (< 0.5 mL/$L_{digestate}$) of water-based antifoaming reagent was added, before being reintroduced into the reactor. Low-dosage water-based antifoaming agents have been suggested to be non-toxic to methanogenic archaea during the anaerobic digestion process [19]. As such, the addition is

not expected to have impacted the performance. The antifoam dosage was repeated periodically to maintain a stable reactor environment and prevent foam from entering the gas lines. In addition, no obvious negative effects on the biomethanation performance were observed.

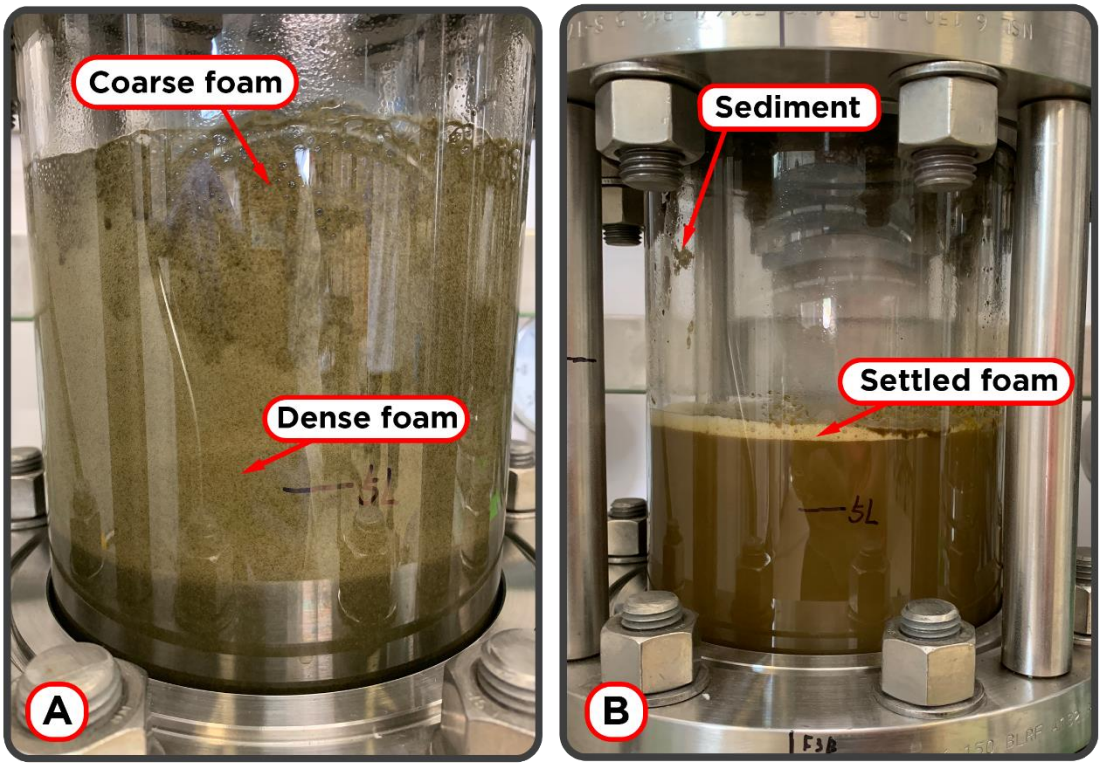


Figure 3.8: Example of reactor liquor before and after antifoaming agent addition. A) Early commissioning stage, with lower reactor volume to investigate the foaming. B) Late-stage commissioning with minimal foaming and higher reactor volume (6 litres). Due to the foaming, sediment is deposited high on the sight glass.

Water condensation: The condensation of moisture was an expected issue of the system due to production of water during the conversion of hydrogen and carbon dioxide to methane and water, as per Equation 3.1. Due to design restrictions, the installed pumps were located at a low point in the system, leading to moisture condensing at higher points, and eventually passing through the pumps, before accumulating at the condensate trap upstream from the diffuser. Coupled with the thermophilic system temperature, water vapour and slug flow (phenomena involving the condensation and accumulation of water droplets in a pipeline, building up to a body of water as the droplets are moved by the circulation of air) were unavoidable due to the vapour condensing at different locations within the system.

The authors recommend the implementation of a detachable moisture trap as per “Rev. 5” in Figure 3.6 to maximise moisture capture. Higher TRL revisions of the system necessitate a redesign of the moisture capture mechanism. The current system is limited by available vertical space.

Manifold: While the authors initially sought to avoid electronic equipment due to the ATEX rating, it is clear that the manually controlled rotameters for the working gases have hindered the quality of the data acquisition process. A common issue encountered has been the 'bobbing' and 'sticking' of the flow indicator. Coupled with non-linear flow controls, the flow rate readings have proved to be inaccurate (See file "[SD6.2] Manifold") and likely have contributed to errors discussed later.

The authors recommend the replacement of the manual rotameters with modular electronic flow controllers (such as "Voegtlin" digital mass flow meters) to ensure accurate flow control of working gases into the system. This corresponds to "Rev. 6" in Figure 3.6.

Diffuser: Due to the design of the system, it was impossible to situate the diffuser plate at the base of the reactor chamber. As a result, the protruding connection meant that approx. 1L of reactor liquor was below the diffuser plate. This resulted in approx. 10cm loss of column height, a significant amount for the reactor scale, which could otherwise have been part of the upgrading process. Additionally, while taking liquid samples, to ensure representative sampling, it is necessary to recirculate 2L of the microbial liquor to ensure a thoroughly mixed sample.

The authors recommend that should a higher TRL iteration of the system be constructed, a novel solution is required to ensure the diffuser is situated at the base of the system. This could be done with custom-designed and manufactured diffusers, with a connection port on the side of the diffuser, in contrast to the current design. This is noted as "Rev. 7" in Figure 3.6.

3.4.2 Discussion of data accuracy

While the commissioning data has been insightful, the authors noticed an issue in the data in the form of a mismatch in the gas throughput balance, based on the measured gas composition levels and measured flow rates. The authors have speculated several ways these errors could have been caused. The data acquisition for the gas flow was carried out in triplicate flow measurements, taken for each reactor (process described in ("(SD2) Standard operating procedure", section 7.2.20 'reactor output gas flow rate measurement'). The gas chromatography readings were sampled simultaneously according to the standard operating procedure. Due to the method of data collection, the errors were identical across the CO_2 volume, mass, and molar balances, as the data are based on the volume flow and gas chromatography data (See Figure 3.9). The errors are suspected to primarily originate from the gas measurement processes. When analysing the samples through the GC, the composition results returned are a percentage. The sum of the measured gases (H_2, CO_2, N_2, O_2, and CH_4) does not equal 100% of the composition, despite no other gas being present (this was verified through GC calibration gas tests). Therefore, the outputs had to be adjusted to account for this systemic inaccuracy using the simple Equation 3.6.

$$\%\ gas_{adjusted} = \frac{\%\ gas_{output}}{\%\ gas_{sum}} * 100 \qquad \text{Equation 3.6}$$

Where $\%gas_{adjusted}$ is the adjusted percentage composition of the analysed gas, $\%gas_{output}$ is the initial GC percentage output gas value, and $\%gas_{sum}$ is the summation of the initial GC gas output percentage values. The calculation is based on the understanding that one mole of CO_2 would generate one mole of CH_4. The adjusted gas composition values were then used with the gas flow rate values to evaluate the individual gas flow rates and compositions. These could then be used to assess the mass and volumetric flow through the system. To verify the data, these values were then used for the mass/molar and volumetric balance

$$\%\ error_{mass\ balance} = 1 - \left(\frac{\frac{gCO_{2out}}{d} + \frac{gCH_{4out}}{d}}{\frac{gCO_{2in}}{d}} \right) \qquad \text{Equation 3.7}$$

This adjustment yields an accurate composition while reducing the error (Table 3.3). This is exemplified in Figure 3.9, where the transparent data columns represent the unadjusted GC data. While this dataset adjustment removes a portion of the error in the data, it does not eliminate all uncertainty. The average errors for $R1_{in}$/ $R1_{out}$, $R2_{in}$/ $R2_{out}$, and $R3_{in}$/ $R3_{out}$ were 12.6%, 13.5%, 24.3% for the unadjusted GC results, and 8.7%, 8.0%, and 15.5% for the adjusted GC results, respectively.

Table 3.3: Day 8 gas composition output and the adjusted outputs.

Day 8	GC output	Percentage (%)		Adjusted (%)
R1 inlet	H_2	74.6	➔	78.6
	CO_2	20.3	➔	21.43
	Total	94.9		100.00
R1 outlet	H_2	40.30	➔	43.58
	CO_2	14.04	➔	15.52
	CH_4	37.83	➔	40.9
	Total	92.17		100

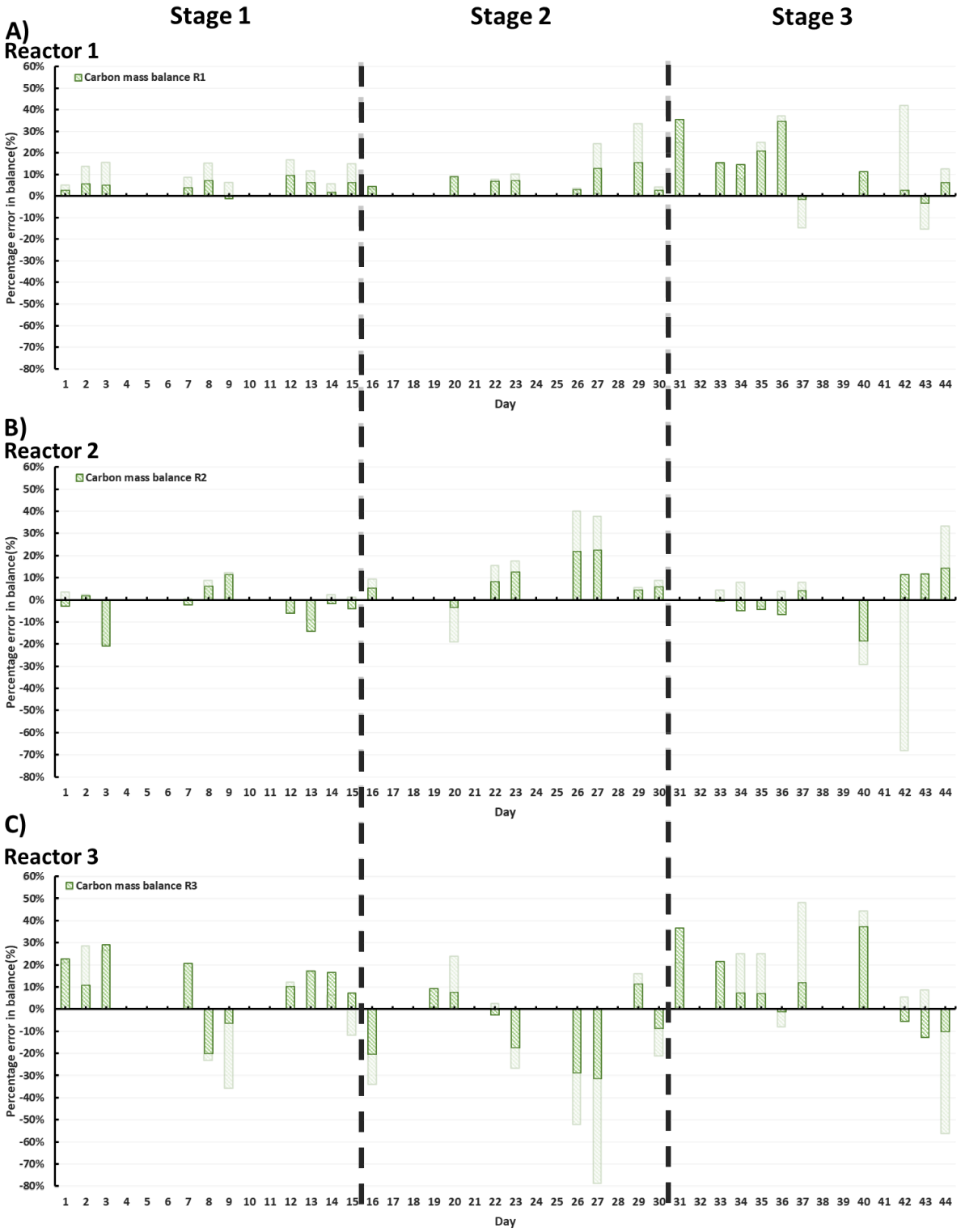


Figure 3.9: Percentage error in the carbon mass balance, across R1, R2 and R3, where; A) Error in balance – Inlet vs. R1 outlet; B) Error in balance – R1 outlet vs. R2 outlet; and C) Error in balance – R2 outlet vs. R3 outlet. Note the faded data columns represent the unadjusted errors in balance, based on Equation 3.7 values. The vertical dashed lines represent the change of flow rate from stages 1-3, as per Table 3.2.

3.5 Conclusion

In this study, a novel biological methanation system was designed and commissioned. The design criteria was based on a previous study carried out by the author. The previous study simulated a cascading three reactor system, proving the system viability. Based on these results, the current study carried out a design and comission of the cascading bubble biological methanation system. The design and commission was carried out in close collaboration with the university health and safety department and contracted engineering companies. The reactor design and commissioning processes were deemed successful. The fabricated system was capable of matching and with future modifications, exceeding the performance of the previously simulated system by Voelklein *et al.*

The authors conclude that a TRL of 4 was achieved in the design of the methanation rig. However, due to the limitations imposed by health and safety, the system was hindered from achieving a higher TRL. It is the authors' recommendation, to achieve a higher system TRL, to house the future reactors in an isolated location with open-air ventilation to avoid the associated complications discussed in this study, maximising the prototype's utility and flexibility.

The fabricated system is capable of matching and exceeding the performance of the simulated work by Voelklein *et al.* [16]. Despite the sub-optimal operation of the system, the system was capable of exceeding the 95% CO_2 conversion levels set out in the previous study, with peak conversions of 72%, 91% and 97% for R1, R2 and R3, respectively. The methane evolution rate across the three reactors averaged 2.5 – 3.4 $L/L_{vr}/d$, matching closely to the 3.6 $L/L_{vr}/d$ of the previous study. The system was shown capable of achieving grid quality levels, with grid quality biomethane (> 95% CH_4) converting most of the CO_2 during the commissioning process.

A major limitation of the experiment came in the restricted design of the system. Due to the risks associated with H_2, any changes or troubleshooting of system issues required communication with the University Health and Safety Officer and the contracted engineering companies. While this chain of command was imposed, the associated delays in electricians and specialist assessment turnaround resulted in months of delays, which resulted in experiments having to be postponed, or restarted. The authors have concluded that several revisions must be considered to the design, should a system be revised at an equal or higher TRL. These changes would include the resizing of flow totalisers and the addition of a water displacement drum for accurate volume measurement.

Acknowledgements

This work was supported by Science Foundation Ireland (SFI) through the MaREI Centre for Energy, Climate and Marine [Grant number 12/RC/2302_P2 and 16/SP/3829] with industrial funding from Gas Networks Ireland through the Green Gas Innovation group; and funding from the SFI zero emission challenge [Grant number 19/FIP/ZE/7565]. The authors would like to extend thanks to co-author Richard O'Shea for his guidance and support in the design of the methanation rig. Dr Gillian Bruton is thanked for her work in managing this project and securing the necessary budgets.

List of References

[1] IPCC, “Climate Change 2021: The Physical Science Basis,” Jun. 2021. [Online]. Available: https://www.ipcc.ch/report/ar6/wg1/downloads/report/IPCC_AR6_WGI_Full_Report.pdf.

[2] European Commission, “Communication from the Commission to the European Parliament, the Council, the European Economic and Social Committee and the Committee of the Regions - A hydrogen strategy for a climate-neutral Europe,” 2020.

[3] EU Directive, “Directive (EU) 2018/2001 of the European Parliament and of the Council of 11 December 2018 on the promotion of the use of energy from renewable sources.” [Online]. Available: http://data.europa.eu/eli/dir/2018/2001/oj.

[4] EirGrid and SONI, “Annual Renewable Energy Constraint and Curtailment Report 2019,” 2020. [Online]. Available: https://www.eirgridgroup.com/site-files/library/EirGrid/Annual-Renewable-Constraint-and-Curtailment-Report-2019-V1.2.pdf.

[5] R. A. Oduro and P. G. Taylor, “Future pathways for energy networks: A review of international experiences in high income countries,” *Renew. Sustain. Energy Rev.*, vol. 171, Jan. 2023, doi: 10.1016/J.RSER.2022.113002.

[6] N. Gray, S. McDonagh, R. O’Shea, B. Smyth, and J. D. Murphy, “Decarbonising ships, planes and trucks: An analysis of suitable low-carbon fuels for the maritime, aviation and haulage sectors,” *Adv. Appl. Energy*, vol. 1, p. 100008, Feb. 2021, doi: 10.1016/J.ADAPEN.2021.100008.

[7] D. Rusmanis, Y. Yang, R. Lin, D. M. Wall, and J. D. Murphy, “Operation of a circular economy, energy, environmental system at a wastewater treatment plant,” *Adv. Appl. Energy*, vol. 8, p. 100109, Dec. 2022, doi: 10.1016/J.ADAPEN.2022.100109.

[8] G. McNamara, “Economic and Environmental Cost Assessment of Wastewater Treatment Systems A Life Cycle Perspective By,” 2018.

[9] IEA, *The Future of Hydrogen*, no. June. OECD, 2019.

[10] S. McDonagh, R. O’Shea, D. M. Wall, J. P. Deane, and J. D. Murphy, “Modelling of a power-to-gas system to predict the levelised cost of energy of an advanced renewable gaseous transport fuel,” *Appl. Energy*, vol. 215, no. January 2018, pp. 444–456, 2018, doi: 10.1016/j.apenergy.2018.02.019.

[11] D. Rusmanis, R. O’Shea, D. M. Wall, and J. D. Murphy, “Biological hydrogen methanation systems – an overview of design and efficiency,” *Bioengineered*, vol. 10, no. 1, pp. 604–634, Jan. 2019, doi: 10.1080/21655979.2019.1684607.

[12] D. Rusmanis, R. O’Shea, D. M. Wall, and J. D. Murphy, “Biological hydrogen methanation systems–an overview of design and efficiency,” *Bioengineered*, vol. 10, no. 1. pp. 604–634, Jan. 01, 2019, doi: 10.1080/21655979.2019.1684607.

[13] R. O’Shea, D. M. Wall, S. McDonagh, and J. D. Murphy, “The potential of power to gas

to provide green gas utilising existing CO2 sources from industries, distilleries and wastewater treatment facilities," *Renew. Energy*, vol. 114, no. 2017, pp. 1090–1100, 2017, doi: 10.1016/j.renene.2017.07.097.

[14] I. Angelidaki *et al.*, "Biogas upgrading and utilization: Current status and perspectives," *Biotechnol. Adv.*, vol. 36, no. 2, pp. 452–466, 2018, doi: 10.1016/j.biotechadv.2018.01.011.

[15] S. Savvas, J. Donnelly, T. Patterson, Z. S. Chong, and S. R. Esteves, "Biological methanation of CO2 in a novel biofilm plug-flow reactor: A high rate and low parasitic energy process," *Appl. Energy*, vol. 202, pp. 238–247, Sep. 2017, doi: 10.1016/j.apenergy.2017.05.134.

[16] M. A. Voelklein, D. Rusmanis, and J. D. Murphy, "Biological methanation: Strategies for in-situ and ex-situ upgrading in anaerobic digestion," *Appl. Energy*, vol. 235, pp. 1061–1071, Feb. 2019, doi: 10.1016/j.apenergy.2018.11.006.

[17] European Commission, "Horizon Europe - Work Programme 2021-2022," no. May, pp. 1–37, 2021, [Online]. Available: https://ec.europa.eu/info/funding-tenders/opportunities/docs/2021-2027/horizon/wp-call/2021-2022/wp-13-general-annexes_horizon-2021-2022_en.pdf.

[18] B. Wu, R. Lin, X. Kang, C. Deng, A. D. W. Dobson, and J. D. Murphy, "Improved robustness of ex-situ biological methanation for electro-fuel production through the addition of graphene," *Renew. Sustain. Energy Rev.*, vol. 152, no. April, p. 111690, Dec. 2021, doi: 10.1016/j.rser.2021.111690.

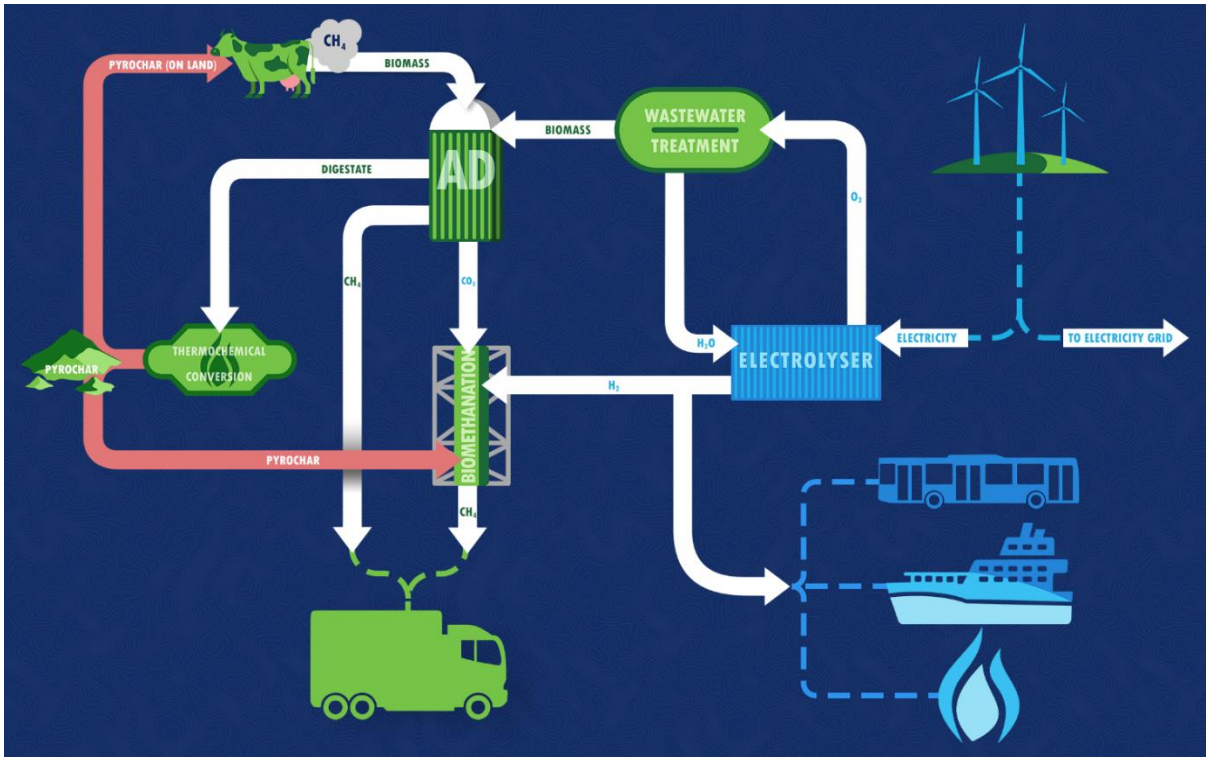
[19] S. Suhartini, S. Heaven, Y. Zhang, and C. J. Banks, "Antifoam, dilution and trace element addition as foaming control strategies in mesophilic anaerobic digestion of sugar beet pulp," *Int. Biodeterior. Biodegradation*, vol. 145, no. May, p. 104812, Nov. 2019, doi: 10.1016/j.ibiod.2019.104812.

4 Electrofuels in a circular economy: A systems approach towards net zero

Davis Rusmanis[1,2] , Yan Yang[1,2], Aoife Long[1,2], Nathan Gray[1,2], Kelvin C. Martins[3], Seán Óg Ó Loideáin[1,4], Richen Lin[1,2,5], Xihui Kang[1,6], Donal Óg Cusack[7] , James G. Carton[1,3], Rory Monaghan[1,4], Jerry D. Murphy[1,2], David M. Wall[1,2, *]

1. SFI MaREI Centre for Energy, Climate and Marine, Ireland.
2. Department of Civil, Structural and Environmental Engineering, School of Engineering and Architecture, University College Cork, Ireland.
3. School of Mechanical & Manufacturing Engineering, Dublin City University, Ireland.
4. Ryan Institute, School of Engineering, National University of Ireland Galway, Ireland.
5. Key Laboratory of Energy Thermal Conversion and Control of Ministry of Education, School of Energy and Environment, Southeast University, Nanjing, 210096, China.
6. Advanced Biofuels and Bioproducts Process Development Unit, Biological Systems and Engineering Division, Lawrence Berkeley National Laboratory, Emeryville, California 94608, United States.
7. DePuy Ireland Unlimited Company, Loughbeg, Ringaskiddy, Cork, Ireland.

Graphical Abstract



Abstract

Decarbonising the hard-to-abate sectors will be necessary in realising a future net-zero economy. Electrofuels store electricity as low carbon energy vectors such as hydrogen or methane which can be used in areas where electrification is not ideal, and as such can facilitate decarbonisation of sectors such as transport, agriculture, and wastewater treatment. In this study, the production of electrofuels was analysed at an industrial site by storing renewable electricity as green hydrogen produced using electrolysis. The analysis highlighted the need for scale in hydrogen production. The cost of hydrogen was calculated at €8.92/kg when a 122 kW electrolyser operated solely on curtailed electricity generated from the industry site was situated at a 65,000 person equivalent municipal wastewater treatment plant. A subsequent integrated and circular approach to electrofuels production was investigated. The oxygen by-product from electrolysis could be utilised for wastewater aeration and reduce the annual electricity usage at the wastewater treatment plant by 3.6%. Furthermore, the carbon dioxide in biogas generated from sewage sludge could be converted to methane through a Sabatier reaction ($4H2 + CO2 \rightarrow CH4 + 2H2O$) as a means of carbon capture and utilisation. The hydrogen produced from the 122 kW electrolyser could convert only 40% of the total carbon dioxide (within the biogas) in a biomethanation process, again supporting the argument for larger electrolyser systems with increased hydrogen production. Pyrolysis of digestate to produce biochar was investigated as a negative emissions technology. If pyrolysis is coupled with anaerobic digestion of feedstocks within 10 km of the industry site savings of 42.7 kt CO2/a could be achieved. In essence, a circular economy approach to electrofuel production could integrate existing electrical, gas and water infrastructure, whilst treating waste, improving the environment, decarbonising agriculture, and storing energy in the form of new low carbon energy vectors for use in heavy transport. Such an approach is vital to progressing future net-zero strategies, however future emissions accountancy processes must adapt to facilitate the benefits of a circular economy.

Highlights

Electrofuel production tackles hard-to-abate sectors in reaching net-zero emissions.

122 kW industry electrolyser could produce 17,100 kg H2/a at a cost of €8.92/kg H2.

Scale can be considered the key enabler for green hydrogen production.

Oxygen from electrolysis could reduce emissions from aeration by 16.04 tCO2eq/a.

Coupling anaerobic digestion with digestate pyrolysis can remove 42.7 kt CO2/a.

Keywords

Electrofuels; Green hydrogen; Biomethanation; Circular economy; Decarbonisation

4.1 Introduction

Whilst a global consensus was reached through the Paris Agreement to reduce greenhouse gas (GHG) emissions and limit global temperature rise below 1.5 °C, the complex logistics necessary to achieve such decarbonisation cannot be understated [1]. Furthermore, the European Green Deal has subsequently mandated that the EU must be climate neutral by 2050 and that all economic sectors should play a role [2]. However, hard-to-abate sectors such as transport, waste management, and agriculture are often overlooked, despite accounting for a significant proportion of emissions. In Ireland for example, agriculture accounted for 37% of annual GHG emissions in 2021 [3]. This highlights the difficulty in reaching a zero-carbon economy. There is no silver bullet solution to such hard-to-abate sectors. Full electrification will not satisfy all long-distance haulage vehicles nor the production of agri-products such as milk and cheese [4]. Holistic approaches are thus required to move towards net zero GHG emissions, facilitated by a circular economy integrating carbon capture and utilisation (CCU) technologies and novel negative emissions technologies (NETs).

4.1.1 The role of electrofuels in reacing net-zero

One method for progressing towards net-zero can be formed through the production of electrofuels. Recent projections have shown the Irish electricity grid will be operating at 80% renewable electricity by 2030 [5]. Whilst this is crucial, renewable wind and solar power introduces the issue of variable renewable energy (VRE) production which can cause the mismatch of energy production and energy demand. If no means for energy storage is available, electricity is curtailed or constrained [6]. Battery technologies can help alleviate this variability of production but are limited by low storage capacity and low discharge time. Of late, electrofuels (or power-to-X systems) have been mooted as a potential flexible energy storage solution complimenting VRE sources [7]. These electrofuels can be gaseous (hydrogen, methane) or liquid (methanol, Fisher-Tropsch diesel), enabling stable, energy dense, and relatively inexpensive forms of energy storage. Previous studies have shown the viability of hydrogen (H_2) production from VRE, relying on bidding strategies to determine the levelized cost of energy for production of H_2 [8], offering viable pathways for green H_2 in a sustainable green economy.

H_2 generated from the electrolysis of water presents a low carbon energy vector that can accommodate the aforementioned hard-to-abate processes which cannot be fully electrified [9]. H_2 can undergo further upgrading to methane (CH_4) when combined with carbon dioxide (CO_2); this can offset natural gas, maximise the utility of existing infrastructure and increase the share of renewable gas in the gas grid [10]. CH_4 can be further used in the production of fertilisers such as ammonia (NH_3), Fisher-Tropsch diesel or methanol (CH_3OH) [11]. The production of these electrofuels offers a green alternative to fossil hydrocarbon fuels that are widely used, particularly in the transport and agriculture sectors. To ensure a green electrofuel, green renewable electricity must be used in the production. This results in a complex problem requiring a complex solution, with a system-of-systems capable of

accommodating variability, capturing carbon, and creating a symbiotic cross-sector relationship. This system-of-systems is not expected to be easy to implement, but this study investigates how society must engage in forward thinking to ensure a sustainable future with sustainable systems.

4.1.2 Circular approach to electrofuel production

In creating a sustainable economy, a circular approach to energy production can enable the re-use of system by-products and establish a circular resource pathway. This can exemplify a system-of-systems approach, allowing previously independent sectors such wastewater treatment to be integrated to the wider energy network. Technologies such as electrolysis produce H_2 and oxygen (O_2), with the O_2 fraction often vented due to its market value not justifying the costs of storage and transport [12]. The capture and utilisation of this O_2 by-product has scarcely been investigated in literature. The investigation of electrofuel production and the utilisation of potential by-products (such as O_2), or the sizing of such systems in real-world applications has not been previously described in detail. Previous literature studies from Gray et al. [13], Lung et al. [14], and Ruggles et al. [15], have focused primarily on the function of electrofuels in the wider energy network.

It has been shown that in conventional wastewater treatment plants (WWTP), the aerobic treatment processes typically contribute up to 50% of the total energy demand of the WWTP [16]. Rusmanis *et al.* demonstrated how the by-product O_2 could replace air used to aerate the activated sludge process [17]. This would reduce the overall energy demand of the facility by a factor of 5, leading to substantial cost savings and GHG reductions [18]. Potential commercial viability for co-location of H_2 and O_2 production at the WWTP has also been previously assessed, with evidence of economic benefit for both electrolysers and the WWTP over a 25-year assessment period [19]. Furthermore, if the water is sufficiently treated it can be supplied back to the electrolyser, again supporting the circular economy approach. During the wastewater treatment process, nutrient rich biomass (primary sludge (PS) and waste activated sludge (WAS)) is removed from the contaminated waters and is often disposed of in landfills, or burned, releasing fugitive emissions [20]. Some WWTPs are equipped with anaerobic digestion (AD) systems, using a consortium of microbes to degrade the sludge and generate biogas. This biogas can be used in a combined heat and power unit to generate heat and electricity that can again be used onsite to offset the use of fossil fuels. Further opportunities for carbon capture and utilisation (CCU) can also be unlocked at the WWTP. Technology coupling such as AD and biomethanation (biological methanation combining H_2 and CO_2) can provide for carbon sequestration. Pilot scale demonstrations such as the “Electrochaea BioCat” plant have already demonstrated the potential symbiosis between a power-to-gas facility and a WWTP [21].

Wu et al. [22] and Lin et al. [23] previously assessed the mass and energy balance and GHG emissions, respectively, for a circular cascading system that integrated anaerobic digestion (AD) and biological methanation to upgrade biogas to high purity CH_4. These studies also

focused on pyrolysing the digestate from AD to produce syngas, pyro-oil and pyrochar and concluded that significant benefits could be attained in using biochar as an additive to the biomethanation process, promoting further symbiosis across the systems. Carbon neutrality will require negative emission technologies (NETs) to capture and store surplus carbon in the atmosphere [24]. NETs such as pyrolysis of the digestate from AD to produce biochar can have multiple functions, serving as a soil enhancer for increased crop productivity and a long-term carbon sequestration pathway.

To create a sustainable economy, a circular approach to the energy model can enable the re-use of system by-products establishing a circular resource pathway across the system-of-systems, allowing previously independent sectors such as wastewater to be integrated into the wider energy network. Technologies such as electrolysis primarily produce H_2 and oxygen (O_2), with the O_2 fraction often vented due to its market value not justifying the costs of storage and transport [12]. The capture and utilisation of this by-product O_2 have scarcely been investigated in literature when documenting circular, cascading systems. Literature has shown that in conventional wastewater treatment plants (WWTP), the aerobic treatment processes typically contribute up to 50% of the total energy demand of the WWTP [16]. The by-product O_2 could replace a fraction of the air used to aerate the activated sludge process, reducing the overall energy demand of the facility by a factor of 5, leading to substantial cost savings and GHG reductions,. The treated water can supply the electrolyser, again supporting the circular economy approach. During the wastewater treatment process, nutrient-rich biomass (Primary Sludge (PS) and Waste Activated Sludge (WAS)) are removed from the contaminated waters and are often disposed of in landfills, or burned, releasing fugitive emissions in the form of CH_4 and other gases. Some WWTPs are equipped with an Anaerobic Digestion (AD) reactor, using acetogenic and acetotrophic microbes to break down the sludge and generate biogas. This gas can be burned in a combined heat and power unit to generate heat and electricity that is fed back into the plant.

Carbon Capture and Utilisation (CCU) technologies such as when coupling AD and biomethanation (combining H_2 and CO_2) create opportunities for carbon sequestration. Pilot scale demonstrations such as the “Electrochaea BioCat” plant offer a good example of symbiosis between a Power-to-gas facility and a WWTP. Potential commercial viability for the co-location of H_2 and O_2 production at the WWTP has been previously assessed, with evidence of economic benefit for both electrolysers and the WWTP over a 25-year assessment period [25]. Other studies on electrofuels have focused primarily on their function in the wider energy network, yet omit the utilisation of by-products (such as O_2), the sizing of such systems, or real-world applications [13]–[15].

Wu et al. [22] and Lin et al. [23] previously assessed the mass and energy balance and GHG emissions, respectively, for a circular cascading system by integrating anaerobic digestion (AD), biological methanation to upgrade biogas to high purity CH_4. These studies focused on

pyrolysing the digestate from AD to produce syngas, pyro-oil and pyrochar. Carbon neutrality will require negative emission technologies (NETs) to capture and store the surplus carbon in the atmosphere [24]. NETs such as pyrolysis of the digestate from AD for the production of biochar can have multiple functions, serving as a soil enhancer for increased crop productivity and a long-term carbon sequestration pathway. Previous studies have also concluded significant benefits in using biochar as a performance-improving additive to the biomethanation process, promoting symbiosis across the systems.

4.1.3 Aims and objectives

In this study, the authors propose a novel cascading, circular economy system, that is based on the production of electrofuels through the capture of otherwise curtailed electricity. The aim of the system is to provide opportunities for improved decarbonisation of the hard-to-abate sectors, such as transport, agriculture, water, and the energy sector. The system-of-systems approach, as illustrated in Figure 4.1, is proposed to demonstrate how the hard-to-abate sectors could be tackled in a future strategy that strives to reach net-zero by reducing multi-sectoral emissions.

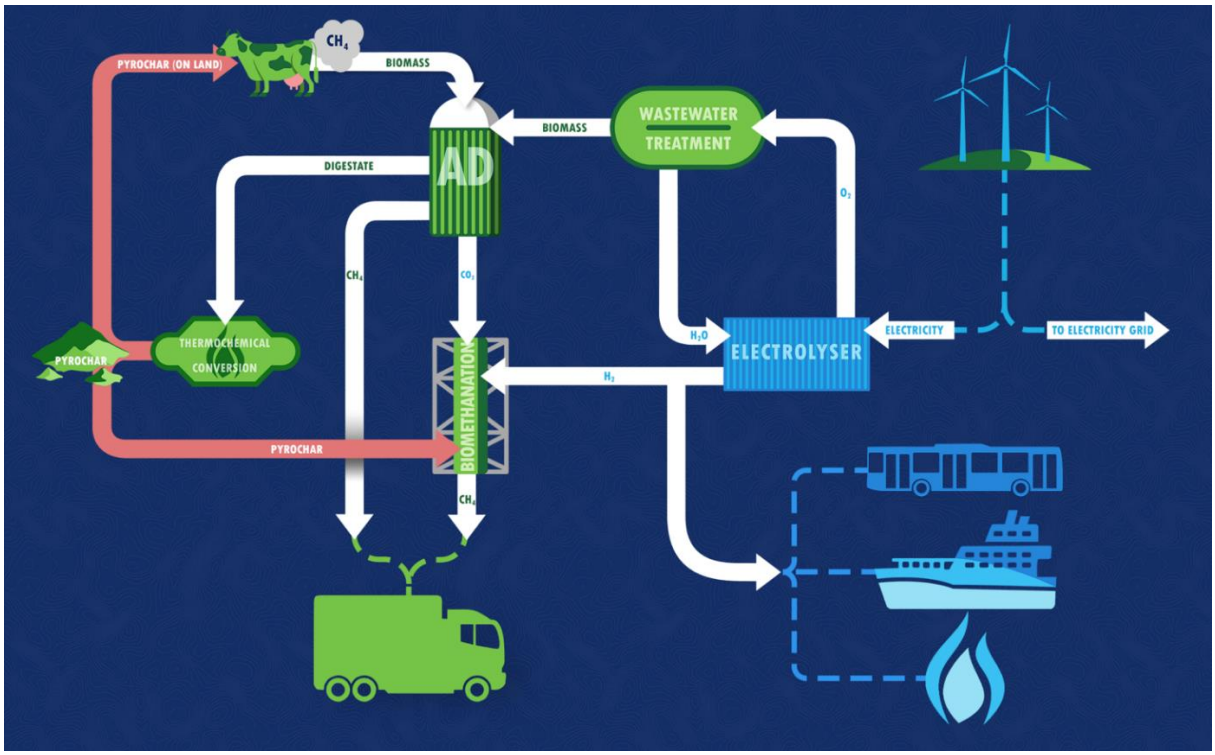


Figure 4.1: The proposed circular electrofuels production system.

The analysis herein considers a feasibility study of the proposed system at a local industrial site in Co. Cork, Ireland, where two existing 3-MWe wind turbines are located onsite, in close proximity to a WWTP of approx. 65,000 population equivalent (PE), with adequate gas and electricity infrastructure situated in the locality. The proposed system underlines the importance of situating electrofuel systems at opportune locations such as municipal wastewater treatment plants, which are frequently co-located with AD plants to process sludge waste from the WWTP aeration process. Municipal WWTPs exist in almost all urban locations and are often situated near existing grid infrastructure (gas and electricity), making WWTPs strategically optimal locations to produce electrofuels, synergising the three sectors of water, gas and electricity [26].

The potential end use of the H_2 and CH_4 electrofuels focuses on decarbonising the local transport network, in the form of hydrogen fuelled buses or a potential hydrogen ferry operating in the local harbour. Upgrading the carbon dioxide (CO_2) fraction of biogas from the AD process to biomethane can significantly increase the yield and simultaneously incorporate CCU technology into the circular economy system. To further expand the circular economy system the model also incorporates NETs through the integration of the pyrolysis of AD produced digestate. Additional feedstock that is available in proximity to the industrial site is also be accounted for to further reduce the potential for GHG emissions of the locality.

To advance beyond the state of the art in the development of the electrofuels in a circular economy concept, the following objectives are proposed for this study:

- Examine the suitability of storing renewable electricity as green hydrogen in terms of application (end-use) and cost (€/kg H2) at the proposed industry site;

- Explore opportunities to decarbonise the wastewater treatment process by integrating an electrolyser and recycling oxygen for aeration;

- Determine the potential for carbon capture and utilisation (CCU) from the coupling of anaerobic digestion and biomethanation technologies in the proposed system;

- Investigate the potential for negative emission pathways through the pyrolysis of digestate;

- Discuss the sustainability considerations to be addressed when implementing a circular economy approach to electrofuel production.Power to hydrogen production at an industrial site

4.2 Methods

The following section presents the methods used in assessing the electrofuels production within the proposed circular system (as per Figure 4.1). The section follows the flow of energy through the proposed system. The investigation starts at the industrial site capturing the surplus wind resource. The assessment of the available wind resource subsequently determines the electrolyser size. In turn, the hydrogen and oxygen resource potential are determined by the chosen electrolyser. This will allow for the evaluation of hydrogen as a potential transport fuel (for buses and a ferry), as well as the potential for emissions reduction in the wastewater treatment process through valorisation of the oxygen. Finally, the wastewater sludge resource is calculated for anaerobic digestion, the biomethanation potential (combination of H_2 and CO_2) is analysed and the subsequent negative emission technology (pyrolysis of digestate) is also investigated.

4.2.1 Potential to store surplus variable renewable energy as green hydrogen

To assess the ability to generate green hydrogen from surplus electricity, an industry site with two existing 3-MW_e wind turbines located in the Lower Harbour in Co. Cork, Ireland was selected as a case study for analysis. Granular data was obtained for the wind turbines, for the year 2019, which included for daily generated electricity, electricity demand on-site, and daily exported electricity to the grid. The data implied that the total electricity generated was 15.3 GWh_e/a with an average capacity factor (the ratio of actual output to the maximum possible output) of 28.7%. Of this total, ca. 12.8% (1.96 GWh_e/a) could be considered surplus to onsite requirement. The majority of the electricity generated was used by the industry across various onsite electrical demands.

4.2.2 Design of electrolyser for the industrial site

The electrolyser is the core component of an electrofuel system. The capital cost of the electrolyser and the cost of electricity are the main factors affecting the overall fuel production cost [27]. Electrolyser costs have reduced by more than 60% in the last decade and are anticipated to decline by more than 50% after 2030 [28]. Currently, the three most common electrolysers for green hydrogen production are the solid oxide electrolysis cells (SOEC), the alkaline electrolysis cells (AEC), and the proton exchange membranes (PEM). Of the 153 completed or planned power-to-gas (electrofuel) projects that are reported in literature, half of the projects have included for PEM electrolysers whilst the other half use AEC systems [10]. An overview of electrolyser characteristics, operating temperature, operating pressure, current density, efficiency, and start-up times are listed in Table 4.1.

Table 4.1: Summary of Electrolyser Technologies in 2020[a]

	AEC	PEM	SOEC
Cell component	Electrodes, membrane diaphragm, alkaline solution	Electrodes, solid polymer electrolyte	Electrodes, ceramic electrolyte
Charge carrier	OH^-	H_3O^+/H^+	O^{2-}
Electrolyte	NaOH or KOH Alkaline solution	Solid Polymer	Ceramic
Operation parameters			
Operating Cell Temperature (°C)	60-90	50-80	700-900
Operating Pressure (bar)	10-30	20-50	1-15
Current Density (A/cm^2)	0.25-0.45	1.0-2.0	0.3-1.0
Flexibility			
Cold Start-up Time	1-2 hour	5-10 minutes	Multiple hours
Load Range (% of nominal load)	20-100	0-100	-100/100
Warm Start-up Time	1-5 mins	< 10 secs	Up to 15 minutes
Efficiency			
Process efficiency (% HHV)	65-82	67-82	80-90
Durability			
Cell Stack Lifetime (k hours)	55-120	60-100	< 10
Efficiency degradation (%/a)	0.25–1.5	0.5–2.5	3–50
Economic			
Investment cost (€/kW)	800-1500	1400-2100	>2000
Maintenance cost (% of investment cost/a)	2-3	3-5	NA
Stage of technology	Mature	Commercial	Demonstration
Comments	• Long cold/warm start-up time can be a major disadvantage if the electrical input is renewable curtailed electricity	• Act dynamically in managing VRE sources • Heavy reliance on the availability of rare metals (e.g., iridium, platinum)/expensive materials. • The degradation of the catalysts leads to a short lifetime	• High energy efficiency • Low emission rate

[a]: Adapted from [21], [29], [30]; HHV: higher heating value

In selecting an electrolyser for the proposed industry site and the existing surplus electricity resource, a PEM system was considered optimal due to its ability to operate at high electrical current densities and variable power supply rates. The two turbines can theoretically produce up to 35,200 kg H_2 annually by utilising all the surplus electricity (see Box S4.1 in supplementary data). However, due to the intermittent nature of VRE, capturing all of it using an electrolyser would not be viable; a system that would be big enough to

capture all the excess energy of the winter months would be lying idle for long periods in the summer, producing hydrogen at very high prices. Thus, choosing the appropriately sized electrolyser requires consideration in terms of how much excess energy could be captured and finding the optimal point between electrolyser capacity, operating hours, and cost. Using the hydrogen production model developed by Gunawan et al. [31] and the analysed hourly wind data from wind turbines, the ideal electrolyser size for the industrial site could then be assessed [31].

4.2.3 Potential end uses for the green hydrogen

The green hydrogen produced could potentially be used directly as a transport fuel, or, injected directly to the existing natural gas grid which is accessible in proximity to the industrial site. At present, only small blends of hydrogen are permitted to the grid and many EU countries have stated a limiting range of 0–10 vol% [32]. It is expected that more injection of hydrogen to the existing natural gas grid will become prevalent in the next decade. For instance, Ireland has a target to introduce 13 vol% of hydrogen to gas network by 2050 [33]. The closest above ground installation (AGI) injection point to the industry site, at which the hydrogen could be injected to the existing gas grid, was located at a 6-km distance away and adjacent to the local WWTP. Preliminary modelling determined that it would be technically feasible to inject hydrogen to the local gas grid as volumes would be below current blending limits in Ireland (<0.1 vol H_2%). However, injection to the grid was calculated to incur an additional cost to hydrogen production assessed of €2.25/kg H_2 for transportation of the compressed gas from the industry site to the location of the AGI; this was assessed using Equations 1–4 below and the assumptions as described in Gunawan et al. [31].

$$LCOH_{trans} = \frac{\sum_{t=0}^{t=\tau WHS} \frac{C_{Inv,}TT}{(1+r)^t} + \sum_{t=0}^{t=\tau WHS} \frac{C_{OM,TT}}{(1+r)^t}}{\sum_{t=0}^{t=\tau WHS} \frac{M_{H_2}}{(1+r)^t}} \quad \text{Equation 4.1}$$

Where;

$LCOH_{trans}$ is the levelised cost of transported hydrogen; $C_{Inv,\,TT}$ is the sum discounted current value of the investment in the tube trailers (TT); *r* is the investment return; *t* is the number of years; and $C_{OM,\,TT}$ is the operation and upkeep expenses over the system lifespan per kg of H_2.

$$C_{OM,TT} = \left(\left(C_{O,TT} + C_{M,TT}\right) \times L_{AGI} \times N_{trip} \times 2\right) + C_{R,TT} \quad \text{Equation 4.2}$$

Equation 4.2 evaluates the complete operation and upkeep costs for the tube trailers. In the equation; $C_{O,\,TT}$ are the operational costs per kilometre for the tube trailer, $C_{M,\,TT}$ are the tube trailer upkeep costs per kilometre, L_{AGI} is the minimal distance between the wind farm and a grid injection location, N_{trip} is the sum trips carried out per annum(the return travel is represented by 2) and $C_{R,TT}$ is a ten-year tube trailer re-examination costs.

$$N_{trip} = \frac{365}{\frac{t_{SV}}{24}} \quad \text{Equation 4.3}$$

$$t_{SV} = M_{TT}/m_{H_2} \quad \text{Equation 4.4}$$

To reduce travel costs for each wind farm, N_{trip} denotes the mean storage period (t_{SV}), based on the mean hourly production in kg/hr (m_{H_2}), and the size of the tube trailer (M_{TT}), as shown in Equation 4.3 and Equation 4.4.

It is also possible to use the hydrogen generated to produce other synthetic gaseous energy carriers such as methane, or liquid energy carriers such as methanol (CH_3OH) [34]. This approach will be investigated in Section 4.2.5 as a means of CCU, that is, combining hydrogen with carbon dioxide to produce methane or methanol.

4.2.4 Oxygen recovery in the wastewater aeration process

The circular economy model can be realised through the integration of the electrolyser at a municipal WWTP which is typically a large energy consumer in municipalities. Oxygen from electrolysis is a valuable resource for the energy-intensive aerobic treatment processes commonly adopted at WWTPs. The aeration energy demand of conventional WWTPs using activated sludge systems, accounts for ca. 50% of the total plant energy due to the pumping of large volumes of compressed air into the aeration tank [16]. When it is considered that oxygen comprises only 21% (volumetric ratio) of air, then pumping air equates to pumping 79% of redundant gas volume (predominately nitrogen) which is not required for aeration. As such, pumping can be reduced by a factor of 5 if pure oxygen is used in aeration. Oxygen from electrolysis can be used at the WWTP to reduce energy costs (pumping O_2 in lieu of air) and as such the carbon footprint associated with the aeration processes [35]. This approach adds value to the oxygen by-product, which may otherwise be vented-off due to lack of cost-effective local solutions. Situating the electrolyser at the WWTP creates an opportunity to partially subsidise hydrogen production and increase its commercial viability [25].

In practice, the oxygen levels in the aeration tank of the WWTP must be maintained constantly to sustain biological activity. Equation 4.5 presents a standard design formula adapted to evaluate the sum oxygen demand for an activated sludge system [36].

$$OD = 0.75 * Q * (BOD_i - BOD_e) + 2 * V_A * \frac{MLSS}{1000} + 4.3 * Q * (Amm_i - Amm_e) - 2.83 * Q * [(Amm_i - Amm_e) - N_e] \quad \text{Equation 4.5}$$

In the equation, OD is the WWTPs hourly oxygen demand, (g/h); Q is the flowrate at inlet of the WWTP, (m^3/h); V_A is the volume of the aeration tank, (m^3); MLSS is the mixed liquor suspended solids in the aeration tank (g/L); BOD_i and BOD_e are the inlet and outlet

concentrations of BOD (g/m^3); Amm_i and Amm_e are the inlet and outlet concentrations of ammoniacal nitrogen (g/m^3), and N_e is the exit flowrate of nitrate nitrogen (g/m^3).

When raw unsettled sewage is processed with extended aeration, the factor of '0.75' changes to '1.0' in Equation 4.5. This is due to omission of the primary settling from the treatment process. These calculations ignore the efficiencies of the shaft and the motor, among other losses. As such, the equations are a simplified estimate of the reality. For higher resolution results, a revised assessment of each individual WWTP is necessary for exact oxygen demand and sludge production is necessary.

4.2.5 Carbon capture and utilisation through biological methanation

Anaerobic digestion at WWTPs is commonly used for the treatment of sewage sludge. This sludge primarily comprises of primary sludge (PS) from the primary sedimentation tank (if one is employed) and waste activated sludge (WAS) from the aeration basin. The primary sedimentation tank removes approximately 50% of the solids and produces a relatively rich primary sludge which offers relatively high gas yields in the AD process (Equation 4.6).

$$PS_{removed} = \frac{50\% \times Q \times TSS \times 24}{1000} \qquad \text{Equation 4.6}$$

In the equation, PS is the removed primary sludge (kg DS/d); Q is the municipal WWTP inlet flowrate (m^3/h); TSS is the municipal WWTP inlet total suspended solids (g/m^3); 50% is the TSS rate of removal from the primary tank. The second biomass removal occurs during the extended aeration process, where WAS is generated as a by converting organic material into cell biomass (Equation 4.7).

$$WAS_{produced} = 0.75 \times \frac{Q \times (BOD_i - BOD_e) \times 24}{1000} \times 0.6 \qquad \text{Equation 4.7}$$

In the equation, WAS refers to the produced waste activated sludge (kg DS/d), 0.75 denotes the 25% of the BOD removed from the wastewater due to the associated 50% TSS removal during primary sedimentation; Q is the municipal WWTP inlet flowrate (m^3/h); BOD_i and BOD_e are the inlet and outlet concentrations of BOD (mg/L), and 0.6 refers to the waste sludge output in kgDS/kg $BOD_{removed}$. The properties of these can be found in Table 4.2.

Table 4.2: AD process yields for primary, and waste activated sludge.

Primary Sludge			Waste Activated Sludge		
SMY	345	L CH_4/kg VS	SMY	87	L CH_4/kg VS
CO_2	33	%	CO_2	50	%
CH_4	67	%	CH_4	50	%
VS/TS	77	%	VS/TS	48	%
Ref.:	[37], [38]		Ref.:	[39]	

SMY – Specific Methane Yield.

To optimise the positioning of the electrolyser at the wastewater treatment facility and to complement oxygen utilisation in the wastewater treatment process, the green hydrogen generated can also be used onsite to upgrade biogas from the AD process to methane via the biological hydrogen methanation process utilising the Sabatier reaction (Equation 4.8).

$$4H_2 + CO_2 \rightarrow CH_4 + 2H_2O, \Delta G_0 = -165\ kJ/mol \qquad \text{Equation 4.8}$$

The reaction is facilitated by hydrogenotrophic methanogenic archaea [32]. As per the equation, a source of CO_2 is required. Biogas produced by sludge digesters at municipal WWTPs can serve as a biogenic source of CO_2.

4.2.6 Integration of pyrolysis as a negative emissions technology

Negative emission technologies (NETs) will be necessary in meeting future climate mitigation scenarios [40]. Thermochemical treatment of digestate in the form of pyrolysis under an oxygen free environment can offer a potential NET pathway. Digestate comprises of water, microbial biomass and slow to degrade substrates, which can be dewatered, and applied to agricultural land as a biofertilizer [41]. Pyrolysis of digestate results in the production of biochar (a stable carbon-rich charcoal like material). Biochar can be applied as a soil enhancer for land-based crop productivity, increasing soil organic content, leading to increased photosynthesis and increased draw-down of CO_2 from the atmosphere, establishing long-term storage of carbon [40]. Additionally, pyrolysing digestate can reduce the agricultural land requirement for digestate application, while producing additional energy in the form of syngas and pyro-oil [42]. A NET system incorporating pyrolysis can enable the production of biochar as a means of long-term CO_2 sequestration from the atmosphere (Figure 4.1). The addition of the process to the existing circular electrofuel production system would maximise the potential for GHG emission reduction.

The key to realising this NET lies in the technology for the pyrolysis of organic feedstock. The stability of biochar depends on the elemental oxygen-to-carbon (O/C) ratio. Biochar requires an O/C ratio below 0.2 for it to possess an approximate half-life of over 1000 years. However, biochar with O/C ratio of 0.2–0.6 has a half-life of 100–1000 years [43]. Biochar can also be used as a carbonaceous additive, which can be recycled back into the digester and into the biological methanation process to enhance CH_4 production through potentially improved direct microbial electron transfer efficiency [44], [45]. Literature has shown that biochar (derived from woody biomass) added to the digestion of seaweed enhanced the CH_4 yields by 17% [42]. Furthermore, the produced syngas from the pyrolysis process could be a supplementary substrate for biological methanation, due to high H_2 and CO_2 content [46]. Implementation of this NET would synergise with the majority of the system components, simultaneously boosting biomethane yields, reducing digestate amounts and increasing net energy outputs. Wu et al. proposed a bespoke circular cascading system with AD as the focal technology, utilising electrofuels and biochar, demonstrating a reduction of 11% in the digestate amount and a 70% increase in biomethane production [22]. The study also claims

that such an integrated system could achieve a 70% increase in the net energy output (in the form of methane), as compared to traditional anaerobic digesters with amine scrubber biogas upgrading technology.

4.2.7 Emissions reduction by integrating anaerobic digestion with pyrolysis

The viability of the NET for GHG emissions reduction depends on the availability of feedstock in the surrounding area for the AD process. This determines the quantity of digestate for the thermochemical process (pyrolysis producing biochar). Increasing the quantity and quality of the pyrolysis products can be achieved through co-pyrolysis of the WWTP sludge and other organic feedstocks available in the locality.

In an Irish context, typical feedstocks for AD include cattle or pig slurry, grass silage, and food waste [47], [48]. The mixing of different AD feedstocks and process conditions for pyrolysis will both impact the biochar yield and its carbon content. For example, pyrolysis of sewage sludge is stated to have a biochar yield of 40.2–54.5% of the feedstock dry weight and an average carbon content of 18.1–31.5% [49], [50]. In contrast, pyrolysing agricultural residues was shown to offer a biochar yield of 23.7% of the feedstock dry weight and an average carbon content of 55–70% [51].

A simple assessment of GHG emission savings through biochar production is presented herein. A reasonable assumption is that based on 100 t dry sewage sludge, at least 26.7 t CO_2 (=100 t dry solids in sewage sludge × 40.2% biochar yield × 18.1% carbon content in feedstock × 3.67 tCO_2/t C) can be sequestered through biochar production via the combined AD and pyrolysis system. Furthermore, the biochar can improve soil fertility through increased soil organic content, enhancing crop growth and yield with the increased photosynthesis efficiency, leading to additional CO_2 sequestration from the atmosphere [52].

4.3 Results and discussion

Based on the methods proposed in Section 4.2, the potential for electrofuel production in a circular economy is now assessed. The following results and discussion section presents the calculations for the industrial site in terms of hydrogen and oxygen production, electrolyser specification, the end-uses for both hydrogen and oxygen, the potential for CCU and the emissions savings from the use of NETs.

4.3.1 Wind resource potential from the industrial site

The percentage of total wind energy dispatched down as compared to the total produced electricity in Ireland in 2019 was 11.4% (ca. 1,448 GWh out of 12,656 GWh) [6], which is not dissimilar to the ratio of surplus electricity (12.8%) at the selected industrial site. This excess electricity resource at the industrial site could now be considered for green hydrogen production through water electrolysis (Figure 4.2). Two end uses were proposed for the hydrogen: 1) direct injection to the existing gas network and 2) utilisation as an advanced transport fuel. A preliminary analysis indicated that the maximum resource of hydrogen that

could be generated at the industrial site was 392,000 m^3 H_2/a or 35,200 kg H_2/a (Box S4.1 in supplementary data).

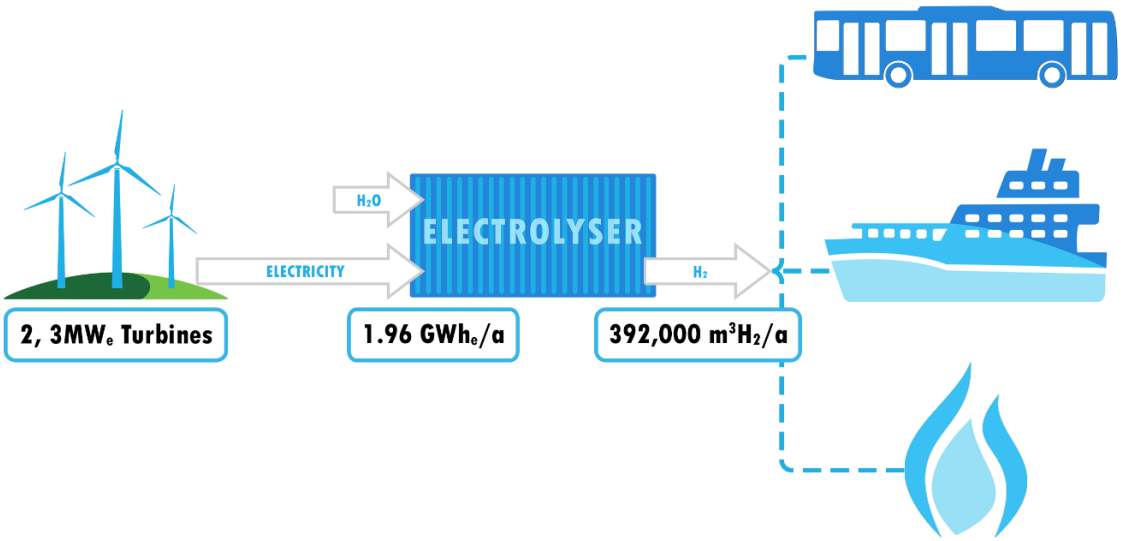


Figure 4.2: Utilisation of all surplus VRE to produce green hydrogen for potential gas grid injection or as a transport fuel.

4.3.2 Electrolyser specifications for the industrial site

Utilising the model developed by Gunawan et al. [31], the optimal electrolyser size was calculated to be 122 kW as per Figure 4.3. Such an electrolyser would have a capacity factor of 74% and produce up to 17,100 kg H_2/a (ca. 190,300 m^3/a) at 60% (LHV) efficiency, representing 48.5% of the aforementioned theoretical resource of hydrogen that could be produced at the site (Box S4.1 in supplementary data). The Levelised Cost of Hydrogen (LCOH) in this case, taking account of the electrolyser size and resource of surplus electricity, was calculated at ca. €8.92/kg H_2, as seen in Figure 4.3.

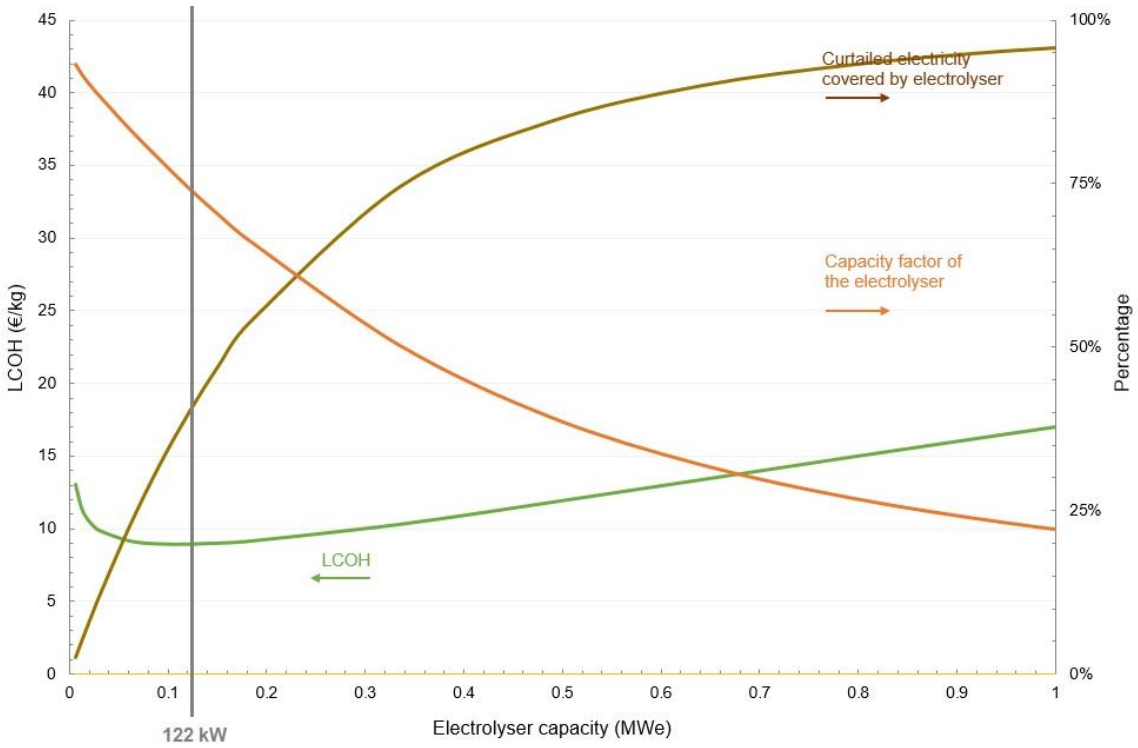


Figure 4.3: Electrolyser capacity and levelized cost of hydrogen. The optimal 122 kW system is represented by a vertical black line intersecting the Capacity Factor curve (orange), the Curtailed Energy Capture curve (brown) and the LCOH curve (green).

The 122 kW electrolyser proposed for the industry site would produce hydrogen at the lowest possible cost of a range of scenarios tested. However, the volume of hydrogen produced is relatively small and the cost is high; €8.92/kg H2 is equivalent to €0.27/kWh, well above commercial natural gas prices at industry scale (ca. €0.03/kWh in 2021) though not dissimilar to prices in 2022 as a result of the geopolitical events in Ukraine. An alternative strategy could be carried out to adopt a larger system and increase the output, although that would result in an even higher LCOH (as per Figure 4.3). This is further illustrated in Figure 4.4, which displays the excess electricity in red throughout the year from the two turbines at the industrial site. The electricity resource captured by the 122 kW electrolyser is shown in green. A decision could be made to increase the quantity of electricity captured by choosing a larger, more expensive electrolyser. Furthermore, an electrolyser at 122 kW is not a commercially available option, the closest available being a 140 kW system which could be obtained by a commercial manufacturer “CPH2” with an investment cost of ca. €428,000.

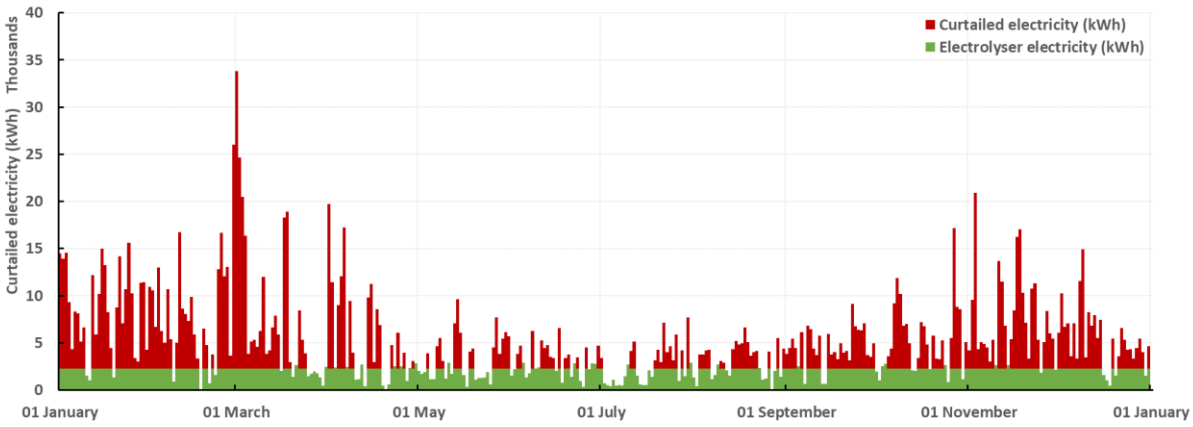


Figure 4.4: Surplus electricity captured by the 122 kW PEM electrolyser at the industrial site.

4.3.3 Hydrogen as a transport fuel

Hydrogen is considered an advanced transport fuel and is particularly suitable for long-distance and heavy-goods transportation [4]. To facilitate a renewable transport sector, it was also proposed that the industry-derived hydrogen resource could be applicable to the local public bus service, or a commuter ferry given the specific industrial site is located in a harbour. An analysis of the associated hydrogen resource of 17,100 kgH_2/a from the industry site suggests the potential to provide the fuel necessary for 5 hydrogen buses providing 4 round trips per day from the industry site to Cork City (38 km round trip); or providing the fuel for 5,512 km of travel for a hydrogen commuter ferry with an estimated capacity of 84 passengers. The full calculations are shown in Box S4.2 in supplementary data. Such an approach would provide a means for zero-emissions transport from the proposed industry site to the local zone of major population.

The evidence presented in Box S4.2 in supplementary data suggests that the quantity of excess electricity is inherently small and most likely insufficient to run one ferry. The electrolyser that would be coupled with these turbines is also relatively small and this exacerbates the cost of hydrogen. The total cost of hydrogen for grid injection (which may be the most likely means of deployment) equates to approximately €10/kg (or €0.3/kWh or €3/L diesel equivalent) when including the cost of production and transportation. This can be compared to an analysis by McDonagh et al. [53] which suggested that the cost of hydrogen needs to be in the order of €4/kg H_2 to be financially viable from offshore wind (in a hybrid model producing electricity and hydrogen) as opposed to curtailment. It is also far above the target cost for 2030 set by the Hydrogen Council of approximately $2.50/kg (equivalent to €2.22/kg at a USD/EUR exchange rate of 0.89) [54].

The key learning from this analysis is that curtailed electricity from two number 3-MW wind turbines on its own would not be sufficient to make hydrogen financially competitive as a transport fuel. This is in agreement with other studies which suggest curtailed electricity alone may not be sufficient for cost effective hydrogen production and increasing operating hours by purchasing cheap electricity from the grid would be a critical function in making green hydrogen cost-effective [8], [55]. In essence, scale can be considered the key enabler

for green hydrogen production and large resources of electricity are required to run electrolysers cost-effectively.

4.3.4 Oxygen recycling to the wastewater treatment process

The total oxygen produced was calculated to be 135,660 kgO_2/a as per Box S4.3 in the supplementary data. Based on the influent wastewater properties (see Table S1 in Box S4.3 in the supplementary data), this oxygen resource accounts for only 8.9% of the estimated demand of the local WWTP in proximity to the industrial site which was sized at a capacity of 65,000 PE.

At WWTPs, fine-bubble diffusers are generally used to diffuse oxygen into the wastewater by pumping air. Transfer rates of 2.0–2.5 kg O_2/kWh_{el} are typically achieved with this standard method [56]. The use of pure oxygen (from electrolysis) can reduce the on-site energy consumption associated with air compression as only approximately one-fifth of the volume is now required [26]. The study by Mohammadpour et al. [35] reported a 550% performance improvement with identical equipment, only by substituting pure O_2 gas in the aeration process, instead of air. This was due to factors such as high solubility, 500% higher O_2 driving force, and a 20% increase in the volumetric mass transfer coefficient for the smaller bubbles (relative to air). Therefore, if the pure oxygen resource from the 122 kW electrolyser (135,660 kg O_2/a) was fully utilised for aeration at the WWTP of 65,000 PE, the electricity saved to transfer oxygen demand would equate to 49.4 MWh_{el}/a (see Box S4.3 in supplementary data). Consequently, CO_2 emissions savings of approximately 16.04 tCO_2eq/a, or an overall reduction of 3.6% could be achieved through a reduction in electricity usage at the WWTP (see Box S4.3 in supplementary data). This analysis assumes that a pure oxygen stream from the electrolyser is added to the aeration system while the existing aeration system utilises air.

4.3.5 Biomethanation and the potential for carbon capture

Biomethanation converts CO_2 to CH_4 through the addition of H_2 in a Sabatier reaction (see Equation 4.8). In consideration of this case study, digestion of sewage sludge at the local WWTP with a design capacity of 65,000 PE has the potential to produce 214,800 m^3 CH_4/a and 118,200 m^3 CO_2/a (see Box S4.4 in supplementary data). Assuming that all of the CO_2 is captured and converted, the CH_4 output from the digester at the local WWTP could be increased by 53.8% (converting 118,200 m^3 CO_2 to CH_4 as per Box S4.4 in supplementary data). However, due to the relatively small electrolyser size (122 kW), there is not enough H_2 produced to capture all of the CO_2 in the biogas from the sludge digester. In the current scenario, the H_2 produced from a 122 kW electrolyser could convert 40% of the total CO_2 produced through a biomethanation process (Box S4.4 in supplementary data). Thus, in this instance, it may be more advantageous for the produced H_2 to be used directly as an advanced transport fuel to decarbonise heavy transport or injected to the local gas grid network as described in Section 4.2.3. However larger scale electrolysers would again enable the potential for carbon capture at the WWTP.

In theory, hydrogen generated from electrolysis could capture CO_2 from any nearby digestion system (not exclusive to WWTP) and could allow for the specific targeting of hard-to-abate sectors such as agriculture. In Ireland, agriculture was responsible for 37.1 % of total GHG emissions in 2020, in which manure management contributed up to 10.3% of these emissions [57]. Hydrogen may potentially be used to capture the CO_2 from agricultural digesters treating slurries and manures to produce biomethane. In this way, hydrogen can offset the requirement for traditional biogas upgrading and the associated costs of such methods. Furthermore, any industry process generating CO_2 emissions would also be suitable for biomethanation, especially, large CO_2 stationary sources including ethanol fermentation plants (nearly 100% CO_2 by vol.) and cement manufacturers (average 20% CO_2 by vol.) where concentrated CO_2 streams exist [58]. This approach is further justified by the inherent corporate social responsibility of such industries in progressing towards carbon neutrality. Figure 4.5 presents a visual summary of the results obtained from the electrofuel in a circular economy system located at the WWTP.

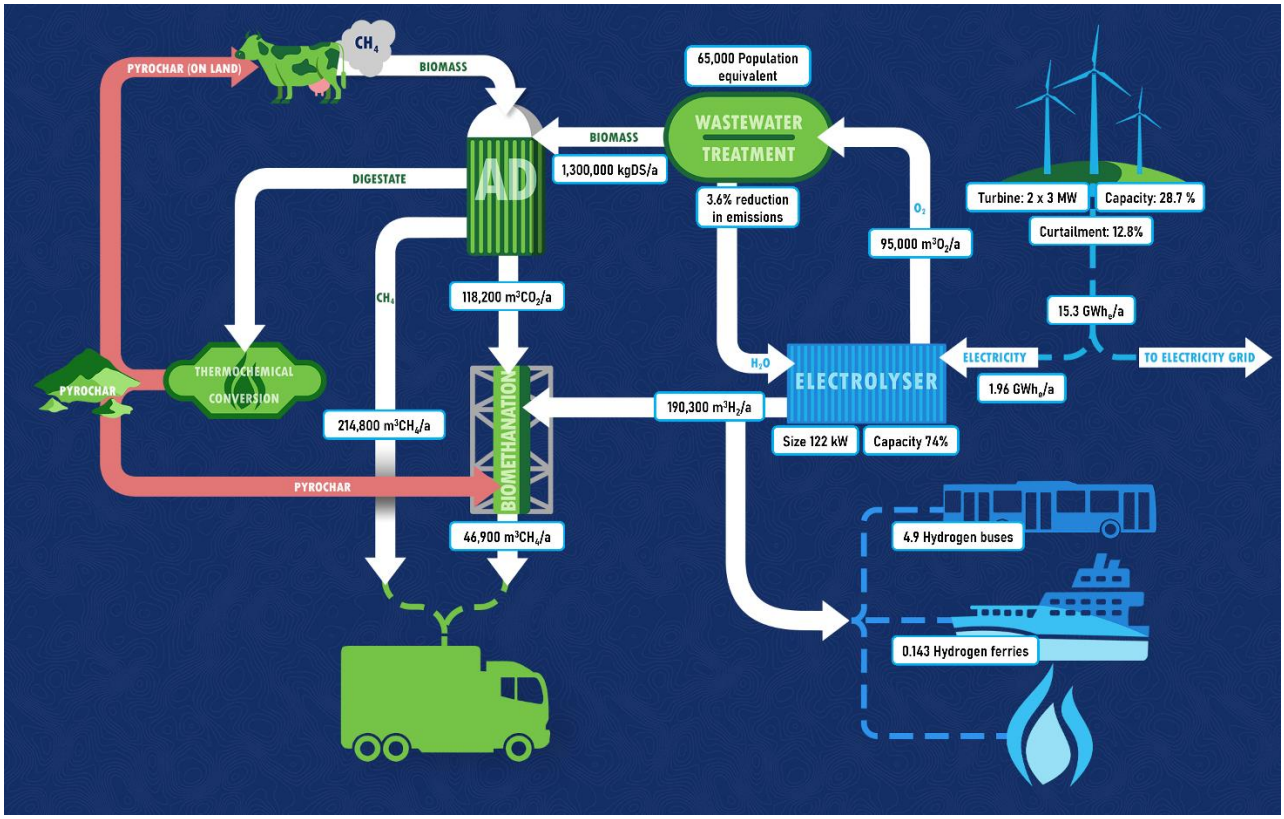


Figure 4.5: Summary flow diagram of the circular economy system at a local industrial site.

4.3.6 Co-locating electrolysers and biomethanation at municipal wastewater treatment plants

WWTPs are usually located in urban locations offering geographically favourable site conditions to produce electrofuels with significant synergies in the coupled sectors (water, gas, electricity). Storage of hydrogen is expensive, but WWTPs with existing AD systems can use hydrogen to upgrade biogas. Co-locating electrolysers and biological methanation systems at existing WWTPs offers numerous benefits such as storage of intermittent renewable energy, decarbonisation of aeration processes at WWTPs with recycled O_2, the offset of traditional biogas upgrading costs (through carbon capture by biological methanation), and decarbonisation of heavy transport through advanced hydrogen, methane, or methanol production. Such developments to date have been scarce. However, the "Electrochaea BioCat" plant located at the local WWTP of 350,000 PE in Avedøre, Denmark demonstrated such novel technology. An on-site 600 kW AEC electrolyser was powered by renewable electricity in conjunction with the local power grid to generate hydrogen which was delivered to an on-site biological methanation reactor. CO_2 was sourced from biogas produced from a biogas plant in the local municipality [18]. Hydrogen and biogas were introduced to the biological methanation system at a stoichiometric ratio of 4:1 (H_2: CO_2) for further conversion to methane. The generated biomethane (which achieved a purity of 97 – 98.6%) was added to the local gas distribution grid, which operates at a pressure of 3 bar [21]. Other novel technologies, such as steam explosion technology has also shown great potential in boosting the biomethane yields. Studies have shown biomethane yield increases of up to 91% (compared to AD alone). This is achieved by breaking down the cellulose, hemicellulose and lignin cell walls of biomass [59]. However, due to the low resolution of the current study, it was deemed that this technology was outside the scope of this paper.

When including for biological methanation, the generated biomethane can be injected into the existing gas grid, allowing for easier transportation, distribution, and utilisation (compared to hydrogen). Biomethane can serve as a low-carbon transport fuel for buses and haulage. Alternatively, biomethane can be further synthesised to methanol. Methanol can be utilised in-situ as an exogenous carbon source in municipal WWTPs for heterotrophic denitrification to achieve low total nitrogen levels, presenting further circularity and enhancing overall the sustainability of the WWTP [60]. Methanol synthesis could also offer a potential solution in the maritime sector where it has been identified as a suitable fuel at a lower investment cost due to limited engine or bunkering modifications of current marine engines and easier storage features [4]. Biomethane and methanol as energy carriers can be used as interim solutions to a future green hydrogen economy. WWTPs can accompany that transformation by providing the currently required type of fuel and reducing the construction of interim solutions.

Overall, the potential for electrofuel production in a circular economy approach offers synergies in three key service sectors: electricity, gas, and water sectors, with numerous benefits such as maximising the use of the existing infrastructure with only minor

modification and enabling the decarbonisation of hard-to-abate sectors (transport, wastewater treatment, industry, and agriculture).

4.3.7 Emission reductions using anaerobic digestion and pyrolysis

Pyrolysis of the digestate (derived from the AD system) to produce biochar has been identified as a potential NET. To assess such an integrated system, a case study was undertaken based on the available feedstock (cattle slurry, food waste and sewage sludge) within the 10 km area surrounding the investigated industrial site. Table 4.3 shows the potential GHG emissions reduction for this area through the proposed circular cascading system. When considering cattle slurry for AD, the fugitive emissions avoided from conventional slurry storage ought to be included in the GHG emissions savings; according to the recast Renewable Energy Directive (REDII), this equates to avoided emissions of 54kgCO_{2e}/t wet weight of slurry [61]. The results show that cattle slurry would comprise the majority of the GHG emissions savings through biogas production and upgrading via biomethanation, and biochar production via pyrolysis, totalling 35.25 ktCO_2 per year (see calculations in Box S4.5 of supplementary data). If all of the H_2 produced is used for biomethanation, ca. 46,900 m^3 CH_4 would be produced, equating to 234 tCO_2 in GHG emissions reductions. However, this represents only 1% of the total CO_2 in the biogas produced from the digested biomass within the 10 km area, due to the limited H_2 production. In effect, to utilise the remaining biogenic CO_2 (99% of the total CO_2), H_2 availability would be necessary in the form of a much larger electrolyser unit. Combining the abovementioned feedstock, the integrated AD and pyrolysis system could potentially reduce emissions in total by 42.7 ktCO_2 per annum via biomethane and biochar production (Table 4.3). It is also worth acknowledging pyrolysis technology offering benefits in enabling negative emissions technologies. Research in the pretreatment of wastewater and digester sludge for pyrolysis has shown to be beneficial in improving the economics of the technology. Dewatering and hydrothermal pretreatment methods have been shown to reduce the drying needs and improve the energy efficiency of the pyrolysis process, adding to the financial feasibility of the technology [62]. The current model developed in this study has not included this technology, the authors wish acknowledge its existence.

Table 4.3: Potential GHG reduction by the proposed circular cascading system. (The quantification of available feedstock in the 10km area surrounding the industrial area, based on a previous study [63]*).*

Feedstock	Resource (kt, fresh matter) [a]	Biogas production potential ($\times 10^3$ m^3)	Biomethane potential ($\times 10^3$ m^3)[b]	GHG reduction from the use of CH_4 ($ktCO_2$)[c]	Avoided methane emissions potential ($ktCO_2$)	GHG reduction from biochar ($ktCO_2$)[d]	Total GHG reduction ($ktCO_2$)[e]
Cattle slurry	**267.93**	**7,127**	**4,287**	**11.31**	**14.47**	**9.46**	**35.25**
Food waste	**12.83**	**3,167**	**1,900**	**5.01**	**/**	**1.52**	**6.54**
Primary Sludge	**0.71 (dry matter)**	**282**	**189**	**0.50**	**/**	**0.19**	**0.69**
Waste Activated Sludge	**0.59 (dry matter)**	**49**	**25**	**0.07**	**/**	**0.16**	**0.22**
Total		**10,625**	**6,401**	**16.89**	**14.47**	**11.33**	**42.7**

a: the TS and VS content of slurry and food waste is modelled at 8.75% and 6.69% [64]*, and 29% and 28%* [65]*, respectively. The biomethane potential of cattle slurry is 16 m^3/t wet weight* [23]*, and food waste is 148 m^3/t wet weight* [65]*; the content of CH_4 and CO_2 are assumed as 60% and 40% respectively. The methane production potential and biogas composition of sewage sludge can be found in* ***Error! Reference source not found.****.*

b: Only including the methane production from the feedstock.

c: The use of methane (energy content of 10 kWh/m^3 CH_4) is modelled as a replacement for diesel consumption; the CO_2 emission factor of diesel is 263.9 g CO_2/kWh

d: Biochar yield from the dry matter of cattle slurry, food waste and sewage sludge (including primary sludge and waste-activated sludge) is conservatively assumed as 20%, 20% and 40%, respectively; the carbon content of the separate biochar is 55%, 55% and 18%, respectively [49], [51].

e: Including the replacement of diesel consumption by biomethane, and the calculation in Box S4.3 in Supplementary data.

4.3.8 The sustainability of the circular electrofuel production systems

The proposed methodology for a circular electrofuel production system integrates multiple processes, with the aim of not only deriving as much energy as possible but also maximising the potential for decarbonisation in the hard-to-abate sectors. Such an approach aligns with the European Green Deal policy proposing a multi-sectoral ambition to decarbonise. However, from an emissions accountancy perspective, some of the key circular attributes of this proposed system of systems are not accounted for.

The main technologies deployed are the electrolyser for generating H_2 and O_2 from surplus electricity; the AD plant for converting organic biomass to biogas; the biological methanation process for converting CO_2 and H_2 to CH_4; and pyrolysis of digestate to produce biochar for CO_2 sequestration. These systems are further integrated with other technologies such as wind turbines at the industrial site and the local wastewater treatment facility. Along with these technologies, the AD feedstock used (for example wastewater sludges, slurries or food wastes) will alter the sustainability of the circular system. For any electrofuel developed (H_2 or CH_4), it will be necessary to meet EU sustainability criteria under the recast Renewable Energy Directive to be certified as renewable [61]. A range of inputs, outputs and processes need to be considered in assessing the circular electrofuel system. Table 4.4 illustrates a list of initial considerations.

Table 4.4: REDII Sustainability considerations for an electrofuel in a circular economy system.

Input	• Residues with no associated emissions (food waste; slurry, WWTP sludge) • Renewable electricity (surplus VRE)
Processes	• Anaerobic digestion • Transportation (feedstock and/or gas) • Wastewater treatment plant • Electrolysis • Biological hydrogen methanation • Compression of H_2/CH_4 • Pyrolysis
Output	• Transport fuel (direct use) • Heat (direct use) • Grid injection
Sustainability Criteria	• REDII • 70% emissions savings for transport fuel as compared to fossil fuel comparator • 80% emissions savings for heat as compared to fossil fuel comparator

The RED recast has a sustainability criterion of a minimum of 70% GHG emissions savings for transport and 80% for heat by 2030 [61]. The criteria to be met for transport are more lenient than for heat due to a higher fossil fuel comparator and a lower requirement for GHG savings [66]. This highlights the exergy of the energy vector; wood chips can provide

heat but not directly power a vehicle while biomethane or H_2 can do both. It is preferable to use a vector suitable for the hard to decarbonise sectors in the hard to decarbonise sector. Thus, the recast renewable energy directive (REDII) does not make it easy to satisfy the sustainability criteria for heat. Furthermore, electrofuels are typically aligned with a transport end use. However, it is evident that aspects of the circular approach presented do not currently benefit from a sustainability accounting process. For instance, whilst the biomethanation system will utilise the biomass derived CO_2 from AD, this is not considered carbon capture according to the recast REDII, and subsequently is not considered an emissions saving. Furthermore, the recast REDII provides no clear guidance for calculating emissions from surplus electricity that would otherwise not be used, which is an increasing issue in a growing VRE energy landscape. These accounting blind spots result in significant hurdles in the efficacy of decarbonising more difficult sectors, and ultimately hinder achieving net-zero goals.

A full life cycle assessment (LCA) would be required to assess the benefits of individual modular systems, while also providing an accurate assessment of the emissions savings such a system could offer to the surrounding industry and the hard-to-abate sectors. As this study has shown, the utilisation of curtailed VRE could offset the use of emission-intense fuels through electrolysis. The use of O_2 could offer reductions in total WWTP electricity demand. Additionally, the by-product CO_2 could be upgraded using the biological methanation process to a low-carbon biomethane when coupled with green H_2 ($4H_2 + CO_2 = CH_4 + 2H_2O$); these energy vectors could be used in the decarbonisation of the hard-to-abate sectors. The inclusion of pyrolysis-derived biochar can affect further emissions savings and improve the ability to comply with the REDII recast sustainability criteria to ensure the progression towards a net-zero economy.

4.3.9 Study limitations and future research

Whilst this study provided a high-level overview for a circular electrofuel production concept, it must be acknowledged that there are limitations to the analysis which may lead to additional questions and the potential for future research. For example, the study can be considered somewhat low-resolution as it focuses primarily on the movement of resources throughout the system. To effectively develop a higher resolution system, it is important that all aspects of the system are developed at a high level of detail. This could include for further analyses of the wastewater treatment process including for detailed designs of the aeration process, sizing of the aeration tanks and the exact influent properties, to determine the oxygen gas transfer efficiency. Furthermore, the wind resource could be assessed on a demand versus production basis, to estimate the periods of availability of the electricity. The investigation of a larger electrolyser size is warranted along with a cost-benefit analysis to determine the economic viability of co-locating the proposed systems, along with a techno-economic analysis for the total cost of the system. Additionally, factors such as the conversion efficiency of specific AD feedstocks and subsequent biogas yields would need to be accurately determined. With respect to the biomethanation process system, conversion

efficiency and rate would need to be determined to evaluate the system ability to upgrade the CO_2 and furthermore the fugitive emissions of the process would need to be established. Nonetheless the system proposed herein provides a valuable roadmap for such technology integration to reduce emissions on a multi-sectoral level. Future research could investigate the integration of the technologies proposed into other industry fields such as distilleries or cement manufacture which offer a CO_2 source for biomethanation and where the products (hydrogen, methane and oxygen) could be utilised favourably.

4.4 Conclusions

In this study, a novel, low resolution circular economy model was developed with the aim of assessing the feasibility of a potential local small scale system. A local industrial site was investigated for its potential size and ability to store variable renewable electricity in the form of green hydrogen using an electrolyser. Using the site as a reference, the paper investigated potential uses of the available electricity, the electrolyser by-product O_2, wastewater treatment plant and anaerobic digester waste.

Based on the site data, a 122 kW proton exchange membrane electrolyser was sized to account for the surplus wind resource available. Recycling of the by-product oxygen generated in electrolysis would supply 8.9% of the oxygen demand for the aeration process of the local 65,000 person equivalent wastewater treatment plant. This would reduce emissions by 16.04 tCO_2eq/a. The hydrogen produced from the electrolyser (190,300 m^3H_2/a) could be used directly as a transport fuel in local buses. Alternatively, the hydrogen could convert 40% of the CO_2 generated in the anaerobic digestion process to biomethane through biological methanation. The levelised cost of hydrogen production was found to be high, at €8.92/kg H_2. Thus, smaller scale systems using intermittent curtailed electricity as described can be deemed difficult to implement. However, larger scale systems with higher capacity factors stemming from more available electricity sources would be more financially feasible and offer significant decarbonisation opportunities.

The paper also investigated potential of negative emissions technologies, such as Pyrolysis. An integrated anaerobic digestion and pyrolysis system could potentially reduce emissions by 42.7 $ktCO_2/a$ via biomethane and biochar production (as a means for long-term CO_2 sequestration). The proposed circular electrofuel system could tackle the hard-to-abate sectors. However, the current emissions accountancy process may ultimately hinder the development of such approaches.

Acknowledgements

This work was supported by Science Foundation Ireland (SFI) through the MaREI Centre for Energy, Climate and Marine [Grant number 12/RC/2302_P2 and 16/SP/3829] with industrial funding from Gas Networks Ireland through the Green Gas Innovation group; and funding from the SFI zero emission challenge [Grant number 19/FIP/ZE/7565]. The authors would like to add thanks to colleagues Richard O'Shea for their time taken in reviewing the manuscript.

References

[1] U. N. F. C. on C. C. UNFCCC, “Conference of the Parties, Adoption of the Paris Agreement, ,” 2015.

[2] European Commission, “The European Green Deal,” *Eur. Comm.*, vol. 53, no. 9, p. 24, 2019.

[3] SEAI, “Energy in Ireland 2022,” 2022.

[4] N. Gray, S. McDonagh, R. O’Shea, B. Smyth, and J. D. Murphy, “Decarbonising ships, planes and trucks: An analysis of suitable low-carbon fuels for the maritime, aviation and haulage sectors,” *Adv. Appl. Energy*, vol. 1, p. 100008, Feb. 2021.

[5] G. of I. Department of Communications, Climate Action and Environment, “Climate Action Plan 2019: to Tackle Climate Breakdown,” 2019.

[6] EirGrid and SONI, “Annual Renewable Energy Constraint and Curtailment Report 2020,” 2021.

[7] M. Lehtveer, S. Brynolf, and M. Grahn, “What Future for Electrofuels in Transport? Analysis of Cost Competitiveness in Global Climate Mitigation,” *Env. Sci Technol*, vol. 53, no. 3, pp. 1690–1697, 2019.

[8] S. McDonagh, R. O’Shea, D. M. Wall, J. P. Deane, and J. D. Murphy, “Modelling of a power-to-gas system to predict the levelised cost of energy of an advanced renewable gaseous transport fuel,” *Appl. Energy*, vol. 215, no. January 2018, pp. 444–456, 2018.

[9] S. McDonagh, P. Deane, K. Rajendran, and J. D. Murphy, “Are electrofuels a sustainable transport fuel? Analysis of the effect of controls on carbon, curtailment, and cost of hydrogen,” *Appl. Energy*, vol. 247, no. November 2018, pp. 716–730, 2019.

[10] M. Thema, F. Bauer, and M. Sterner, “Power-to-Gas: Electrolysis and methanation status review,” *Renew. Sustain. Energy Rev.*, vol. 112, pp. 775–787, 2019.

[11] IEA, *The Future of Hydrogen*, no. June. OECD, 2019.

[12] S. Pascuzzi, A. S. Anifantis, I. Blanco, and G. S. Mugnozza, “Electrolyzer performance analysis of an integrated hydrogen power system for greenhouse heating a case study,” *Sustain.*, vol. 8, no. 7, pp. 1–15, 2016.

[13] N. Gray, R. O’Shea, B. Smyth, P. N. L. Lens, and J. D. Murphy, “What is the energy balance of electrofuels produced through power-to-fuel integration with biogas facilities?,” *Renew. Sustain. Energy Rev.*, p. 111886, Nov. 2021.

[14] H. Lund *et al.*, “The role of sustainable bioenergy in a fully decarbonised society,” *Renew. Energy*, vol. 196, pp. 195–203, Aug. 2022.

[15] T. H. Ruggles, J. A. Dowling, N. S. Lewis, and K. Caldeira, “Opportunities for flexible electricity loads such as hydrogen production from curtailed generation,” *Adv. Appl. Energy*, vol. 3, p. 100051, Aug. 2021.

[16] A. G. Capodaglio and G. Olsson, “Energy issues in sustainable urban wastewater management: Use, demand reduction and recovery in the urban water cycle,” *Sustain.*, vol. 12, no. 1, p. 266, Dec. 2020.

[17] D. Rusmanis, Y. Yang, R. Lin, D. M. Wall, and J. D. Murphy, “Operation of a circular economy, energy, environmental system at a wastewater treatment plant,” *Adv. Appl. Energy*, vol. 8, p. 100109, Dec. 2022.

[18] D. T. Laurent Lardon Lars Krosgaard, “Technical and economic analysis of biological methanation,” 2020.

[19] Jacobs and Yarra Valley Water, “Towards a zero carbon future. Yarra Valley Water,” 2020.

[20] L. Appels, J. Baeyens, J. Degrève, and R. Dewil, “Principles and potential of the anaerobic digestion of waste-activated sludge,” *Prog. Energy Combust. Sci.*, vol. 34, no. 6, pp. 755–781, Dec. 2008.

[21] J. Liebetrau P. Kornatz, U. Baier, D. Wall, and J. D. Murphy., “Integration of Biogas Systems into the Energy System: Technical aspects of flexible plant operation,” IEA Bioenergy Task 37, 2020.

[22] B. Wu, R. Lin, R. O’Shea, C. Deng, K. Rajendran, and J. D. Murphy, “Production of advanced fuels through integration of biological, thermo-chemical and power to gas technologies in a circular cascading bio-based system,” *Renew. Sustain. Energy Rev.*, vol. 135, p. 110371, Jan. 2021.

[23] R. Lin, R. O’Shea, C. Deng, B. Wu, and J. D. Murphy, “A perspective on the efficacy of green gas production via integration of technologies in novel cascading circular bio-systems,” *Renew. Sustain. Energy Rev.*, vol. 150, p. 111427, 2021.

[24] Y. Gao, X. Gao, and X. Zhang, “The 2 °C Global Temperature Target and the Evolution of the Long-Term Goal of Addressing Climate Change—From the United Nations Framework Convention on Climate Change to the Paris Agreement,” *Engineering*, vol. 3, no. 2, pp. 272–278, Apr. 2017.

[25] Jacob, “Jacobs Yarra valley water towards a zero carbon future,” 2020. [Online]. Available: https://www.jacobs.com/sites/default/files/2020-06/jacobs-yarra-valley-water-towards-a-zero-carbon-future.pdf.

[26] M. Schäfer, O. Gretzschel, and H. Steinmetz, “The Possible Roles of Wastewater Treatment Plants in Sector Coupling,” *Energies*, vol. 13, no. 8, 2020.

[27] S. Brynolf, M. Taljegard, M. Grahn, and J. Hansson, “Electrofuels for the transport sector: A review of production costs,” *Renew. Sustain. Energy Rev.*, vol. 81, pp. 1887–1905, Jan. 2018.

[28] EU Directive, “Powering a climate-neutral economy: An EU Strategy for Energy System Integration,” 2020.

[29] A. Buttler and H. Spliethoff, “Current status of water electrolysis for energy storage, grid balancing and sector coupling via power-to-gas and power-to-liquids: A review,” *Renew. Sustain. Energy Rev.*, vol. 82, pp. 2440–2454, Feb. 2018.

[30] N. A. Burton, R. V. Padilla, A. Rose, and H. Habibullah, “Increasing the efficiency of hydrogen production from solar powered water electrolysis,” *Renew. Sustain. Energy Rev.*, vol. 135, p. 110255, Jan. 2021.

[31] T. A. Gunawan, A. Singlitico, P. Blount, J. Burchill, J. G. Carton, and R. F. D. Monaghan, “At what cost can renewable hydrogen offset fossil fuel use in Ireland’s gas network?,” *Energies*, vol. 13, no. 7, p. 1798, Apr. 2020.

[32] D. Rusmanis, R. O’Shea, D. M. Wall, and J. D. Murphy, “Biological hydrogen methanation systems – an overview of design and efficiency,” *Bioengineered*, vol. 10, no. 1, pp. 604–634, Jan. 2019.

[33] GNI, “Vision 2050 A Net Zero Carbon Gas Network for Ireland,” 2019.

[34] S. Schemme, R. C. Samsun, R. Peters, and D. Stolten, “Power-to-fuel as a key to sustainable transport systems - An analysis of diesel fuels produced from CO2 and renewable electricity,” *Fuel*, vol. 205, pp. 198–221, 2017.

[35] H. Mohammadpour, R. Cord-Ruwisch, A. Pivrikas, and G. Ho, “Utilisation of oxygen from water electrolysis – Assessment for wastewater treatment and aquaculture,” *Chem. Eng. Sci.*, vol. 246, p. 117008, Dec. 2021.

[36] I. Environmental Protection Agency, “Wastewater Treatment Manuals,” 1997.

[37] W. Wei *et al.*, “Zero valent iron enhances methane production from primary sludge in anaerobic digestion,” *Chem. Eng. J.*, vol. 351, pp. 1159–1165, Nov. 2018.

[38] W. Wei *et al.*, “Enhanced high-quality biomethane production from anaerobic digestion of primary sludge by corn stover biochar,” *Bioresour. Technol.*, vol. 306, p. 123159, Jun. 2020.

[39] R. M. Potdukhe, N. Sahu, A. Kapley, and R. Kumar, “Co-digestion of waste activated sludge and agricultural straw waste for enhanced biogas production,” *Bioresour. Technol. Reports*, vol. 15, p. 100769, Sep. 2021.

[40] EASAC, “EASAC report on negative emission report,” 2018.

[41] F. Guilayn, M. Rouez, M. Crest, D. Patureau, and J. Jimenez, “Valorization of digestates from urban or centralized biogas plants: a critical review,” *Rev. Environ. Sci. Bio/Technology*, vol. 19, no. 2, pp. 419–462, Jun. 2020.

[42] C. Deng, R. Lin, X. Kang, B. Wu, R. O’Shea, and J. D. Murphy, “Improving gaseous biofuel yield from seaweed through a cascading circular bioenergy system integrating anaerobic digestion and pyrolysis,” *Renew. Sustain. Energy Rev.*, vol. 128, p. 109895, 2020.

[43] K. A. Spokas, “Review of the stability of biochar in soils: predictability of O: C molar ratios,” *Carbon Manag.*, vol. 1, no. 2, pp. 289–303, 2010.

[44] R. Lin, J. Cheng, L. Ding, and J. D. Murphy, “Improved efficiency of anaerobic digestion through direct interspecies electron transfer at mesophilic and thermophilic temperature ranges,” *Chem. Eng. J.*, vol. 350, pp. 681–691, 2018.

[45] B. Wu *et al.*, “Graphene Addition to Digestion of Thin Stillage Can Alleviate Acidic

Shock and Improve Biomethane Production," *ACS Sustain. Chem. Eng.*, vol. 8, no. 35, pp. 13248–13260, Sep. 2020.

[46] C. Li, X. Zhu, and I. Angelidaki, "Carbon monoxide conversion and syngas biomethanation mediated by different microbial consortia," *Bioresour. Technol.*, vol. 314, p. 123739, 2020.

[47] R. O'Shea, D. M. Wall, I. Kilgallon, J. D. Browne, and J. D. Murphy, "Assessing the total theoretical, and financially viable, resource of biomethane for injection to a natural gas network in a region," *Appl. Energy*, vol. 188, pp. 237–256, Feb. 2017.

[48] M. A. Voelklein, R. O' Shea, A. Jacob, and J. D. Murphy, "Role of trace elements in single and two-stage digestion of food waste at high organic loading rates," *Energy*, vol. 121, pp. 185–192, Feb. 2017.

[49] A. Zielińska, P. Oleszczuk, B. Charmas, J. Skubiszewska-Zięba, and S. Pasieczna-Patkowska, "Effect of sewage sludge properties on the biochar characteristic," *J. Anal. Appl. Pyrolysis*, vol. 112, pp. 201–213, 2015.

[50] A. Callegari and A. Capodaglio, "Properties and Beneficial Uses of (Bio)Chars, with Special Attention to Products from Sewage Sludge Pyrolysis," *Resources*, vol. 7, no. 1, p. 20, Mar. 2018.

[51] F. Monlau, C. Sambusiti, E. Ficara, A. Aboulkas, A. Barakat, and H. Carrère, "New opportunities for agricultural digestate valorization: current situation and perspectives," *Energy Environ. Sci.*, vol. 8, no. 9, pp. 2600–2621, 2015.

[52] Y. Ding *et al.*, "Biochar to improve soil fertility. A review," *Agron. Sustain. Dev.*, vol. 36, no. 2, pp. 1–18, 2016.

[53] S. McDonagh, S. Ahmed, C. Desmond, and J. D. Murphy, "Hydrogen from offshore wind: Investor perspective on the profitability of a hybrid system including for curtailment," *Appl. Energy*, vol. 265, p. 114732, May 2020.

[54] H. Council, "Path to hydrogen competitiveness A cost perspective," 2020. [Online]. Available: https://hydrogencouncil.com/en/path-to-hydrogen-competitiveness-a-cost-perspective/.

[55] S. McDonagh, D. M. Wall, P. Deane, and J. D. Murphy, "The effect of electricity markets, and renewable electricity penetration, on the levelised cost of energy of an advanced electro-fuel system incorporating carbon capture and utilisation," *Renew. Energy*, vol. 131, pp. 364–371, Feb. 2019.

[56] J. Drewnowski, A. Remiszewska-Skwarek, S. Duda, and G. Łagód, "Aeration Process in Bioreactors as the Main Energy Consumer in a Wastewater Treatment Plant. Review of Solutions and Methods of Process Optimization," *Processes*, vol. 7, no. 5, p. 311, May 2019.

[57] EPA, "Greenhouse gas emissions Ireland," 2019. [Online]. Available: https://www.epa.ie/ghg/agriculture/.

[58] John Bradshaw *et al.*, "Sources of CO2," J. F. H. Ismail El Gizouli, Ed. 2018.

[59] N. Dutta, R. Garrison, M. Usman, and B. K. Ahring, “Enhancing methane production of anaerobic digested sewage sludge by advanced wet oxidation & steam explosion pretreatment,” *Environ. Technol. Innov.*, vol. 28, p. 102923, Nov. 2022.

[60] Y. C. Su, S. Sathyamoorthy, and K. Chandran, “Bioaugmented methanol production using ammonia oxidizing bacteria in a continuous flow process,” *Bioresour Technol*, vol. 279, pp. 101–107, 2019.

[61] EU Directive, “Directive (EU) 2018/2001 of the European Parliament and of the Council of 11 December 2018 on the promotion of the use of energy from renewable sources (recast),” *Off. J. Eur. Union*, vol. 2018, no. L 328, pp. 82–209, 2018.

[62] C. Li *et al.*, “A process combining hydrothermal pretreatment, anaerobic digestion and pyrolysis for sewage sludge dewatering and co-production of biogas and biochar: Pilot-scale verification,” *Bioresour. Technol.*, vol. 254, pp. 187–193, Apr. 2018.

[63] R. O’Shea, I. Kilgallon, D. Wall, and J. D. Murphy, “Quantification and location of a renewable gas industry based on digestion of wastes in Ireland,” *Appl. Energy*, vol. 175, no. 2016, pp. 229–239, 2016.

[64] D. M. Wall, P. O’Kiely, and J. D. Murphy, “The potential for biomethane from grass and slurry to satisfy renewable energy targets,” *Bioresour. Technol.*, vol. 149, pp. 425–431, 2013.

[65] J. D. Browne and J. D. Murphy, “Assessment of the resource associated with biomethane from food waste,” *Appl. Energy*, vol. 104, pp. 170–177, 2013.

[66] A. Long, A. Bose, R. O’Shea, R. Monaghan, and J. D. Murphy, “Implications of European Union recast Renewable Energy Directive sustainability criteria for renewable heat and transport: Case study of willow biomethane in Ireland,” *Renew. Sustain. Energy Rev.*, vol. 150, p. 111461, Oct. 2021.

5 Operation of a circular economy, energy, and environmental system at a wastewater treatment plant

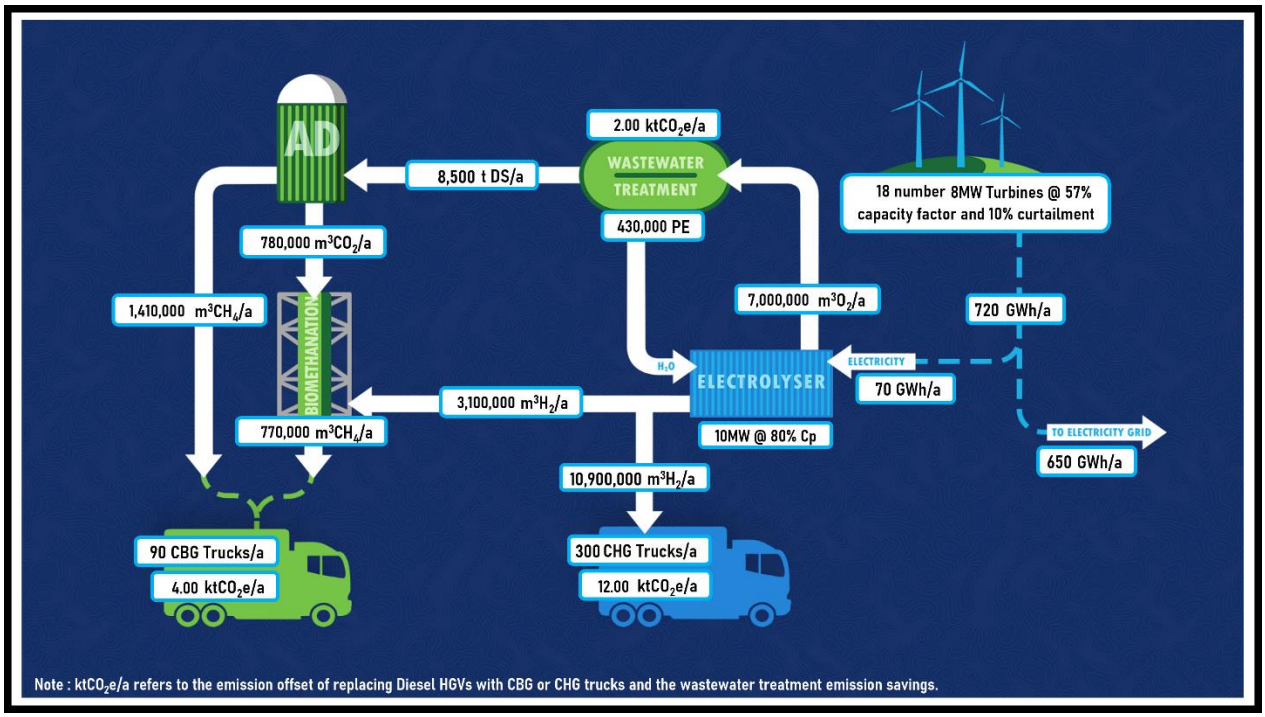
Rusmanis, Davis[1,2], Yang, Yan[1,2], Lin, Richen[1,2], Wall, David M.[1,2], Murphy, Jerry D.[1,2,*]

1. MaREI Centre, Environmental Research Institute, University College Cork, Ireland.
2. Civil, Structural and Environmental Engineering, School of Engineering and Architecture, University College Cork, Cork, Ireland

Abstract

Decarbonising economies and improving the environment can be enhanced through circular economy, energy, and environmental systems integrating electricity, water, and gas utilities. Hydrogen production can facilitate intermittent renewable electricity through reduced curtailment of electricity in periods of overproduction. Positioning an electrolyser at a wastewater treatment plant with existing sludge digesters offers significant advantages over stand-alone facilities. This paper proposes co-locating electrolysis and biological methanation technologies at a wastewater treatment plant. Electrolysis can produce oxygen for use in pure or enhanced oxygen aeration, offering a 40% reduction in emissions and power demand at the treatment facility. The hydrogen may be used in a novel biological methanation system, upgrading carbon dioxide (CO_2) in biogas from sludge digestion, yielding a 54% increase in biomethane production. A 10MW electrolyser operating at 80% capacity would be capable of supplying the oxygen demand for a 426,400 population equivalent wastewater treatment plant, producing 8,500 tTS/a of sludge. Digesting the sludge could generate 1,409,000 m^3CH_4/a and 776,000 m^3CO_2/a. Upgrading the CO_2 to methane would consume 22.2% of the electrolyser-generated hydrogen and capture 1.534 $ktCO_2e$/a. Hydrogen and methane are viable advanced transport fuels that can be utilised in decarbonising heavy transport. In the proposed circular economy, energy, and environment system, sufficient fuel would be generated annually for 94 compressed biomethane gas (CBG) heavy goods vehicles (HGV) and 296 compressed hydrogen gas fuel cell (CHG) HGVs. Replacement of the equivalent number of diesel HGVs would offset approximately 16.1 $ktCO_2e$/a.

Graphical Abstract



Highlights

Curtailed electricity from a 144 MW offshore wind farm can supply a 10MW electrolyser.

A 10 MW electrolyser can supply O_2 to a 426,400-person wastewater treatment facility.

Only 22% of the H_2 is required for methanation of biogas from sludge digestion.

Pure O_2 aeration can result in a 40% reduction in emissions at the treatment facility.

Excess H_2 and biomethane could together fuel 390 heavy goods vehicles.

Keywords

Electrolyser; wastewater treatment; biological methanation; circular economy; decarbonisation; heavy-goods vehicles.

5.1 Introduction

5.1.1 The benefits of circular economy, energy, and environmental systems

The European Commission has set out a definite strategy towards climate neutrality by 2050 with significant emphasis on diversification of energy sources, and a move away from traditional independent, vertical energy value chains towards integrated energy systems with multiple pathways and energy carriers; hydrogen is an essential element of this future integrated decarbonised energy system [1]. Traditional linear energy systems are susceptible to disruptions; it is suggested that circular economy energy systems offer more resilient pathways. Recent events such as the war in Ukraine have underlined this need for diversification and restructuring of the European energy model and indeed beyond energy into the need for renewable hydrogen molecules in essential chemicals such as ammonia (NH_3) and methanol production (CH_3OH).

In the transition from fossil fuels, challenges arise with the integration of intermittent renewable energy sources. The temporal mismatch of variable electricity production with increases in demand for electrification of heat and transport places significant stresses on the present electricity grid. Methods to alleviate this are necessary for any intermittent renewable energy source, be it wind or solar or other. In the Irish context (which is very much an island with limited integration into other electricity grids), the majority of renewable energy is sourced from wind, which often produces periods of surplus electricity (necessitating curtailment) due to variability in production and demand.

Developments in electrolyser technologies will facilitate hydrogen-based systems that can capture this otherwise surplus electricity, with expected 60-70% conversion efficiencies and flexibility in operation (fast start-up) and scale. The by-product of splitting water in electrolysis, oxygen may be considered to be of relatively low value and is often vented to the atmosphere [2]. However, wastewater treatment processes require significant volumes of oxygen for the aerobic microbes in aeration basins. Integration of electrical utilities (facilitation of variable renewable electricity) with water utilities (through positioning electrolysers at WWTPs to generate oxygen for aeration basins) creates a novel system which should reduce planning issues by positioning gas utilities (hydrogen and methane) at existing wastewater treatment plant sites whilst reducing the carbon footprint of wastewater treatment. This circular economy energy and environmental system would utilise cost-effective brownfield sites, avoiding competition with greenfield sites and allowing for the valorisation of the oxygen gas above and beyond the production of hydrogen. Hydrogen systems have been proposed in The United Kingdom [3]. The Renewable Energy Directive outlines the necessity for guarantees of origin for renewable gases to be considered renewable; hydrogen cannot be considered renewable through connection with the existing national electricity grid (with associated fossil fuel-sourced electricity) [4]. The integration of renewable energy sources and interconnectivity of electrical, water and gas utilities are an exemplar for the implementation of the EU climate neutrality strategy.

5.1.2 Dispatch down of variable renewable electricity

Within power control centres, renewable energy is prioritised by scheduling and dispatch algorithms. Sometimes, it is not feasible to accommodate all prioritised generation, due to excess production or to maintain the safe operation of the power system, either on local or system-wide network levels. This is called *dispatch-down* and may occur for two reasons. *Constraint* refers to the limitations of the localised distribution network in its inability to handle high levels of generated wind energy and is solved by shutting off a subset of wind turbines to alleviate the strain on the network. C*urtailment* refers to the limitation of system-wide networks, where the relative end-use demand is low compared to supply, resulting in the reduction of any or all wind generation to alleviate the problem [5].

In 2020, wind energy made up 36.4% (13,768 GWh) of the total electricity demand (and 85.6% of renewable electricity) in the all-Ireland region; a further 12.1% of renewable electricity (1,909 GWh) was lost due to dispatch-down (Figure 5.1) [6]. This level of dispatch down was an increase of 901GWh from the 2019 report (1,008GWh)[7]. This restricted turbine operation affects the overall efficiency of wind turbines and with more wind energy deployment expected, curtailment becomes of increasing concern and magnitude. The intermittent nature of wind will cause increasing variability in energy generation as more wind is accepted to the grid.

Figure 5.2 depicts the breakdown of energy generation for the island of Ireland in 2020, with the total captured energy making up 87.3% of the potential availability [7]. Curtailment can be discussed under three headings: System Non-Synchronous Penetration (SNSP) (Equation 5.1); Rate of Change of Frequency (ROCOF/Inertia); and High frequency/Minimum generation.

- SNSP limit refers to the amount of variable renewable electricity allowed on the grid at any given time and is defined as:

$$SNSP = \frac{Wind\ generation + Imports}{System\ demand + Exports} \qquad \text{Equation 5.1}$$

- ROCOF/Inertia refers to situations when the loss of a large single infeed is unacceptably high leading to low system inertia resulting in the necessity to dispatch down variable renewable energy sources such as from wind turbines.
- High Frequency/Minimum generation is the alleviation of emergency high-frequency events or facilitating the minimum level of conventional generation to satisfy reserve requirements, priority dispatch, or to provide ramping capabilities.

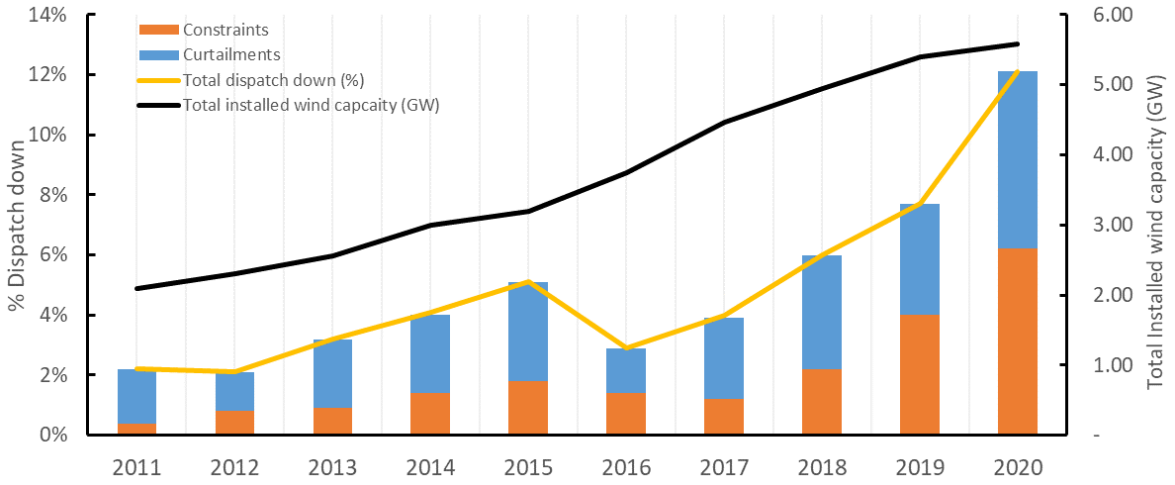
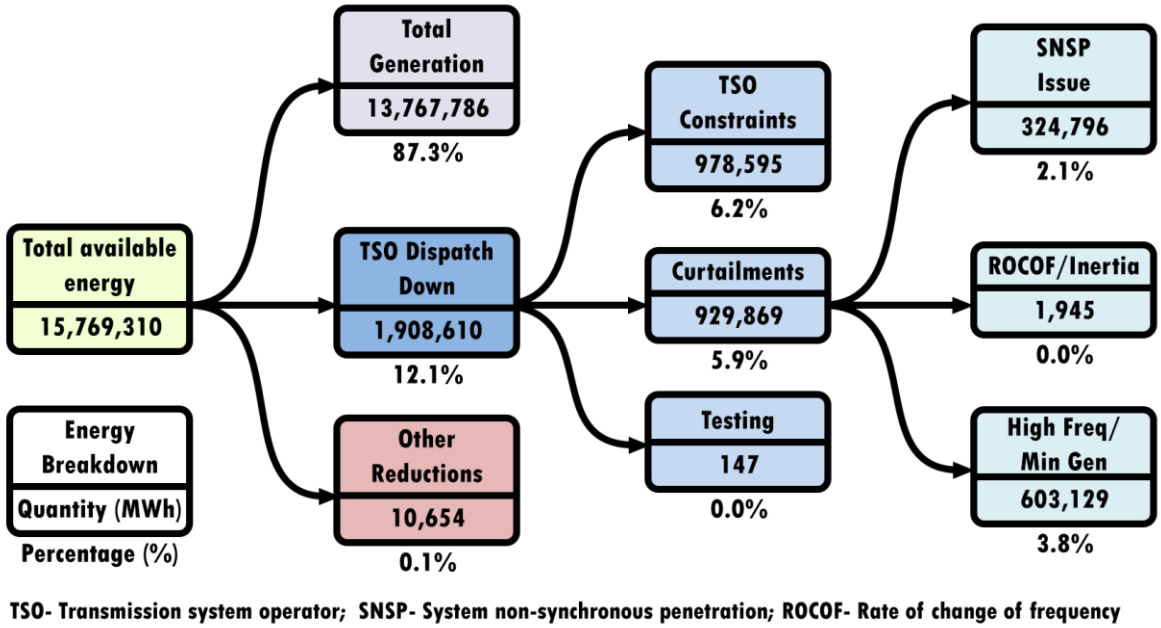


Figure 5.1: Yearly breakdown of wind dispatch-down levels into constraints and curtailments on the island of Ireland.



'Other reductions' include developer outages and testing. Certain reductions are outside of the control of Transmission System Operators (TSO) and are not logged. Therefore, Total available energy ≠ Generation + TSO dispatch down + Other reductions.

Figure 5.2: Graphical representation of Ireland's all-island wind dispatch-down in 2020.

A breakdown of the dispatch-down reveals that curtailment makes up most of the dispatch-down electricity in the past decade (Figure 5.1), accounting for, on average 62.6% of the dispatch-down. As such, an investigation into the capture and use of curtailed electricity is a key consideration going forward. Uncaptured electricity is forecasted to be a significant issue in the future, with projects such as the DS3 program ("Delivering a Secure, Sustainable Electricity System" programme), focusing on system performance, policies, and tools that seek to resolve these issues [8],[9]. Ireland is forecasted to install 3.5 GW of offshore wind farms by 2030 [10]. This additional instalment will likely lead to a higher percentage

dispatch-down within the electricity grid. Thus, the potential for converting electricity to alternative energy vectors is of great interest, in particular, the production of hydrogen through electrolyser technologies to alleviate growing dispatch-down losses.

5.1.3 Hydrogen production via electrolysis

Hydrogen has typically been produced through steam methane reforming (SMR), by splitting fossil natural gas into hydrogen and carbon monoxide. This form of hydrogen is termed 'grey hydrogen'. This method typically produces H_2 with a high CO_2 emission intensity (c. 91 gCO_2/MJ) without carbon capture and storage [11]. The future of hydrogen should ideally be 'green hydrogen' derived via electrolysis of renewable electricity. Electrolysis is an electrochemical process, that uses electrical energy as a driver for chemical reactions. Water can be split into its prime constituents of Oxygen (O_2) and Hydrogen (H_2) as per Equation 5.2**Error! Reference source not found.**

$$2H_2O \rightarrow 2H_2 + O_2 \qquad \text{Equation 5.2}$$

The alkaline electrolysis cell (AEC) has been the state-of-the-art electrolyser technology but may not be ideally suited to intermittent operation. Proton exchange membrane (PEM) technology is more suited to on/off operation and is expected to replace the AEC as the state of the art with further cost reductions expected with the maturity of the technology [12]. The conversion of electricity to hydrogen in this manner is termed 'power to gas'.

5.1.4 Circular economy, energy, and environmental systems at wastewater treatment plants

Wastewater treatment plants (WWTPs) are an integral part of environmental conservation. The process has undergone multiple developments, with the most common technologies in operation being Sequential Batch Reactors (SBRs) and more traditionally, oxidation ditches and activated sludge plants. In 2018, the EU reported 25,906 active urban WWTP facilities with a population equivalence (PE) greater than 2,000 [13]. The power demand of these plants can be substantial, with aeration accounting for approximately half of the electrical demand of WWTPs as shown in Figure 5.3 [14]. Many of these plants can be characterised by ageing activated sludge aeration technologies, and thus an opportunity exists to enhance the technical performance of such facilities. WWTPs account for 1.3% of global GHG emissions [15],[16]. Utilising oxygen-enriched air (as opposed to air which is only 21% Oxygen) in aeration can lower energy demand and aid the decarbonisation of WWTPs. As of 2014, the US reported that up to 15% of all municipal wastewater treatment was undertaken using pure oxygen in aerobic WWTPs [17]. This study explores the potential for a circular economy, energy, and environmental system at a WWTP and its ability to act as an energy conversion hub. The traditionally isolated sectors of electricity, gas, and water can be combined in a symbiotic relationship using an integrated and cascading systems approach.

Electrolysers are more likely to be effective in locations where existing infrastructure can be enhanced and renewable energy and water are readily available; this is likely at WWTPs [18]. Municipal WWTPs are an integral part of environmental protection associated with

growing urbanisation and industrialisation. The energy-intensive activated sludge process is still at the heart of current sewage treatment technologies [19]. The specific electricity consumption depends on the size of WWTP, ranging from 37-96 kWh_{el}/PE/a with an average of 72 kWh_{el}/PE/a [20]. The oxygen required for the removal of the Biological Oxygen Demand (BOD), is supplied by injecting compressed air (blowers/compressors) into the system. A study by Capodaglio and Olsson reported the energy use of aeration ranging from 50-70% of the total municipal WWTP demand applying aerobic activated sludge processes, matching closely the work presented by Drewnowski et al. [14],[21]. WWTPs have gained much attention of late under concepts such as “water resource recovery”, “circular economy”, energy-efficient resource recovery and reuse from wastewater treatment and energy-neutral or even net-energy-positive systems [22],[23]. Co-locating electrolysers at WWTPs for electricity storage in the form of gaseous energy vectors, renewable electricity facilitation and utilising oxygen from the electrolysis for enhanced purification processes can facilitate a circular economy, energy, and environmental system and aid in the decarbonisation of such processes.

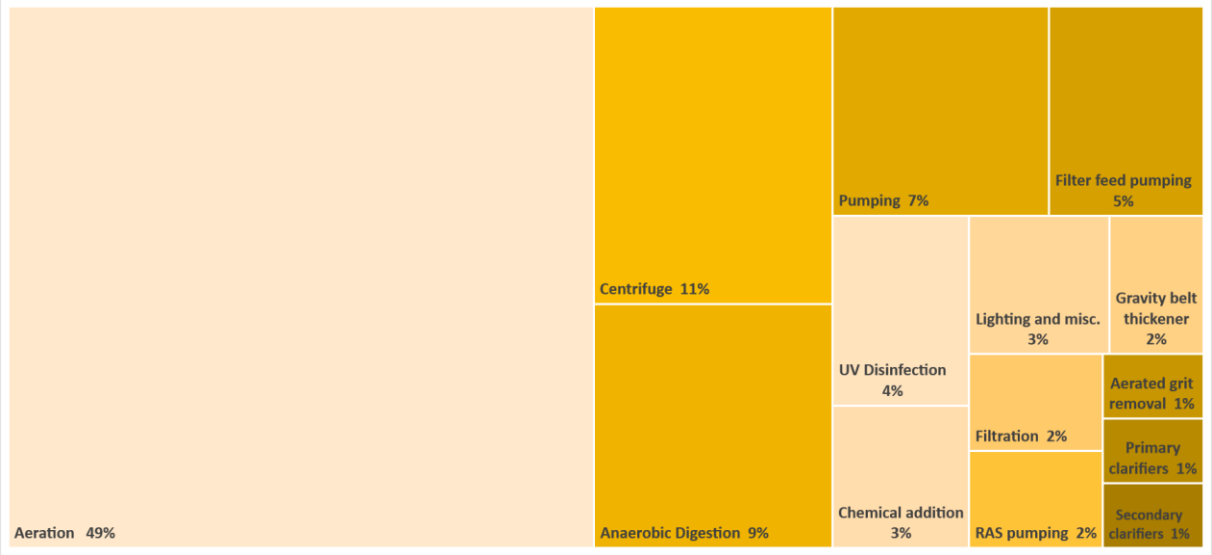


Figure 5.3: Breakdown of wastewater treatment plants (WWTP) power demand. Adapted from [14].

5.1.5 Anaerobic Digestion at WWTPs

In wastewater treatment, the aeration process removes most of the biological matter, and in doing so generates waste-activated sludge (WAS). Anaerobic digestion (AD) is a common technology for the treatment of this sludge at municipal WWTPs producing renewable energy in the form of biogas. Estimates for WWTP sludge disposal can account for 40 to 60% of the cost of the sewage treatment process [24],[25]. Biogas is typically comprised of 50-70% CH_4 and 30-50% CO_2. It can be used as an energy source by combustion in a CHP unit or flared when not required, the latter resulting in significant emissions [26]. Examining the literature it can be reported that only 15 of 1,100 WWTPs in Ireland had on-site AD systems in 2018 [27],[28]; 39% of examined wastewater treatment facilities (24 out of 61) used AD in Colorado, US in 2019 [29]; 8% (26 out of 340) of WWTPs had AD systems implemented in

Catalonia, Spain in 2015 [30], and in Austria, most WWTPs with PE greater than 20,000 have integrated AD systems [31]. The biogas produced can be used to maintain the AD reactor temperature and provide some of the power demand for a WWTP [31]. Biogas can also undergo upgrading to biomethane (traditionally through water scrubbing to remove CO_2 and other gases) and be injected into the existing gas grid network or compressed and used as a compressed biomethane gas (CBG) fuel in haulage. Typically, most WWTPs with AD tend to simply combust biogas in boilers for temperature control in AD systems, with the surplus biogas flared and CO_2 released back into the atmosphere [30]. Gaseous emissions (typically methane with a global warming potential of 28 times that of CO_2) from sludge and biogas flaring account for the majority of GHG emissions from WWTPs, if not properly managed [31]. Therefore, the efficient use of biogas and carbon capture at WWTPs can significantly reduce the carbon footprint whilst providing unique energy conversion methods.

5.1.6 Biological hydrogen methanation

Biological hydrogen methanation (BHM) is a promising technology for the conversion of electricity to biomethane via electrolysis and an application of the Sabatier reaction (Equation 5.3).

$$4H_2 + CO_2 \rightarrow CH_4 + 2H_2O\ , \Delta G_0 = -165\ kJ/mol \qquad \text{Equation 5.3}$$

The process is a viable alternative to traditional (and often energy-intensive and costly) biogas upgrading processes. Utilising specific archaea of the *Methanothermobacter* genus, it is possible to convert H_2 and CO_2 to CH_4 with small amounts of water as a by-product of the process. The mechanics of the process involve the introduction of the working gases into a bioreactor environment via coarse diffusion, followed by high-intensity mixing to break up the gas bubbles and promote gas dissolution within the liquid [32]. Other methods such as fine and nano-bubble diffusion have also been investigated, albeit on a small scale [33].

Biomethane produced from the BHM process can increase CH_4 yields by 50-70%, depending on the injected biogas composition from the AD process [32]. The BHM process converts the injected H_2 and CO_2 gas at a molar ratio of 4: 1 to grid-quality CH_4. In addition to the generation of green, renewable energy, carbon capture and reuse is another significant benefit of the technology. Integrated BHM technology allows for the capture of otherwise emitted CO2, and further conversion to CH4. The use of this technology, combined with access to a renewable H2 supply can offer a pathway for the integration of electrical, gas, and water utilities in a circular economy, energy, and environmental decarbonisation system.

5.1.7 Aims and objectives

Currently, there is a minimum of literature on sizing methods for an electrolyser positioned at an existing WWTP supplying oxygen to extended aeration facilities and hydrogen to sludge digesters for biomethanation. This paper seeks to fill this gap in the state of the art

by presenting a model whereby electrolysis and biomethanation technologies are positioned at existing and future WWTPs. The electrolyser size will depend on the O_2 supply for aeration systems, or H_2 supply to biomethanation for biogas upgrading from sludge digestion. The entire circular economy, energy, and environmental system allows for the interaction of previously independent sectors of water, electricity, and gas.

The innovation in this paper is the production of a model which will allow the determination of the relationship between the size of a wind farm supplying renewable electricity, the size of the electrolyser, the generated hydrogen (H_2) and oxygen (O_2) for use to aid in the decarbonisation of the WWTP and production of advanced fuels (CH_4 and H_2) for hard to decarbonise sectors. The initial power analysis will aid in understanding the benefits of using and capturing the dispatch down electricity, and the necessary accommodation required to ensure cost-effective electrolyser operation times.

The key questions asked in this paper are as follows:

1. What is the relationship between the size of a wind farm, dispatch down and the size of an electrolyser?
2. What is the relationship between electrolyser size and the oxygen requirement in a wastewater treatment plant?
3. What portion of H_2 produced from the electrolyser is required to upgrade the digested sludge biogas to biomethane via biological methanation and what resource or process will be the limiting factor of the system?
4. What emissions savings can be achieved at the wastewater treatment plant?
5. In assessing the end-use of renewable gases, how many diesel trucks can be offset with the generated H_2 and CH_4?

5.2 Methodology

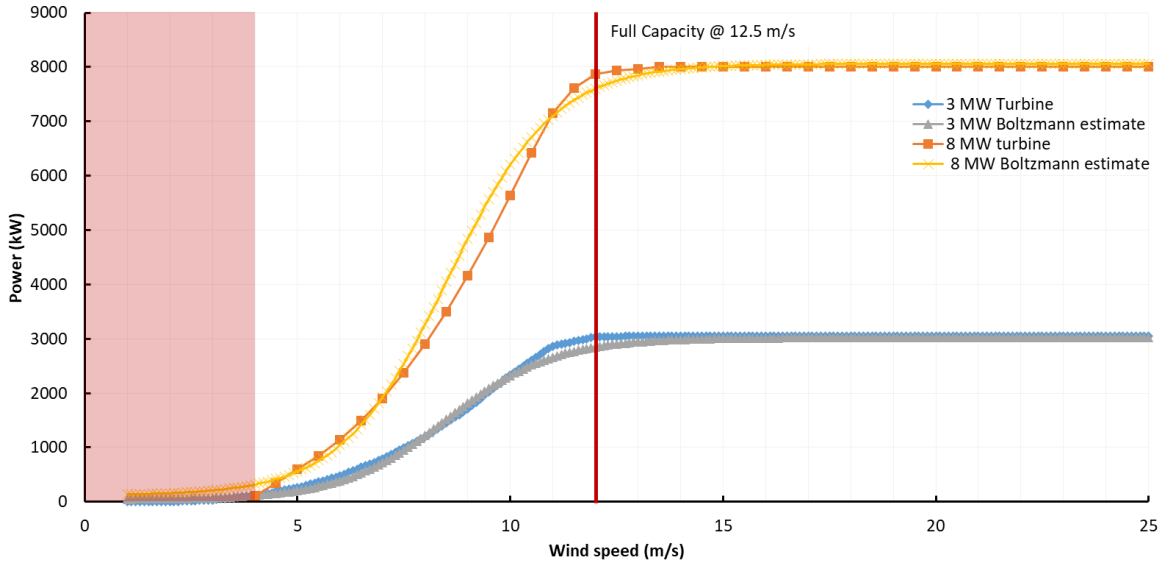
5.2.1 Relationship between the size of a wind farm, dispatch down and the size of an electrolyser

5.2.1.1 Wind energy resource assessment

Wind energy production was simulated with an approximated turbine power curve through a Boltzmann curve. Using “ORIGIN” data analysis software, a generic equation to calculate wind turbine power output for a given turbine size and wind speed was created with the input of industrial wind turbine power curves (Equation 5.4) [34],[35]. Due to the similar nature of turbine power curves, the Boltzmann curve was scalable for a turbine of a given size to generate the approximate power output. Figure 5.4 shows the performance comparison of two industrial wind turbines and the Boltzmann estimate of the turbine power curves. The Boltzmann estimate has a mean average prediction error of 1-2%, omitting the 4 m/s estimate error, which skews the result due to low initial generation values (high percentage variance) of the power curve.

$$MWh\ output = MW_{WT} * \left(\frac{1.00754 + (1.00754 - 0.01468)}{1 + e^{\left(\frac{WS - 8.5245}{1.24505}\right)}} \right) \quad \text{Equation 5.4}$$

Where 'MWh output' is the hourly power output of a wind turbine at a given wind speed (WS) and turbine size (MW_{WT}).



The red zone indicates wind speeds below the cut-in (less than 4m/s) speed for typical wind turbines.

Figure 5.4: Wind turbine power curve compared to the Boltzmann estimate to investigate the estimated reliability.

One onshore and two offshore scenarios were assessed. The reason for the two offshore scenarios (approximately 50 km offshore) was due to high south-westerly wind speeds in the north-western regions and calmer winds in the eastern region (Table 5.1). The wind datasets were obtained from "BrightWind" for the Offshore (North-West [N54.941, E-10.312], East coast [N°53.536, E°-5.400]) and Onshore (Central Ireland [N53.500, E-7.629]) scenarios. The Offshore East coast calculations are used as the exemplary scenario as they were found to be representative of forecasted wind turbine capacity factors [36].

Table 5.1: Annual wind conditions for locations across Ireland, offshore and onshore.

Scenario	Cp_{WT}	Offline hrs/a	Online hrs/a	% Time offline	% Green electricity	% Brown electricity
Offshore wind (North-west)	63.6%	603	8,162	6.9%	88.4%	11.6%
Offshore wind (East)	57.0%	663	8,102	7.6%	83.7%	16.3%
Onshore wind	32.1%	934	7,830	10.7%	69.0%	31.0%

Note: The "% Brown electricity" column in Table 5.1 refers to electricity pulled from the grid to maintain electricity production for a 10 MW electrolyser at an 80% capacity factor. As such the "% Green electricity" column in Table 5.1 relates to the percentage share of energy demand used by the electrolyser from wind turbines.

The wind data was recorded at an elevation of 100 metres from the ground. To represent accurate wind speeds at turbine hub height (reference 8 MW turbine hub height of 110m) [34], wind speed adjustments were made using a basic form of the power-law profile (Equation 5.5) [37].

$$u = u_r * \left(\frac{z}{z_r}\right)^{\alpha} \quad \text{Equation 5.5}$$

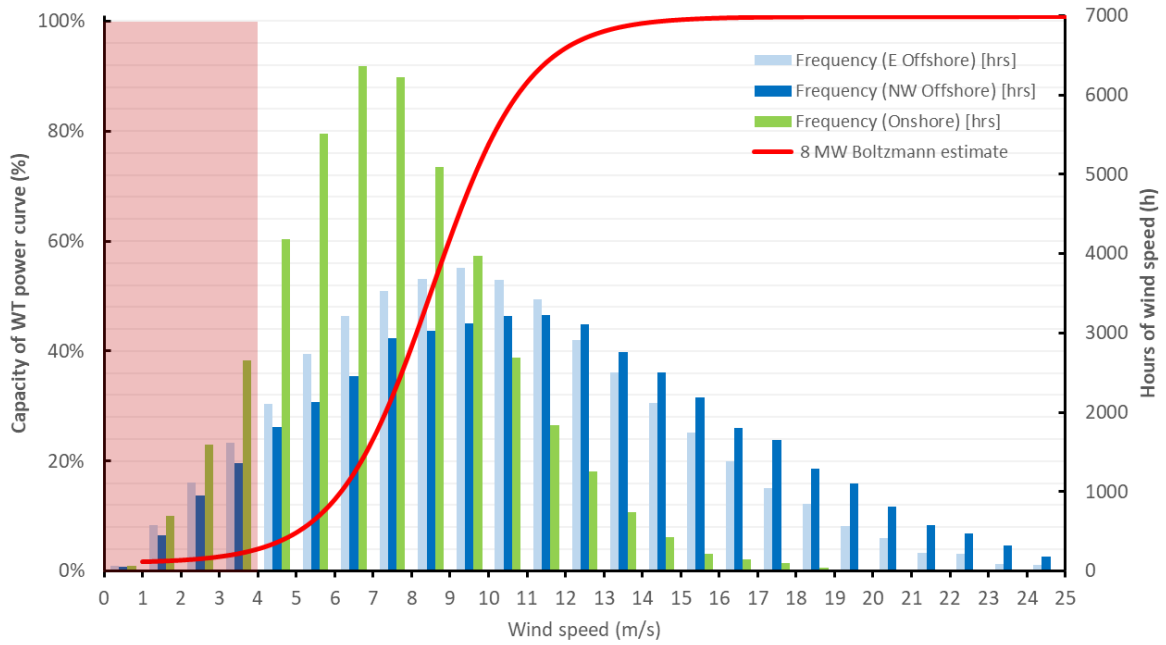
Where u is the wind speed at height z, and u_r is the reference wind speed at a reference height z_r. The wind shear exponent (power law exponent) α was modified on an hour-to-hour basis with the original data as reference height and wind speed (Equation 5.6) [37].

$$\alpha = \frac{0.37 - 0.088 \ln(U_r)}{1 - 0.088 \ln\left(\frac{z_r}{10}\right)} \quad \text{Equation 5.6}$$

Where α is the wind shear exponent, u_r and z_r are reference wind speed and height. Datasets for each scenario are at hourly intervals, spanning 5 years (2015-2019). Table 5.1 shows the wind turbine capacity factors (Cp_{WT}) of 32.1%, 57.0% and 63.6% as calculated for 'Onshore', 'Offshore East' and 'Offshore North-west' scenarios, respectively. The values generated were similar to those presented by the IEA [38]. The increase in offline hours is visualised in Figure 5.5 due to higher frequencies of sub 4m/s wind speeds in onshore scenarios.

The data was used to calculate the potential generated electricity of a common offshore wind turbine size (8 MW) with a custom curtailment percentage (10%), based on the current trend of annual curtailment in an Irish context (Figure 5.1). This allowed for a reliable approximation of the possible capture of curtailed electricity, and the size of the electrolyser suitable for the available energy (discussed in section 5.3.1). The estimated wind energy potential includes 2% power losses and 1.5% wake effect-related losses [39].

Due to intermittent power generation, some of the required electricity must be siphoned from the grid, under the assumption that the electrolyser always operates at 80% capacity, or approximately 7000 hours annually (see Figure 5.5**Error! Reference source not found.** in section 5.3.1). This is necessary to maintain the economic viability of the electrolyser [40]. For the offshore wind east scenario, approximately 83.7% of the used energy would be from wind turbines, whilst the other 16.3% would be brown electricity siphoned from the grid to maintain the electrolyser operating at an 80% capacity factor.



The red zone indicates wind speeds below the cut-in (less than 4 m/s) speed for typical wind turbines (cut-out greater than 25 m/s).

Figure 5.5: Comparison of On/Off-shore wind speed frequencies.

5.2.1.2 Hydrogen resource from the electrolyser

The electrolyser calculations follow a standard procedure (see section 5.3.1), with assumptions as per Box 5.1. The simplified calculation used in this work is representative of real-life electrolyser performance operating in a linear relation of power supply to H_2 and O_2 production. A capacity factor of 80% was assumed for the electrolyser under an assessment from McDonagh et al. [40] outlining the necessity of high system run hours for financial viability. A present-day electrolyser efficiency of 60% (LHV) or 72% (HHV) was assumed for a PEM electrolyser operating under a 2020 efficiency scenario [11],[40]. Higher electrolyser efficiencies are forecasted in the future, with 2030 PEM electrolyser efficiency estimates of up to 74% (LHV) [11]. As such the approach employed in this work may be assumed to be conservative.

5.2.2 Oxygen demand, sludge production and biogas produced

5.2.2.1 Oxygen demand at a wastewater treatment plant

To calculate the oxygen demand of a WWTP, a modified equation used for wastewater treatment oxygen demand was adapted for an activated sludge system, based on literature [41],[42] and code of practice values [43]. The subsequent calculations for the sludge production were similarly obtained. Assumptions made in the calculations were acquired from the literature and are synthesised in Box 5.1 [43],[44]. Assumptions for the oxygen demand and sludge calculations can be found in Table 5.2.

In practice, a WWTP must maintain a certain level of oxygen in the aeration tank to sustain biological activity. Equation 5.7 shows an adapted standard design equation to determine the total Oxygen demand in an activated sludge system [41].

$$OD = 0.75 * Q * (BOD_i - BOD_e) + 2 * V_A * MLSS/1000 + 4.3 * Q * (Amm_i - Amm_e) - 2.83 * Q * [(Amm_i - Amm_e) - N_e] \quad \text{Equation 5.7}$$

Where: OD is the oxygen demand of the WWTP, (g/h); Q is the inflow of a municipal WWTP, (m^3/h); V_A is the aeration tank volume, (m^3); MLSS is the mixed liquor suspended solids in the aeration tank (g/L). The BOD_i and BOD_e are the inflow and outflow concentrations of BOD (g/m^3); Amm_i and Amm_e are the inflow and outflow concentrations of ammoniacal nitrogen (g/m^3), and N_e is the outflow of nitrate nitrogen (g/m^3).

It should be noted that when primary sedimentation is not employed, and crude unsettled sewage is treated in extended aeration then the "0.75" value is changed to "1.0". These calculations do not consider the motor and shaft efficiencies and other losses and as such serve as simplified estimates of real-life scenarios. For further accuracy, a detailed design of the plant is required for more accurate oxygen demand and sludge production.

The total oxygen demand may be broken down as the sum of:

- Carbonaceous oxygen demand: $(0.75 * Q * (BOD_i - BOD_e))$
- Endogenous oxygen demand: $(2 * V_A * MLSS/1000)$
- Nitrification oxygen demand: $(4.3 * Q * ((Amm_i - Amm_e))$
- Less oxygen derived from denitrification in an anoxic zone: $(2.83 * Q * [(Amm_i - Amm_e) - N_e])$

Equations from other sources were also assessed (calculations not shown) to determine the most suitable estimation of WWTP oxygen demand. Results obtained from Equation 5.7 were compared with other methodologies and industry estimations to verify calculation integrity. It was found that Equation 5.7 offered the most conservative results out of the three assessed [41],[42],[43]. Again, as per the hydrogen resource from the electrolyser, a conservative approach is adopted.

The aeration tank volume (V_A) used in the oxygen demand was calculated using Equation 5.8 which highlights the dependence on the sediment retention time [43]

$$V_A = \frac{\theta_c \times Q_w \times X_r}{X} \quad \text{Equation 5.8}$$

Where: V_A is the aeration tank volume, (m^3); θ_c is the sediment retention time, (d); Q_w is the Waste activated sludge (WAS) flow rate (m^3/d); X_r is the waste sludge production ratio (kg/m^3), and X is the mixed liquor suspended solids (MLSS) in the aeration tank (kg/m^3).

5.2.2.2 Sludge production at a wastewater treatment plant

Typically, wastewater treatment removes sludge at two stages; the first takes place within the primary settling tanks, which removes approximately 50% of the solids in the wastewater (Equation 5.9). This Primary Sludge (PS) is rich in biomass, generating higher gas

yields in AD (see section 5.3.3). The second stage is at the end of the extended aeration process, where the Waste Activated Sludge (WAS) is produced due to the conversion of organic material into cell biomass [25] (Equation 5.10).

$$PS_{removed} = \frac{50\% \times Q \times TSS \times 24}{1000} \quad \text{Equation 5.9}$$

Where PS is the primary sludge removed (kg TS/d); Q is the inflow of a municipal WWTP (m^3/h); TSS is the total suspended solids (g/m^3); 50% is the TSS removal rate in the primary tank.

$$WAS_{produced} = 0.75 \times \frac{Q \times (BOD_i - BOD_e) \times 24}{1000} \times 0.6 \quad \text{Equation 5.10}$$

Where, WAS is the Waste activated sludge produced (kg TS/d), 0.75 accounts for 25% removal of BOD in the wastewater associated with 50% TSS removal in primary sedimentation. Variable Q is the respective inflow of a municipal WWTP (m^3/h); BOD_i and BOD_e are the inflow and outflow concentrations of BOD (mg/L) to the extended aeration basin, and 0.6 is the waste sludge production in kgTS/kg $BOD_{removed}$.

5.2.2.3 Biogas production from primary and waste-activated sludge

The reuse of sludge from the WWTP process is an important step for maximising the sustainability of the process. It is essential to discern the difference between the two types of sludge digested. As shown in Table 5.2, the yield of CH_4 and CO_2, and the biodegradation within the AD process varies significantly.

Table 5.2: Primary sludge and Waste Activated Sludge AD yield characteristics.

Primary Sludge			Waste Activated Sludge		
SMY	345	L CH_4/kg_{VS}	SMY	87	L CH_4/kg_{VS}
CO_2 %	33	%	CO_2 %	50	%
CH_4 %	67	%	CH_4 %	50	%
VS/TS	77	%	VS/TS	48	%
Ref.:	[45],[46]		Ref.:	[25]	

5.2.3 Biological hydrogen methanation

Assuming a CO_2 conversion of 98.6% for biological hydrogen methanation [44], CO_2 is converted to CH_4 through the addition of H_2 from the electrolyser as described in Equation 5.3. Assumptions made are listed in Box 5.1.

5.2.4 What emissions savings can be achieved at the wastewater treatment plant?

Emission savings for the WWTP have been estimated based on the O_2 volume demand reduction using pure O_2 aeration instead of air. The typical energy demand value for air aeration is 2.25 kgO_2/kWh (1.58 m^3O_2/kWh), for standard fine bubble diffusers, based on data from Drewnowski et al. and as indicated in Figure 5.3 [14]. This corresponds to 7.542

m^3air/kWh to supply the necessary equivalent O_2 (20.95% volume O_2 in the air). Mohammadpour et al. investigated the use of pure O_2 in the WWTP aeration process, yielding a far higher oxygen transfer of 12.5 kgO_2/kWh [47]. As discussed by Mohammadpour et al, the 5.5-fold increase in O_2 transfer has been attributed to the complex behaviour of the pure gas. Factors such as higher solubility of O_2 in the liquid, up to a 20% higher volumetric mass transfer coefficient for small bubbles (compared to air) and five times higher driving force for O_2 all contribute to this increased efficiency. Emissions due to aeration energy demand of electricity with a carbon intensity of 0.484 $kgCO_2eq$/kWh and a price of 0.07 €/kWh were used in the calculation of emission and cost reductions [16],[48],[49] as highlighted in Box 5.1.

5.2.5 End-use of renewable gases in fuelling trucks

Using biomethane and hydrogen as alternative energy vectors in the hard-to-abate sectors can potentially offer further significant emissions reductions. In this analysis, both H_2 and CH_4 were proposed as transport fuels for heavy goods vehicles (HGVs). Fuel types were compared based on the emissions per litre of fuel type. Diesel, compressed biomethane gas (CBG) and compressed hydrogen gas used in fuel cell trucks (referred to as simply CHG) were assessed based on the typical fuel and engine efficiencies found across the literature, (Table 5.3 and Box 5.1). See Table S5.1 and Figure S5.1 in Supplementary data for supporting evidence for these numbers. The energy, mass and emissions of fuels are given on a per kilometre basis, estimated from literature data and HGV truck specifications, specifically MJ/km energy use of HGVs. An annual HGV mileage of 60,000 km/truck was assumed for calculations [50],[51]. In Table 5.3, the CO_2 emissions for H_2 have been calculated based on the percentage of brown electricity used annually for the electrolyser, thus the emissions can vary significantly as alterations to the model are made.

Table 5.3: Vehicle efficiencies and properties.

	Avg. fuel consumption		Avg. CO_2 emissions			
	(kg Fuel/km)	(MJ/km)*	($kgCO_2$/km)	($kgCO_2$/kg Fuel)	(gCO_2/MJ)	Reference
Diesel HGV	0.287	12.2	0.922	3.207	75.27	[51],[52],[53],[54]
CBG HGV	0.275	13.8	0.217	0.789	15.77	[51],[54],[55]
CHG HGV	0.055	6.6	0.243	4.405	36.68	[16],[54],[55]

** - Values averaged from literature. The rest of the values rely on the literature values.*

Due to these H_2 emissions, the use of H_2 in biomethanation offsets the inherent carbon neutrality of biomethane, resulting in small but notable emissions from the use of the fuel

Box 5.1: Assumptions and data used in the analysis

Wind turbine size	8	MW
Electrolyser size	10	MW
Electrolyser capacity factor (Cp)	80	%
Electrolyser Efficiency (LHV)	60	%
H_2 properties (LHV) [0°C, 1 atm]	3.002	kWh/m^3
	11.126	m^3/kg
	0.002	kg/mol
O_2 properties [0°C, 1 atm]	0.032	kg/mol
	1.428	kg/m^3
Molar ratio H_2 : CH_4 in biomethanation	4 : 1	
Molar ratio H_2 : O_2 in electrolyser	2 : 1	
Standard aerator power demand	2.25	kgO_2/kWh
O_2 aerator power demand	12.5	kgO_2/kWh
Global average electricity CO_2 intensity	0.484	$kgCO_2e/kWh_{el}$
Electricity sale price	0.07	€/kWh
CBG (CH_4) LHV	50.04	MJ/kg
	13.9	kWh/kg
Density	0.716	kg/m^3
Molar mass	0.016	kg/mol
Specific CO_{2eq} emission	0.789	$kgCO_2e/kg_{CBG}$
Specific CO_{2eq} emission	0.104	gCO_2e/MJ_{CBG}
CHG (H_2) LHV	120.24	MJ/kg
	33.4	kWh/kg
	0.090	kg/m^3
	0.002	g/mol
Average HGV mileage	60,000	km/a
Diesel LHV	846	kg/m^3
	42.60	MJ/kg
	36.04	MJ/L
	3.21	$kgCO_2e$/kg Diesel

5.3 Discussion and Results

5.3.1 The relationship between the size of a wind farm, dispatch down and the size of an electrolyser

From Box 5.2 it may be seen that an average production of 39,913 MWhel is generated by an 8MW turbine (in an Eastern offshore scenario with 57.0% capacity as per Table 5.1). Operation of an electrolyser using the 10% curtailment of electricity over the year (similar to present curtailment levels as per Figure 5.1) would require 18 number wind turbines of 8 MW size to supply a 10 MW electrolyser (83.7% renewable electricity share). Of the total electricity produced 718.4 GWh_{el}/a, 90% (649 GWh_{el}/a) may be sent to the electricity grid while 70 GWh_{el}/a (from the 10% curtailment) would be sent to the electrolyser.

From Box 5.3 it may be seen that a 10 MW electrolyser operating at a capacity of 80% averaged over the year with an energy efficiency of 60% will generate 14,000,000 m3 H2 and 7,000,000 m3 of oxygen per annum. Due to the temporal mismatch of wind energy, 16.3% of the electrolyser electricity demand is siphoned from the grid as brown electricity (Table 5.5) to maintain the 80% capacity of the electrolyser (Table 5.5**Error! Reference source not found.**). With an average brown electricity CO_2 intensity of 0.484 $kgCO_2e/kWh$ [16], the average CO_2 intensity of the electricity used by the Electrolyser would be 0.079 $kgCO_2e/kWh$ (4.4 $kgCO_2e/kgH_2$).

Box 5.2: Relationship between wind farm, dispatch down and size of the electrolyser.

Using Equation 5.4, wind energy generated at hourly intervals, over a 5-year period was averaged.

$$\text{MWh output} = MW_{WT} * \left(\frac{1.00754+(1.00754-0.01468)}{1+e^{\left(\frac{WS-8.5245}{1.24505}\right)}} \right)$$

Table 5.4 shows the produced electricity and capacity factors for the east coast scenario with a turbine size of 8 MW. The wind speed (WS) in hourly intervals over a 5-year period is summarised and synthesised in Table 5.4.

Table 5.4: Annual and average 8MW turbine capacity factors (Offshore – East coast scenario).

Year	kWh_{el}/Turbine/a	MWh_{el}/Turbine/a	Wind Turbine Capacity factor (Cp_{WT})
2015	41,518,040	41,518	59.2%
2016	38,392,507	38,393	54.8%
2017	40,541,351	40,541	57.9%
2018	39,440,507	39,441	56.3%
2019	39,670,679	39,671	56.6%
Average	39,912,617	39,913	57.0%

$10\ MW_{Electrolyser} \times 80\%_{Cp} \times 8760 = 70{,}080 \frac{MWh}{a}$ Electrolyser electricity demand

$70{,}080\,\frac{\text{MWh}}{\text{a}} \div \left(39{,}913\,\frac{\text{MWh}}{\text{Turbine*a}} * 10\%_{\text{curtailed}}\right)$ = 18 wind turbines at 10% curtailment

18 wind turbines$*39{,}913\,\frac{\text{MWh}}{\text{Turbine*a}} \div 1000 = 718.4\,\frac{\text{GWh}}{\text{a}}$ total electricity from 18 wind turbines

Box 5.3: Electrolyser assessment

Electrolyser power demand:

$$10\ \text{MW}_{\text{Electrolyser}} \times 80\%_{\text{Cp}_{\text{EL}}} \times 8760 = 70{,}080\,\frac{\text{MWh}}{\text{a}}$$ Electrolyser electricity demand

$70{,}080\,\frac{\text{MWh}}{\text{a}} \times 60\%_{\text{LHV efficiency}} = \mathbf{42{,}048\,\frac{MWh}{a}}$ Electricity converted directly to H_2 and O_2.

H_2 generated:

Where:

H_2 Molar weight = 0.002 kg/mol

O_2 Molar weight = 0.032 kg/mol

$$\frac{42{,}048\,\frac{\text{MWh}}{\text{a}} \times 1000}{3.002_{\text{LHV}}\,\frac{\text{kWh}}{\text{m}^3}} = \mathbf{14{,}006{,}700\,\frac{m^3H_2}{a}}$$

$14{,}006{,}700\,\frac{\text{m}^3\text{H}_2}{\text{a}} \div 11.126\,\frac{\text{m}^3}{\text{kg}} = 1{,}258{,}900\,\frac{\text{kgH}_2}{\text{a}}$

$1{,}258{,}900\,\frac{\text{kgH}_2}{\text{a}} \div 0.002_{\text{H2 MW}}\,\frac{\text{kg}}{\text{mol}} = 624{,}465{,}400\,\frac{\text{Moles H}_2}{\text{a}}$

O_2 generated:

As per Equation 5.2, $2H_2O \rightarrow 2H_2 + O_2$ leading to twice as many moles of H2 produced as O2. Thus:

$624{,}465{,}400\ \frac{\text{Moles H}_2}{\text{a}} \div 2 = 312{,}232{,}700\ \frac{\text{Moles O}_2}{\text{a}}$

$312{,}232{,}700\ \frac{\text{Moles O}_2}{\text{a}} \times 0.032_{\text{O2 MW}}\,\frac{\text{kg}}{\text{mol}} = 9{,}987{,}400\,\frac{\text{kg O}_2}{\text{a}}$

$9{,}987{,}400\,\frac{\text{kg O}_2}{\text{a}} \div 1.428_{\text{O}_2\text{Density}}\ \frac{\text{kg}}{\text{m}^3} = \mathbf{6{,}994{,}000\,\frac{m^3O_2}{a}}$

Using an electrolyser to capture dispatch-down electricity can prove to be an effective way to maximise the capture of energy from a turbine whilst minimising the carbon footprint of the hydrogen produced. Assuming 10% curtailment, a 10 MW electrolyser at 80% capacity is capable of capitalising on 8.17% of the 10% curtailment, thus reducing curtailment to 1.82% (Figure 5.6**Error! Reference source not found.**). A possible solution for capturing this remaining curtailed electricity could be a small battery storage system, designed to capture the outlier peaks and discharge to provide power for the electrolyser, theoretically allowing for 100% capture of otherwise curtailed electricity.

Reliance on brown electricity from the grid will always be an issue if pulling curtailed variable renewable electricity (VRE) from a single wind farm unless the electrolyser is significantly undersized for the wind farm (see Figure 5.7**Error! Reference source not found.**). In Figure 5.7**Error! Reference source not found.**, the left axis shows the number of turbines required to satisfy the electricity demand of the electrolyser (in this case, a 10 MW electrolyser). The X-axis indicates the assumed initial curtailment (% of wind turbine generated electricity going to the electrolyser) of the wind turbines. Finally, the right axis indicates the residual curtailment after the electrolyser siphons its share from the curtailed electricity used in the electrolyser. The uneven curtailment increase is due to a reduction in allocated wind turbines required to satisfy the electrolyser demand with increased curtailment, leading to a reduction in the number of turbines allocated. Higher curtailment results in fewer turbines required. However, as the curtailed electricity increases, available electricity may exceed the electrolyser demand, resulting in excess electricity generated, beyond the capacity of the electrolyser; this results in an undersized electrolyser.

The output of these figures suggests that exclusive reliance on the wind turbines for electricity supply to the electrolyser to generate hydrogen is not feasible in maintaining adequate capacity. As per Table 5.1, 12-31% of the generated electricity would be missing if relying exclusively on wind turbines, owing to a mismatch in supply and demand. As such, electricity from the national grid, which has a carbon intensity, is required for the operation of the electrolysers [61].

Table 5.5: Annual electrolyser electricity origin and annual remaining curtailed electricity (East coast scenario).

Year	Green electricity share	Brown electricity share	Annual curtailed electricity
2015	85.9%	14.1%	1.94%
2016	81.0%	19.0%	1.78%
2017	85.1%	14.9%	1.83%
2018	83.2%	16.8%	1.79%
2019	83.0%	17.0%	1.78%
Average	83.7%	16.3%	1.82%

Note: Annual percentage of green and brown electricity share sums up to meet the assigned Electrolyser 80% capacity (i.e. – Green 83.7% + Brown 16.3% = 100% of the 10 MW electrolyser @ 80% capacity).
Curtailed electricity post electrolysis power demand, i.e. 10% - 1.82% = 8.17% of electricity produced by turbines recovered from curtailment.

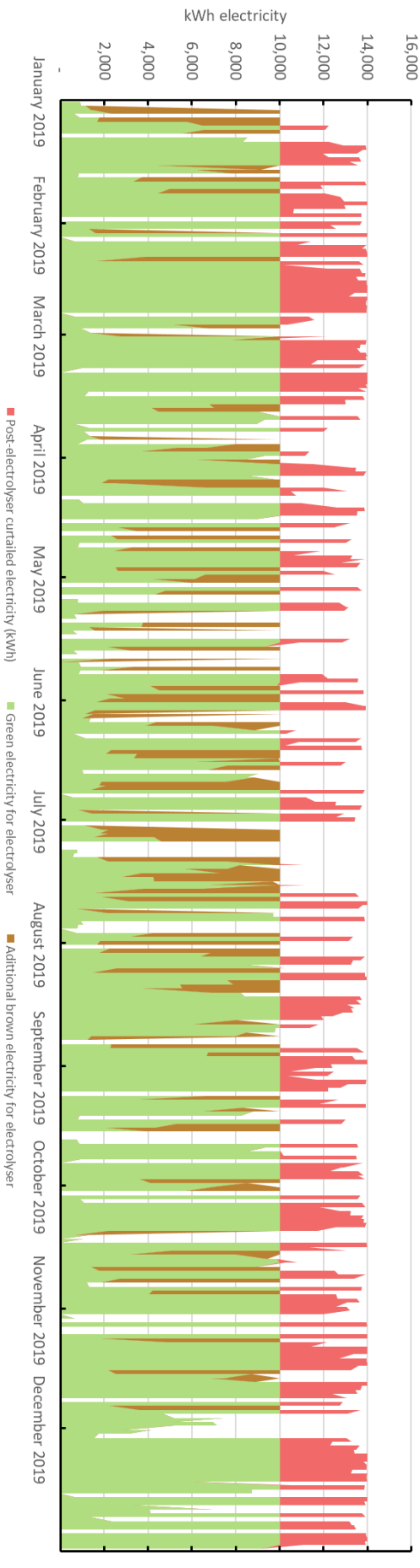
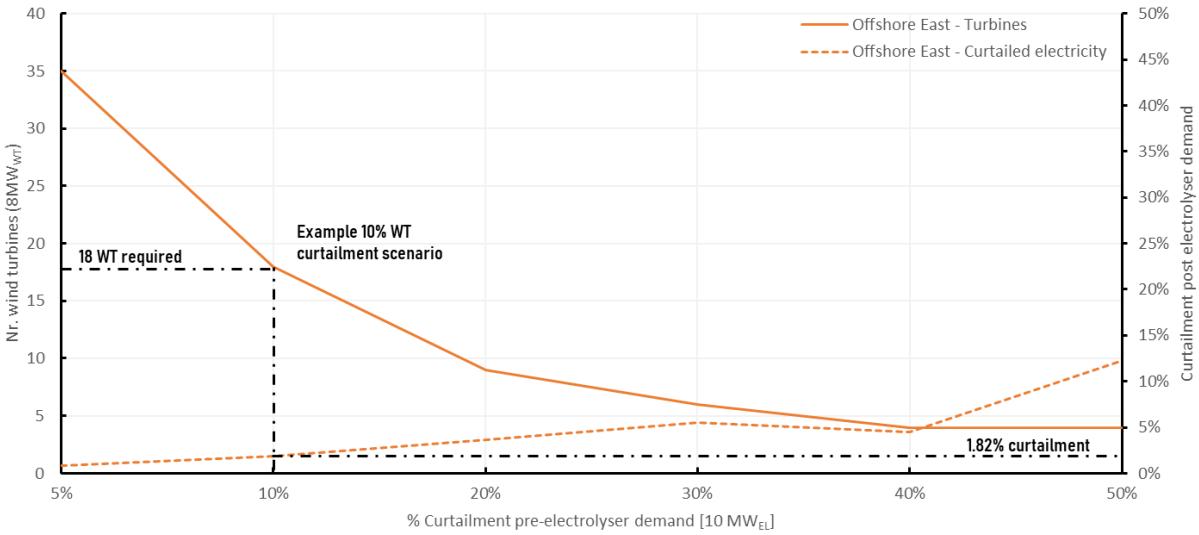


Figure 5.6: Representation of an annual (2019) electrolyser power demand (10MW @ 80% capacity), with available green VRE, denoted as green (84% of total), and siphoned additional brown electricity denoted as brown (16% of total). The remaining curtailed electricity is denoted as red (1.82%).



The dashed black line indicates Offshore East, 10MW scenario. The left axis shows the number of turbines (solid orange line) required for the chosen scenario. The right axis (dashed orange line) indicates the 'left-over' curtailed electricity after electrolyser demand.

Figure 5.7: Relationship of the number of wind turbines (8MW) required to supply the energy demand of an electrolyser (10MW @ 80% capacity) with increased curtailment, and the resulting increase in curtailment post electrolyser demand.

5.3.2 Relationship between electrolyser size and oxygen demand in an extended aeration basin.

From Box 5.4 it may be seen that for a 426,400 PE wastewater treatment plant 27,344 kg O_2 would be required per day which equates to c. 6,994,000 m^3O_2/a generated by the electrolyser. In an Irish context, this is equivalent to the WWTP of Cork which is the 2nd largest city in Ireland. The capital city, Dublin is served by a WWTP of 1.6 million PE, which would correspond to an approximate 39 MW electrolyser. On record, there are 7 municipal WWTPs in Ireland with population equivalents in the range 100,000 – 200,000 PE (corresponding to electrolyser sizes between 2.5 and 5 MW), totalling 3.1 million PE which is equivalent to 62% of the population [56]; however much of the population equivalent is likely to come from industry sources.

Box 5.4: WWTP oxygen demand and sludge production

Table 5.6: WWTP Influent liquid properties based on PE of 426,400. Code of practice values for a single PE.

Influent variables			Code of practice (Per Person)		
Q	3,554	m^3/h	Flow	0.2	m^3/PE/d
V_A	46,907	m^3	BOD	60	g/PE/d
BOD_i	300	g/m^3	Ammonia (NH_4-N)	4.5	g/PE/d
BOD_e	25	g/m^3	TSS	60	g/PE/d
MLSS (X)	3000	g/m^3	Sludge production	60	g_{TS}/PE/d
Amm_i	22.50	g/m^3	Waste sludge production (X_r)	0.6	kg_{TS} WAS/m^3
Amm_o	0.5	g/m^3	Solid concentration in clarifier	11	g/L
N_e	1	g/m^3	Sediment retention time	10	d
TSS in primary sludge	50	%	WAS flow rate (Q_w)	23,453	kg/day

Ref: [57], [42], [58] *Note: Influent variable values are for PE 426,400*

Aeration tank volume

$$\theta_c \frac{d}{1} \times Q_w \frac{m^3}{d} \times X_r \frac{kg}{m^3} / X \frac{kg}{m^3} = V_A \ m^3 \text{ from Equation 5.8.}$$

$$10\ d \times 23{,}453 \frac{m^3}{d} \times 0.6 \frac{kg}{m^3} / 3 \frac{kg}{m^3} = 46{,}907\ m^3$$

Oxygen Demand

$$OD = 0.75 \times Q \frac{m^3}{h} \times (BOD_i - BOD_e) \frac{g}{m^3} + 2\ V_A m^3 \times (MLSS \frac{g}{m^3} \times 0.001) + 4.3 \times$$
$$Q \frac{m^3}{h} \times (Amm_i - Amm_e) \frac{g}{m^3} - 2.83 * Q \frac{m^3}{h} * [(Amm_i - Amm_e) - N_e] \frac{g}{m^3}$$

$$OD = 0.75 \times 3{,}554 \frac{m^3}{h} \times (300-25) \frac{g}{m^3} + 2 \times (46{,}907) m^3 \times (3{,}000 \frac{g}{m^3} \times 0.001) + 4.3 \times 3{,}554 \frac{m^3}{h} \times$$
$$(22.50 - 0.5) \frac{g}{m^3} - 2.83 \times 3{,}554 \frac{m^3}{h} \times \left[(22.50-0.5) \frac{g}{m^3} - 1 \frac{g}{m^3}\right]$$

$$OD = 963{,}394 \frac{g}{h} + 11{,}676 \frac{g}{h} + 441{,}877 \frac{g}{h} - 277{,}598 \frac{g}{h} = 1{,}139{,}310 \frac{g}{h}$$

$$1{,}139{,}310 \frac{g}{h} \div 1000 \times 24 = \mathbf{27{,}344} \frac{\mathbf{kgO_2}}{\mathbf{d}}$$

$$27{,}344 \frac{kgO_2}{d} \times 365.25 \frac{d}{a} \div 1.428_{O_2 Density} \frac{kg}{m^3} = 6{,}993{,}829 \frac{m^3 O_2}{a} \approx \text{Electrolysis } O_2 \text{ production}$$

$$27{,}344 \frac{kgO_2}{d} \div 0.064 \frac{\frac{kgO_2}{PE}}{d} = \mathbf{426{,}400\ PE}$$

Value of $0.064 \frac{\frac{kgO_2}{PE}}{d}$ *obtained in Figure 5.9.*

The developed model (as represented in Figure 5.8**Error! Reference source not found.**) shows a linear relationship between the electrolyser size, the population equivalent (PE) of the WWTP, the H_2 and O_2 generation from the electrolysis process, and the number of 8MW wind turbines required for the 10% curtailment scenario. It is pertinent that the 10 MW

electrolyser producing 14,006,700 m^3H_2/and 6,994,000 m^3O_2/a, equates to the oxygen demand of a 426,400 PE WWTP.

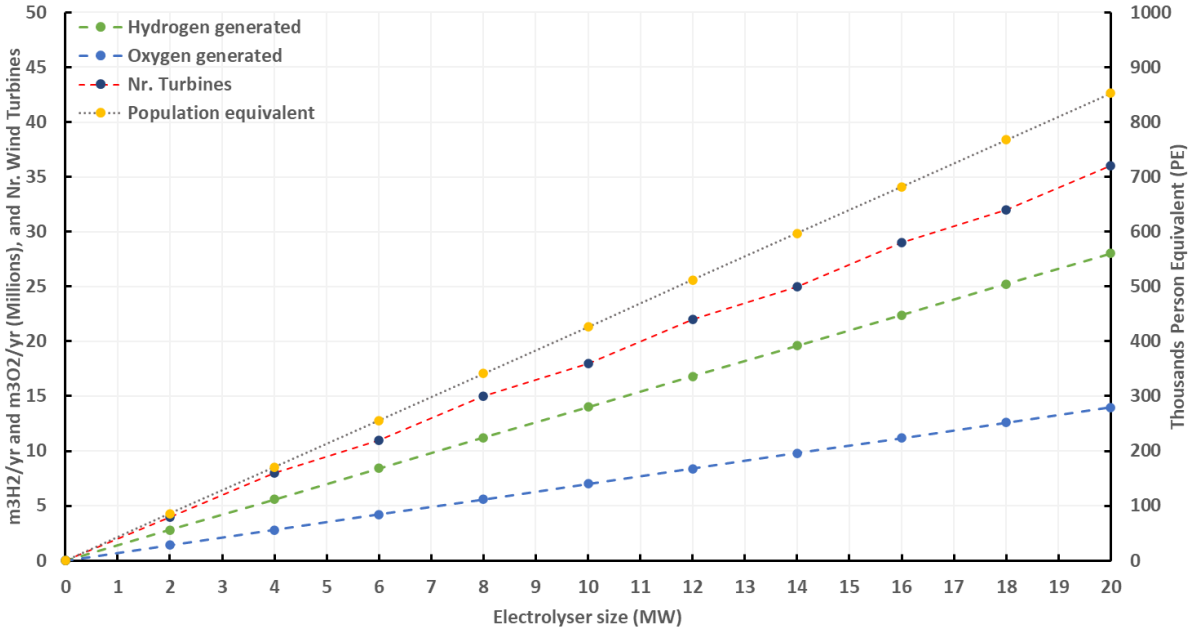


Figure 5.8: Electrolyser size vs H_2 and O_2 generated, and the number of wind turbines (8MW, 10% curtailment) required to supply oxygen to a wastewater treatment plant in an offshore wind (East) scenario.

A relationship was developed for a population equivalent oxygen demand and sludge production based on Equation 5.7 and the code of practice values (as per Box 5.4). Equation 5.7 and the methodology in Box 5.4 were used to assess oxygen demand and sludge generation for 10,000 – 1,000,000 PE. The results of the range were plotted and the slope presents an oxygen demand of 64.1 gO_2/PE/d and sludge production of 54.8 gTS_{Sludge}/PE/d (Figure 5.9**Error! Reference source not found.**).

Based on the calculated relationship, for a WWTP of approximately 426,400 PE capacity the oxygen required is 27.343 t/d which is equivalent to that which would be produced by the 10 MW electrolyser (27.343 t/d * 1000 kg/t * 365.25 days per year / 1.428 kg/m^3 = 6,994,000 m^3/a). The WWTP would produce 23.3 tTS/d (8,500 tTS/a) of which, 45.2% is waste activated sludge and 54.8% is primary sludge.

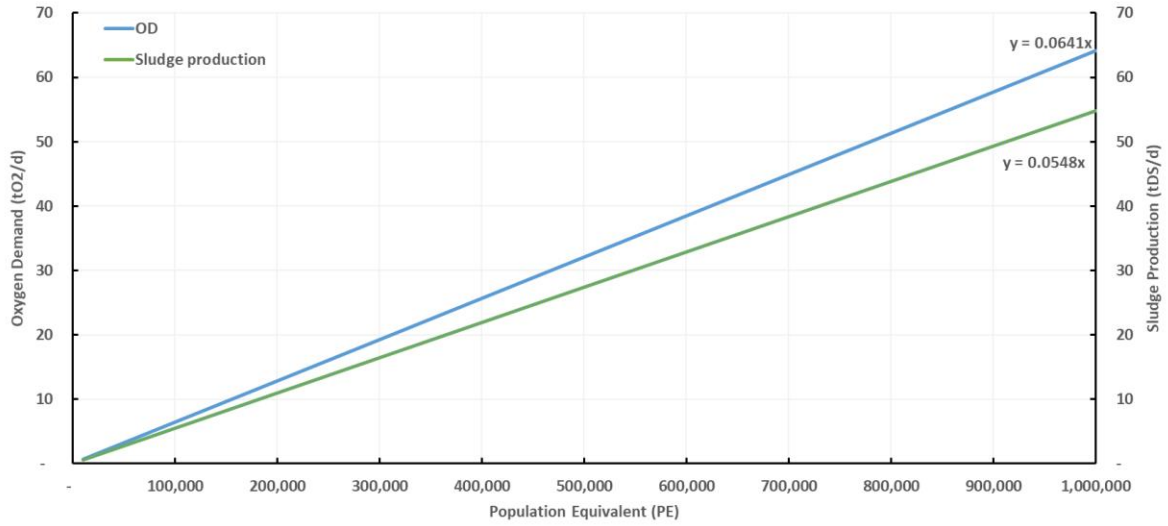


Figure 5.9: Oxygen demand and Sludge production relationship to WWTP PE based on a sludge production of 54.8 g TS/PE/d and 64.1 gO2/PE/d.

5.3.3 The H_2 required to upgrade the digested sludge biogas to biomethane

From Box 5.5 it may be noted that an estimated 12,793 kgTS/d of primary sludge and 10,554 kgTS/d of waste activated sludge is generated at the WWTP. AD produces 1,409,006 m^3CH_4/a of which 89% comes from primary sludge (1,248,027 m^3CH_4/a) and 11% comes from WAS (160,979 m^3CH_4/a).

The CO_2 generated in the biogas is modelled as reacted with hydrogen from the electrolyser in a biological methanation reactor; this increases the methane production by 54.3%. The hydrogen for this process equates to 22.2% of that produced from the 10MW electrolyser. This shows that oxygen demand is the critical parameter in matching an electrolyser to a wastewater treatment plant. If the model was to convert all of the H_2 into CH_4, a WWTP of approx. 1.92 million PE would be required to produce enough sludge to generate the necessary amount of CO_2 to react with H_2.

Box 5.5: Digestion of sludge, biogas and biological methanation

Sludge production:

Total solids in the Primary Sludge correspond to 50% of the TSS in the wastewater:

$$\text{Primary Sludge (PS) removal} = \frac{50\% \times Q \times TSS \times 24}{1000} = \frac{50\% \times 3{,}554 \frac{m^3}{hr} \times 300 \frac{g}{m^3} \times 24 \frac{h}{d}}{1000} = \mathbf{12{,}793 \frac{kgTS}{d}}$$

$$\text{WAS production} = 0.75 \times \frac{Q \times (BOD_i - BOD_e) \times 24 \frac{h}{d}}{1000} \times 0.6 = \frac{3{,}554 \frac{m^3}{hr} \times (300-25) \frac{g}{m^3} \times 24 \frac{h}{d}}{1000} * 0.6 \frac{kgTS}{kg\ BOD} = \mathbf{10{,}554 \frac{kgTS}{d}}$$

Total Sludge production = PS removal + WAS production

$$12{,}793 \frac{kgTS}{d} + 10{,}554 \frac{kgTS}{d} = 23{,}347 \frac{kgTS}{d} \times 365.25 = \mathbf{8{,}527{,}429 \frac{kgTS}{a}}$$

Digestion of PS:

$$12{,}793 \frac{kgTS}{d} \times 77\%VS \times 345 \frac{LCH_4}{kgVS} \div 1000 = \mathbf{3{,}417 \frac{m^3CH_4}{d}}$$

$3{,}417\ \frac{m^3CH_4}{d} \times 365.25 = \mathbf{1{,}248{,}027}\ \frac{\mathbf{m^3CH_4}}{\mathbf{a}}$

$\frac{1{,}248{,}027\ \frac{m^3CH_4}{a}}{67\%} \times 33\% = \mathbf{614{,}700}\ \frac{\mathbf{m^3CO_2}}{\mathbf{a}}$

Digestion of WAS:

$10{,}554\ \frac{kgTS}{d} \times 48\%VS \times 87\ \frac{LCH_4}{kgVS} \div 1000 = \mathbf{441}\ \frac{\mathbf{m^3CH_4}}{\mathbf{d}}$

$441\ \frac{m^3CH_4}{d} \times 365.25 = \mathbf{160{,}979}\ \frac{\mathbf{m^3CH_4}}{\mathbf{a}}$

$\frac{160{,}979\ \frac{m^3CH_4}{yr}}{50\%} \times 50\% = \mathbf{160{,}979}\ \frac{\mathbf{m^3CO_2}}{\mathbf{a}}$

Total CH_4 from PS and WAS $= 1{,}248{,}027\ \frac{m^3CH_4}{a} + 160{,}979\ \frac{m^3CH_4}{a} = \mathbf{1{,}409{,}006}\ \frac{\mathbf{m^3CH_4}}{\mathbf{a}}$

Total CO_2 from PS and WAS $= 614{,}700\ \frac{m^3CO_2}{a} + 160{,}979\ \frac{m^3CO_2}{a} = \mathbf{775{,}679}\ \frac{\mathbf{m^3CO_2}}{\mathbf{a}}$

Reaction of 775,679 m^3CO_2/a with H_2 in a biomethanation system:

$4H_2 + CO_2 \rightarrow CH_4 + 2H_2O$

$\frac{775{,}679\ \frac{m^3CO_2}{a} \times 4_{\text{molar ratio}}}{14{,}006{,}700\ \frac{m^3H_2}{a}} = \mathbf{22.2\%}$ of generated H_2 used in upgrading CO_2 .

$775{,}679\ \frac{m^3CO_2}{a} \times 98.6\%_{\text{BHM efficiency}}$ produces $\mathbf{764{,}819}\ \frac{\mathbf{m^3CH_4}}{\mathbf{a}}$

Use of $3{,}102{,}716\ \frac{m^3H_2}{a}$ in biomethanation results in a **54.3%** increase in CH_4 yield, totalling:

$1{,}409{,}006\ \frac{m^3CH_4}{a} + 764{,}819\ \frac{m^3CH_4}{a} = \mathbf{2{,}173{,}825}\ \frac{\mathbf{m^3CH_4}}{\mathbf{a}}$

Processing of 8,527,429 kgTS/a of sludge from a 426,400 PE WWTP produces a biogas mixture of 1,409,006 m^3CH_4/a and 775,679 m^3CO_2/a. The corollary of the electrolyser size on the WWTP size can be seen in Figure 5.8**Error! Reference source not found.**. Capturing the CO_2 from the AD process with biological hydrogen methanation technology allows for the upgrading of biogas that would otherwise require 'scrubbing' to bring the biomethane purity to the grid standard. With biological hydrogen methanation, an additional yield of 764,819 m^3CH_4/a is generated (98.8% conversion), by consuming the CO_2 and 3,102,716 m^3H_2/a, or 22.2% of the electrolyser generated H_2. This additional CH_4 equates to a 54.3% increase in the CH_4 yield, totalling 2,173,825 m^3CH_4/a. The capture of just this CO_2 is equivalent to a savings of 1.534 $ktCO_2/a$. The relationship between the WWTP and generated sludge and subsequent gas production is shown in Figure 5.10**Error! Reference source not found.**.

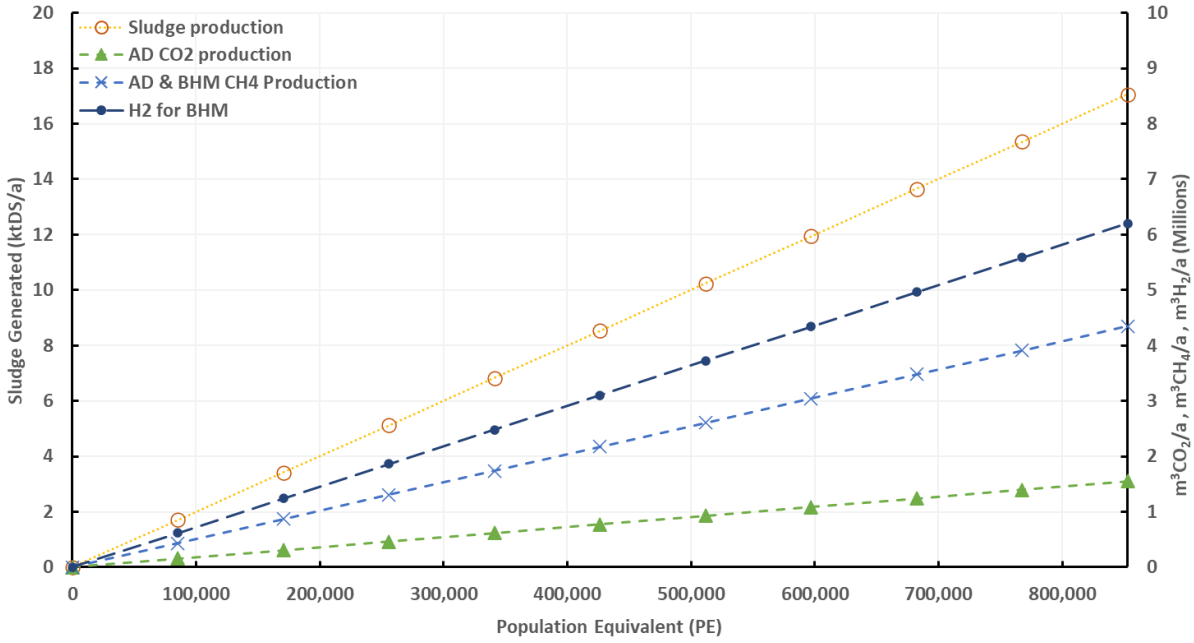


Figure 5.10: WWTP PE relationship to sludge generated, and resultant m^3 CH_4 and CO_2 produced from the digestion of sludge.

5.3.4 Emissions savings achieved at the wastewater treatment plant

It may be seen in Box 5.6 that by use of pure O_2 aeration instead of air aeration an 80% reduction in aeration electricity demand (from 4,440 MWh/a to 799 MWh/a) may be affected. When we consider that aeration is typically 49% of the power demand, the overall WWTP electricity demand (and the associated GHG emissions) may be reduced by 40% through O_2 use. In an Irish context, if the nine largest WWTPs in Ireland were to switch to pure O_2 aeration, 8 $ktCO_{2e}/a$ would be saved. A total of 3,000 decarbonised HGVs (2,200 CHG HGVs and 800 CBG HGVs) could be fuelled with a total emissions savings of c. 133 $ktCO_{2e}/a$.

Box 5.6: Emission savings associated with the reduction in aeration requirements. This excludes biogas/sludge/renewable methane/flaring reduction.

Aeration energy demand and emissions

$$27{,}344\ \frac{kgO_2}{d} \div 2.25\ \frac{kgO_2}{kWh} \times 365.25 \div 1000 = \mathbf{4{,}440}\ \frac{\mathbf{MWh_{el}}}{\mathbf{a}}$$ *(Aeration power demand)*

$$4{,}440\ \frac{MWh_{el}}{a} \div 49\%_{\text{Aeration power demand}} = \mathbf{9{,}060}\ \frac{\mathbf{MWh_{el}}}{\mathbf{a}}$$ *(Estimated total WWTP power demand)*

$$9{,}060\ \frac{MWh_{el}}{a} \times 49\%_{Aeration} \times 0.484\ \frac{kgCO_2}{kWh} \div 1000 = \mathbf{2.149}\ \frac{\mathbf{ktCO_{2eq}}}{\mathbf{a}}$$ *(Aeration emissions)*

$$9{,}060\ \frac{MWh_{el}}{a} \times 51\%_{WWTP} \times 0.484\ \frac{kgCO_2}{kWh} \div 1000 = \mathbf{2.236}\ \frac{\mathbf{ktCO_{2eq}}}{\mathbf{a}}$$ *(Other WWTP emissions)*

$$2.149\ \frac{ktCO_{2eq}}{a} + 2.236\ \frac{ktCO_{2eq}}{a} = \mathbf{4.385}\ \frac{\mathbf{ktCO_{2eq}}}{\mathbf{a}}$$ Total annual WWTP emissions.

Pure O_2 aeration scenario

$27{,}344\ \frac{kgO_2}{d} \div 12.5\ \frac{kgO_2}{kWh} \times 365.25 \div 1000 = \mathbf{799}\ \frac{\mathbf{MWh_{el}}}{\mathbf{a}}$ *(O_2 Aeration power demand fraction)*

Energy and associated emissions savings due to switching to pure O_2:

$799\ \frac{MWh_{el}}{a} \times 0.484\ \frac{kgCO_2}{kWh} \div 1000 = \mathbf{0.387}\ \frac{\mathbf{ktCO_{2eq}}}{\mathbf{a}}$ *(O_2 Aeration emissions)*

$4{,}440\ \frac{MWh_{el}}{a} - 799\ \frac{MWh_{el}}{a} = \mathbf{3{,}641}\ \frac{\mathbf{MWh_{el}}}{\mathbf{a}}$ *(O_2 Aeration power savings)*

$3{,}641\ \frac{MWh_{el}}{a} \times 0.484\ \frac{kgCO_2}{kWh} \div 1000 = \mathbf{1.762}\ \frac{\mathbf{ktCO_{2eq}}}{\mathbf{a}}$ *(O_2 Aeration emission savings)*

$1.762\ \frac{ktCO_{2eq}}{a} \div 4.385\ \frac{ktCO_{2eq}}{a} = \mathbf{40.2\%}$ *(Reduction in emissions at WWTP)*

$799\ \frac{MWh_{el}}{a} \div \left(\left(9{,}060\ \frac{MWh_{el}}{a} \times 51\%\right) + 799\ \frac{MWh_{el}}{a}\right) = \mathbf{14.7\%}$ *(O_2 Aeration as a % of the WWTP power demand)*

$3{,}641\ \frac{MWh_{el}}{a} \times 0.07\ \frac{€}{kWh} \times 1000 = \mathbf{250{,}000}\ \frac{\mathbf{€}}{\mathbf{a}}$ *(Annual savings due to switching to pure O_2 aeration)*

5.3.5 How many diesel trucks can be offset with the generated H_2 and CH_4?

Investigation of the end-use of H_2 and CH_4 was carried out by assessing their potential use in replacing diesel HGVs, as a method for emission reduction in transport and haulage. The CH_4 (2,173,825 m^3 CH_4/a) produced via combining biogas from the digestion of sludge and biomethanation, plus the remaining hydrogen (10,903,984 m^3 H_2/a) can power 94 CBG HGVs and 296 CHG (fuel cell) HGVs, and in doing so offset 16.022 $ktCO_{2e}$/a (Box 5.7). The specific value used for CBG HGV calculations of 0.789 $kgCO_2e/kgCH_4$ equates to 15.8 gCO_2e/MJ. The basis for this figure is that the biogas from anaerobic digestion is assumed to be carbon neutral. However, methane generated via biological hydrogen methanation carries the carbon footprint of the hydrogen via electrolysis associated with the emission intensity of the brown electricity used in electrolysis (16.3% for offshore wind east as identified in Table 5.1). The exaggeration of the emission intensity in the hydrogen is due to the electrolyser efficiency (taken conservatively as 60%). The resulting value of 15.8 g $CO2_e$/MJ may be contrasted with the fossil fuel comparator of 94 gCO_2/MJ in the recast renewable energy directive [59]. Indeed, Long and Murphy (2019), presented results for biomethane as a transport fuel which suggested sustainability in line with the recast Renewable Energy Directive at a carbon footprint of less than 32.9 g CO_2/MJ [59]. In Ireland, as of December 2020, there were a total of 39,922 HGVs, most of which were diesel fuelled [60]. This would equate to a 7.2% conversion of the entire Irish fleet. To convert all 39,922 diesel HGVs, this

would equate to approximately a 1 GW size electrolyser (enough O_2 for a 42.6 million WWTP PE) to switch all HGVs in Ireland to green HGVs (29,600 CHG HGVs and 9,400 CBG HGVs), with 1,800 $ktCO_{2e}/a$ savings, based on the current outlined scenario.

Box 5.7: Emission savings based on the displaced number of diesel HGV trucks

***Diesel Trucks** (Refer to Table 5.3, Box 5.1 & Box 5.5 for data used in this Box)*

$$2{,}173{,}825\frac{m^3CH_4}{a}\ (\text{Box 5.5})\times 0.716\frac{kg}{m^3}\left(=1{,}556{,}459\frac{kg\ CH_4}{a}\right)\times 50.04\frac{MJ}{kg}=77{,}885{,}131\frac{MJ}{a}$$

$$77{,}885{,}131\frac{MJ}{a}\div 42.60\ \frac{MJ}{kg}\ (\text{Diesel})=1{,}828{,}289\frac{kg\ Diesel}{a}$$

$$1{,}828{,}289\frac{kg\ Diesel}{a}\times 3.21\ \frac{kg\ CO_2e}{kg\ Diesel}\div 1000\div 1000=5.863\frac{kt\ CO_2e}{a}$$

$$1{,}828{,}289\frac{kg\ Diesel}{a}\div 0.287\ \frac{kg\ Diesel}{km}_{Average}=6{,}360{,}889\frac{km_{Diesel}}{a}$$

$$6{,}360{,}889\frac{km_{Diesel}}{a}\div 60{,}000\frac{km}{a}_{HGV}=106\frac{Trucks_{Diesel}}{a}$$

$$5.863\frac{kt\ CO_2e}{a}\times 1000\div 106\frac{Trucks_{Diesel}}{a}=\mathbf{55.3}\frac{\mathbf{t\ CO_2e}}{\mathbf{a}}\ \textbf{\textit{Per diesel HGV}}$$

Compressed biomethane gas (CBG) Trucks

$$1{,}556{,}459\frac{kg\ CH_4}{a}\times 0.789\frac{kg\ CO_2e}{kg\ CH_4}\div 1000\div 1000=1.228\frac{kt\ CO_2e}{a}$$

$$1{,}556{,}459\frac{kg\ CH_4}{a}\div 0.275\ \frac{kg\ CH_4}{km}_{Average}=5{,}654{,}299\frac{km_{CBG}}{a}$$

$$5{,}654{,}299\frac{km_{CBG}}{a}\div 60{,}000\frac{km}{a}_{HGV}=\mathbf{94}\frac{\mathbf{Trucks_{CBG}}}{\mathbf{a}}$$

$$1.228\frac{kt\ CO_2e}{a}\times 1000\div 94\frac{Trucks_{CBG}}{a}=\mathbf{13.07}\frac{\mathbf{t\ CO_2e}}{\mathbf{a}}\ \textbf{\textit{Per CBG HGV}}$$

To calculate the emissions savings, it is assumed 94 diesel trucks are replaced by the CBG trucks:

$$94\frac{Trucks_{diesel}}{a}\times 55.3\frac{t\ CO_2e}{a}\div 1000-94\frac{Trucks_{CBG}}{a}\times 13.07\frac{t\ CO_2e}{a}\div 1000$$

$$=\mathbf{3.970}\ \frac{\mathbf{kt\ CO_2e}}{\mathbf{a}}\ \textbf{\textit{Emissions savings}}$$

Compressed hydrogen gas (CHG) in fuel cell Trucks (using remaining H_2 from electrolysis)

$14{,}006{,}700\ \frac{m^3H_2}{a} - 3{,}102{,}716\ \frac{m^3H_2}{a}_{BHM} (=10{,}903{,}984\ \frac{m^3H_2}{a}) \times 0.0899\ \frac{kg}{m^3} = \mathbf{980{,}050\ \frac{kgH_2}{a}}$

$980{,}050\ \frac{kgH_2}{a} \div 0.055\ \frac{kg\ H_2}{km}_{Average} (=17{,}787{,}339\ \frac{km_{CHG}}{a}) \div 60{,}000\ \frac{km}{a}_{HGV} = \mathbf{296\ \frac{Trucks_{CHG}}{a}}$

$980{,}050\ \frac{kgH_2}{a} \times 4.405\ \frac{kg\ CO_2e}{kg\ H_2} \div 1000 \div 1000 = 4.317\ \frac{kt\ CO_2e}{a}$

$4.317\ \frac{kt\ CO_2e}{a} \times 1000 \div 296\ \frac{Trucks_{CHG}}{a} = \mathbf{14.585\ \frac{t\ CO_2e}{a}}$ ***Per CHG HGV***

To calculate the emissions savings, it is assumed 296 diesel trucks are replaced by CHG trucks.

$296\ \frac{Trucks_{diesel}}{a} \times 55.3\ \frac{t\ CO_2e}{a} \div 1000 - 296\ \frac{Trucks_{CHG}}{a} \times 14.585\ \frac{t\ CO_2e}{a} = \mathbf{12.052\ \frac{kt\ CO_2e}{a}}$ ***Emissions savings***

Emissions savings using CBG and CHG trucks instead of diesel trucks = $\mathbf{16.022\ \frac{kt\ CO_2e}{a}}$

Assessing the annually generated biomethane from both the AD and the biomethanation process (2,173,825 m^3CH_4/a), a fuel efficiency comparison was investigated for the different HGVs. The values chosen for fuel efficiency (Table 5.3) would suggest that on average, compressed biomethane (CBG) HGVs had the highest energy use of the three engine types (13.8 MJ/km), as compared to diesel (12.2 MJ/km) and compressed hydrogen (6.6 MJ/km). The emissions per km however, present a different perspective of the optimal fuel engine combination. Due to the low carbon footprint of the biomethane used for CBGs, these generated the lowest emissions. Biomethane emissions are comprised of the H_2 emission intensity, as some H_2 is used for the biomethanation process. In the case of hydrogen, it was found that the CO_2 intensity of the fuel was due to the significant share of brown electricity used in electrolysis. In our scenario, the CHG HGV had an emission intensity of 36.68 gCO_2/MJ (based on 16.3% brown electricity at a carbon intensity of 484 g CO_2/kWh in an electrolyser with an efficiency of 60%) [16]. In the case of compressed biomethane (CBG HGV), the CO_2 intensity of 15.77 gCO_2/MJ (Table 5.3) was also influenced by the hydrogen used in biomethanation. Using CH_4 and H_2 as fuel in HGV transport can offer significant CO_2 savings when sourced sustainably. The 94 CBG HGVs fuelled per annum had an average emission rate of 13.07 tCO_{2e}/truck/a (**Error! Reference source not found.**), totalling 3.970 $ktCO_{2e}/a$ in emissions savings (Box 5.7). The 296 CHG trucks had an emission rate of 24.954 tCO_{2e}/truck/a, resulting in 12.052 $ktCO_{2e}/a$ in total emissions savings (Box 5.7). Table 5.7**Error! Reference source not found.** outlines the relative comparison of the three truck technologies based on the same energy value in fuel which is equivalent to the methane produced.

Table 5.7: Comparison of fuel type performance (with an equivalent energy use [MJ calculated as per Box 5.7]) for HGVs at an annual mileage of 60,000 km.

Fuel type	MJ/a	kg Fuel/a	$ktCO_2$ emitted/a	$ktCO_2$ reduction/a	trucks/a	tCO_{2truck}/a
Diesel	77,885,131	1,828,289	5.863	-	106	55.30
CBG	77,885,131	1,556,459	1.228	4.634	94	13.07
CHG	77,885,131	647,748	2.853	3.009	196	14.56

Figure 5.11**Error! Reference source not found.** shows this corollary of electrolyser size to the number of diesel HGVs displaced and the resulting emissions reductions.

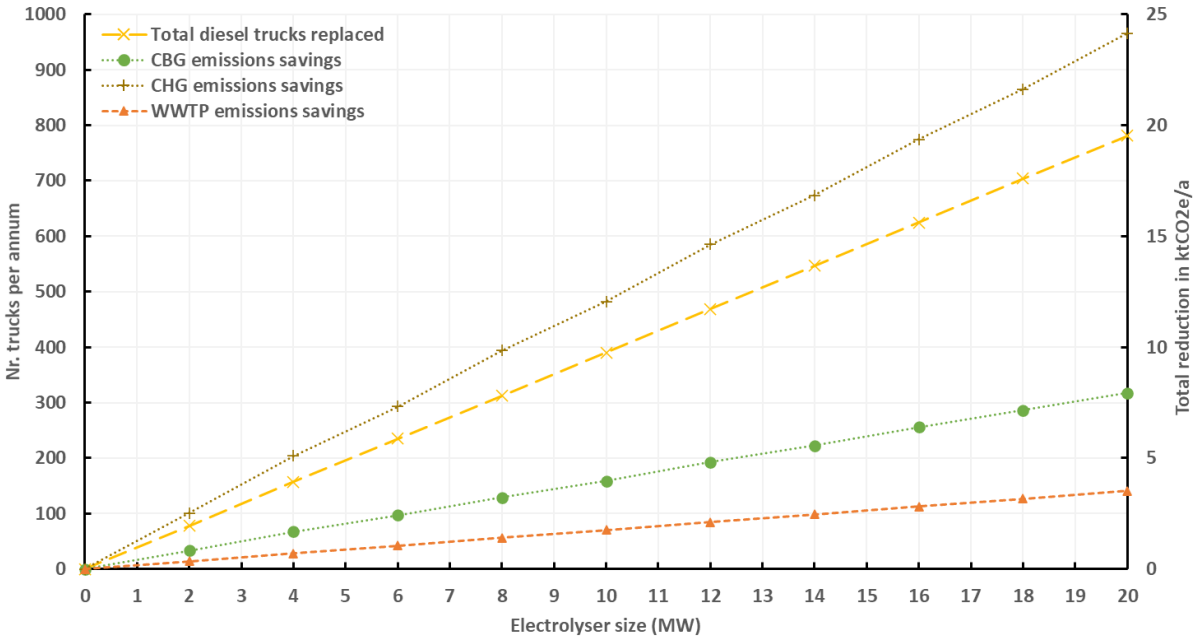


Figure 5.11: Relationship of electrolyser size to the number of diesel trucks replaced, emission savings using biomethane (CBG) and hydrogen (CHG) trucks in units of $ktCO_2e/a$ and the WWTP emission reductions ($ktCO_2e/a$) due to the switch to pure O_2.

5.3.6 Alternative configurations

The described scenario was designed to provide for the oxygen demand of the aeration basin. The electrolyser was shown to generate a volume of H_2 significantly above the amount of hydrogen required for ex-situ biomethanation of the biogas from sludge digestion. There is a range of alternative scenarios or variations in configurations of this model which could be used. One such scenario could size the electrolyser to convert the biogas from sludge digestion to pure CH_4 via biological methanation; this would be approximately 5 times smaller (c. 2MW electrolyser) as only 22% of the hydrogen is required for biomethanation in the assessed model. In this revised configuration the WWTP could use an enriched O_2 blend, rather than pure O_2. Another model or configuration could keep the 10MW electrolyser matching the O_2 demand of the 426,4000 PE WWTP but increase the biogas produced through the importation of other feedstock (such as grass silage or food waste) from the surrounding area to increase the biogas production by a factor of about 5

to produce the necessary CO_2. Only one gaseous vector (methane) is then produced. In other configurations or systems, the produced CH_4 may be injected into a nearby gas injection point, allowing for the decarbonisation of the gas grid. This could also be done with H_2, albeit at low blend volumes. The system could be used for 'power-to-X' processes such as ammonia (NH_3) via the Haber Bosch process or methanol (CH_3OH).

5.3.7 Limitations of the research and recommendations for future research.

While this study seeks to provide a broad perspective of the circular economy, energy, and environmental system model, the authors are conscious of potential perceived limitations and questions related to a further depth of analysis within specific technologies. Most aspects of the model focus solely on the movement of energy through the system. The detailed design of the individual systems and components has not been addressed due to the exponential complexity involved in the full design of each component (wind turbine, electrolysis technology and operation, specifics of wastewater treatment facility such as O_2 storage, H_2 storage, ex-situ biomethane system, service stations for hydrogen and methane, truck types). However, the authors wish to note some immediate considerations for future research.

For the wind turbine facilities, research is required in: connectivity to the electrolyser; simulation of an hourly load for the electricity market; system marginal cost profile for electricity; mechanical and electrical considerations, and a techno-economic assessment.

For the wastewater treatment and electrolysis system, further research is required in: aeration tank sizing; compressor and blower sizes to solve for transfer efficiency of gases; short-term storage and compression of pure O_2 for the aeration processes. Additional research is necessary in hydrogen sulfide gas removal; H_2 storage and grid injection; a scenario involving a contract with a wind facility for higher capacity factors; mechanical and electrical calculations, and a techno-economic assessment.

For the anaerobic digestion and biomethanation systems and end-use of gaseous fuels, research is required in: detailed design of the digester and biomethanation systems; end-use facilities; detailed assessment of the fuelling facilities for trucks; mechanical and electrical considerations; alternative grid injection route, and a techno-economic assessment. The authors recognise that the use of steam explosion treatment can also significantly enhance the biogas yields, while also reducing the drying requirements for the pyrolysis.

5.4 Conclusion

This paper developed on the model in the previous chapter. In an effort to simulate a large scale system, an offshore wind farm annual electricity production was simulated using publically available data. The study highlights the relationship across the system and the energy balance of said system. The product hydrogen and biomethane were also evaluated on their ability to displace traditional hydrocarbon fuels, as well as the potential emissions savings based on this displacement.

A 10 MW PEM electrolyser, operating at 80% capacity would require a 144MW (18 x 8MW) wind farm operating off the east coast of Ireland at 57.0% Cp_{WT}, with an assumed 10% curtailment scenario. The electrolyser would produce 14,006,700 m^3H_2/a and 6,994,000 m^3O_2/a. Some 16% additional brown grid electricity would be required to satisfy the electricity demand of the electrolyser. The oxygen produced (6,994,000 m^3O_2/a) would be capable of supplying the oxygen demand of a WWTP of 426,400 PE. This relationship has a downstream effect on the rest of the process, as it is governed by scale. The 426,400 PE WWTP as modelled generates 8,500 tTS/a of sludge which when digested should generate 1,409,000 m^3CH_4/a, and 775,700 m^3CO_2/a.

The use of biological methanation can upgrade the biogas to biomethane by reacting with the hydrogen from the electrolyser, yielding an additional 764,800 m^3CH_4/a. This increases the annual CH_4 yield by 54%, totalling 2,173,800 m^3CH_4/a. The hydrogen required in this process is 3,102,700 m^3H_2/a, 22% of that generated by the electrolyser. As such, it may be said that the oxygen demand of the WWTP is more critical that the hydrogen demand of a biomethanation system (used to upgrade the biogas produced in digesting primary and waste activated sludge) in assessing the sizing of an electrolyser at a WWTP.

Replacing the traditional air aeration of the wastewater treatment process with pure O_2 can result in a 40% reduction in emissions from the treatment facility. The additional biomethane produced in digesting the wastewater sludge and the hydrogen from the electrolyser not used in biomethanation, together can be used as a sustainable green fuel in road haulage, a hard-to-abate sector. As modelled, a 16.022 $ktCO_2e$/a reduction may be achieved through the replacement of 390 diesel trucks with 94 CBG trucks and 296 CHG trucks.

Acknowledgements

This work was supported by Science Foundation Ireland (SFI) through the MaREI Centre for Energy, Climate and Marine [Grant number 12/RC/2302_P2 and 16/SP/3829] with industrial funding from Gas Networks Ireland through the Green Gas Innovation group; and funding from the SFI zero emission challenge [Grant number 19/FIP/ZE/7565]. The authors would like to add thanks to colleagues Richard O'Shea and Nathan Gray for their time taken in reviewing the manuscript.

List of References

[1] EU Directive. Powering a climate-neutral economy: An EU Strategy for Energy System Integration [Internet]. Vol. 4, European Commission. 2020. Available from: https://eur-lex.europa.eu/legal-content/EN/ALL/?uri=COM:2020:299:FIN

[2] Pascuzzi S, Anifantis AS, Blanco I, Mugnozza GS. Electrolyzer performance analysis of an integrated hydrogen power system for greenhouse heating a case study. Sustain. 2016;8(7):1–15.

[3] Dykes A. ScottishPower plans 100MW green hydrogen plant at Felixstowe [Internet]. Energy Voice. 2022 [cited 2022 Aug 22]. Available from: https://www.energyvoice.com/renewables-energy-transition/hydrogen/uk-hydrogen/433894/scottishpower-plans-100mw-green-hydrogen-plant-at-felixstowe

[4] European Parliament. Directive (EU) 2018/2001 Of The European Parliament and of the council on the promotion of the use of energy from renewable resources (recast) [Internet]. Official Journal of the European Union. 2018 [cited 2019 Aug 26]. Available from: https://eur-lex.europa.eu/eli/dir/2018/2001/oj

[5] EirGrid and SONI. Annual Renewable Energy Constraint and Curtailment Report 2018 [Internet]. 2019. Available from: https://www.eirgridgroup.com/site-files/library/EirGrid/Annual-Renewable-Constraint-and-Curtailment-Report-2018-Non-Technical-Summary-V1.0.pdf

[6] EirGrid and SONI. Annual Renewable Energy Constraint and Curtailment Report 2020 [Internet]. 2021 [cited 2021 May 26]. Available from: https://www.soni.ltd.uk/media/documents/Annual-Renewable-Constraint-and-Curtailment-Report-2020-V1.0.pdf

[7] EirGrid and SONI. Annual Renewable Energy Constraint and Curtailment Report 2019 [Internet]. 2020. Available from: https://www.eirgridgroup.com/site-files/library/EirGrid/Annual-Renewable-Constraint-and-Curtailment-Report-2019-V1.2.pdf

[8] Steurer M, Fahl U, Voß A, Deane P. Curtailment: An option for cost-efficient integration of variable renewable generation?. An option for cost-efficient integration of variable renewable generation? [Internet]. Europe's Energy Transition: Insights for Policy Making. Elsevier Inc.; 2017. 97–104 p. Available from: http://dx.doi.org/10.1016/B978-0-12-809806-6.00015-8

[9] EirGrid Group. The DS3 Programme [Internet]. 2015 [cited 2021 Oct 19]. Available from: https://www.eirgridgroup.com/how-the-grid-works/ds3-programme/

[10] Department of Communications, Climate Action and Environment G of I. Climate Action Plan 2019: to Tackle Climate Breakdown [Internet]. 2019. Available from: https://www.dccae.gov.ie/en-ie/climate-action/topics/climate-action-plan/Pages/climate-action.aspx

[11] IEA. The Future of Hydrogen [Internet]. The Future of Hydrogen. OECD; 2019. Available from: https://www.oecd-ilibrary.org/energy/the-future-of-hydrogen_1e0514c4-en

[12] Schmidt O, Gambhir A, Staffell I, Hawkes A, Nelson J, Few S. Future cost and performance of water electrolysis: An expert elicitation study. Int J Hydrogen Energy [Internet]. 2017 Dec 28 [cited 2021 Feb 26];42(52):30470–92. Available from: https://linkinghub.elsevier.com/retrieve/pii/S0360319917339435

[13] European Environment Agency, The Water Information System for Europe. Urban waste water directive treatment plants data viewer [Internet]. 2018 [cited 2021 Mar 23]. Available from: https://www.eea.europa.eu/themes/water/european-waters/water-use-and-environmental-pressures/uwwtd

[14] Drewnowski J, Remiszewska-Skwarek A, Duda S, Łagód G. Aeration Process in Bioreactors as the Main Energy Consumer in a Wastewater Treatment Plant. Review of Solutions and Methods of Process Optimization. Processes [Internet]. 2019 May 24;7(5):311. Available from: https://www.mdpi.com/2227-9717/7/5/311

[15] Hannah Ritchie. Sector by sector: where do global greenhouse gas emissions come from? [Internet]. Our World In Data. 2020. Available from: https://ourworldindata.org/ghg-emissions-by-sector#licence

[16] International Energy Agency. IEA: World Energy Outlook 2018 [Internet]. IEA. 2018 [cited 2021 Mar 24]. Available from: https://www.iea.org/reports/world-energy-outlook-2018

[17] Larrea A, Rambor A, Fabiyi M. Ten years of industrial and municipal membrane bioreactor (MBR) systems – lessons from the field. Water Sci Technol [Internet]. 2014 Jul 1 [cited 2021 Apr 27];70(2):279–88. Available from: http://iwaponline.com/wst/article-pdf/70/2/279/471049/279.pdf

[18] Jacobs, Yarra Valley Water. Towards a zero carbon future. Yarra Valley Water [Internet]. 2020. Available from: https://www.jacobs.com/sites/default/files/2022-03/jacobs-yarra-valley-water-towards-a-zero-carbon-future.pdf

[19] van Loosdrecht MCM, Brdjanovic D. Anticipating the next century of wastewater treatment. Science (80-) [Internet]. 2014 Jun 27;344(6191):1452–3. Available from: https://www.science.org/doi/10.1126/science.1255183

[20] Gruber-Glatzl W, Brunner C, Meitz S, Schnitzer H. From the Wastewater Treatment Plant to the Turnstiles of Urban Water and District Heating Networks. Front Sustain Cities [Internet]. 2020 Nov 27 [cited 2021 Mar 5];2:523698. Available from: https://www.frontiersin.org/articles/10.3389/frsc.2020.523698/full

[21] Capodaglio AG, Olsson G. Energy issues in sustainable urban wastewater management: Use, demand reduction and recovery in the urban water cycle. Sustain [Internet]. 2020 Dec 29 [cited 2021 Mar 23];12(1):266. Available from: https://www.mdpi.com/2071-1050/12/1/266

[22] Hao X, Furumai H, Chen G. Resource recovery: Efficient approaches to sustainable water and wastewater treatment. Water Res [Internet]. 2015 Dec;86:83–4. Available from: http://dx.doi.org/10.1016/j.watres.2015.10.063

[23] Zhang X, Liu Y. Circular economy is game-changing municipal wastewater treatment technology towards energy and carbon neutrality. Chem Eng J [Internet].

2022;429(May 2021):132114. Available from: https://doi.org/10.1016/j.cej.2021.132114

[24] Andreoli C V, von Sperling M, Fernandes F. Sludge Treatment and Disposal. Water Intell Online [Internet]. 2015 Dec 30;6:9781780402130–9781780402130. Available from: https://library.oapen.org/bitstream/id/2cfbc8d9-8306-4c26-8b13-27e213a14f26/640145.pdf

[25] Potdukhe RM, Sahu N, Kapley A, Kumar R. Co-digestion of waste activated sludge and agricultural straw waste for enhanced biogas production. Bioresour Technol Reports. 2021 Sep 1;15:100769.

[26] Paolini V, Petracchini F, Segreto M, Tomassetti L, Naja N, Cecinato A. Environmental impact of biogas: A short review of current knowledge. J Environ Sci Heal - Part A Toxic/Hazardous Subst Environ Eng [Internet]. 2018 Aug 24 [cited 2021 Mar 23];53(10):899–906. Available from: https://www.tandfonline.com/doi/full/10.1080/10934529.2018.1459076

[27] Environmental Protection Agency. Urban Waste Water Treatment in 2018 [Internet]. Official Journal of the European Union. 2019. 40–52 p. Available from: http://eur-lex.europa.eu/legal-content/EN/TXT/PDF/?uri=CELEX:31991L0271&from=EN

[28] Murphy JD, Gustafsson M, Ammenberg J. Task 37 Biogas Country Report Summaries [Internet]. IEA Bioenergy. 2020. Available from: https://task37.ieabioenergy.com/country-reports.html

[29] Pfluger A, Coontz J, Zhiteneva V, Gulliver T, Cherry L, Cavanaugh L, et al. Anaerobic digestion and biogas beneficial use at municipal wastewater treatment facilities in Colorado: A case study examining barriers to widespread implementation. J Clean Prod [Internet]. 2019 Jan 1 [cited 2021 Mar 4];206:97–107. Available from: https://linkinghub.elsevier.com/retrieve/pii/S0959652618328841

[30] Silvestre G, Fernández B, Bonmatí A. Significance of anaerobic digestion as a source of clean energy in wastewater treatment plants. Energy Convers Manag [Internet]. 2015 Sep 10 [cited 2021 Mar 4];101:255–62. Available from: https://linkinghub.elsevier.com/retrieve/pii/S019689041500480X

[31] Shen Y, Linville JL, Urgun-Demirtas M, Mintz MM, Snyder SW. An overview of biogas production and utilization at full-scale wastewater treatment plants (WWTPs) in the United States: Challenges and opportunities towards energy-neutral WWTPs. Renew Sustain Energy Rev [Internet]. 2015;50:346–62. Available from: http://dx.doi.org/10.1016/j.rser.2015.04.129

[32] Rusmanis D, O'Shea R, Wall DM, Murphy JD. Biological hydrogen methanation systems–an overview of design and efficiency [Internet]. Vol. 10, Bioengineered. 2019 [cited 2020 Jan 29]. p. 604–34. Available from: https://www.tandfonline.com/doi/full/10.1080/21655979.2019.1684607

[33] Fan Y, Lei Z, Guo Z, Huang W, Wang D, Wang X, et al. Enhanced solubilization of solid organics and methane production by anaerobic digestion of swine manure under nano-bubble water addition. Bioresour Technol. 2020 Mar 1;299:122512.

[34] Desmond C, Murphy J, Blonk L, Haans W. Description of an 8 MW reference wind turbine. J Phys Conf Ser [Internet]. 2016 Sep [cited 2021 Aug 26];753:092013. Available from: https://iopscience.iop.org/article/10.1088/1742-6596/753/9/092013

[35] ENERCON. Product portfolio [Internet]. p. 1–19. Available from: https://www.enercon.de/fileadmin/Redakteur/Medien-Portal/broschueren/EC_WEA_EN.pdf

[36] International Energy Agency. Offshore Wind Outlook 2019 [Internet]. 2019 [cited 2021 Aug 25]. Available from: https://www.iea.org/reports/offshore-wind-outlook-2019

[37] Manwell JF, McGowan JG, Rogers AL. Theory, Design and Application. In: Wind Energy Explained. 2010. p. 45–7.

[38] International Energy Agency. Offshore Wind Outlook 2019 [Internet]. 2019. Available from: https://www.iea.org/reports/offshore-wind-outlook-2019

[39] McDonagh S, Ahmed S, Desmond C, Murphy JD. Hydrogen from offshore wind: Investor perspective on the profitability of a hybrid system including for curtailment. Appl Energy [Internet]. 2020 May 1 [cited 2020 Apr 7];265:114732. Available from: https://linkinghub.elsevier.com/retrieve/pii/S0306261920302440

[40] McDonagh S, O'Shea R, Wall DM, Deane JP, Murphy JD. Modelling of a power-to-gas system to predict the levelised cost of energy of an advanced renewable gaseous transport fuel. Appl Energy [Internet]. 2018;215(January 2018):444–56. Available from: https://doi.org/10.1016/j.apenergy.2018.02.019

[41] Environmental Protection Agency. Primary, Secondary and Tertiary Treatment. Waste Water Treatment Manuals. 1997. 27–28 p.

[42] George Tchobanoglous, Franklin L. Burton HDS. Wastewater Engineering : Treatment and Reuse (Fourth Edition). Vol. 179, Metcalf & Eddy, Inc. 2003. 317 p.

[43] Davis ML. Water and Wastewater Engineering : Design principles and practice. McGraw-Hill Companies Inc.; 2010.

[44] Von Sperling M. Wastewater Characteristics, Treatment and Disposal. Water Intell Online [Internet]. 2015 Dec 30 [cited 2021 Apr 29];6:292. Available from: https://www.iwapublishing.com/sites/default/files/ebooks/9781780402086.pdf

[45] Wei W, Cai Z, Fu J, Xie GJ, Li A, Zhou X, et al. Zero valent iron enhances methane production from primary sludge in anaerobic digestion. Chem Eng J. 2018 Nov 1;351:1159–65.

[46] Wei W, Guo W, Ngo HH, Mannina G, Wang D, Chen X, et al. Enhanced high-quality biomethane production from anaerobic digestion of primary sludge by corn stover biochar. Bioresour Technol. 2020 Jun 1;306:123159.

[47] Mohammadpour H, Cord-Ruwisch R, Pivrikas A, Ho G. Utilisation of oxygen from water electrolysis – Assessment for wastewater treatment and aquaculture. Chem Eng Sci. 2021 Dec 31;246:117008.

[48] Robescu LD, Presură E. Reducing carbon footprint of a wastewater treatment plant using advanced treatment and renewable energy sources. Environ Eng Manag J. 2017;16(5):1055–62.

[49] Enerpower. Feed in Tariffs Ireland [Internet]. [cited 2021 Apr 29]. Available from: https://enerpower.ie/portfolio-item/feed-in-tariffs-ireland/

[50] Sustainable Energy Authority of Ireland. Energy in Ireland 2020 Report. 2020 [cited 2021 Mar 10];(2):1–45. Available from: https://www.seai.ie/publications/Energy-in-Ireland-2020.pdf

[51] Ricardo Energy & Environment, Kollamthodi S. The role of natural gas and biomethane in the transport sector. Transp Environ Rep [Internet]. 2016;(1):1–85. Available from: https://www.transportenvironment.org/discover/?_article_type=publications

[52] Langshaw L, Ainalis D, Acha S, Shah N, Stettler MEJ. Environmental and economic analysis of liquefied natural gas (LNG) for heavy goods vehicles in the UK: A Well-to-Wheel and total cost of ownership evaluation. Energy Policy [Internet]. 2020 Feb;137(November 2019):111161. Available from: https://doi.org/10.1016/j.enpol.2019.111161

[53] Smajla I, Sedlar DK, Drljača B, Jukić L. Fuel switch to LNG in heavy truck traffic. Energies. 2019;12(3).

[54] ICCT, Moultak M, Lutsey N, Hall D. Transitioning to zero-emission heavy-duty freight vehicles. Int Counc Clean Transp [Internet]. 2017;(September):53. Available from: www.theicct.org

[55] Department for Business E& IS. Greenhouse gas reporting: conversion factors 2020 [Internet]. Government Digital Service. 2020 [cited 2021 Apr 7]. p. 1. Available from: https://www.gov.uk/government/publications/greenhouse-gas-reporting-conversion-factors-2020

[56] European Commission. European Commission urban waste water website: Ireland [Internet]. [cited 2022 Aug 22]. Available from: https://uwwtd.eu/Ireland/download

[57] Environmental Protection Agency I. Wastewater Treatment Manuals. Management. 1997.

[58] Smallbone A, Jia B, Atkins P, Roskilly AP. The impact of disruptive powertrain technologies on energy consumption and carbon dioxide emissions from heavy-duty vehicles. Energy Convers Manag X. 2020 Apr 1;6:100030.

[59] Long A, Murphy JD. Can green gas certificates allow for the accurate quantification of the energy supply and sustainability of biomethane from a range of sources for renewable heat and or transport? Renew Sustain Energy Rev [Internet]. 2019 [cited 2021 Nov 25];115. Available from: https://sci-hub.se/https://doi.org/10.1016/j.rser.2019.109347

[60] Department of Transport. Ten-year Strategy for the Haulage Sector. First Consultation Document [Internet]. 2021. Available from: https://assets.gov.ie/131011/9ec09053-

9c24-4860-9f98-d81d08206e4a.pdf

[61] SEAI. Common conversion factors for energy use in Ireland [Internet]. 2020. Available from: https://www.seai.ie/data-and-insights/seai-statistics/conversion-factors/

6. Conclusions and Recommendations

The development of novel power-to-gas technologies presents opportunities for a solution to the major challenge of matching the energy demand to the variability of renewable electricity generation technologies. Integrating electrolysers and biomethanation technologies could offer sustainable pathways for hard-to-abate sectors such as haulage, aviation, and shipping, which rely heavily on traditional fossil hydrocarbon fuels. Hydrogen produced from electrolysis (from *preferable* curtailed or surplus electricity) and biogas (produced from the digestion of organic waste) may be upgraded in a biomethanation process to gas grid specification biomethane (or renewable methane) via reaction of CO_2 (within biogas) and hydrogen (from electrolysis). The biomethane vector may be viewed as a decentralised energy storage method and/or an alternative energy vector for haulage.

Current biomethanation systems present various obstacles across different systems. Financially sustainable biomethanation systems require optimisation of the methane evolution rate by improving the gas transfer rates while limiting the parasitic energy demand of the system. Optimising the retention times and overall performance will mean increased dispatchability of the systems during periods of excessive variable renewable electricity production, increased gas grid demand, or demand in renewable haulage transport fuel. With increasing technology readiness level (TRL) capital costs are expected to fall as systems become more compact, and a specific optimised design is produced in bulk.

The proposed circular economy and energy system in this thesis seeks to combine the novel biomethanation technology with wind turbines, wastewater treatment plants (WWTPs), anaerobic digesters and electrolysers to create a symbiotic relationship across the previously independent sectors of water, gas, and electricity.

6.1. Conclusions

This thesis addresses a number of objectives throughout its chapters. In-depth summaries are thoroughly discussed at the end each respective chapter. This chapter highlights the key points of the thesis, collating the results of the previous thesis chapters into an overarching conclusions section.

Chapter 2 serves as a literature review for the anaerobic digestion and the biomethanation technologies. The chapter primarily identified a knowledge gap in the state of the art of biomethanation technology. This gap being the ex-situ methanation technology. It was evident that biomethanation technology was not yet mature, with current designs borrowing from the anaerobic digestion reactor, which use impeller agitation. The authors thus proposed investigating novel dissolution technologies.

Based on the conclusions drawn from the previous chapter, Chapter 3 focused on the design and commission of the cascading diffusion based biological methanation system. The experiment was deemed successful. The system was capable of matching the

performance of the previously simulated system by Voelklein et al. (2019). The authors concluded that a TRL of 4 was achieved for the biomethanation rig. The fabricated system was capable of exceeding the 95% CO_2 conversion levels set out in the previous simulations by Voelklein et al. (2019), with peak conversions of 72%, 91% and 97% for three contiguous sequential ex-situ biomethanation rigs named R1, R2, and R3, respectively [1]. The methane evolution rate across the three reactors averaged 2.5 – 3.4 $L/L_{vr}/d$, matching closely to the 3.6 $L/L_{vr}/d$ of the previous study by Voelklein et al. (2019). The system was capable of achieving grid-quality biomethane (> 95% CH_4) and was capable of converting the majority of the CO_2 to methane during the commissioning process. The development of the novel biomethanation technology opens opportunities for more advanced and versatile biomethanation systems. Such an adaptive technology could be coupled with existing technologies like anaerobic digesters, co-locating them on farms, or wastewater treatment plants (As seen in the following chapters). This symbiosis promotes the circular economy pathway and enable the production of green energy from biological waste. This symbiosis is crucial if Ireland is to reduce its overall emissions by 51% by 2030 and achieve carbon neutrality by 2050.

Chapter 4 departed from the lab-scale studies and single system assessment seen in the previous chapters. A model was developed with the intent of integrating a range of technologies, including a biomethanation system, into a circular energy hub. This consisted of an electrolyser located at a wastewater treatment plant, with an anaerobic digester and a biomethanation system. A local pyrolysis station was also investigated to assess the potential for biochar production from the wastewater sludge, and the wider local region in an effort to explore negative emission pathways. In collaboration with the local industry, data was obtained from two turbines to assess the potential available electricity. It was found that a 122 kW electrolyser using surplus variable renewable electricity could supply 8.9% of the oxygen demand necessary for the aeration of an aeration basin treating the wastewater for a 65,000 person equivalent (PE) wastewater treatment plant by recycling the by-product oxygen from the electrolysis process to the aeration basin. The electrolyser produced H_2 could convert 40.2% of the CO_2 generated in the anaerobic digestion of sludge at the 65,000 PE wastewater treatment plant. The resulting levelised cost of hydrogen production was modelled at €8.92/kg H_2. This price could not currently justify smaller-scale systems using intermittent curtailed electricity as presented. The co-located 122 kW electrolyser at the WWTP utilised otherwise vented O_2, offering some operational cost reductions for the WWTP, through reduced air compression demand in the aeration basin. CO_2 emissions (and electricity usage) could potentially be reduced by an estimated 16.04 tCO_2eq/a (3.6%) due to the associated reduced pumping requirements. The circular energy and economy model has a viable negative carbon emissions pathway through the integration of pyrolysis to produce biochar as a way for long-term CO_2 sequestration through increased soil organic content and as a result, increased photosynthesis. Integrating anaerobic digestion (AD) and a pyrolysis system could potentially reduce GHG emissions by up to 42.7 kt CO_2 through the production of biomethane (from agricultural and food residue, within a 10 km radius) and biochar in a 2035 scenario. Applying the methodologies to establish sustainability criteria

within the EU Renewable Energy Directive (REDII) would suggest transport as the favourable end-use pathway for renewable gaseous fuels, due to the lower GHG emission savings requirement (70% for transport versus 80% for heat). In the case of biological methanation with the CO_2 originating from biogas, the REDII criteria do not recognise this as carbon capture nor is it considered an emission saving.

Lastly, Chapter 5 explored an ideal case scenario for the potential benefits of a large scale 'system-of-systems'. The system primarily focused on the energy flow across the systems. A method for the assessment of necessary wind electricity, turbine size was developed based on the wind resource data sets used. The chapter also investigates the end use of the biomethane and hydrogen resources, in the form of compressed CH_4 and H_2 gas trucks. It was concluded that a 10 MW proton exchange membrane (PEM) electrolyser with an 80% operating capacity necessitates a 144MW wind farm operating at 57.0% capacity factor (Cp_{WT}) in a 10% curtailment scenario to satisfy the energy demand of the electrolyser. Due to the variable nature of the wind turbines, an additional 16% of brown grid electricity is necessary to satisfy the electricity demand of the electrolyser. The electrolyser-produced oxygen (6,994,000 m^3O_2/a) would be capable of supplying the oxygen demand of a WWTP with a population equivalent of 426,400. The modelled 426,400 WWTP could generate 8,500 tDS/a of biological sludge, generating 1,409,000 m^3CH_4/a, and 775,700 m^3CO_2/a when digested in an anaerobic digester. Biological methanation can upgrade the CO_2 component to biomethane by reacting with the hydrogen from the electrolyser, yielding an additional 764,800 m^3CH_4/a, increasing the annual CH_4 yield by 54%, totalling 2,173,800 m^3CH_4/a. This process requires 3,102,700 m^3H_2/a, 22% of the electrolyser generated gas (14,006,700 m^3H_2/a). Using pure O_2 in the aeration process of the WWTP instead of air (which is 79% nitrogen) can reduce emissions of the treatment facility by 40%. By digesting the WWTP sludge and upgrading via biomethane, a sustainable compressed biogas fuel can be generated to displace 94 diesel trucks and the remaining hydrogen could displace the diesel required in a further 296 diesel trucks. The total emission savings from the displacement of 390 diesel trucks with green fuel alternatives of compressed biomethane and hydrogen fuel trucks could reduce emissions by 16.022 $ktCO_2e/a$.

The collaboration of the previously independent sectors of water, gas and electricity allows for tackling the emissions across multiple sectors through the development of these circular energy hubs. The capture of otherwise curtailed electricity with the goal of producing green energy would poise Ireland to lead the charge in meeting the emission reduction goals in a lucrative and efficient manner. The integration of anaerobic technology allows for the decarbonisation of the agriculture sector. Using pyrolysis and for negative emissions technologies and treated digestate for biological fertilisers can significantly improve the emissions reduction in this sector.

6.2. Recommendations

6.2.1. Recommendations for Industry

The author recommends the consideration of the evident benefits of the proposed 'system-of-systems' (SoS) model in the wider industry context. To reach the sustainability criteria set out by the Renewable Energy Directive, the previously independent sectors (such as gas, electricity, water, and others), must undertake significant restructuring. Existing wastewater treatment plants have long lifespans, many equipped with inefficient technologies causing excess emissions. Planning problems associated with building upon greenfield sites could be avoided through the co-location of the anaerobic digesters, biomethanation plants and electrolysers at the local wastewater treatment plants. The potential capture of otherwise curtailed electricity would also create an opportunity for the industry to further reduce the levelised cost of energy.

6.2.2. Recommendations for Policymakers

From the policymaker's perspective, the proposed 'system-of-systems' is particularly notable at the time of this thesis, where the ongoing war in Ukraine has caused disruptions in the price of energy. The dependence on a single source of gas or electricity highlights how fragile linear systems can become in the face of external factors. Shifting towards sustainable and circular economies will benefit all stakeholders. Due to the previous (pre-war) low cost of fossil hydrocarbons, current systems have become reliant on unreliable Russian oil and gas. Incentives must be introduced to stimulate the industry and economy to shift away towards sustainable alternatives.

Countries such as Denmark have already set a strong narrative of departing from fossil hydrocarbons through the government's drafting of the Green Gas Strategy proposal, with an outlook of extending biogas production to account for 70% of the total gas consumption by 2030. This includes the upgrading of CO_2 and the production of 'Power-to-X' products such as methanol. Boosting this shift through subsidies and amenable framework conditions facilitates the shift toward sustainable green energy. As such, Ireland has a unique opportunity to unite the electricity and gas sectors through capture or surplus electricity during low demand by producing green low carbon gas.

6.2.3. Recommendations for Communities

From a community perspective, the co-location of the power-to-X systems at wastewater treatment plants can provide the localities (especially isolated) with job opportunities, stable energy prices, biofertilisers for farms and lower overall pollution. If the generated energy can be used back in the community, self-sufficiency may also be achieved. System co-location at existing brownfield sites offers minimal disruptions, noise and odour pollution as the power-to-gas systems require low maintenance and little to no heavy machinery during operation. These self-sufficient communities can then further incentivise the growth of the locality.

6.2.4. Recommendations for future research

This thesis demonstrates the development of a novel cascading biomethanation system operating at a technology readiness level of 4. The prototype rig is capable of reaching higher methane evolution rate values with increased gas throughput through optimisation and revision of the utilised microbial cultures. As discussed in Chapter 3, several system revisions have been proposed to update the rig to extend its operational capabilities, with capabilities of achieving a TRL of 5. The changes range from easy transition to use of pure culture *Methanothermobacter* archaea, additional moisture traps, replacement of digital flow meters and digitised flow measurement; to more complex revisions such as introduction of isolation valves, reworking of the reactor base and diffuser connections. These downstream experiments open the opportunity for the design and commission of an industry-scale demonstration plant in the future, ideally collaborating with existing local industries. A demonstration-scale experiment could allow for a TRL of 7-8.

The low-resolution 'System-of-Systems' modelled in Chapter 4, is ripe for revision and restructuring into a high-resolution model capable of being representative of the real-life performance of such systems. The author acknowledges the thesis would have benefited from a techno-economic assessment of the circular economy system. While it was initially desired to implement said assessment, the development of the existing model revealed the complexity of accurately assessing the outputs of the model. This iteration of the model used generalised assumptions, avoiding a high resolution model. The high-resolution model would also present an opportunity to determine the levelised costs of the produced hydrogen, methane, oxygen, and the potential emissions savings of integrating such a system into the wider industrial community. The additional analysis could assess the potential benefits of otherwise curtailed electricity from wind or solar technologies and the associated potential emission savings. The higher resolution model should also include sub-processes such as the sludge pretreatment for the biogas yield enhancement is also a crucial pathway that would be beneficial to explore. Sludge pretreatment can increase the biomethane yields, reduce total solids sent to pyrolysis, and improve sludge dewaterability, reducing the drying needs prior to pyrolysis. Integrating said technology ought to be integrated for the higher resolution model, aiding in the economy feasibility of the proposed system. A high resolution model could also include for the option to situate the 'system of systems' near harbour or airports, by producing Fischer-Tropsch fuels for green maritime and aviation.

With the said high-resolution model, a minimal WWTP size may also be identified for the co-location of an electrolysis or biomethanation system, determined by a cost-benefit analysis. The author suggests that such a system would benefit from a more advanced model than just the use of an Excel spreadsheet. Either more advanced use of the integrated Visual Basic Analysis (VBA) programming language is necessary, or a complex model based on MATLAB (Python) code is to generate dynamic results from the model.

Chapter 2 - Supplementary data

The purpose of Box S2.1 is to provide a comparison of the use of methane (CH_4) and hydrogen (H_2) as an energy carrier gas. An energy transmission of 1GW_{th} was chosen as an arbitrary value of energy required to be transmitted.

BOX S2.1

		Methane	Hydrogen
Density	kg/m³	6.585	0.8085
Viscosity	CP	1100	880
LHV	MJ/kg	50	119.9

Gas grid pressure: 1MPa
Temperature: 25°C
Energy transmission: 1,000MW_{th} (Arbitrary number chosen for comparison.)
Hydrogen mass flow & Volume flow:

$$\frac{1000}{119.9}\frac{MW_{th}}{\frac{MJ}{kg}} = 8.34\frac{kg}{s} = \frac{8.34}{0.8085}\frac{kg/s}{kg/m^3} = 10.315\frac{m^3}{s}$$

Pressure drop:

$$= 4.0156\frac{kPa}{km_{pipe}}$$

Specific work:

$$\frac{4.0156}{0.8085}\frac{\frac{kPa}{km_{pipe}}}{kg/m^3} = 4.967\frac{kJ}{kg_{H2}\,.\,km_{pipe}}$$

Power:

$$4.967\frac{kJ}{kg_{H2}\,.\,km_{pipe}} * 8.34\frac{kg}{s} = 41.42\frac{kW}{km_{pipe}}$$

Methane Mass flow:

$$\frac{1000}{50}\frac{MW_{th}}{\frac{MJ}{kg}} = 20\frac{kg}{s}$$

Volume flow:

$$\frac{20}{6.585}\frac{kg/s}{kg/m^3} = 3.037\frac{m^3}{s}$$

Pressure drop:

$$1.477\frac{kPa}{km_{pipe}}$$

Specific work and power:

$$\frac{1.477}{6.585}\frac{\frac{kPa}{km_{pipe}}}{kg/m^3} = 0.224\ \frac{kJ}{kg_{CH4}\,.\,km_{pipe}} * 20\ kg/s = 4.48\frac{kW}{km_{pipe}}$$

Chapter 3 - Supplementary data

[SD 1] Supplementary Figures

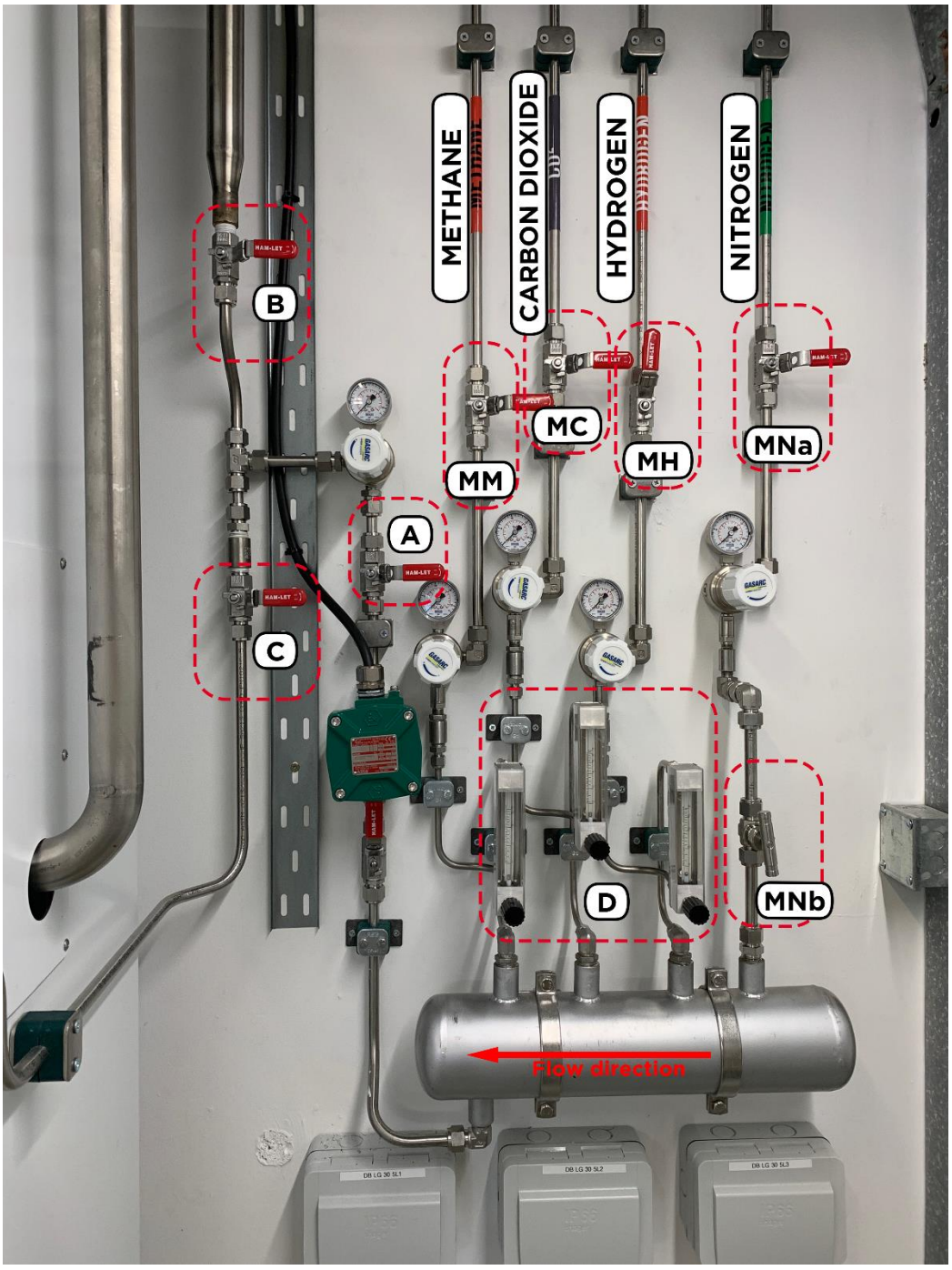


Figure S3.1: The external manifold panel before gas entry into the reactor skid. Where A- Manifold manual Parker A-Lok valve outlet valve (Post-solenoid valve); B- Manual Parker A-Lok valve leading to atmosphere (System by-pass for venting); C- Manual Parker A-Lok valve leading to the system inlet; D- Manual rotameters for methane, hydrogen and carbon dioxide); MO- Manual Parker A-Lok valve for the Manifold outlet (Pre solenoid valve); MM- Manual Parker A-Lok valve for the methane supply; MC- Manual Parker A-Lok valve for the carbon dioxide supply; MH- Manual Parker A-Lok valve for the hydrogen supply; MNa- Manual Parker A-Lok valve for the nitrogen supply; MNb- Needle valve for the regulation of nitrogen supply downstream.

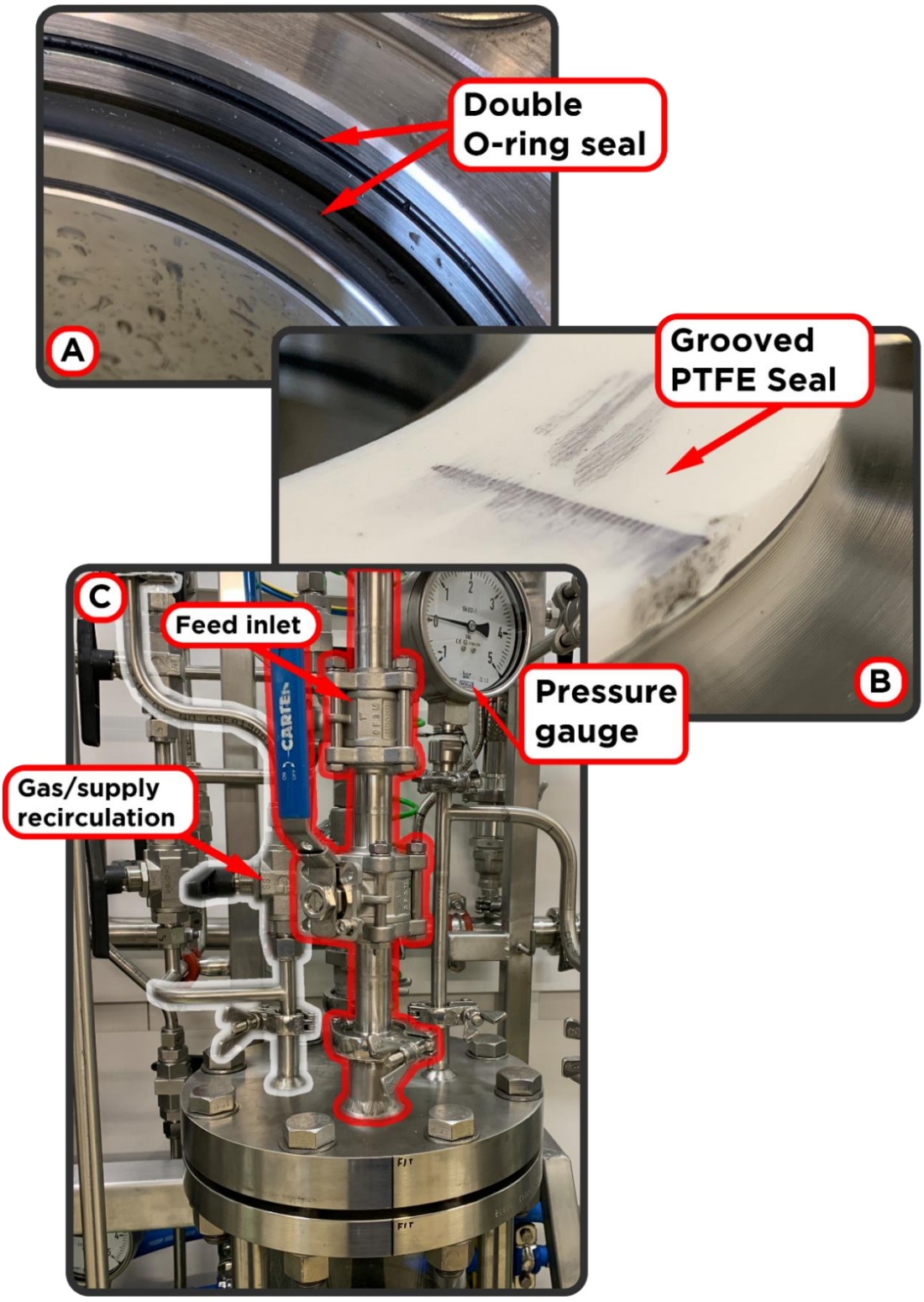


Figure S3.2: Annotated reactor components, where: Image A- Double O-ring seal of the bottom sight glass (identical for top flange); Image B- Grooved PTFE ring seated between two flanges for an airtight seal; Image C- Top flange reactor connections, Supply and gas recirculation lines, feed inlet line and pressure gauge/outlet line. Behind the feed inlet is a pressure safety valve, which cannot be observed in Image C.

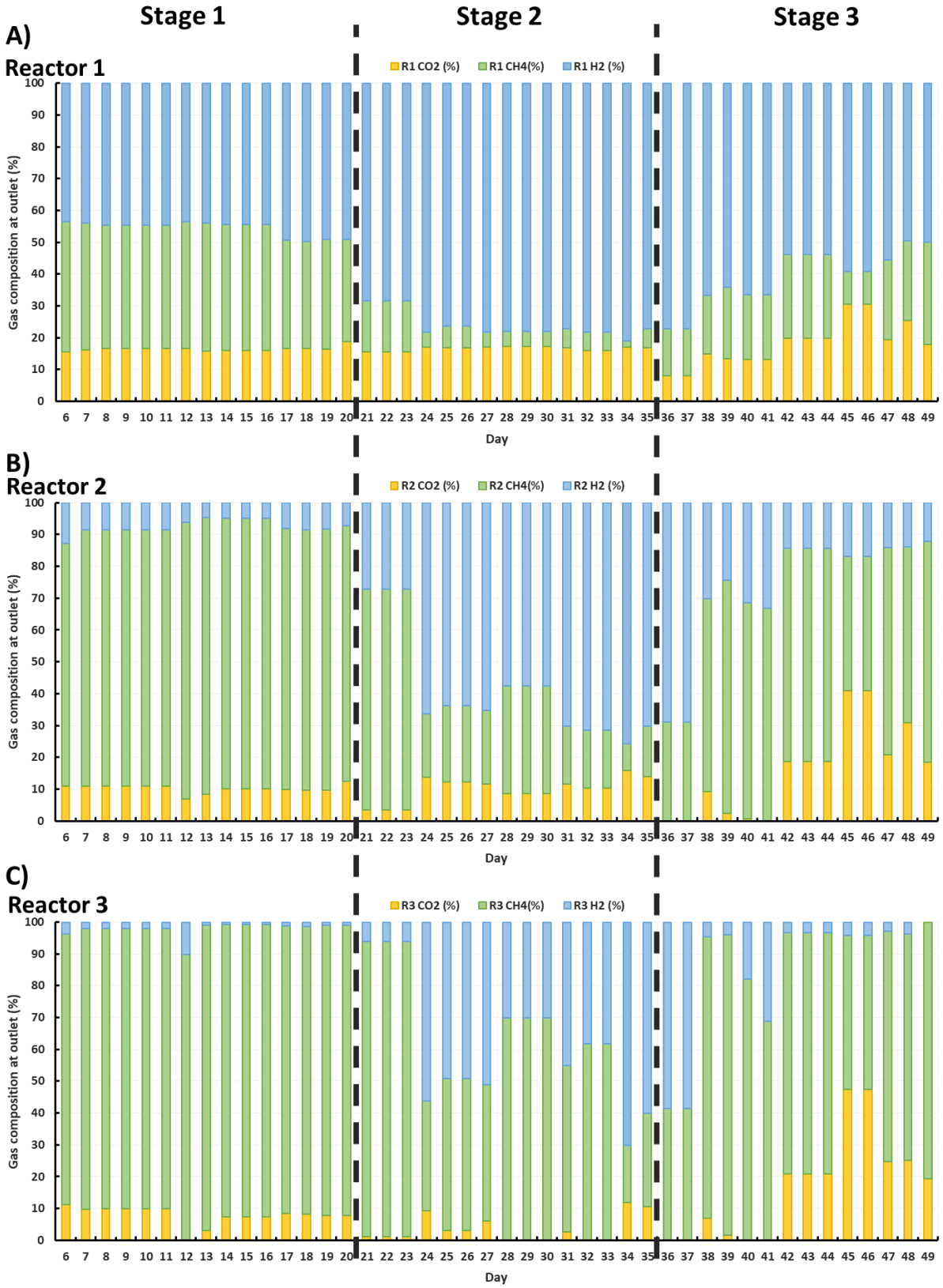


Figure S3.3: Gas composition across R1 (A), R2(B), and R3 (C). Where the reactor was shut off, or gas composition was not measured (e.g. weekends), gas composition from the previous day was substituted for better visualisation.

Table S3.1: Summary table of average Stage 1 performance across all three cascading system reactors.

		Stage 1			
		$R1_{in}$	$R2_{in}$	$R3_{in}$	$R3_{out}$
Gas retention time	h	-	0.79	1.78	2.58
Reactor vol.	L	-	8	8	8
Working vol.	L	-	6	6	6
Bubble column height	m	-	0.54	0.54	0.54
Chamber height	m	-	0.43	0.43	0.43
Chamber ID	m	-	0.15	0.15	0.15
Gas inflow					
H2:CO2 ratio		3.7	2.8	0.8	0.3
H2	%	78.7%	45.7%	7.7%	2.1%
CO2	%	21.3%	16.5%	10.3%	7.8%
CH4	%	-	37.8%	82.0%	90.2%
Avg. H2in	L/Lvr/d	34.9	7.6	0.8	0.2
Avg. CO2in	L/Lvr/d	9.4	2.7	1.1	0.6
Avg. CH4in	L/Lvr/d	0.0	6.3	8.4	7.5
MER	L/Lvr/d	-	6.30	2.11	-0.87
MER_{avg}	L/Lvr/d	-	-	-	0.42
Average gas conversion					
H2	%	-	78.2%	97.7%	99.5%
CO2	%	-	70.9%	88.8%	93.1%

Note: $R3_{out}$ – MER is negative due to the suspected errors in the mass balance, resulting in lower methane flow at the outlet than at the inlet.

Table S3.2: Summary table of average Stage 2 performance across all three cascading system reactors.

		Stage 2			
		$R1_{in}$	$R2_{in}$	$R3_{in}$	$R3_{out}$
Gas retention time	h	-	0.44	0.67	1.05
Reactor vol.	L	-	8	8	8
Working vol.	L	-	6	6	6
Bubble column height	m	-	0.54	0.54	0.54
Chamber height	m	-	0.43	0.43	0.43
Chamber ID	m	-	0.15	0.15	0.15
Gas inflow					
H2:CO2 ratio		4.3	4.6	5.7	9.9
H2	%	81.3%	76.4%	62.1%	41.9%
CO2	%	18.7%	16.6%	10.9%	4.2%
CH4	%	-	7.0%	27.0%	53.9%
Avg. H2in	L/Lvr/d	51.9	34.4	16.5	8.1
Avg. CO2in	L/Lvr/d	12.0	7.5	2.9	0.8
Avg. CH4in	L/Lvr/d	0.0	3.2	7.2	10.4
MER	L/Lvr/d	-	3.16	4.03	3.20
MER_{avg}	L/Lvr/d	-	-	-	0.58
Average gas conversion					
H2	%	-	33.6%	68.2%	84.4%
CO2	%	-	20.5%	69.2%	91.3%

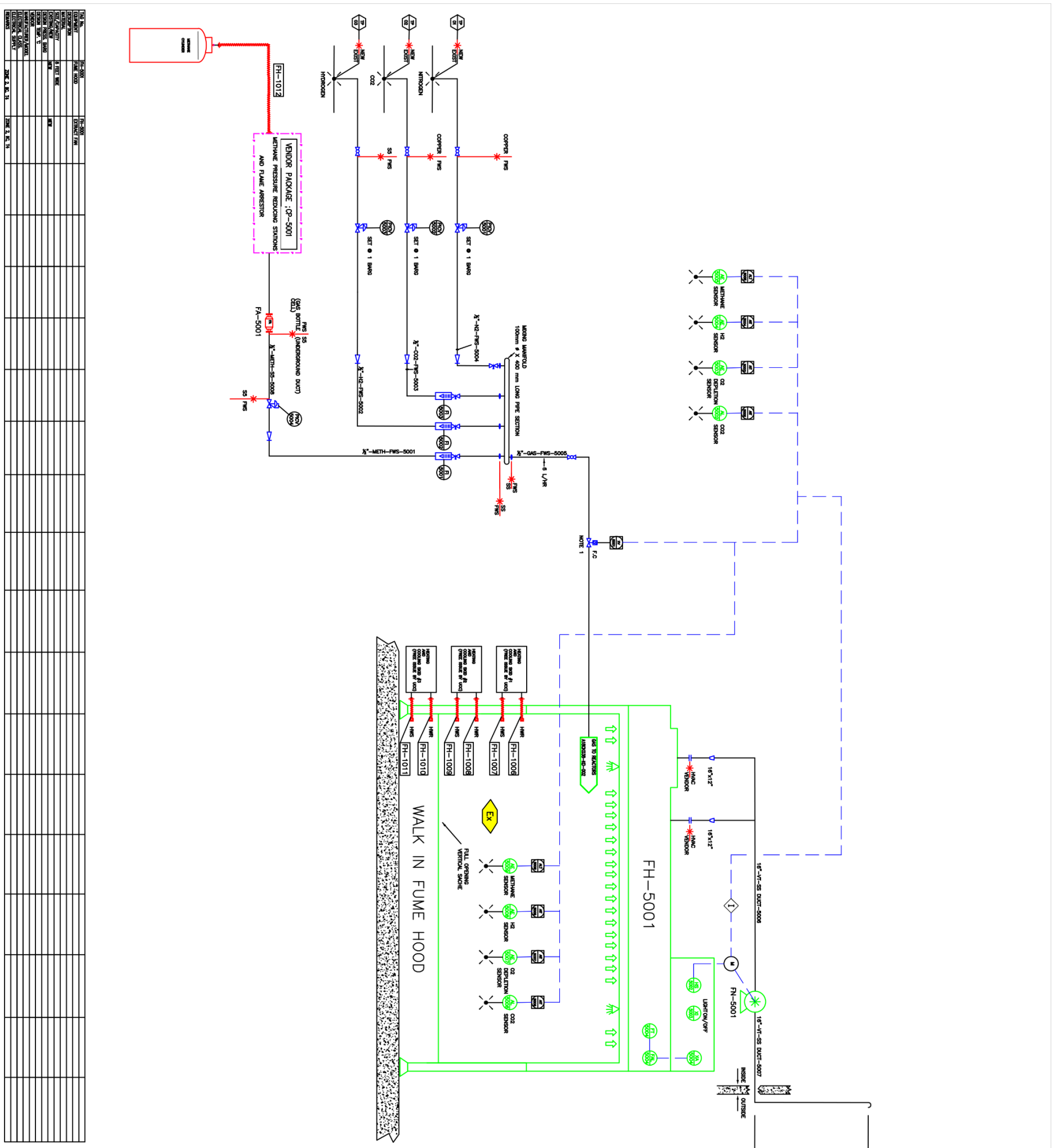
Table S3.3: Summary table of average Stage 3 performance across all three cascading system reactors.

		Stage 3			
		$R1_{in}$	$R2_{in}$	$R3_{in}$	$R3_{out}$
Gas retention time	h	-	0.72	1.31	1.96
Reactor vol.	L	-	8	8	8
Working vol.	L	-	6	6	6
Bubble column height	m	-	0.54	0.54	0.54
Chamber height	m	-	0.43	0.43	0.43
Chamber ID	m	-	0.15	0.15	0.15
Gas inflow					
H2:CO2 ratio		3.6	3.3	2.8	1.3
H2	%	78.3%	61.1%	36.8%	20.0%
CO2	%	21.7%	18.5%	13.1%	15.1%
CH4	%	-	20.4%	50.1%	65.0%
Avg. H2in	L/Lvr/d	34.9	13.3	5.4	2.0
Avg. CO2in	L/Lvr/d	9.6	4.0	1.9	1.5
Avg. CH4in	L/Lvr/d	0.0	4.5	7.4	6.4
MER	L/Lvr/d	-	4.46	2.91	-1.01
MER_{avg}	L/Lvr/d	-	-	-	0.35
Average gas conversion					
H2	%	-	61.7%	84.5%	94.4%
CO2	%	-	57.3%	79.5%	84.3%

Note: $R3_{out}$ – MER is negative due to the suspected errors in the mass balance, resulting in lower methane flow at the outlet than at the inlet.

NOTE: [SD2] SOP Section has been moved to the end of the Appendices. This has been moved to preserve readability of the thesis.

[SD 3] A18CK038- KD-001



D	30.04.19	ISSUE FOR TENDER	JDC	PF	JL	CH
C	15.04.19	ISSUE FOR TENDER	JDC	PF	JL	CH
B	05.04.19	ISSUE FOR DESIGN	JDC	PF	JL	CH
A	03.04.19	ISSUE FOR COMMENT	JDC	PF	JL	CH
REV	DATE	DESCRIPTION	DRN.	DES.	CHKD.	APPR.

STATUS: ISSUE FOR TENDER

CLIENT:

DPS

THIS DRAWING IS THE PROPERTY OF DPS AND SHALL NOT BE USED, REPRODUCED OR DISCLOSED TO ANYONE WITHOUT THE PRIOR WRITTEN PERMISSION OF DPS AND SHALL BE RETURNED UPON REQUEST.

PROJECT: ERI LAB LG 30 UPGRADE

TITLE: P&ID WALK IN FUME HOOD FH-1001

PROJECT No.	A1 SCALE	DISCIPLINE	
A18CK038	N/A	PROCESS	
CLIENT DRAWING NO.	DRAWING NO.	SHT	REV
N/A	A18CK038-KD-001	1/1	D

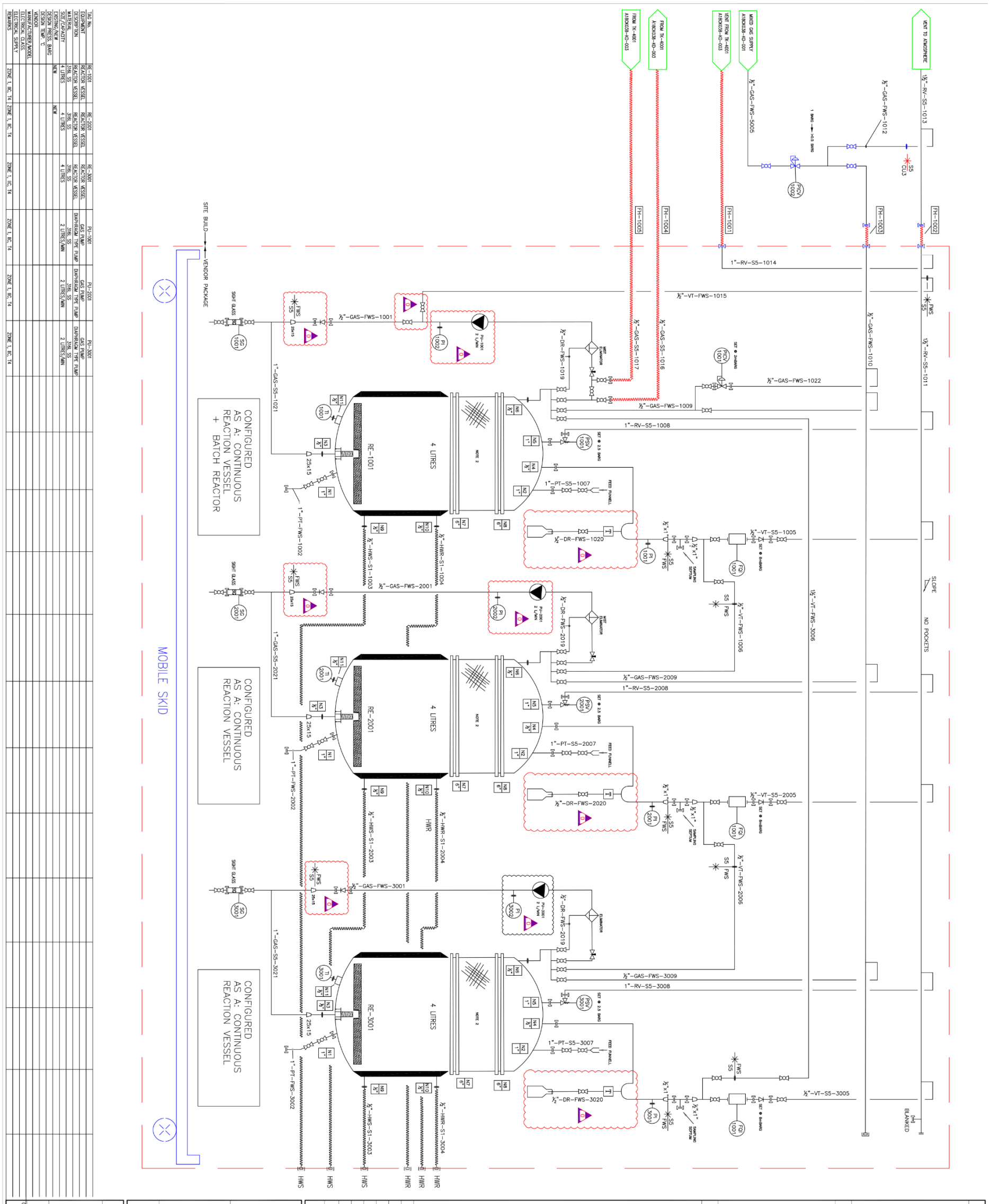
NOTES

1) XV-1001 CLOSES ON DETECTION OF:
- HYDROGEN RICH ENVIRONMENT
OR
- CO2 RICH ENVIRONMENT
OR
- METHANE RICH ENVIRONMENT
OR
- OXYGEN DEPLETED ENVIRONMENT
OR
- FAN IS TURNED OFF OR POWER TO FAN IS LOST

LEGEND

HOLDS

[SD 4] A18CK038- KD-002



TAG No.	RE-1001	RE-2001	RE-3001	PU-1001	PU-2001	PU-3001
EQUIPMENT	REACTOR VESSEL	REACTOR VESSEL	REACTOR VESSEL	GAS PUMP	GAS PUMP	GAS PUMP
DESCRIPTION	REACTOR VESSEL	REACTOR VESSEL	REACTOR VESSEL	DIAPHRAGM TYPE PUMP	DIAPHRAGM TYPE PUMP	DIAPHRAGM TYPE PUMP
MATERIAL	316L SS	316L SS	316L SS	316L SS	316L SS	316L SS
SIZE/CAPACITY	4 LITRES	4 LITRES	4 LITRES	2 LITRES/MIN	2 LITRES/MIN	2 LITRES/MIN
DESIGN/NEW	NEW	NEW	NEW			
DESIGN PRESS. BARG						
DESIGN TEMP. °C						
VENDOR						
MANUFACTURER/MODEL						
ELECTRICAL CLASS						
ELECTRICAL SUPPLY						
REMARKS	ZONE 1, IIC, T4	ZONE 1, IIC, T4	ZONE 1, IIC, T4	ZONE 1, IIC, T4	ZONE 1, IIC, T4	ZONE 1, IIC, T4

NOTES

1. REACTIONS ARE LOCATED WITHIN AN ATEX RATED WALK IN FUME HOOD (SEE A18CK038-KD-001 FOR DETAILS).
2. MAIN BODY OF REACTION VESSEL INCORPORATES A SIGHT GLASS.

LEGEND

- CU3 : COPPER TUBING
- FWS : SS TUBING WITH PARKER A-LOCK COMPRESSION FITTINGS.
- S5 : 316L SS TUBING WITH ASME BPE TRICLAMP FITTINGS
- S1 : SCH 10 316L SS PIPING

HOLDS

REV	DATE	DESCRIPTION	DRN.	DES.	CHKD.	APPR.
STATUS		ISSUE FOR CONSTRUCTION				
A	03.04.19	ISSUE FOR COMMENT	JOC	PF	JL	OH
B	05.04.19	ISSUE FOR DESIGN	JOC	PF	JL	OH
C	15.04.19	ISSUE FOR TENDER	PR	PF	JL	OH
D	24.04.19	ISSUE FOR TENDER	JOC	PF	JL	OH
E	30.04.19	ISSUE FOR TENDER	JOC	PF	JL	OH
0	28.02.20	ISSUE FOR CONSTRUCTION	PR	PF	JL	OH

CLIENT

UCC Coláiste na hOllscoile Corcaigh, Éire University College Cork, Ireland

DPS

THIS DRAWING IS THE PROPERTY OF DPS AND SHALL NOT BE USED, REPRODUCED OR DISCLOSED TO ANYONE WITHOUT THE PRIOR WRITTEN PERMISSION OF DPS AND SHALL BE RETURNED UPON REQUEST.

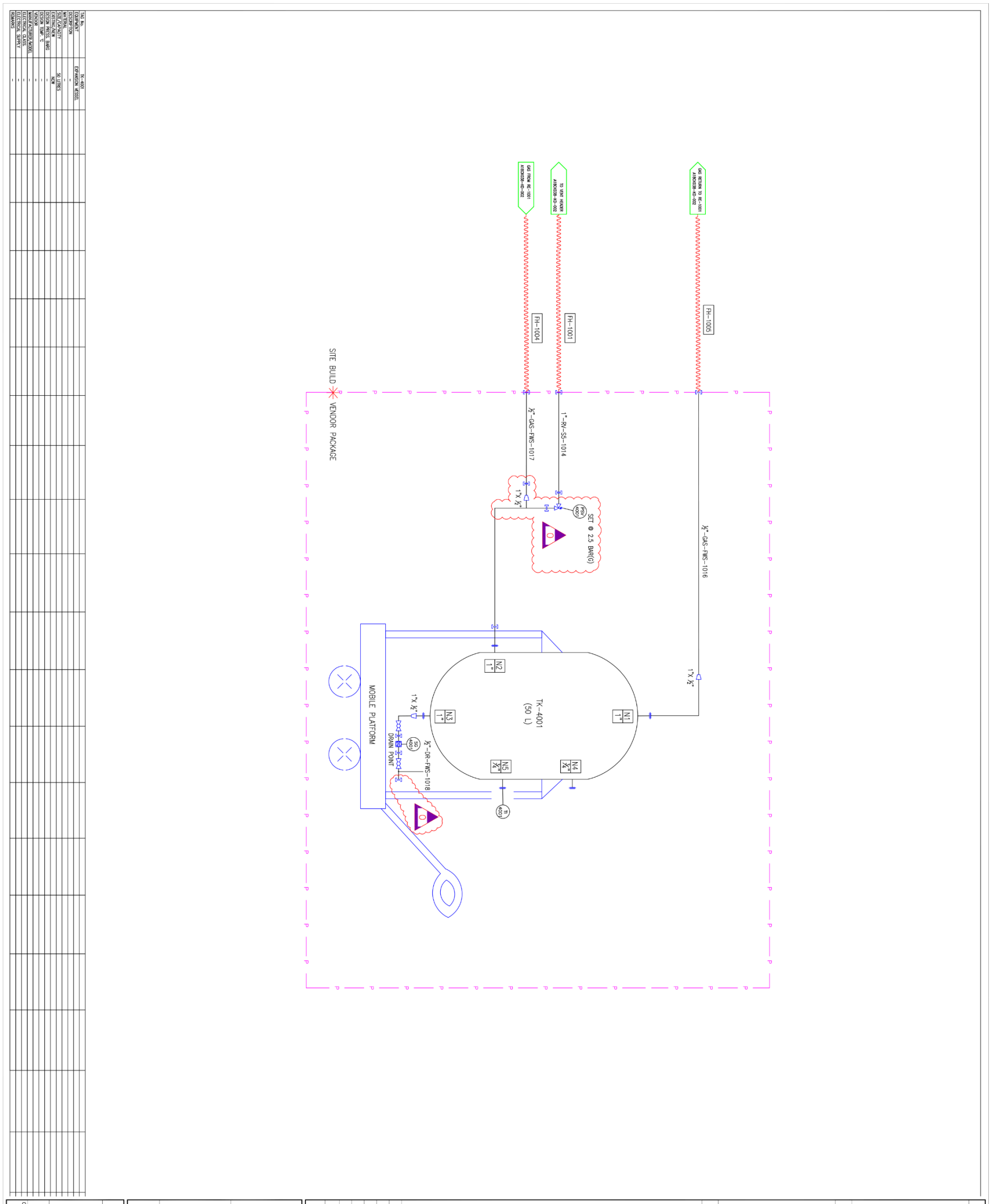
PROJECT: ERI LAB LG-30 UPGRADE

TITLE: P&ID FOR 3 NO. 4 LITRE BIO-REACTOR VESSELS

PROJECT No.	A1 SCALE	DISCIPLINE	
A18CK038	N/A	PROCESS	
CLIENT DRAWING NO.	DRAWING NO.	SHT	REV
N/A	A18CK038-KD-002	1/1	0

P:\2018\A18CK038\24 Drawings\01-WIP\07-Process\KD\A18CK038-KD-002

[SD 5] A18CK038- KD-003



[SD 6] Methanation rig

[SD 6.1] Diffuser images

Additional footage of large bubble coalescence may be found in the electronic supplementary data folders.



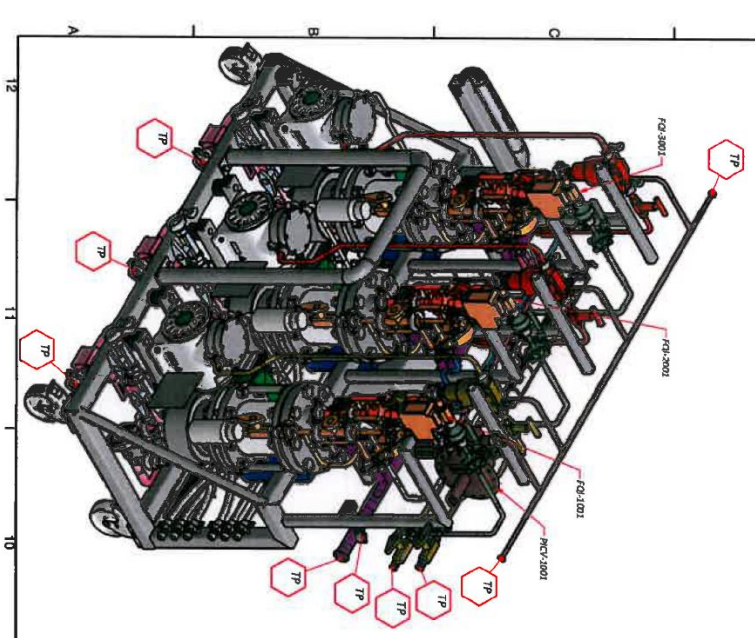


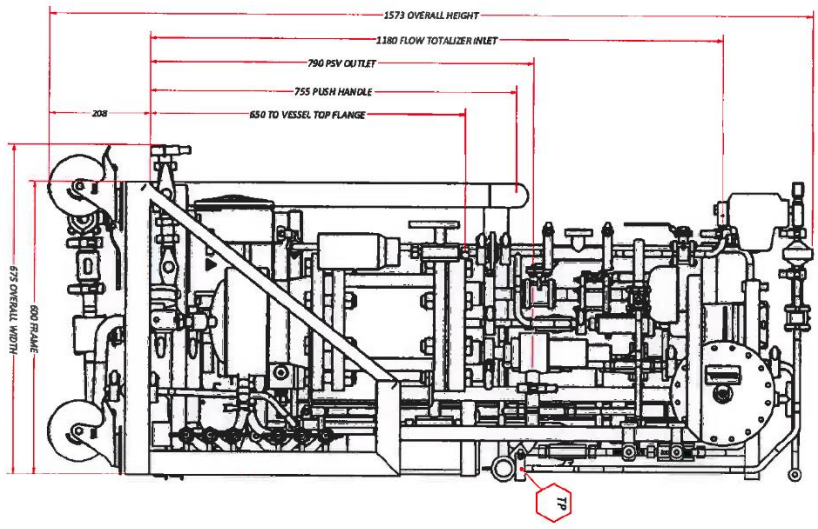
[SD 6.2] Manifold

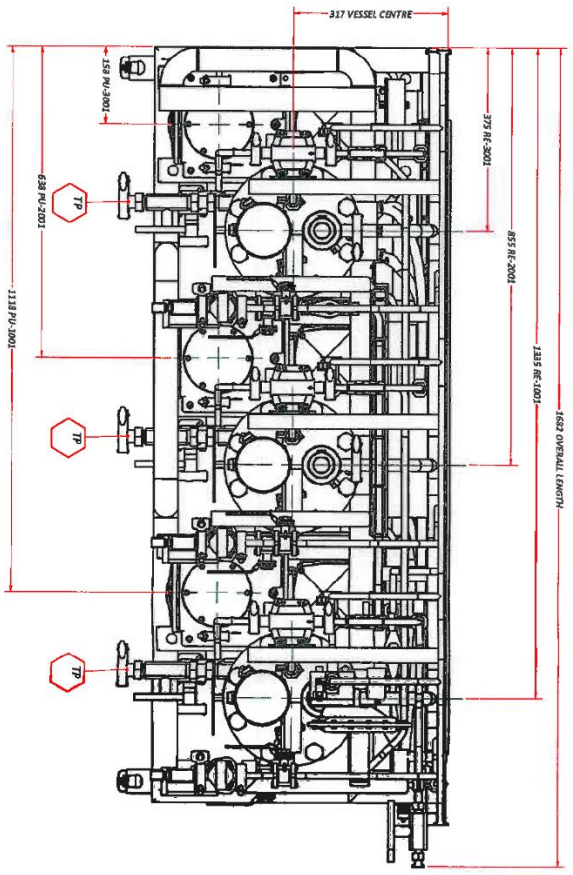
Manifold supplementary data comprises of video footage of the fluctuating manifold rotameter, exhibiting the issue associated with the flow measurement in the main text of the paper. For the purpose of the thesis publication, still frames from the video have been taken to showcase the issue of flow fluctuations. The approximate flow fluctuations shown vary between approximately 8-12 NL/h due to the non-linear flow measurements, especially at the lower range of the rotameter.

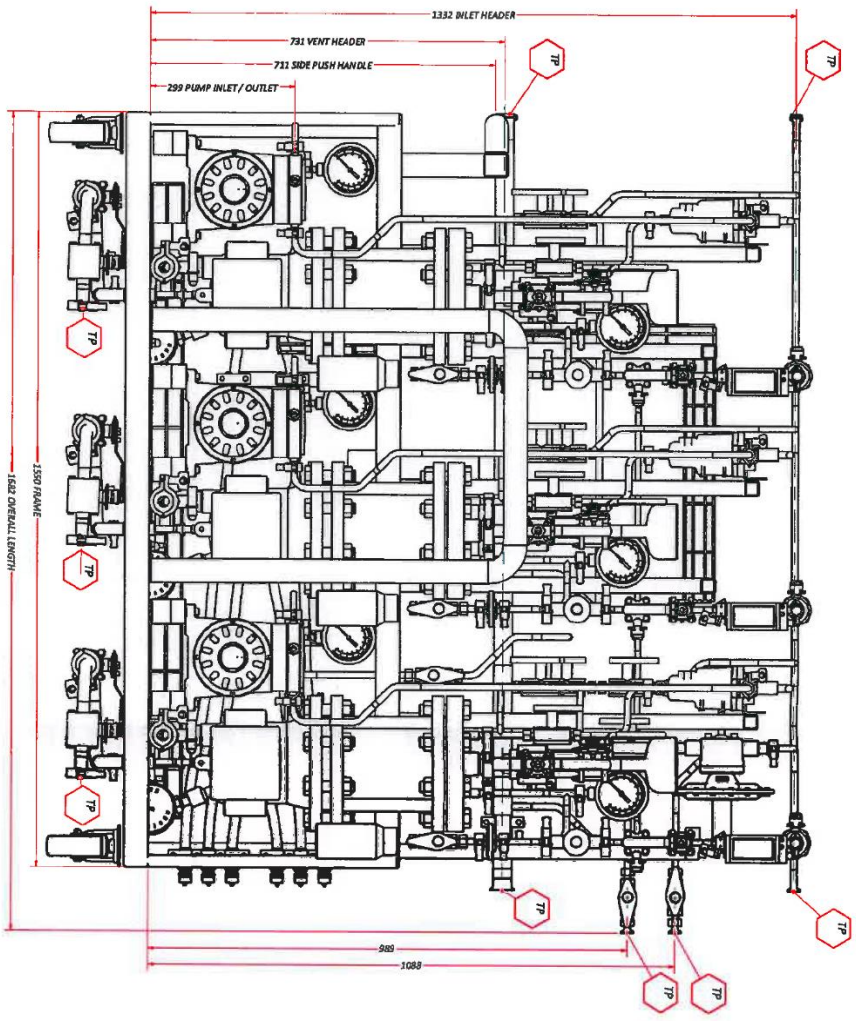


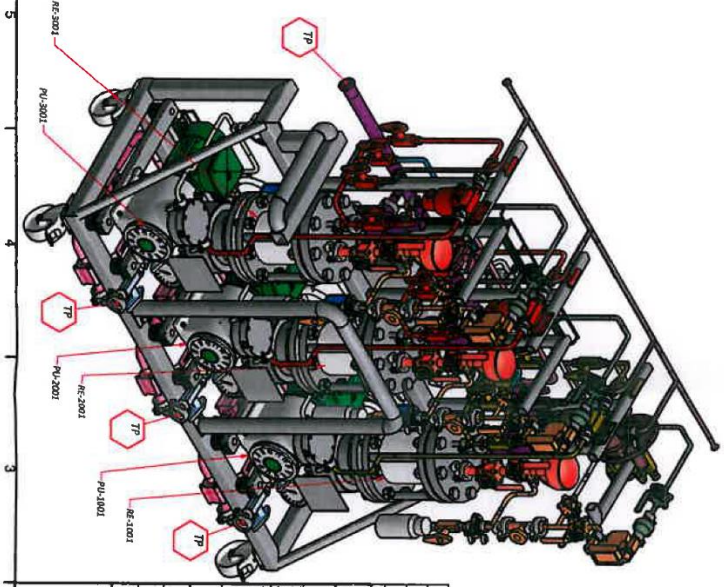
[SD 6.3] General Arrangement Drawings

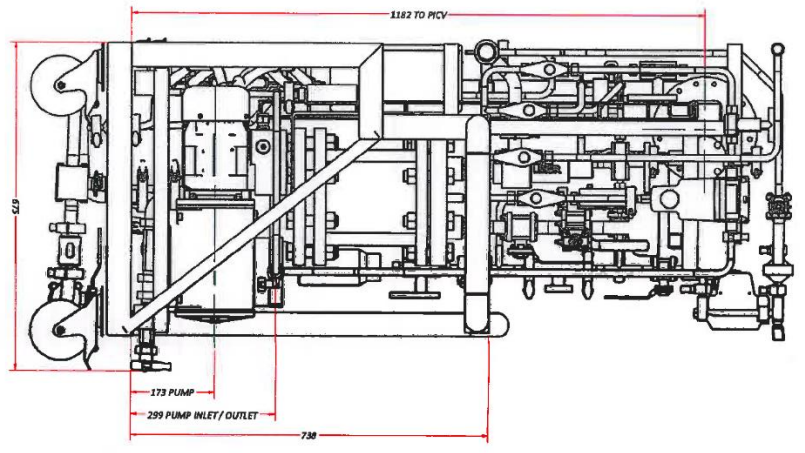












GENERAL ARRANGEMENT NOTES:

1. ALL DIMENSIONS ARE IN MILLIMETERS AND ARE SUBJECT TO A MANUFACTURING TOLERANCE OF +/- 15mm FOR PIPING AND +/-5mm FOR FRAME. CHANGES MAY OCCUR DURING CONSTRUCTION.
2. ALL BOX SECTION 304SS MILL FINISH & CONSISTS OF 50x50x3 SHS & 30x30x3 SHS ONLY. ALL WELDS ON FRAME TO BE AS LAID & ACID CLEANED.
5. ALL SLOPED LINES TO HAVE MIN SLOPE ACCORDING TO ASME BPE GSD2 (TABLE SD-2.4.3.1-1) (0.57deg).
6. ESTIMATED EMPTY WEIGHT OF COMPLETE SKID IS APPROX. 490kg

DRAWING STATUS

Preliminary Design ☐
Issued For Approval ☐
Issued For Construction ☐
As Built ☒

Issued By: R.Mc Evoy
Date: 22 JUL 2020

REV	DESCRIPTION	DATE	DRWN	APPRV
REVISION HISTORY				
1	AS BUILT	22 JUL 2020	RME	MM
0	FOR CONSTRUCTION	20 MAR 2020	RME	MM

CLIENT: UCC
PROJECT TITLE: ERI LAB LG-30 UPGRADE
PROJECT NUMBER: TPUC001
TITLE: REACTOR SKID GA
DWG NO: TPUC001-GAD-001 REVISION: 1
DRAWN BY: R.Mc Evoy DATE: 20 MAR 2020
CHECKED BY: M.Madden DATE: 20 MAR 2020
SIZE: A1 SCALE: N.T.S SHEET: 1 of 2

BCD
Railway Road
Charleville
Co.Cork
IRELAND
Tel: +353 (63) 30200
Fax: +353 (63) 30201
Web: www.bcdir

[SD 7] Flow totaliser conversion table

FLOW EQUIVALENCY TABLE FOR DIFFERENT GASES

Parameter/ Gas	CO2 (calibration gas)	Nitrogen	Hydrogen	Methane	Oxygen
Chemical Composition	CO2	N2	H2	CH4	O2
Molecular weight	44	28	2	16	32
Density (Kg/M3) @ 1.0 Bar(A)	1.964	1.250	0.089	0.714	1.429
Density (Kg/M3) @ 1.2 Bar(A)	2.357	1.500	0.107	0.857	1.714
(assume pressure & Temperature unchanged)	1.00	1.25	4.69	1.66	1.17
Scaling Calibration factor N2	*0.80*	***1.00***	*3.74*	*1.32*	*0.94*
Scaling Calibration factor H2	*0.21*	*0.27*	***1.00***	*0.35*	*0.25*
Scaling Calibration factor CH4	*0.60*	*0.76*	*2.83*	***1.00***	*0.71*
Scaling Calibration factor O2	*0.85*	*1.07*	*4.00*	*1.41*	***1.00***

Factor = $\sqrt{\left(\frac{SG_{Scale}}{SG_{New}}\right)\times\left(\frac{P_{New}}{P_{Scale}}\right)\times\left(\frac{T_{Scale}}{T_{New}}\right)}$	CO2 (calibration gas)	Nitrogen	Hydrogen	Methane	Oxygen
Flow (NL/HR)	19	23.82	89.12	31.51	22.28
Flow (NL/HR)	20	25.07	93.81	33.17	23.45
Flow (NL/HR)	30	37.61	140.71	49.75	35.18
Flow (NL/HR)	40	50.14	187.62	66.33	46.90
Flow (NL/HR)	50	62.68	234.52	82.92	58.63
Flow (NL/HR)	60	75.21	281.42	99.50	70.36
Flow (NL/HR)	70	87.75	328.33	116.08	82.08
Flow (NL/HR)	80	100.29	375.23	132.66	93.81
Flow (NL/HR)	90	112.82	422.14	149.25	105.53
Flow (NL/HR)	100	125.36	469.04	165.83	117.26
Flow (NL/HR)	110	137.89	515.95	182.41	128.99
Flow (NL/HR)	120	150.43	562.85	199.00	140.71
Flow (NL/HR)	130	162.96	609.75	215.58	152.44
Flow (NL/HR)	140	175.50	656.66	232.16	164.16
Flow (NL/HR)	150	188.03	703.56	248.75	175.89
Flow (NL/HR)	160	200.57	750.47	265.33	187.62

Chapter 4 - Supplementary data

Box S4.1: Calculation of maximum H_2 production using surplus electricity from the two 3 MW_e wind turbines

The generated electricity by the two wind turbines (provided data): 15.34 GWh_e/a.
Surplus electricity from the two wind turbines (provided data): 1.96 GWh_e/a.
The percentage of surplus electricity to the total generated electricity:

$$\frac{1.96}{15.34} \times 100\% = 12.78\%$$

H_2 density is 0.0899 kg/Nm^3 with a lower heating value of 33.33 kWh/kg and a lower energy density of 3.00 kWh/m^3 [1].
Assuming an electrolyser with a system efficiency of 60% $_{LHV}$ and an energy consumption of 5.00 kWh_e/m^3 H_2 [2].
The maximum H_2 production from the curtailed electricity would be (if all surplus electricity is used):

$$\frac{1.96\frac{GWh}{a}}{5.0\frac{kWh}{m^3 H_2}} = 392{,}000\,\frac{m^3 H_2}{a} \; or \; 35{,}200\,\frac{kg H_2}{a}$$

Box S4.2: Hydrogen potential for fuelling buses and commuter ferries at the industrial site.

Hydrogen bus

Assuming the hydrogen fuel cell bus has an energy consumption of 2.11 kWh/km [3] and based on a range of 450 km, the hydrogen capacity of the bus can be calculated as follows:

Range = 450 km

Energy consumption = 2.11 kWh/km

Hydrogen capacity = (450 km × 2.11 kWh/km) × = 950 kWh

LHV of hydrogen = 33.3 kWh/kg

Mass of hydrogen required = 950 kWh ÷ 33.3 kWh/kg = 28.49 kg

The average daily travel distance for a bus in Dublin, Ireland is calculated as 150 km/bus/day based on the data from Central Statistics Office (CSO) on Public transport [4].

Number of days between refuelling: 450 km ÷ 150 km/day = 3 days

Therefore, the number of buses that can be fuelled per year from the hydrogen produced at the industrial site:

$$\frac{17{,}100\,\frac{kgH_2}{year}}{\left(\frac{365\ days}{3\ days}\right) \times 28.49\ kgH_2} = 4.9\ buses$$

Hydrogen ferry

A travel distance of 112 km/ferry/day is assumed (equal to 4 round trips per day between the harbour and Cork City). A ferry fuelled by liquid hydrogen has an estimated fuel capacity of 2090 kg H_2 and a range of 673 km based on the specifications and route information used for the Zalophus (a passenger ferry with an estimated 84-passenger capacity) in the San Francisco Bay [5]. The fuel efficiency is equivalent to 0.32 km/kg H_2 or 0.0097 km/kWh or 0.0023 km/MJ.

The number of round trips each ferry can run using each tank of fuel:

$$\frac{672.3\ \text{km}}{28\ km} = 24\ round\ trips$$

If the ferry does 4 round trips per day from the harbour to Cork City:

$$\frac{672.3\ \text{km}}{112\ \text{km}} = 6\ days\ between\ refuelling$$

The number of times the ferry can be re-fuelled per year

$$\frac{17{,}100\,\frac{kgH_2}{yr}}{(2090kg)} = 8.2\,refills$$

8.2 refills at 6 days between refills suggests each system can provide 49 days of ferry travel, therefore:

Hydrogen sufficient to fuel ferry for:

$$672.3\ \text{km} * 8.2\ \text{refills} = 5512\ \text{km}$$

If the ferry operates every day of the year, then 7 such electrolyser systems are required per ferry, travelling 112 km per day.

Box S4.3: Calculation of the saved CO_2 emissions by on-site utilisation of oxygen from water electrolysis for aeration at a conventional municipal WWTP

Production of hydrogen:

17,100 kg H_2/a (190,254 m^3H_2/a) (based on H_2 produced from 122 kW electrolyser at a capacity factor of 74%)

Corresponding production of oxygen:

Based on the mass balance of water electrolysis (the weight ratio of H_2:O is 1:7.94)

$$17{,}100\ kgH_2/a \times 7.94 = 135{,}660\ kgO_2/a$$

$$135{,}660\frac{kgO_2}{a} \div 365.25 = 371.3\frac{kgO_2}{d}\ through\ electrolysis\ production$$

Oxygen demand of 65,000 WWTP aeration basin:

Table 4.2: Influent properties based on nearby WWTP PE of 65,000.

Inlet variables			COP (/ Person)		
Q	542	m^3/h	Inflow	0.2	m^3/PE/d
V_A	7,150	m^3	BOD	60	g/PE/d
BOD_i	300	g/m^3	Ammonia (NH_4-N)	4.5	g/PE/d
BOD_e	25	g/m^3	TSS	60	g/PE/d
MLSS (X)	3	g/m^3	Sludge production	60	g_{TS}/PE/d
Amm_i	22.50	g/m^3	Waste sludge generation (X_r)	0.6	kg_{TS} WAS/m^3
Amm_o	0.5	g/m^3	Solids concentration in clarifier	11	g/L
N_e	1	g/m^3	Sediment residence time	10	d
TSS removal from primary settling	50	%	WAS flow rate (Q_w)	3,575	kg/day

References used: [6]–[8] *Note: Inlet variable values are calculated for PE of 65,000.*
WAS – Waste Activated Sludge, COP – Code of practice

Application of Equation 4.5, calculation oxygen demand for WWTP of 65,000 PE:

$$\mathrm{OD} = 0.75 \times 542\frac{m^3}{h} \times (300 - 25)\frac{g}{m^3} + 2 \times (7{,}150)m^3 \times \left(3{,}000\frac{g}{m^3} \times 0.001\right) + 4.3 \times 542\frac{m^3}{h} \times (22.50 - 0.5)\frac{g}{m^3} - 2.83 \times 542\frac{m^3}{h} \times \left[(22.50 - 0.5)\frac{g}{m^3} - 1\frac{g}{m^3}\right]$$

$$\mathrm{OD} = 111{,}719\frac{g}{h} + 42{,}900\frac{g}{h} + 51{,}242\frac{g}{h} - 32{,}191\frac{g}{h} = 173{,}669\frac{g}{h}$$

$$173{,}669\frac{g}{h} \div 1000 \times 24 = 4{,}168\frac{kgO_2}{d} \approx 1{,}522{,}384\frac{kgO_2}{a}\ production$$

The CO_2 emissions intensity for electricity production in Ireland was 0.325 $kgCO_2e$/kWh in 2019 [9]. Assuming the WWTP applies typical fine-bubble diffusers with an average transfer rate of 2.25 kg O_2/kWh, and an average transfer rate of 12.5 kgO_2/kWh for pure oxygen, then if the produced oxygen from electrolysis is fully used to supply oxygen demand at the WWTP, the electricity saved is:

Aeration energy demand and emissions:

$4{,}168\,\frac{kgO_2}{d} \div 2.25\,\frac{kgO_2}{kWh} \times 365.25 \div 1000 = \; 677\,\frac{MWh_{el}}{a}$ *(Aeration power demand)*

Aeration power demand typically 49% of WWTP power demand

$677\,\frac{MWh_{el}}{a} \div 49\%_{\substack{Aeration \\ power\ demand}} = 1{,}381\,\frac{MWh_{el}}{a}$ *(Estimated total WWTP power demand)*

$1{,}381\,\frac{MWh_{el}}{a} \times 49\%_{Aeration} \times 0.325\,\frac{tCO_2}{MWh} = 220\,\frac{tCO_{2eq}}{a}$ *(Aeration emissions)*

$1{,}381\,\frac{MWh_{el}}{a} \times 51\%_{WWTP} \times 0.325\,\frac{tCO_2}{MWh} = 229\,\frac{tCO_{2eq}}{a}$ *(Other WWTP emissions)*

$220\,\frac{tCO_{2eq}}{a} + 229\,\frac{tCO_{2eq}}{a} = 448\,\frac{tCO_{2eq}}{a}\ Total\ annual\ WWTP\ emissions.$

Associated energy and emissions reduced by the switch to pure O_2:

Pure O_2 aeration fraction

$371.3\,\frac{kgO_2}{d} \div 12.5\,\frac{kgO_2}{kWh} \times 365.25 \div 1000 = \; 10.85\,\frac{MWh_{el}}{a}$

Remaining Air aeration fraction

$\left(4{,}168\,\frac{kgO_2}{d} - \; 371.3\,\frac{kgO_2}{d} =\right) 3{,}797\,\frac{kgO_2}{d} \div 2.25\,\frac{kgO_2}{kWh} \times 365.25 \div 1000 = \; 616.3\,\frac{MWh_{el}}{a}$

Overall savings at WWTP

$677\,\frac{MWh_{el}}{a} - 10.85\,\frac{MWh_{el}}{a} - \; 616.3\,\frac{MWh_{el}}{a} = 49.4\,\frac{MWh_{el}}{a}$ *(WWTP energy savings)*

$49.4\,\frac{MWh_{el}}{a} \times 0.325\,\frac{tCO_{2eq}}{MWh} = 16.04\,\frac{tCO_{2eq}}{a}$ *(WWTP emissions savings)*

$16.04\,\frac{tCO_{2eq}}{a} \div 448\,\frac{tCO_{2eq}}{a} = 3.6\%$ *(Percentage reduction in emissions at the WWTP)*

$616.3\,\frac{MWh_{el}}{a} \div \left(\left(1{,}381\,\frac{MWh_{el}}{a} \times 51\%\right) + \; 616.3\,\frac{MWh_{el}}{a}\right) = 47.1\%$ *(Enriched O_2 aeration power demand as a % of the WWTP power demand [down from 49%])*

Box S4.4: Calculation of sludge production, biogas and biological methanation converting CO_2 to methane.

The removal rate of TSS in the primary sediment tank is 50% [10]. The amount of sewage sludge (from the primary sedimentation tank and aeration tanks) at the local WWTP with a design capacity of 65,000 PE is calculated below:

Production of sludge:

The total solids found in the primary sludge correspond to half of the total suspended solids in the wastewater at the inlet:

$$Primary\ Sludge\ (PS)\ removal = \frac{50\% \times Q \times TSS \times 24}{1000} = \frac{50\% \times 542\frac{m^3}{h} \times 300\frac{g}{m^3} \times 24\frac{h}{d}}{1000} = 1{,}950\frac{kgTS}{d}$$

$$WAS\ production = 0.75 \times \frac{Q \times (BOD_i - BOD_e) \times 24\frac{h}{d}}{1000} \times 0.6 =$$

$$\frac{542\frac{m^3}{hr} \times (300-25)\frac{g}{m^3} \times 24\frac{h}{d}}{1000} * 0.6\frac{kgTS}{kg\ BOD} = 1{,}609\frac{kgTS}{d}$$

Total Sludge production = PS removal + WAS production

$$\left(1{,}950\frac{kgTS}{d} + 1{,}609\frac{kgTS}{d} =\right) 3{,}559\frac{kgTS}{d} \times 365.25 = 1{,}299{,}833\ \frac{kgTS}{a}$$

Digestion of PS:

$$1{,}950\frac{kgTS}{d} \times 77\% VS/DS \times 345\frac{LCH_4}{kgVS} \div 1000 = 521\frac{m^3CH_4}{d}$$

$$521\ \frac{m^3CH_4}{d} \times 365.25 =\ 190{,}236\ \frac{m^3CH_4}{a}$$

$$\frac{190{,}236\frac{m^3CH_4}{a}}{67\%} \times 33\% = 93{,}698\frac{m^3CO_2}{a}$$

Digestion of WAS:

$$1{,}609\frac{kgTS}{d} \times 48\%\frac{VS}{TS} \times 87\frac{LCH_4}{kgVS} \div 1000 = 67.2\frac{m^3CH_4}{d}$$

$$67.2\frac{m^3CH_4}{d} \times 365.25 =\ 24{,}538\frac{m^3CH_4}{a}$$

$$\frac{24{,}538\frac{m^3CH_4}{yr}}{50\%} \times 50\% = 24{,}538\frac{m^3CO_2}{a}$$

$$Total\ CH_4\ from\ PS\ and\ WAS = 190{,}236\frac{m^3CH_4}{a} + 24{,}538\frac{m^3CH_4}{a} = 214{,}774\frac{m^3CH_4}{a}$$

$$Total\ CO_2\ from\ PS\ and\ WAS = 93{,}688\frac{m^3CO_2}{a} + 24{,}538\frac{m^3CO_2}{a} = 118{,}237\frac{m^3CO_2}{a}$$

Biological methanation:

The reaction of 118,237 m^3CO_2/a with 17,100 kg H_2/a [190,254 m^3H_2/a] from the electrolyser (Box 4.3) in a biomethanation system yields:

$$\frac{190{,}254\ \frac{m^3H_2}{a}}{118{,}237\ \frac{m^3CO_2}{a} \times 4_{molar\ ratio}} = 40.2\%\ of\ generated\ CO_2\ converted\ by\ H_2\ upgrading.$$

$$190{,}254\ \frac{m^3H_2}{a} \div 4 \times 98.6\%_{BHM\ efficiency}\ produces\ 46{,}897\ \frac{m^3CH_4}{a}$$

Using 190,254 $\frac{m^3 H_2}{a}$ in the biomethanation process results in a **21.8%** improvement in the CH_4 yield, totalling:

$$214{,}774\,\frac{m^3 CH_4}{a} + 46{,}897\ \frac{m^3 CH_4}{a} = 261{,}672\,\frac{m^3 CH_4}{a}$$

Box S4.5: Calculation of biomethane production and GHG emissions reduction from the use of biomethane

Taking cattle slurry (total solid content of 8.75%) as an example:

(1) Basic conversion factor and energy content:

1 m^3 CH_4 = 36 MJ = 10 kWh

1 m^3 biogas = 36 MJ * 60% (methane content) = 21.6 MJ

CO_2 emission factor of diesel = 0.264 kg CO_2/kWh

Slurry management bonus = -54 kg CO_2/twwt slurry

(2) Biomethane production

Biomethane production from cattle slurry = 267,930 twwt/a × 16 m^3/twwt ≈ 4,287 × 10^3 m^3/a.

It is assumed that the content of CH_4 and CO_2 in biogas is 60% and 40%, respectively; as such, the CH_4 and CO_2 production is calculated as follows:

V_{CO2} = (4,287 × 10^3 m^3/60%) × 40% = 2,840 × 10^3 m^3/a;

Therefore, the total amount of CO_2 in biogas production from cattle slurry, food waste and sewage sludge (including primary sludge and waste activated sludge) were calculated as 4,225 × 10^3 m^3/a. However, as the produced H_2 from the electrolyser was only 190,207 m^3/a, this could only convert 47,552 m^3 (190,207/4) CO_2, which accounts for only 1.13% (47,552/(4,225 × 10^3)) of the total amount of CO_2 in the produced biogas.

(3) GHG emissions reduction from replacement of diesel consumption:

Energy content in biomethane: E_{CH4} = 4,287 × 10^3 m^3 × 10 kWh/m^3 = 4,287 × 10^4 kWh;

CO_2 emission savings by replacing diesel = 4,287 × 10^4 kWh × 0.264 kg CO_2/kWh = 11.31 kt CO_2;

(CO_2 emission reduction from avoided methane production via digestion of slurry:

CO_2 emission savings by digesting slurry = 267,930 twwt/a × 54 kg CO_2/twwt slurry = 14.47 kt CO_2

(5) GHG emissions from biochar production:

CO_2 sequestrated by biochar = 267,930t × 8.75% × 20% × 55% × 3.67 = 9.46 kt CO_2.

Total CO_2 emission reduction from slurry digestion = 11.31 kt + 14.47 + 9.46 = 35.24 kt.

Supplementary references

[1] Ludwig-Bölkow-Systemtechnik, “Hydrogen Data,” 2020. [Online]. Available: http://www.h2data.de/.

[2] IEA, The Future of Hydrogen, no. June. OECD, 2019.

[3] Byrne Ó Cléirigh Consulting, “Report on Diesel and Alternative Fuel Bus Trials – Addendum,” 2022.

[4] CSO Ireland, “Transport Omnibus 2018,” 2018. [Online]. Available: https://www.cso.ie/en/releasesandpublications/ep/p-tranom/transportomnibus2018/publictransport/.

[5] J. J. Minnehan and J. W. Pratt, “Practical Application Limits of Fuel Cells and Batteries for Zero Emission Vessels,” Sandia Unltd. Release, vol. SAND2017-1, pp. 1–71, 2017.

[6] H. D. S. George Tchobanoglous, Franklin L. Burton, Wastewater Engineering : Treatment and Reuse (Fourth Edition), vol. 179, no. 18. 2003.

[7] A. Smallbone, B. Jia, P. Atkins, and A. P. Roskilly, “The impact of disruptive powertrain technologies on energy consumption and carbon dioxide emissions from heavy-duty vehicles,” Energy Convers. Manag. X, vol. 6, p. 100030, Apr. 2020.

[8] I. Environmental Protection Agency, “Wastewater Treatment Manuals,” 1997.

[9] SEAI, “Common conversion factors for energy use in Ireland,” 2020. [Online]. Available: https://www.seai.ie/data-and-insights/seai-statistics/conversion-factors/.

[10] M. Von Sperling, Wastewater characteristics, treatment and disposal. IWA publishing, 2007.

Chapter 5 - Supplementary data

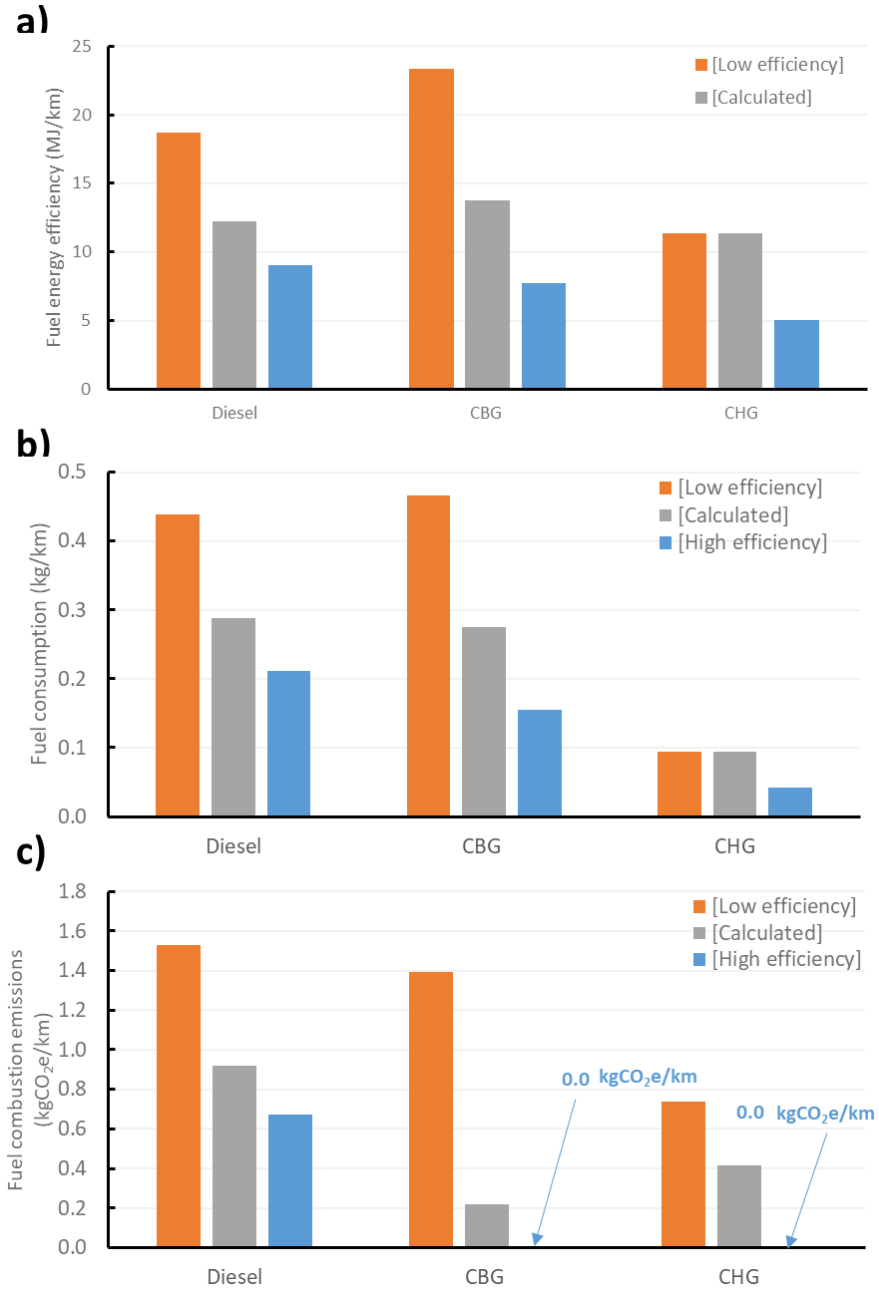


Figure S5.1: Fuel and HGV comparison (Lower is better); a) HGV Tank-to-Wheel efficiency (MJ/km); b) Fuel consumption (kg/km); c) Fuel combustion emissions ($kgCO_2e$/km). Adapted from Table S5.1.

Table S5.1: Low, average, and high-efficiency scenarios for HGV fuel and engine types.

	[Low efficiency]			[Calculated]			[High efficiency]		
	$kgCO_2e$/km	kg/km	MJ/km	$kgCO_2e$/km	kg/km	MJ/km	$kgCO_2e$/km	kg/km	MJ/km
Diesel	1.530	0.439	18.700	0.922	0.287	12.2	0.672	0.212	9.0
CBG	1.390	0.467	23.350	0.217	0.275	13.8	0.000	0.155	7.7
CHG	0.740	0.094	11.352	0.243	0.055	6.6	0.000	0.042	5.1
Mileage				60,000 km/a					
Reference				[1–9]					

Supplementary References

[1] Quiros DC, Smith J, Thiruvengadam A, Huai T, Hu S. Greenhouse gas emissions from heavy-duty natural gas, hybrid, and conventional diesel on-road trucks during freight transport. Atmos Environ. 2017 Nov 1;168:36–45.

[2] Ricardo Energy & Environment, Kollamthodi S. The role of natural gas and biomethane in the transport sector. Transp Environ Rep [Internet]. 2016;(1):1–85. Available from: https://www.transportenvironment.org/discover/?_article_type=publications

[3] Smallbone A, Jia B, Atkins P, Roskilly AP. The impact of disruptive powertrain technologies on energy consumption and carbon dioxide emissions from heavy-duty vehicles. Energy Convers Manag X. 2020 Apr 1;6:100030.

[4] Langshaw L, Ainalis D, Acha S, Shah N, Stettler MEJ. Environmental and economic analysis of liquefied natural gas (LNG) for heavy goods vehicles in the UK: A Well-to-Wheel and total cost of ownership evaluation. Energy Policy [Internet]. 2020 Feb;137(November 2019):111161. Available from: https://doi.org/10.1016/j.enpol.2019.111161

[5] Gas Networks Ireland. The future of transport - Case Study: Comparison of a natural gas truck versus a diesel truck. 2014;1–6. Available from: https://www.gasnetworks.ie/business/natural-gas-in-transport/celtic-linen-case-study/CNG_Case_Study.pdf

[6] ICCT, Moultak M, Lutsey N, Hall D. Transitioning to zero-emission heavy-duty freight vehicles. Int Counc Clean Transp [Internet]. 2017;(September):53. Available from: www.theicct.org

[7] Smajla I, Sedlar DK, Drljača B, Jukić L. Fuel switch to LNG in heavy truck traffic. Energies. 2019;12(3).

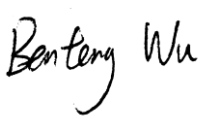
[8] Department for Business E& IS. Greenhouse gas reporting: conversion factors 2020 [Internet]. Government Digital Service. 2020 [cited 2021 Apr 7]. p. 1. Available from: https://www.gov.uk/government/publications/greenhouse-gas-reporting-conversion-factors-2020

[9] International Energy Agency. World Energy Outlook 2018 – Analysis [Internet]. Flagship report — November 2018. 2018 [cited 2021 Mar 24]. Available from: www.iea.org/weo

Chapter 2 – [SD 2] Standard Operating Procedure

SOP Version	1			
SOP Title	Biological Hydrogen Methanation system			
	NAME	TITLE	SIGNATURE	DATE
Author	Davis Rusmanis	PhD Student		21/02/2023
Reviewer	Richard O'Shea	Senior Postdoctoral Researcher		
Authoriser				

Effective Date:	10/07/2020
Review Date:	

READ BY			
NAME	TITLE	SIGNATURE	DATE
Richard O'Shea	Senior Postdoctoral Researcher		14/12/2020
Davis Rusmanis	PhD Student		14/12/2020
Benteng Wu	PhD Student		14/12/2020

Change Log

SOP version.	Effective Date	Significant Changes/ Comment	Previous SOP no.
1	20/01/2020	Initial draft V0.0	N/A
2	03/10/2020	V1.0	V0.0
3	15/11/2021	V1.1 – Addition of Benteng's intermittent feeding SOP.	V1.0
4	21/02/2023	V1.2 – Reformatting and minor revisions of SOP	V1.1

CONTENTS

[SD 2] Standard Operating Procedure 182
1. PURPOSE 185
2. INTRODUCTION 185
3. SCOPE 187
4. DEFINITIONS 187
5. RESPONSIBILITIES 187
6. HEALTH AND SAFETY 188
7. METHODOLOGY 189
7.1 Flow chart and BHM reactor skid P&ID 189
7.2 Set up and operation of BHM reactor skid 191
7.2.1 Securing the reactor skid 191
7.2.2 Connecting the reactor skid 191
7.2.3 Connecting the expansion vessel 192
7.2.4 Filling of Heating Jackets 193
7.2.5 Fume hood operation and system start up 194
7.2.6 External gas supply 197
7.2.7 Safe state configuration 198
7.2.8 Manifold Purging 198
7.2.9 Mixed gas preparation 201
7.2.10 Total System Purging and Flushing 202
7.2.11 R1 Batch Operation - Single Reactor Batch operation 203
7.2.12 R1 + R2 + R3 Batch Operation – Multiple Reactor Batch Operation 205
7.2.13 R1, R2 or R3 Continuous Operation 207
7.2.14 R1 & R2 In-series 211
7.2.15 R2 & R3 In-series 213
7.2.16 R3 & R1 In-series 215
7.2.17 R1, R2, R3 In-series 217
7.2.18 R1, R2, R3 Continuous Parallel 219
7.2.19 System reset 221
7.2.20 Reactor output gas flow rate measurement 222
7.2.21 Input gas flow rate measurement 225
7.2.22 Intermittent gas supply 227

7.3 Gas Sampling 227
7.4 Gas chromatography 228
7.5 General maintenance 228
7.5.1 Water bath 228
7.5.2 Condensate traps 228
7.5.3 Sampling septum replacement 229
7.6 Liquid Substrate Sampling 230
7.7 Sample testing 231
7.7.1 pH 231
7.8 Reactor feeding 231
7.9 Sample to storage 232
7.10 Reactor vessel dismantling 232
8. MAINTENANCE 233
8.1 Making/Breaking connections 233
8.2 Inspections 233
8.2.1 Leak Inspections: Nitrogen Leaks 233
8.2.2 Leak Inspections: Hydrogen and Methane Leaks 234
8.3 Equipment maintenance checks 235
9. FORMS/TEMPLATES TO BE USED 236
10. INTERNAL AND EXTERNAL REFERENCES 236
10.1 Internal References 236
10.2 External References 236
11. RISK ASSESSMENT 237

1. PURPOSE

This manual details the safe; practice, operation, and handling of the biological hydrogen methanation (BHM) reactor skid. The purpose of this SOP is to provide an in-depth, systematic operation of the three-reactor system, allowing the user to set up different system operations by manipulation of the valves. This SOP complies with necessary lab safety regulations, as well as the HAZOP feedback issued by the contracted parties [HAZOP amendments, not incl. until handover of project] [Internal References]. Additionally, this project seeks to comply with the zoning regulations set out by the contracted company - DPS and the UCC Buildings & Estates department.

2. INTRODUCTION

The designed experiments are based on the Sabatier process:

$$4H_2 + 2\ CO_2 \rightarrow CH_4 + 2H_2O,\ \Delta H = -165\ kJ/mol$$

The reaction of CO_2 with H_2 results in the production of CH_4 with heat and water as by-products. The heat produced by the exothermic process in the reactors is negligible as the heat losses of the system will far exceed those generated by the process.

H_2 is a difficult gas to work with due to the unique properties of the element. It is the lightest gas, and the molecule is the smallest of the elements. This necessitates complex storage solutions to prevent gas leaks. Working with H_2 can be cumbersome, especially with elevated pressures.

The design of this reactor skid maximises the safety of the operators and minimises the risk of combustion of volatile gases and leaking of inert asphyxiating gases into the laboratory. Several limitations to the experiments exist as a result.

The system allows for varied operational set-ups, ranging from single reactor operation in parallel to cascading in-series operation across all three reactors, acting as a single system.

The BHM rig is comprised of three ATEX-rated reactors, each with a maximum 6L working volume. An optional Batch process expansion vessel, 50L volume is also part of the system, on a separable trolley. The provisional flowrate of the system (limited by the flow totaliser) is as follows:

Table 1: Krohne flow totaliser specifications.

Tag No.	P&ID	Fluid	Pressure	Temperature	Flow rate required	Instrument selected	Comment
FI-5003	A18CK038-KD-001	CO_2	0.5 Bar(g)	Ambient	0.9 NL/Hr to 7.8 NL/Hr	Type: Krohne DK48 Miniature variable area flowmeter 0.9 NL/Hr to 7.8 NL/Hr Stainless Steel construction. Stainless steel float. c/w Needle valve to regulate flow. c/w Glass tube & analogue scale. Design Pressure range: 0 -10 Bar(g) Design Temperature range: 5°C -100°C End connections: ¼" NPT(F) Screwed connections	Normal = 1,013 bar abs; 0°C
FI-5001	A18CK038-KD-001	CH_4	0.5 Bar(g)	Ambient	0.9 NL/Hr to 7.8 NL/Hr	Type: Krohne DK48 Miniature variable area flowmeter 0.9 NL/Hr to 7.8 NL/Hr Stainless Steel construction. Stainless steel float. c/w Needle valve to regulate flow. c/w Glass tube & analogue scale. Design Pressure range: 0 -10 Bar(g) Design Temperature range: 5°C -100°C End connections: ¼" NPT(F) Screwed connections	Normal = 1,013 bar abs; 0°C
FI-5002	A18CK038-KD-001	H_2	0.5 Bar(g)	Ambient	3.12 NL/Hr to 31.2 NL/Hr	Type: Krohne DK48 Miniature variable area flowmeter 3.12 NL/Hr to 31.2 NL/Hr Stainless Steel construction. Stainless steel float. c/w Needle valve to regulate flow. c/w Glass tube & analogue scale. Design Pressure range: 0 -10 Bar(g) Design Temperature range: 5°C -100°C End connections: ¼" NPT(F) Screwed connections	Normal = 1,013 bar abs; 0°C

3. SCOPE

The scope of the SOP is to function as a guide to setting up, operating, and maintaining the reactor system, allowing new operators to become familiar with the system by following the SOP document. Arrangement schematics for the reactor and valves are presented, with diagrams visualising the final valve arrangement for each system configuration. Procedures for reactor commission, connection to power supply, supplementary works and general maintenance can also be found within the SOP. It is important to follow the Health and safety advice of the SOP as the potential risk outcomes may be severe, leading to death and/or severe damage to the surrounding environment.

This SOP does ***NOT*** apply where experiments beyond H_2 are concerned, such as anaerobic digestion. Should other processes besides BHM take place, a re-evaluation of the BHM rig suitability is essential and an updated SOP must be developed.

4. DEFINITIONS

BHM – Biological hydrogen methanation
CH_4 – Methane
H_2 – Hydrogen
CO_2 – Carbon Dioxide
N_2 - Nitrogen
R1, R2, R3 – Reactor 1, Reactor 2, Reactor 3
Purging – Purging the system of foreign gases with inert N_2 gas.
Flushing – Flushing the system of inert N_2 with the working gases. Namely H_2, CO_2 and CH_4, a mixture of two or three of the gases.
MC – Manifold Carbon Dioxide valve.
MH – Manifold Hydrogen valve.
MM – Manifold Methane valve.

5. RESPONSIBILITIES

Operators – The responsibility of the operators is to carry out experiments, including set up and decommissioning, with the reactor skid in a safe manner.

Note: The authors recommend for new operators of the system familiarise and practice with the system, using water as the reactor medium and N_2 as the gas. Only once comfortable with the operation, should flammable gases be used.

Due to safety concerns, and to ensure correct operating procedures are followed, **it is required to have two operators at any time to cross-reference and proof-check the interactions with the reactor set-up**. Ensure **ALL** operators are fully trained in the operation of the BHM rig with sufficient knowledge in understanding the process and procedures to follow in (de)commissioning, feeding and maintenance of the BHM system and the risks associated with the system.

6. Health and Safety

All ignition sources are prohibited within the Zone classification boundary marked on the floor surrounding the BHM rig in LG30 when the rig is in operation.
The following items are prohibited:

- **Naked flames**
- **Personal electronic equipment (including; cameras, laptops, phones, and watches)**
- **All electronic devices that are not ATEX rated**

Operators are also required to wear properly earthed anti-static bracelets when inside the Zone classification boundary operating the BHM rig

Owing to the flammable nature of the working gases used in the BHM rig and the hazard that they pose to personnel operating the BHM rig, it is vital that all personnel who operate the BHM rig;

- Are aware of the hazards and risks associated with the operation of the BHM rig.
- Have completed the required training and are deemed competent in BHM rig operation.
- Are familiar with the ERI emergency evacuation procedures.

Hazards and Risks:
Details of the hazards of operating the BHM rig and their associated risks as outlined in the Risk Assessment folders.
Personnel operating the BHM rig must read these documents and understand the potential hazards and risks.

Training:
The researchers operating the BHM rig are required to undertake the following training to be qualified for the operation of the rig:
Familiarity with the BHM rig SOP (This document) and associated checklists.
Basic training/information on electrical hazards.
Personnel must be deemed competent in the operation of the BHM rig before their use of the BHM rig

Emergency Procedures:
The incorrect use of the BHM rig could result in an emergency. Personnel operating the BHM rig must familiarise themselves with the correct course of action to take in the event of an emergency as per ERI guidelines provided in *'ERI SOP 02: Emergency evacuation procedures (ERI Building)'* for detailed procedures.

7. Methodology

7.1 Flow chart and BHM reactor skid P&ID

The flow chart in Figure 1 outlines the procedures necessary to ensure minimal risk for gas leaks and contamination and ensure the health and safety of the operators of the hydrogen reactor skid.

When first connecting the reactor skid or restarting from dormancy periods, operators must ensure the first ten steps are carried out before introducing any volatile gases.

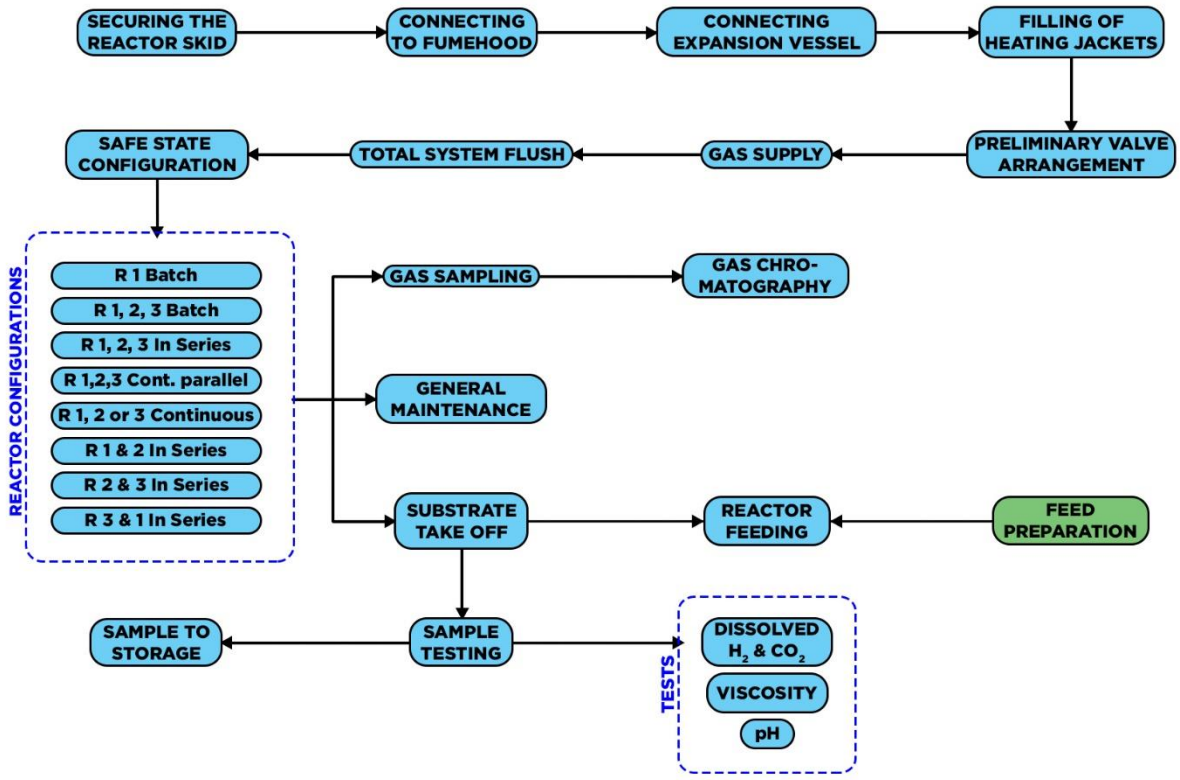


Figure 1: Preliminary procedure flow diagram for Hydrogen reactor skid set-up and operation.

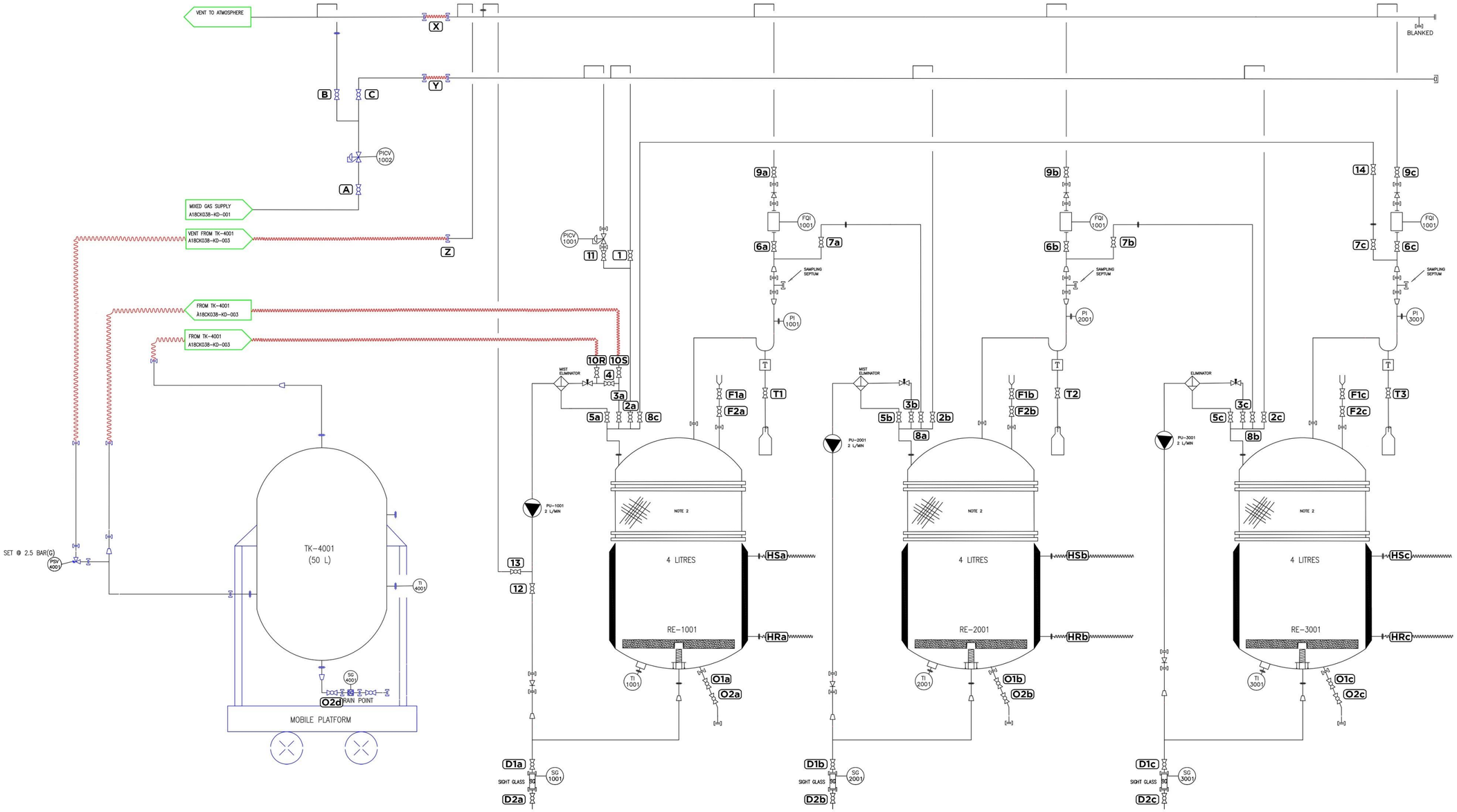


Figure 2: Preliminary P&ID schematic of the Biological Hydrogen Methanation Skid (Adapted from P&ID – A18CK038-KD-004 and A18CK038-KD-003).

7.2 Set up and operation of BHM reactor skid

Before the reactor skid may be used, it is crucial to observe all procedures in the safe setup of the reactor system. The following sections must be followed to set up the BHM skid according to the manufacturers (BCD), design engineers (DPS), and UCC Buildings & Estate safety recommendations.

7.2.1 Securing the reactor skid

The skid must first be safely moved into the fume hood by a minimum of ***2 people***.

1. Ensure that the fume hood sash is lifted ***fully*** before attempting to roll the skid in.
2. The skid castors must be unlocked to wheel in the skid.
3. Due to space issues, care must be taken so as not to risk damaging the skid, piping, or fume hood while manoeuvring. Move the skid into place.
4. Once in place, lock the casters to prevent unwanted movement of the skid.

Refer to the '7.2.1 - 7.2.8 - Reactor commission.xlsx' checklist when operating the system for verification.

7.2.2 Connecting the reactor skid

1. Connections for gas supply (Connection Y) and venting to the atmosphere (Connection X). The connections are in the upper right area of the fume hood.
2. Connect the heating jackets to the appropriate supply and return lines. ($HS_{a, b, c}$ and $HR_{a, b, c}$). Ensure no circulation liquid leaks exist once connected. Leaks can cause a slip or electrical hazards if leaking on the reactor or cables.

Figure 3: Connected water supply and return lines to the BHM rig. It is advised the placement of the heating pumps is to be at a lower elevation than the heating jackets, to ensure no air pockets are present in the jackets.

3. Before connecting any electrical cables, ensure the control box power is switched off.
4. The electrical supply for gas pumps, flow totalisers and thermocouples are connected using the electrical cords labelled: PU-1001, PU-2001, and PU-3001 and the blue power cable for the (Figure 4).
5. The cables must skirt along the wall of the fume hood and laboratory as much as possible to minimise a trip hazard or damage to the cables. Ensure the connection is securely connected and the safety latches are fixed firmly on the socket plugs.
6. Ensure any excess lengths of cable are in a safe, dry, and hazard-free area ***outside*** of the fume hood.
7. The earth cable connected to the BHM rig and the expansion vessel (when in use) must be securely connected to the earth bar, located to the right of the fume hood along the western wall of LG30.
8. When turning on the fume hood extraction, ensure that a window is open in the laboratory, to provide sufficient airflow into the room.



Figure 4: Connected three-phase plugs into the main reactor control box. Black cables labelled as PU-1001, PU-2001 and PU-3001, Blue labelled cable.

9. Once these steps are carried out, the system is ready for the next section.

Refer to the '7.2.1 - 7.2.8 - Reactor commission.xlsx' checklist when commissioning the system for verification.

7.2.3 Connecting the expansion vessel

As the expansion vessel will not always be used in the operation of the system, it may be left disconnected when not required. The vessel must be connected for the first system purge to eliminate foreign gases and ensure the vessel contains only inert N_2 gas.

1. Connect the expansion vessel via the flexible hose couplings (Connections Z, 10S and 10R).
2. Gas flow to the expansion vessel is controlled via valves 10S (supply) and 10R (return).
3. Follow sections 7.2.8 and 7.2.10 for purging of the expansion vessel.
4. Once the expansion vessel has been purged, valves 10S and 10R may be closed when the expansion vessel is not in use, isolating it from the main system.
5. The drainage valves (O1d and O2d) located at the bottom of the expansion vessel must also be closed.
6. Ensure that connection Z is secure for the pressure safety valve ventilation, located on the expansion vessel TK-4001.

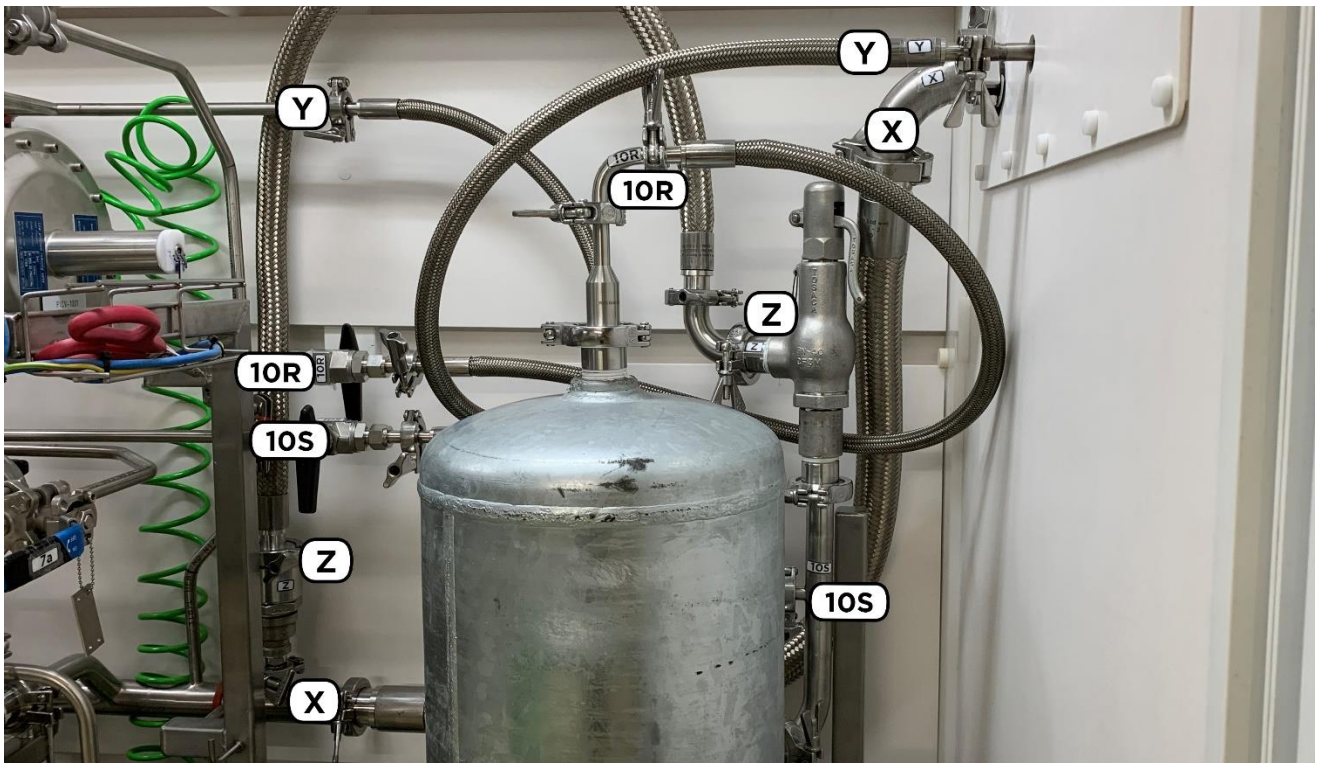


Figure 5: Location of Connection Z and valves/connections 10S and 10R.

Refer to the '7.2.1 - 7.2.8 - Reactor commission.xlsx' checklist when commissioning the system for verification.

7.2.4 Filling of Heating Jackets

1. To fill up the reactor water jackets, connect the hot water supply hose to the top inlet $HS_{a,b,c}$ of the heating jacket. Connect the hot water return hose to the bottom outlet $HR_{a,b,c}$.
2. The heaters should be placed at a higher elevation to the reactor jackets, to ensure the removal of air pockets in jackets. Ensure the water level in the water heater is full. Turn on the water circulator and set the desired temperature.
3. As the water jacket fills with circulating water, the water level in the circulator will drop. Fill up the water circulator when this occurs to ensure continued operation until the water level no longer drops.
4. The water circulator reservoir must remain open to the atmosphere until the desired temperature is reached. This is to avoid pressurisation of the water circulator due to the thermal expansion of water as it is heated.
5. Before continuing with the set-up, ensure **ALL VALVES** are closed, ensuring a 'safe state' from which valves can be configured.

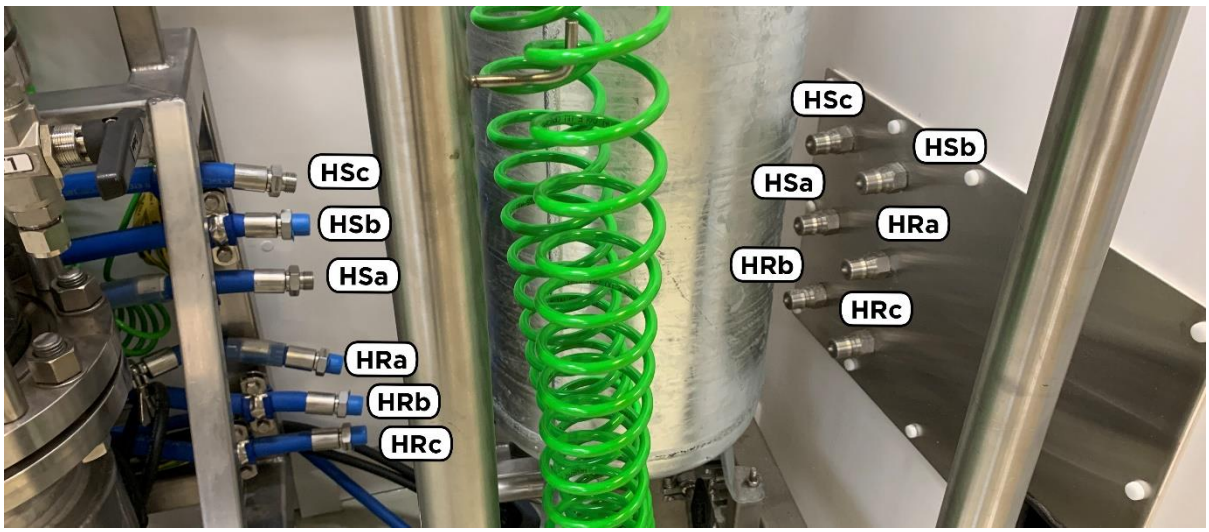


Figure 6: Connection points for each water heater supply and return. Common labels indicate the intended connections and the subsequent water bath connections located outside of the fume hood.

Note: If filling the water baths during reactor commissioning, ensure the temperature of the heating unit reaches the required temperature before isolating the reactor (e.g. batch mode). Isolating a reactor before temperature acclimatisation may result in unwanted over-pressurisation of the reactors due to the thermal expansion of gases within the reactor, as the water jackets heat the system.
Refer to the '7.2.1 - 7.2.8 - Reactor commission.xlsx' checklist when commissioning the system for verification.

7.2.5 Fume hood operation and system start up

Before turning on the BHM rig and gas supply, the fume hood must be turned on. A safety interlock system connects the fume hood and the gas supply. The solenoid valves which supply gas to the BHM rig will not open unless the fume hood is turned on. Additionally, the gas pumps on the BHM rig will not turn on until the fume hood is turned on.

1. Ensure that the BHM rig and expansion tank (if required) is fully contained within the fume hood.
2. Ensure that the fume hood sash is closed.
3. Turn off the valves supplying gas to the gas mixing manifold.
4. Turn on the fume hood control panel by turning the main breaker switch on the control panel.

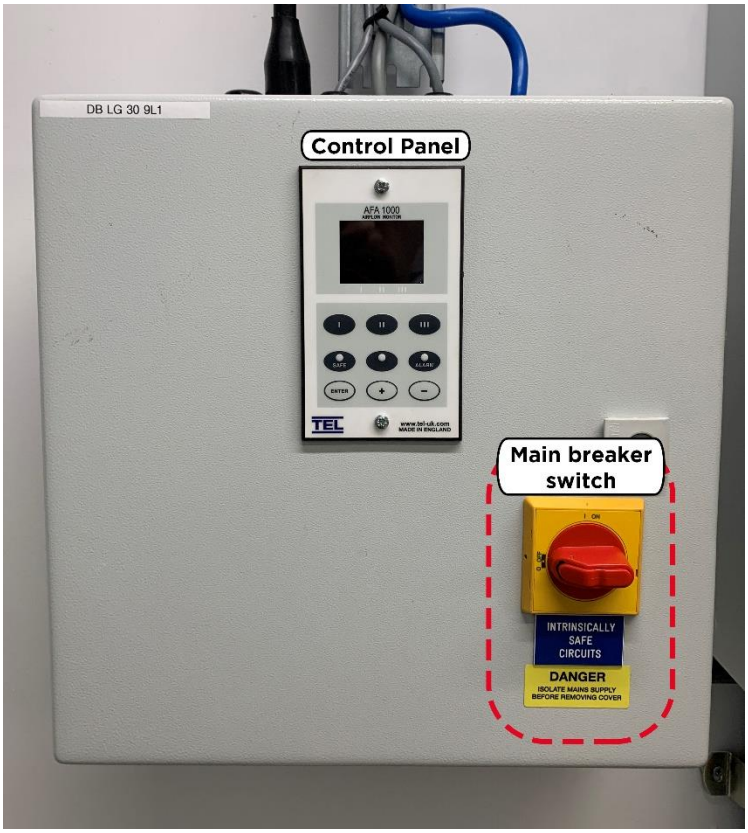


Figure 7: Fume hood control panel highlighting the main breaker switch.

1. The fume hood control panel will now be energised. An alarm may sound stating that the airflow through the fume hood is too low.
2. Turn on the fume hood extract fan by pressing the “Fan On” button on the fume hood control panel. The control panel display will show the fan start-up message and the fan status should change from “Fan Off” to “Fan On”.
3. Once the fume hood fan is turned on the airflow through the fume hood will increase and the fume hood alarm will stop sounding.
4. To turn on the BHM rig, turn the main circuit breaker on the BHM rig control panel.

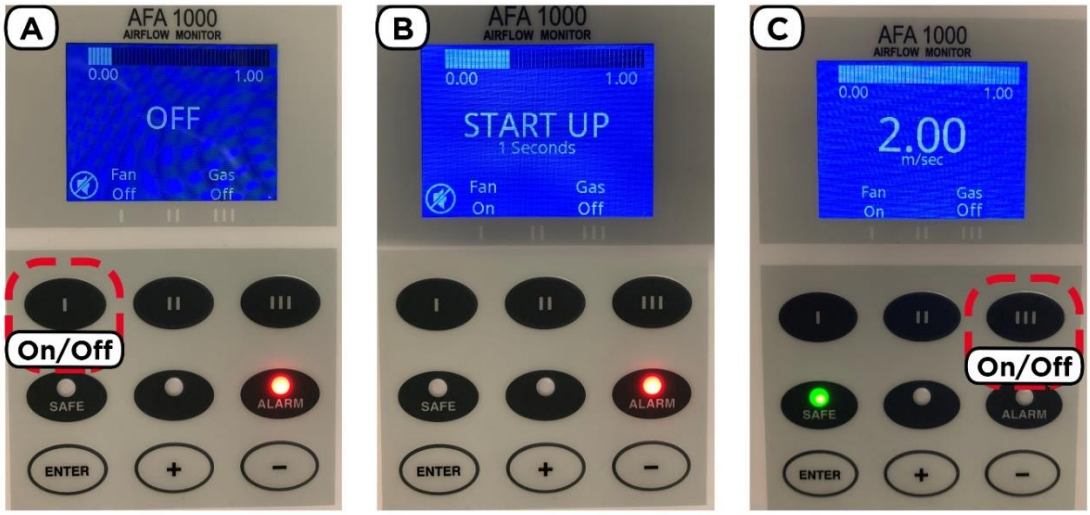


Figure 8: (a) Fume hood control panel with fan and gas off after switching on the breaker. (b) Control panel with the fan in the start-up sequence. (c) Fume hood operating and ready to receive a gas supply. Button highlighted in (c) for gas supply switch.

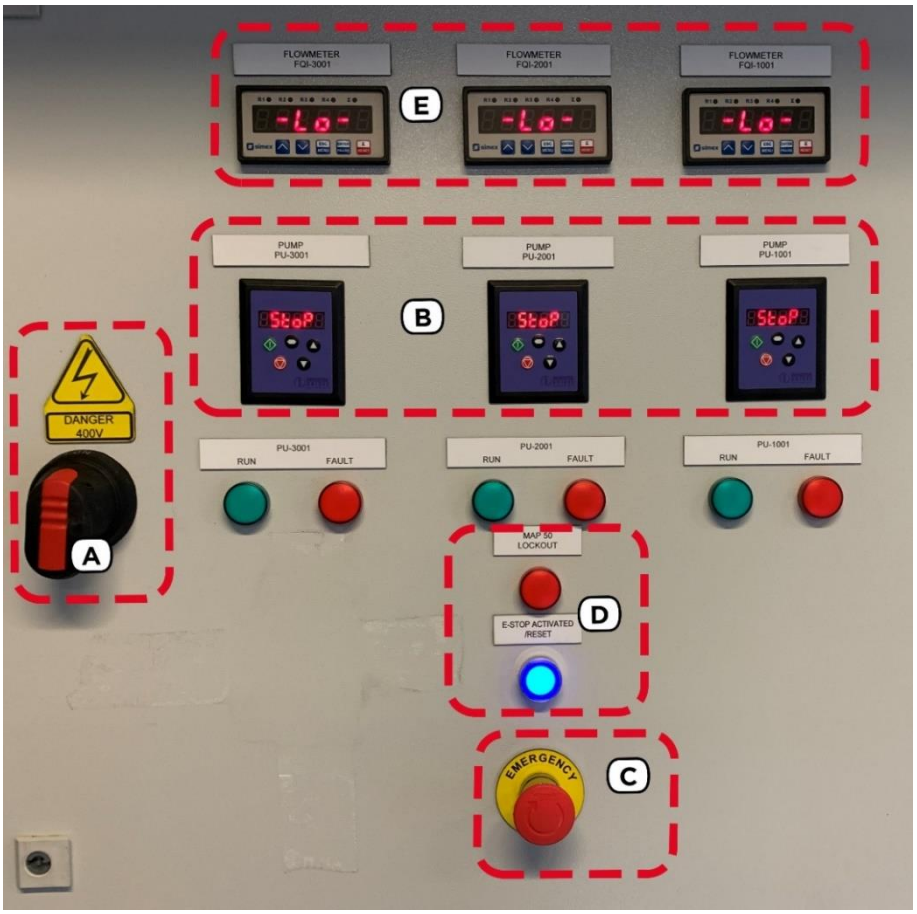


Figure 9: BHM Rig main control panel - A: Main power switch, B: Pump controls, C: Emergency shut off button, D: MAP 50 Lockout, "MAP 50" lockout is on during initial start-up and must be switched off by pressing the "E-stop/reset" button. E: Flow meter controls.

1. When the BHM rig panel is turned on, the “MAP 50” lockout button will be illuminated. This means that the BHM rig control panel will not turn on the gas pumps until the gas supply to the gas manifold is turned on.
2. To turn on the gas supply to the manifold, press the “Gas On” button on the fume hood control panel. There should be an audible “click” as the solenoid valves open. Gas can now flow through the solenoids. The gas will not enter the manifold as the manually actuated valves on the gas lines upstream of the manifold are still closed.
3. The BHM rig control panel can now be fully activated by pressing the “MAP 50” lockout button. This allows for the gas pumps to be turned on and their speed controlled using the VSD controllers on the BHM rig control panel.
4. The system is now fully energised and ready to use.

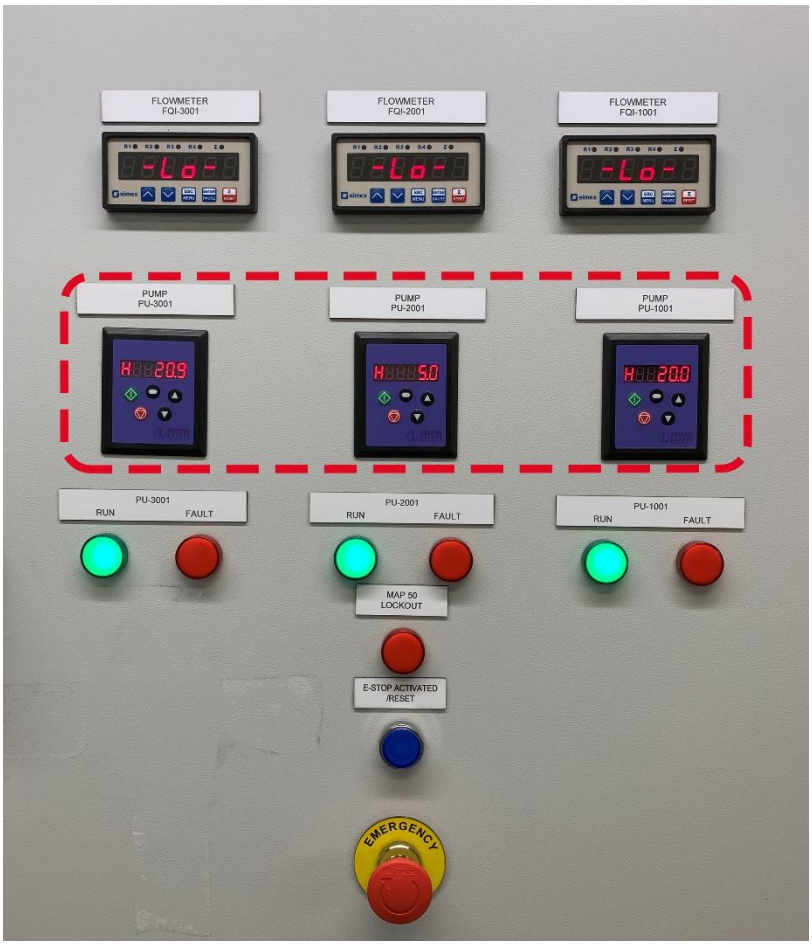


Figure 10: BHM Rig control panel fully operational. Highlighted are pump controls with pumps operating at set speeds.

7.2.6 External gas supply

Before the system can be purged with nitrogen gas, the gas supply must be first set up. This is carried out by opening valves of relevant gas cylinders in the gas and blast bunkers; namely, CH_4, H_2, CO_2, and N_2.
Ensure these are opened and correctly connected to the supply lines. Refer to 'Gas cylinder SOP.docx'. The gas bunker ought to be operated by trained personnel to ensure the correct cylinders are opened safely and according to protocol. Ensure H_2, CH_4, CO_2 and N_2 lines are all open for the experiment.
Refer to the '7.2.1 - 7.2.8 - Reactor commission.xlsx' checklist when operating the system for verification.

7.2.7 Safe state configuration

Ensure sections 7.2.1 - 7.2.6 have been correctly carried out before the following steps are conducted. **Safe state configuration requires the operators to shut all valves.**
Before the system is purged or flushed, no operation can take place, as it is necessary to ensure the safe configuration of valves. **ALL** valves should be closed, this is referred to as the 'safe state' configuration of valves.
The following valves are to be opened before any gas introduction takes place.

- Valves $D1_{a, b, c}$
- $O1_d$
- T1,T2,T3

These valves must stay open as often as possible, to ensure moisture collection in condensate traps and to prevent condensation in the gas line.
Refer to the '7.2.1 - 7.2.8 - Reactor commission.xlsx' checklist when operating the system for verification.

7.2.8 Manifold Purging

Manifold purging using N_2 gas must first be carried out before mixing the gases or purging the BHM system. To prepare the inert and mixed gases which will be used during the experiment, follow the procedure :
Note: Refer to Figure 2 and

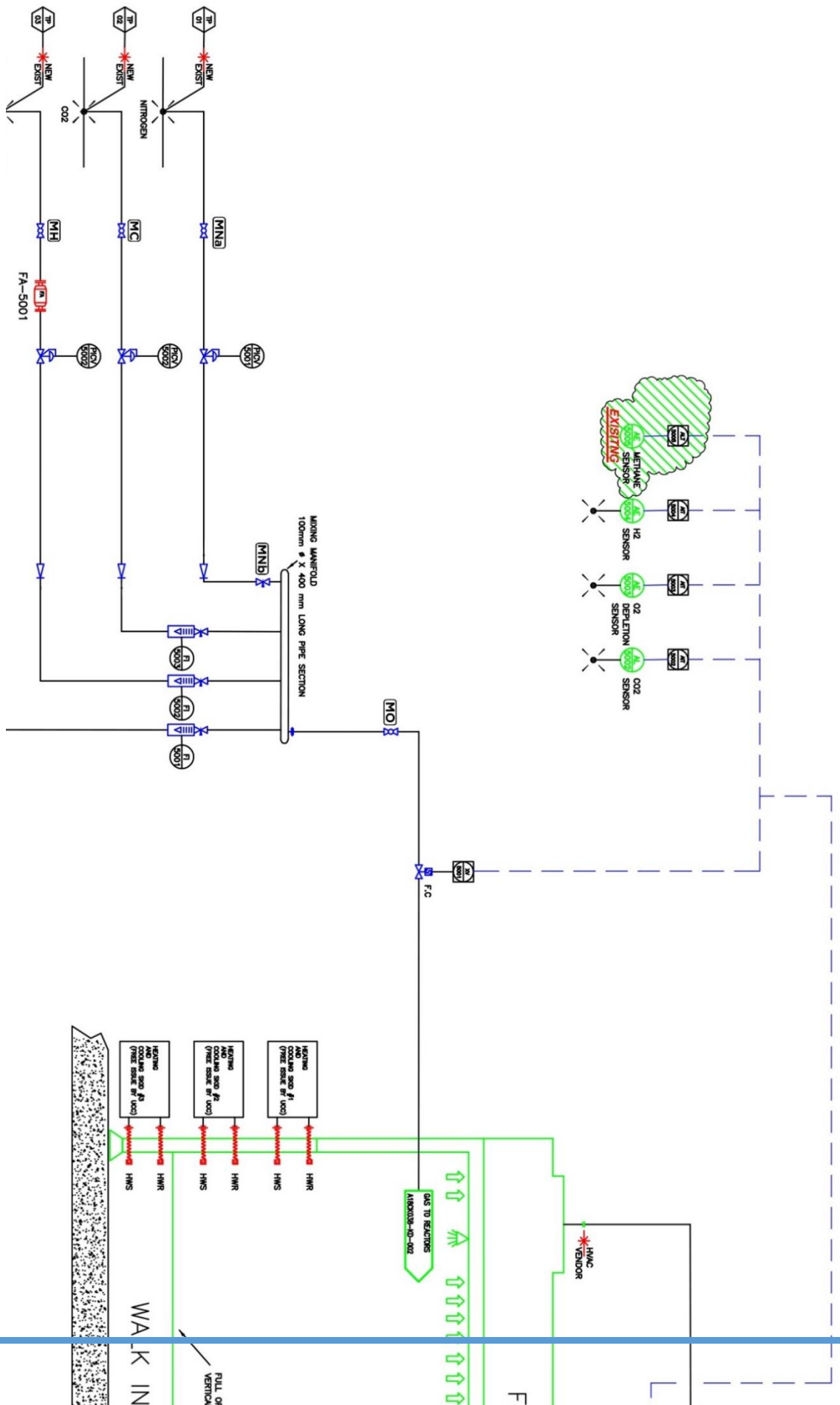


Figure 12: Gas supply and Manifold P&ID as per A18CK038-KD-001.

for valve reference.

1. Ensure previous sections (7.2.1 to 7.2.6 inclusive) have been carried out before commencing the current section.
2. Ensure the reactor system and manifold is in the 'safe state' (All valves in the closed position).
3. Purge the manifold line with N2. Open valves B, A, MO, MNb and MNa (Located on the manifold, see Figure 11). Purge for 3 minutes*.
4. The purging times of the system are preliminary and are not indicative of the finalised times required to adequately flush the system. It is advised to use gas detectors at the atmosphere vents to determine the times more precisely.
5. Bring the manifold to the 'safe state'.

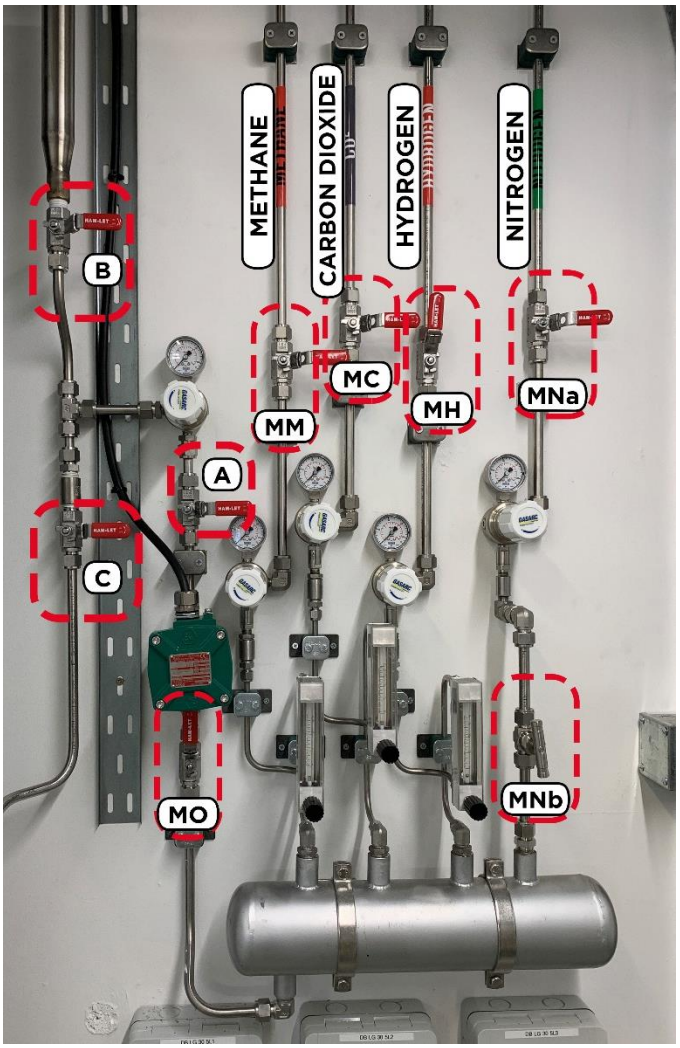


Figure 11: Labelled fume hood external lines supply and manifold.

Refer to the '7.2.1 - 7.2.8 - Reactor commission.xlsx' checklist when commissioning the system for verification.

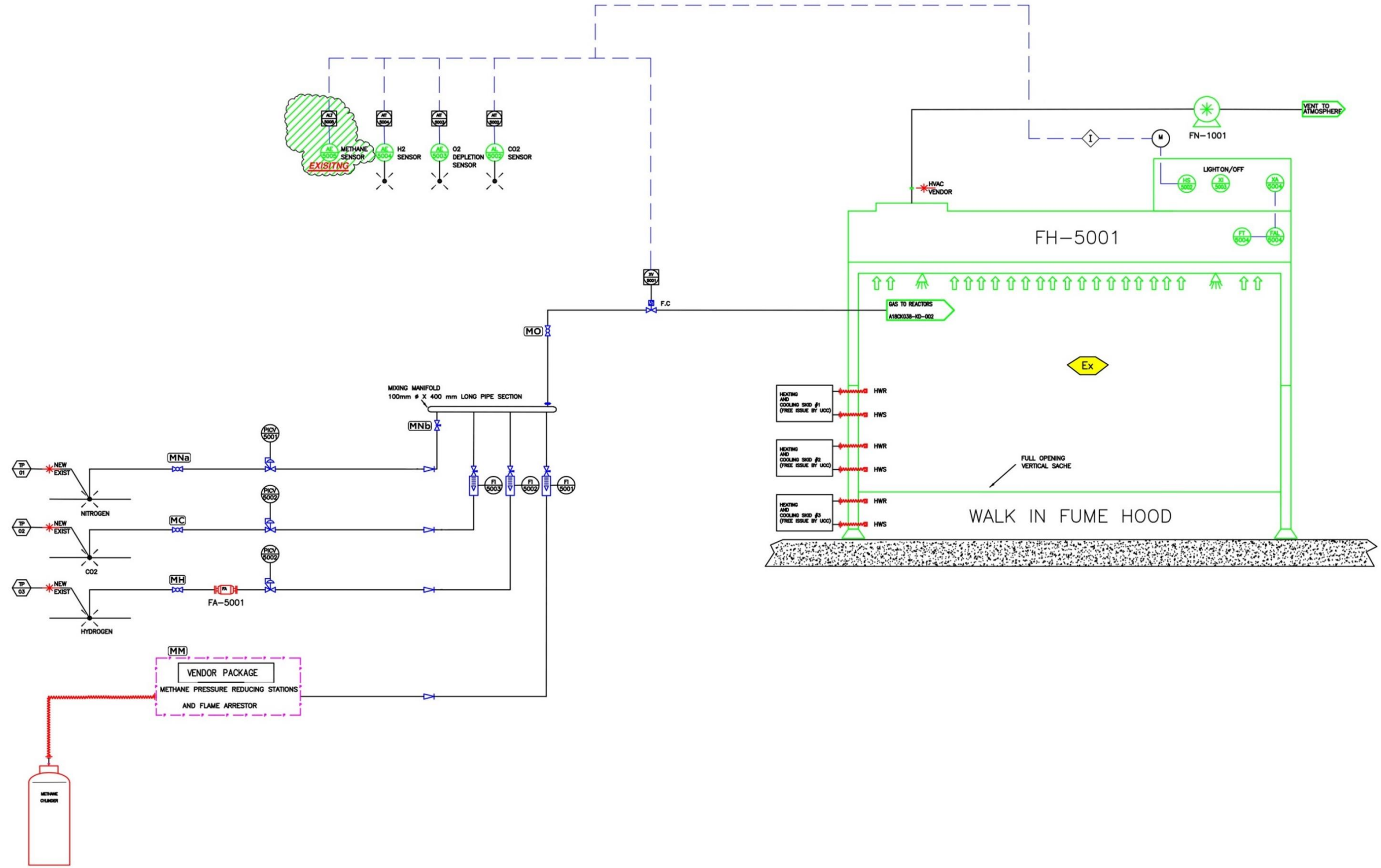


Figure 12: Gas supply and Manifold P&ID as per A18CK038-KD-001.

7.2.9 Mixed gas preparation

CONTINUE ONLY ONCE 7.2.8 IS CARRIED OUT

Note: Refer to Figure 2 and

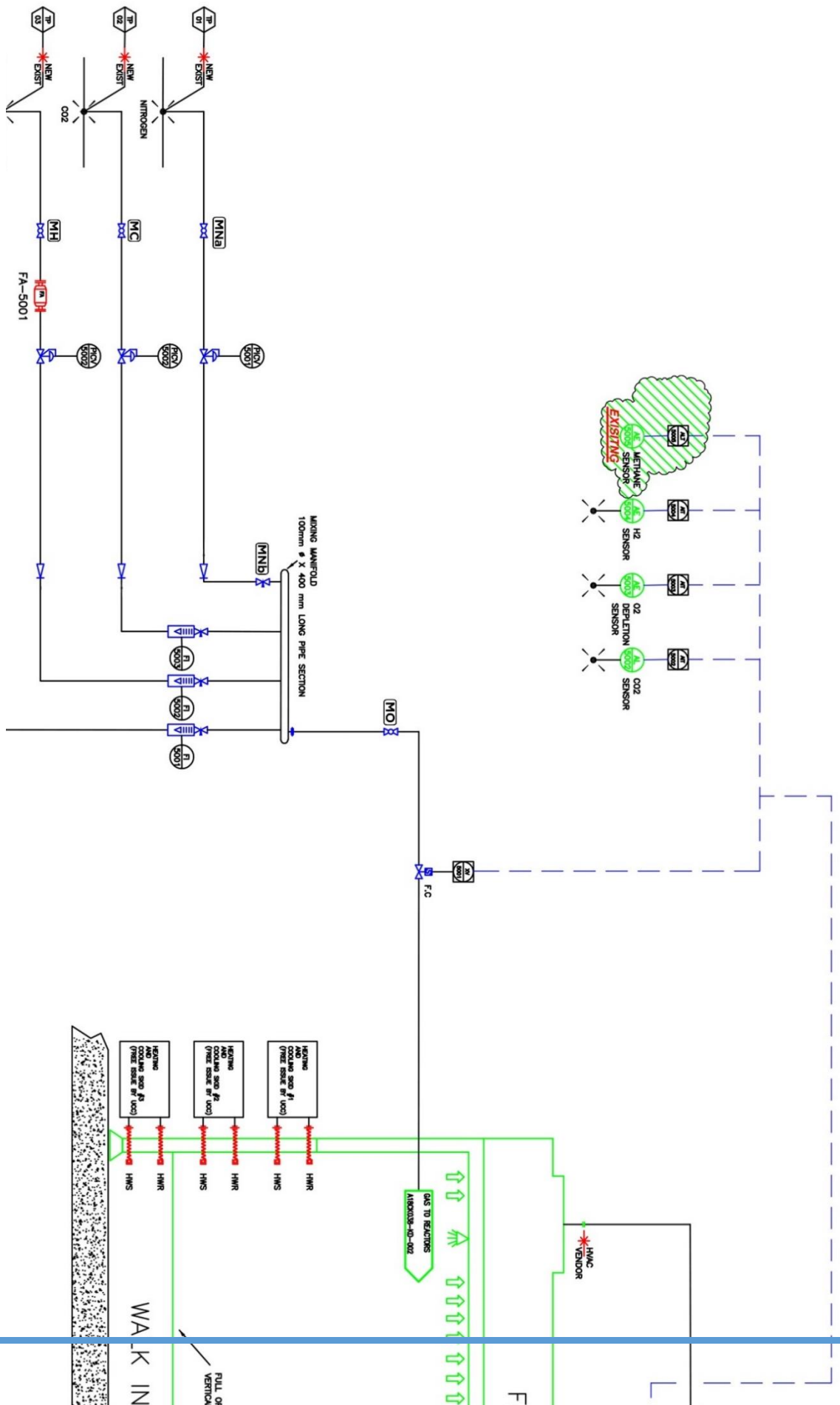


Figure 12: Gas supply and Manifold P&ID as per A18CK038-KD-001.

for valve reference.

Before commencing experiments, follow sections 7.2.11 - 7.2.18 for the relevant BHM skid operational setup after flushing.

If preparing gas for purging or flushing, follow the steps for N_2 only (for purging) or a mixture of working gases (For flushing once the system has been purged).

7.2.9.1 N2 gas preparation

1. When setting working gas flow rates, an unobstructed flow path must first be created. For N2, valves B, A, MN_a and MN_b must be opened.
2. Purge for 3 minutes*.
3. The purging times of the system are preliminary and are not indicative of the finalised times required to adequately flush the system. Use gas detectors at vents to determine the times more precisely.
4. Once ready to purge the BHM system, close valve B and open valve C.

7.2.9.2 H2, CO2, CH4 gas preparation

1. While setting working gas flow rates, an unobstructed flow path must first be created. For H2, CO2 and CH4, valves B, A, MO, MC, MH and/or MM must be opened. This allows the working gases to flow through the flow controllers (FI-5001, FI-5002 and FI-5003).
2. From this point, the working gases may be set to the required flow rate. Typically, H2 and CO2 flows are set to a molar ratio of 4:1, which applies to volume per unit of time. If measuring the flow rate in mass per unit of time, the ratio is 5.46 H2: 1 CO2. As the flow rate is being set, the gas will bypass the BHM skid and vent to the atmosphere via the BHM vent gas lines outside the fume-hood, to prevent improper gas compositions from entering the reactor.
3. Once the flow has stabilised for all gases, the manifold is ready for flushing. Close valve B and open valve C to let the mixture into the BHM skid.
4. Flush for the required amount of time, as indicated in the respective section followed. If the system is in continuous operation, leave the gas supply on.

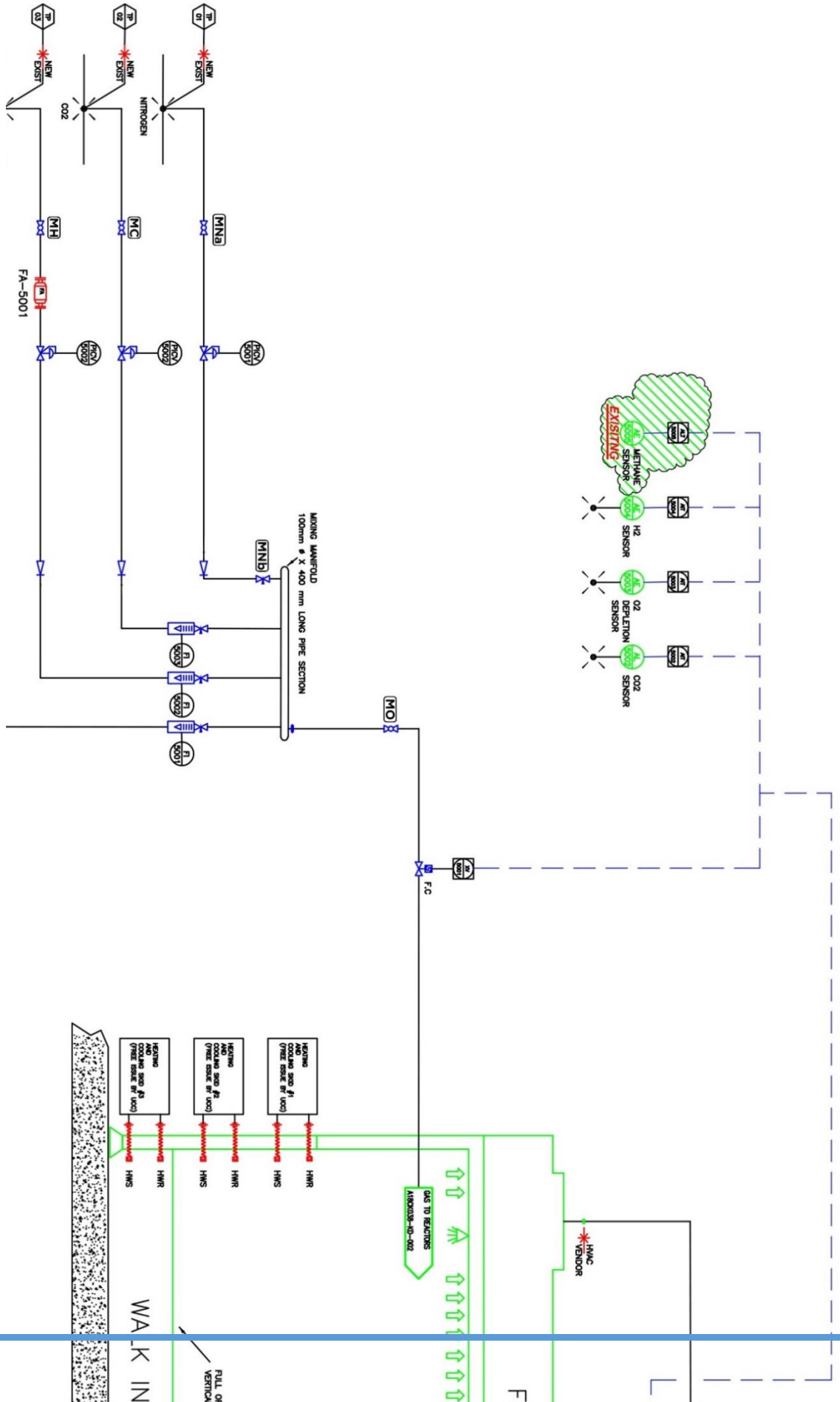
Refer to the '7.2.1 - 7.2.8 - Reactor commission.xlsx' checklist when operating the system for verification.

7.2.10 Total System Purging and Flushing

CONTINUE ONLY ONCE 7.2.9 IS CARRIED OUT

As H_2 and CH_4 are flammable gases, the system must be first purged with N_2 to minimise the risk of flammable gases mixing with O_2 and minimising the risk of combustion of the gases.
It is recommended to purge the system with N_2 before (re)starting experiments. For prolonged exposure to the external environment, purging the lines should be repeated, as O_2 may enter the headspace of the reactors and pose a risk. Refer to Figure 2 and

Figure 12: Gas supply and Manifold P&ID as per A18CK038-KD-001.



for valve reference.

When first purging the system, it is recommended to flush the system in a parallel reactor configuration to maximise the gas removal rate and minimise the dissolution of gases into the reactor liquor. Anaerobic microbes may suffer if exposed to elevated O_2 levels.

1. Refer to section 7.2.8 for manifold and gas set-up.
2. Before purging, ensure valves 1, $2_{a,b,c}$, $3_{a,b,c}$, 4, $5_{a,b,c}$, 12, $6_{a,b,c}$ and $9_{a,b,c}$ are open for parallel purging of reactors.
3. Once confirmed, open valves A, MO, MN_b and MN_a.
4. Once ready to purge the main system, set N2 flow to the maximum, and open valve C to let the inert gas enter the system. Purge for at least 4 minutes.*
5. Open valves $7_{a,\,b}$ and $8_{a,\,b}$.
6. Close valves $2_{b,\,c}$, $6_{a,\,b}$ and $9_{a,b}$. Purge for an additional 4 minutes.*
7. Open 2_b, 6_a 7_c, 8_c, 9_a and 14.
8. Close 2_a, 7_a, 8_a, 9_c and 6_c. Purge for an additional 5 minutes.*
9. Close valves 1 through 14. (BHM rig valves)
10. Open valves 1,2_a,3_a,10S,10R,5_a and 13 to purge the expansion vessel.
11. Purge for 10 minutes.*
12. Ensure valves are in the safe state once purging has been completed.

** The purging times of the system are preliminary and are not indicative of the finalised times required to adequately flush the system. It is advised to use gas detectors at the atmosphere vents to determine the times more precisely.*

Once the purging with N_2 has been completed, the N_2 gas supply must be **shut off** and **all** valves closed once more.

For continuous processes, purging needs to be carried out for the entire system thoroughly, as flammable gases may leak into unused lines. Prolonged seepage may result in a combustible gas mixture. Thus, if a cascade across all three reactors is to be used for experiments, *purging of all system lines is required*.

Repeat steps 1 - 12, after preparing the mixed working gas in section 7.2.9.

Repeat steps 1 - 12, at the end of an experiment, purging with N_2 as per section 7.2.9.

Refer to the '7.2.9 - Total System Purge & Flush.xlsx' checklist when operating the system for verification.

7.2.11 R1 Batch Operation - Single Reactor Batch operation

1. Ensure previous sections (7.2.1 to 7.2.10 inclusive) have been carried out before commencing the current section.
2. Ensure the reactor system is in the **'safe state'**.
3. For batch operation, ensure TK-4001 mobile expansion vessel is properly connected to the main system at valves 10S and 10R.
4. Ensure the gas lines have been purged and flushed as per section 7.2.10. Open valves 11 and 2_a.

5. Valves 3_a, 10S and 10R are opened to allow for flow to the expansion vessel and back. Valve 4 must remain closed to ensure correct gas circulation.
6. Open valves 5_a and 12.
7. Ensure the mixed gas supply is set according to section 7.2.9.
   At this stage, the pump speed should be set to the maximum flow*
   ** The limit of the diffuser and pump should be determined and restricted to the lower of the two to ensure the longevity of the equipment.*
8. Once the system has been purged and flushed as per section 7.2.9; close valves MC, MH and MM (

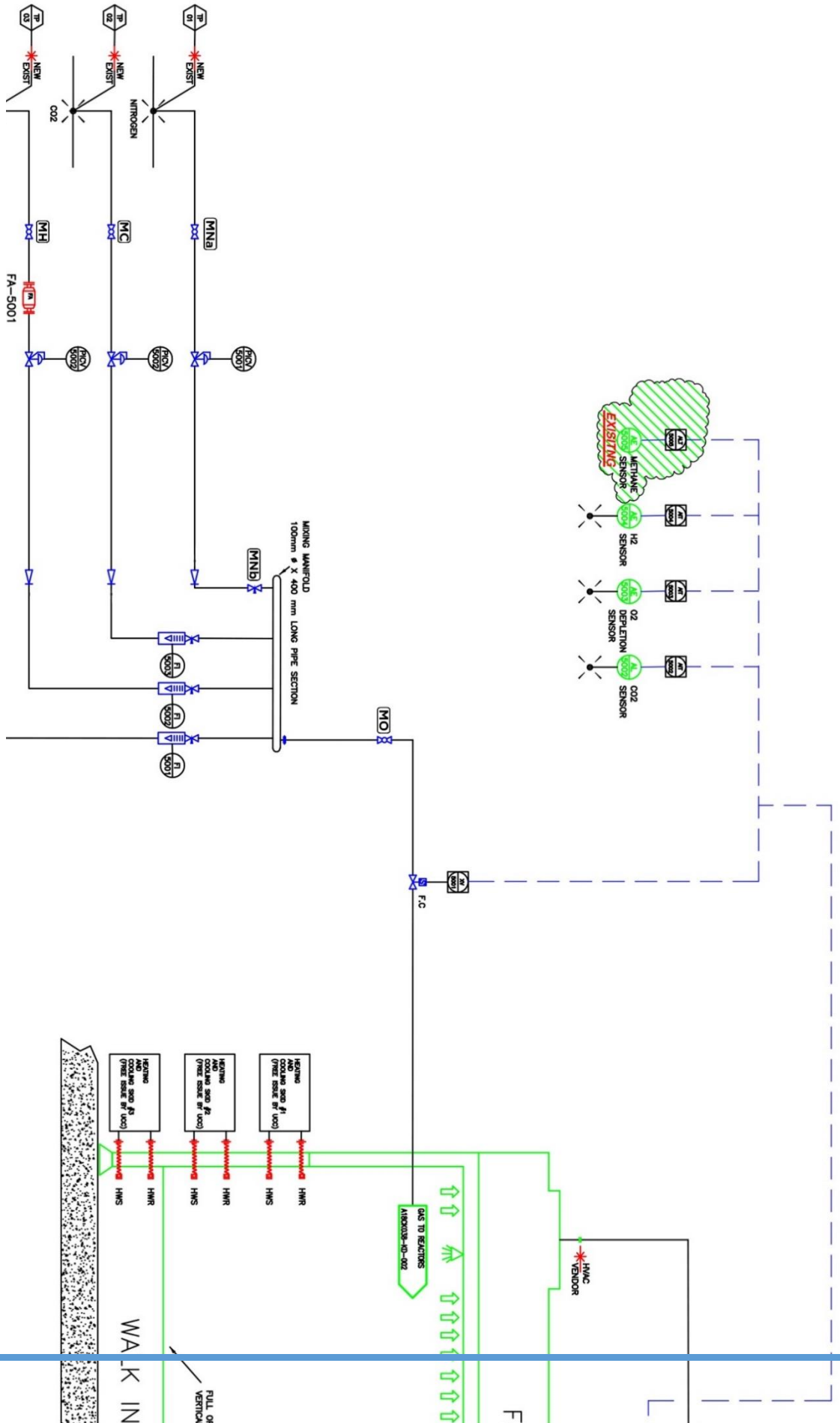


Figure 12: Gas supply and Manifold P&ID as per A18CK038-KD-001.

9.).
10. Verify the correct valve arrangement is carried out (Steps 1-8).
11. Ensure the recirculation pump PU-1001 is recirculating gas. Close valves 1, 6_a and 9_a.
12. Purge the manifold once more with N_2 as per section 7.2.8. Once done so, open valves MN_a and MN_b, MO, A, C and 11.
13. Ensure valves $O2_d$, and $D1_a$ are open to allow for the capture of condensate in the gas lines. Check valve T1 for any condensate build-up in the line leading away from the reactor. Caution must be taken in losing volumes of gas due to these checks, in batch scenarios.

The batch system is now set up to operate for the desired retention time. Figure 13 shows the final flow arrangement of the system.

Note: Due to the nature of the system, reliably measuring gas volume in the system is not possible in batch operation. The rigid walls mean gas will need to be calculated from the gas composition acquired through the GC and the calculated volume of the reactor headspace, expansion vessel and the volume of intermittent piping.
Refer to the '7.2.10 - R1 Batch Operation - Single Reactor Batch operation.xlsx' checklist when operating the system for verification.

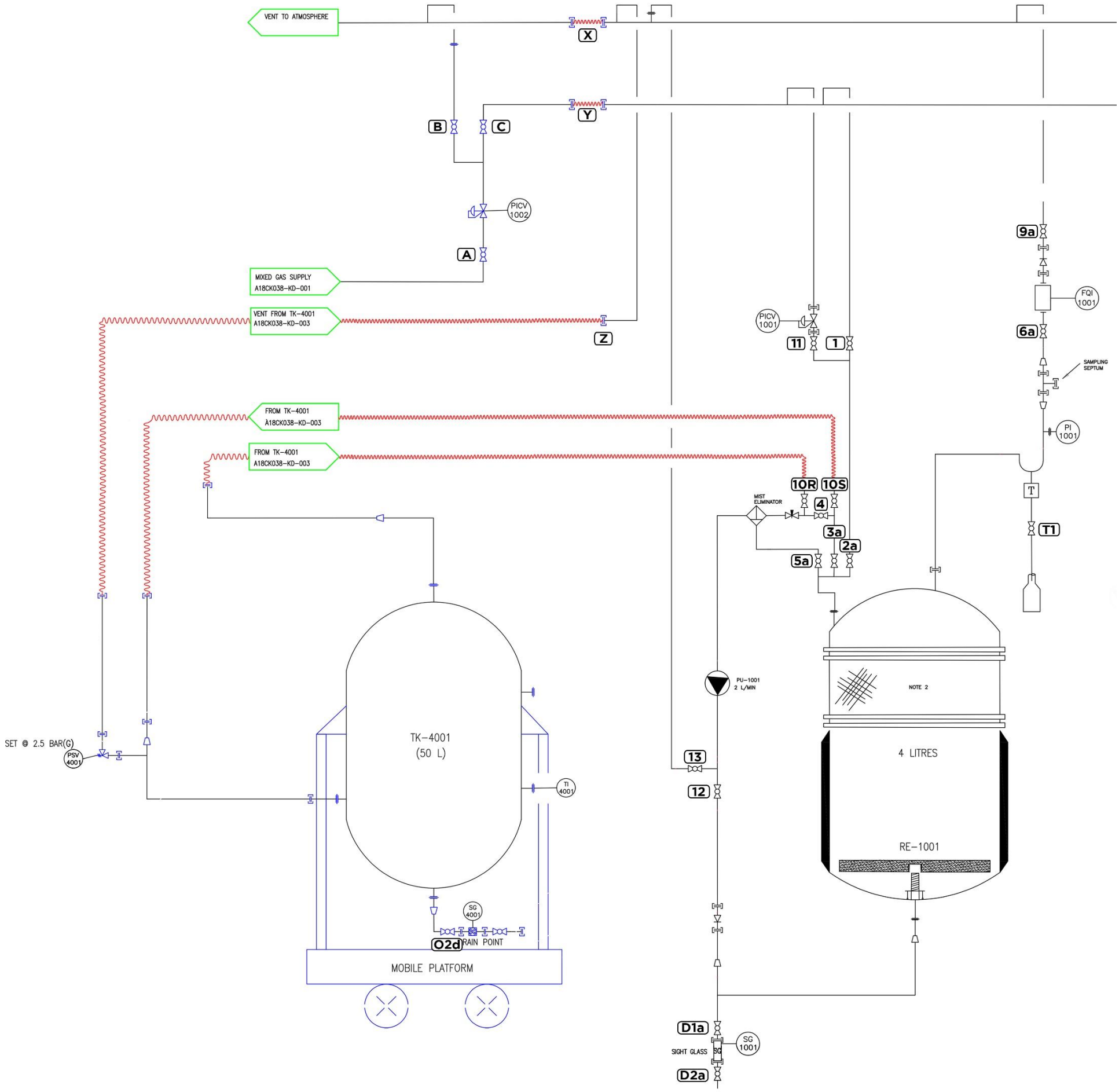


Figure 13: Final valve arrangement for R1 Batch system set up (non-essential lines excluded).

7.2.12 R1 + R2 + R3 Batch Operation – Multiple Reactor Batch Operation

1. Ensure previous sections (7.2.1 to 7.2.10 inclusive) have been carried out before commencing the current section.
2. Ensure the reactor system is in the **'safe state'**.
3. For batch operation, ensure TK-4001 mobile expansion vessel is properly connected to the main system at valves 10S and 10R.
4. Ensure the gas lines have been purged and flushed as per section 7.2.10. Open valves 11 and 2_a.
5. Open valves $3_{a,b,c}$,$5_{a,b,c}$,$7_{a,b,c}$,$8_{a,b,c}$,10S,10R, 12 and 14.
6. The pump speed should be set to the desired circulation rate*.
   ** The limit of the diffuser and the pump should be determined and restricted to the lower of the two to ensure the longevity of the equipment.*
7. Ensure the gas pumps PU-1001, PU-2001 and PU-3001 are circulating gas. Ensure valves 1, $2_{a,b,c}$, $6_{a,b,c}$ and $9_{a,b,c}$ are closed.
8. Purge the manifold once more with N_2 as per section 7.2.8. Once done so, open valves MN_a and MN_b, MO, A, C and 11.
9. Ensure valves $D1_{a,b,c,d}$ are open to allow for the capture of condensate in the gas lines. Check valves T1, T2 and T3 for any condensate build-up in the lines leading away from the reactors. Caution must be taken in losing volumes of gas due to these checks, in batch scenarios.

The three-reactor recirculating batch system is now set up to operate until the operators decide to stop it. Figure 14 shows the final flow arrangement of the system.

Note: Due to the nature of the system, reliably measuring gas volume in the system is not possible in batch operation. The rigid walls mean gas will need to be calculated from the gas composition acquired through the GC and the calculated volume of the reactor headspace, expansion vessel and the volume of intermittent piping.

Refer to the '7.2.11 - R1 + R2 + R3 Batch Operation - Multiple Reactor Batch operation.xlsx' checklist when operating the system for verification.

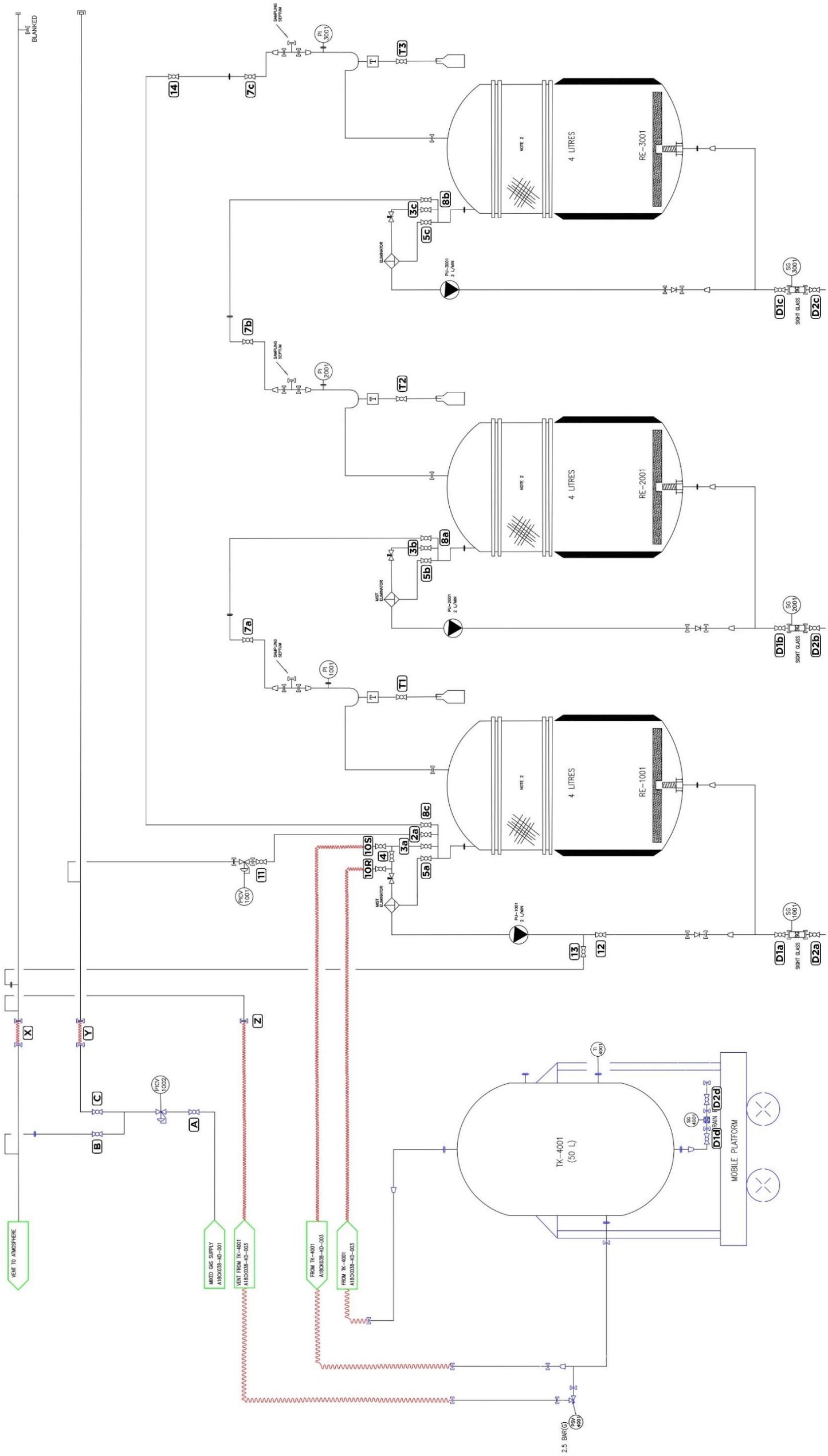


Figure 14: Final valve arrangement for R1,2,3 Batch system set up (non-essential lines excluded).

7.2.13 R1, R2 or R3 Continuous Operation

1. Ensure previous sections (7.2.1 to 7.2.10 inclusive, except 7.2.3 as the expansion vessel is not required for continuous operation.) have been carried out before commencing continuous operation set-up.
2. Ensure the reactor system is in the '**safe state**'.
3. After a total system purge and flush (section 7.2.10), decide which reactor will be run for the experiment; R1 (valves denoted with a subscript - a), R2 (valves denoted with a subscript - b) or R3 (valves denoted with a subscript - c).
4. Ensure valves 1, 2, 3, 4, 5, 6, 9 and 12 (of the chosen reactor – a [Figure 15], b [Figure 16] or c [Figure 17]) are open for the working gases (H_2, CO_2, CH_4) to allow the working gas mixture to flow through the BHM system.
   Note: Valves 1, 4 and 12 are only found on the Reactor 1 system.
5. Ensure valves D1,2 or 3 are open to allow for the capture of condensate in the gas lines. Check valves T1, T2 or T3 for any condensate build-up in the lines leading away from the reactors. Caution must be taken in losing volumes of gas due to these checks.
6. Once confirmed, refer to section 7.2.9 to prepare the gas mixture for the system gas supply.
7. Once the working gas mixture is prepared, close valve B and open valve C to let the working gas mixture flow into the BHM skid. Monitor the reactor flushing for several minutes to ensure consistent gas flow (observe flow regulators).
8. At this stage, pump PU-1001 speed should be set to the desired circulation rate*.
   **The limit of the diffuser and the pump should be determined and restricted to the lower of the two to ensure the longevity of the equipment.*
9. Once the system has been purged and flushed, ensure valves C, A, MO, MC, MH and MM remain open (

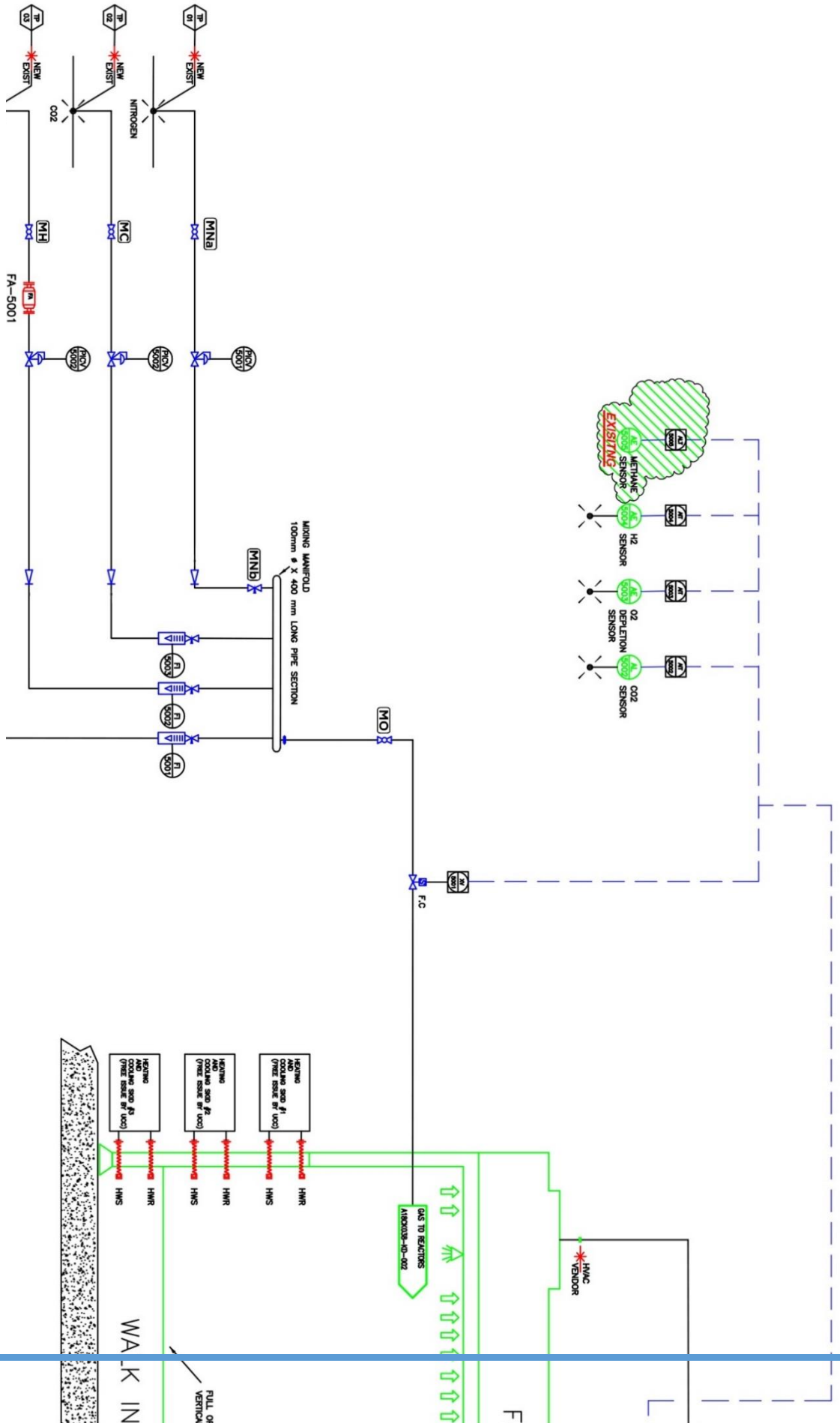


Figure 12: Gas supply and Manifold P&ID as per A18CK038-KD-001.

10.).

The single reactor continuous system is now set up to operate until the operators decide to stop it. Figure 15 shows the final flow arrangement of the system.
Note: For depiction, Reactor R1 is seen in Figure 15*; Reactor R2 in* Figure 16 *and Reactor R3 in* Figure 17*.*
Refer to the '7.2.12 - R1, R2 or R3 Continuous Operation.xlsx' checklist when operating the system for verification.

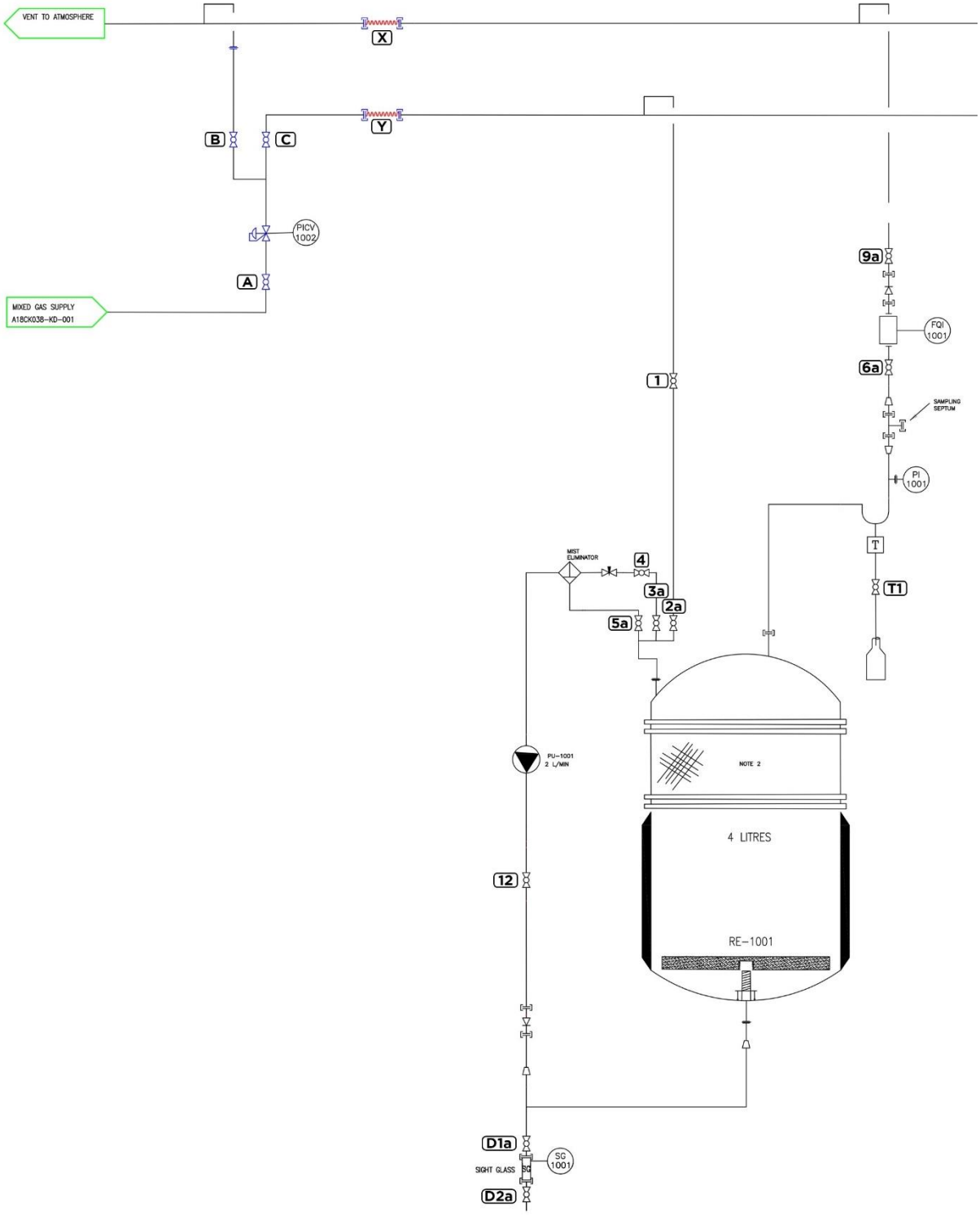


Figure 15: Final valve arrangement for R1 continuous reactor system set-up (non-essential lines excluded).

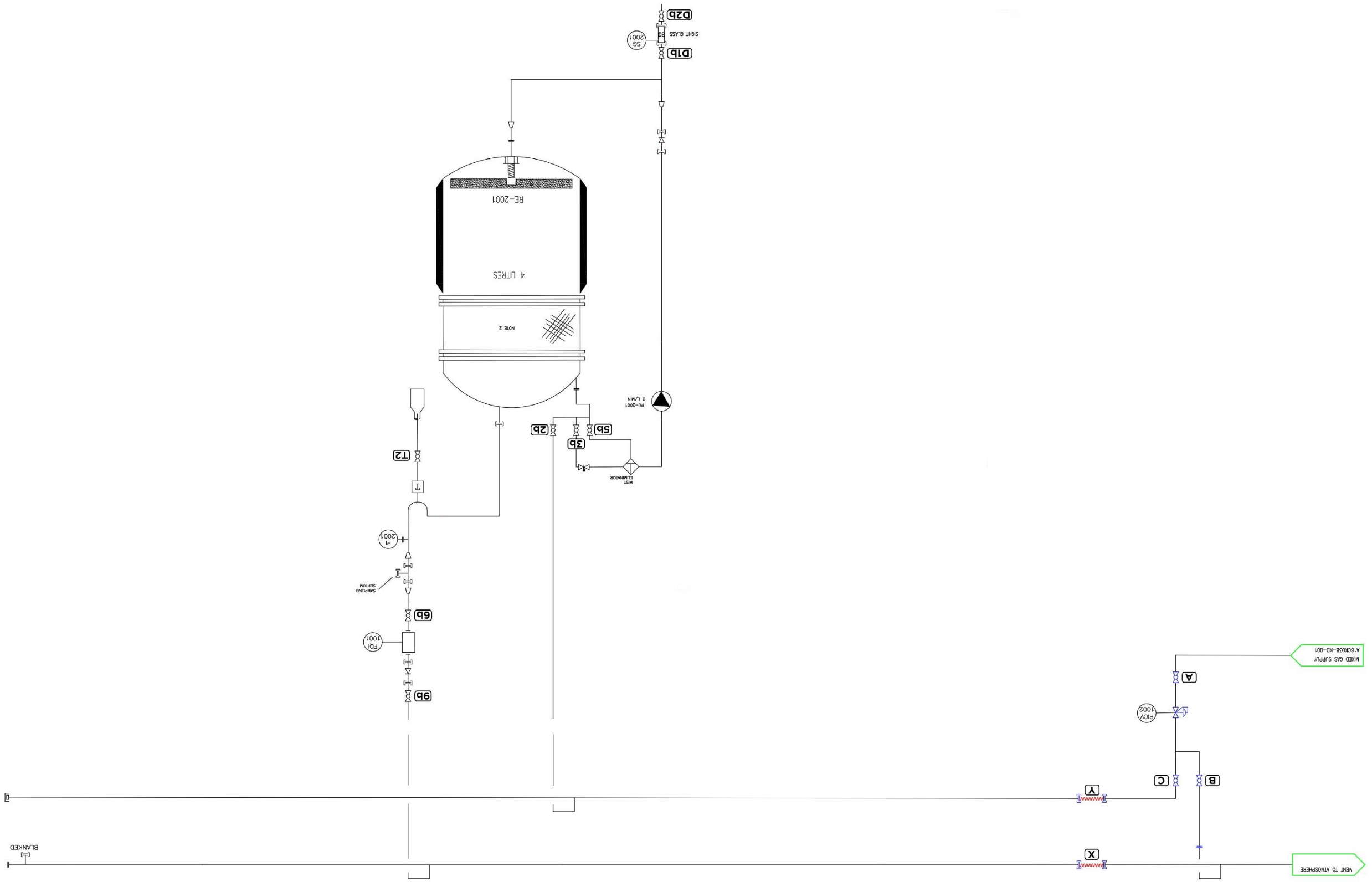
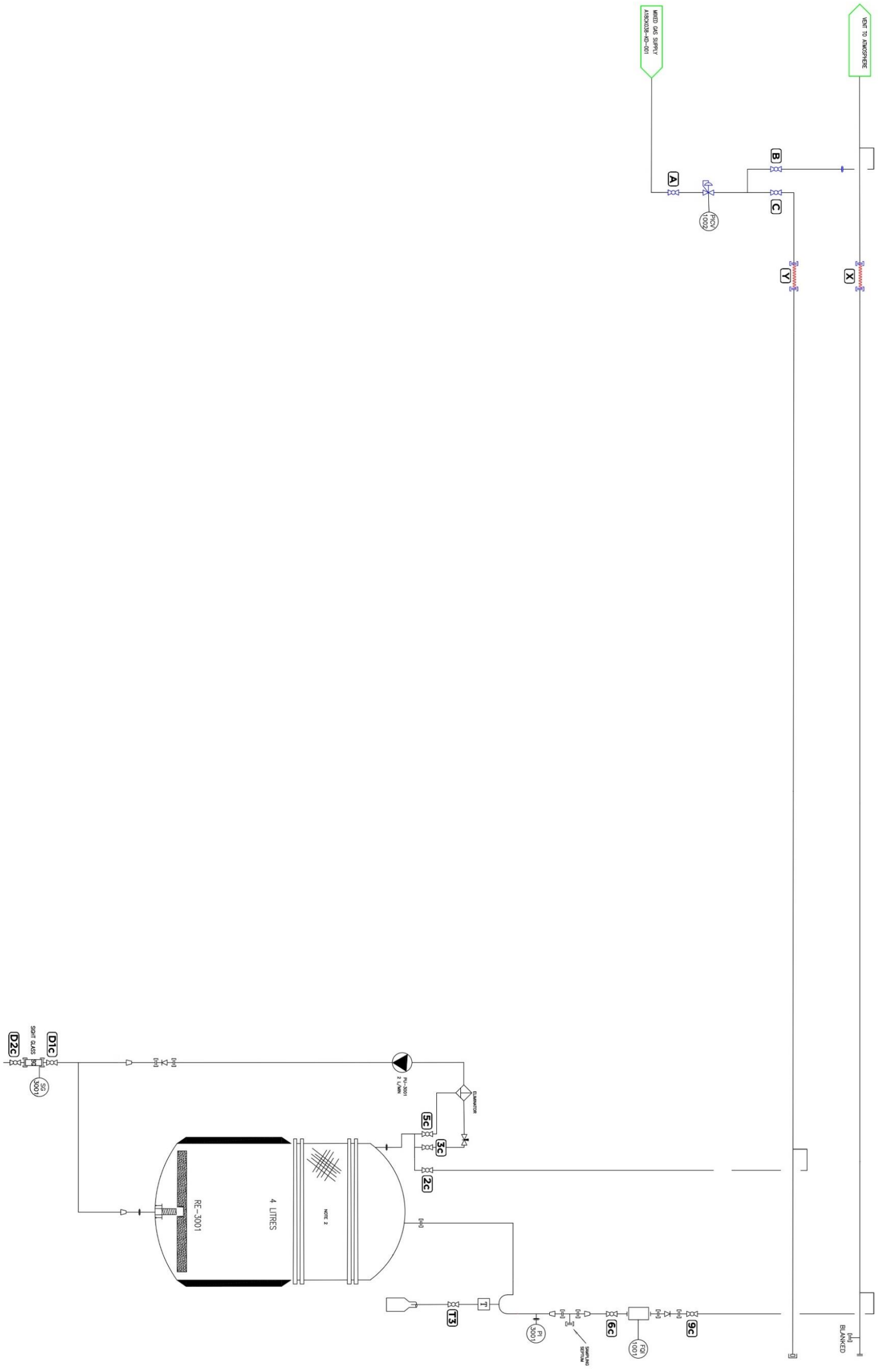


Figure 16: Final valve arrangement for R2 continuous reactor system set-up (non-essential lines excluded).

Figure 17: Final valve arrangement for R3 continuous reactor system set-up (non-essential lines excluded).



7.2.14 R1 & R2 In-series

1. Ensure previous sections (7.2.1 to 7.2.10 inclusive, except 7.2.3 as the expansion vessel is not required for continuous operation.) have been carried out before commencing continuous operation set-up.
2. Ensure the reactor system is in the '**safe state**'.
3. Ensure valves 1, 2_a, $3_{a,b}$, 4, $5_{a,b}$, 7_a, 8_a, 6_b, 9_b and 12 are open for the working gases.
   Note: Valves 1, 4 and 12 are only found on the Reactor 1 system.
4. Ensure valves $D1_{a,b}$ are open to allow for the capture of condensate in the gas lines. Check valves T1 and T2 for any condensate build-up in the lines leading away from the reactors. Caution must be taken in losing volumes of gas due to these checks.
5. Once confirmed, refer to section 7.2.9 to prepare the gas mixture for the system gas supply.
6. Once the mixed working gas has been prepared, close valve B and open valve C to let the mixture into the system. Monitor the gas flow for several minutes to ensure consistent flow (observe flow regulators).
7. At this stage, pumps PU-1001 and PU-1002 speeds should be set to the desired circulation rates*.
   ** The limit of the diffuser and the pump should be determined and restricted to the lower of the two to ensure the longevity of the equipment.*
8. Once the system has been purged and flushed, ensure valves C, A, MO, MC, MH and MM remain open (

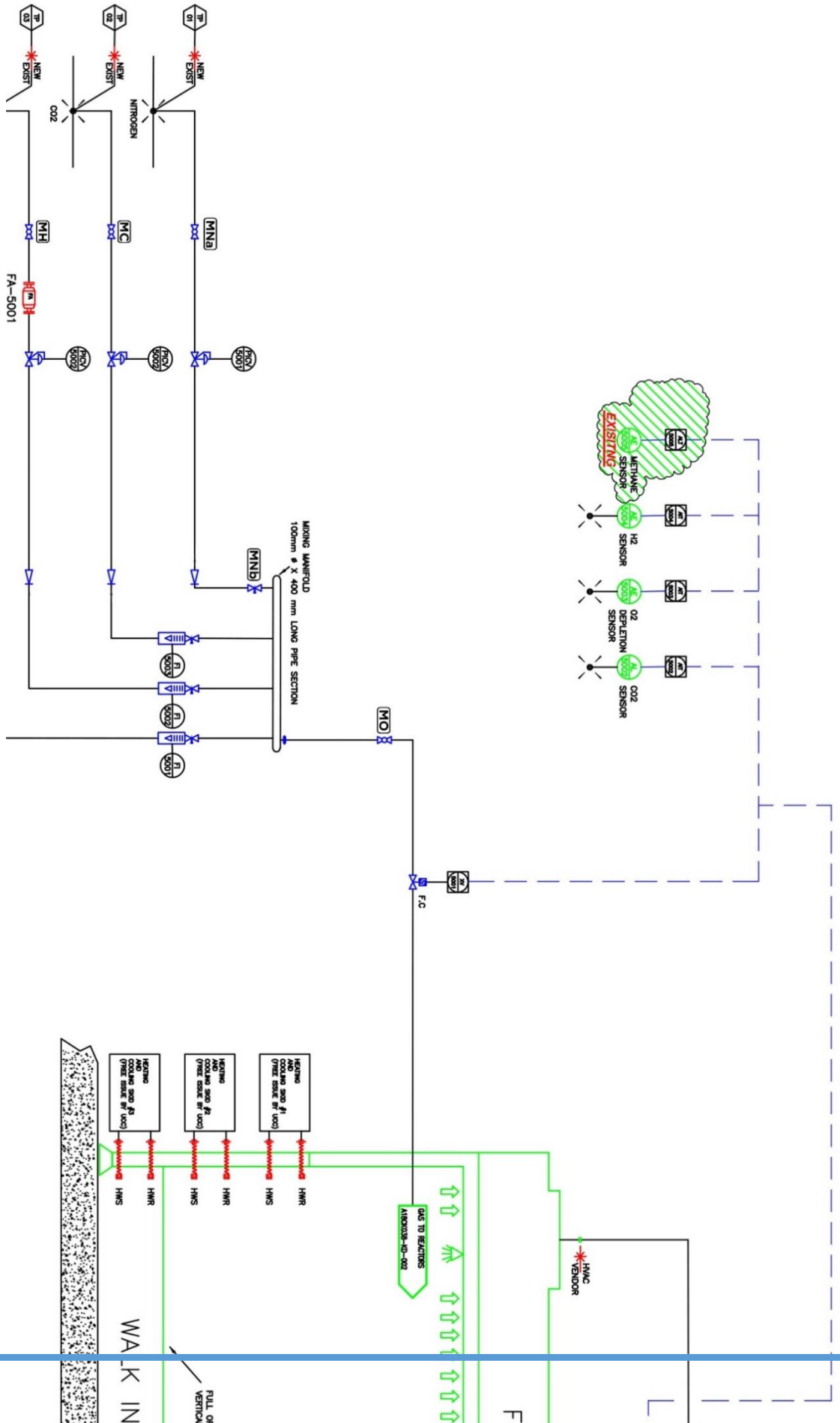


Figure 12: Gas supply and Manifold P&ID as per A18CK038-KD-001.

9.).

The R1 and R2, two-reactor continuous in-series system is now set up to operate until the operators decide to stop it. Figure 18 shows the final flow arrangement of the system.

Refer to the '7.2.13 - R1 & R2 In-series.xlsx' checklist when operating the system for verification.

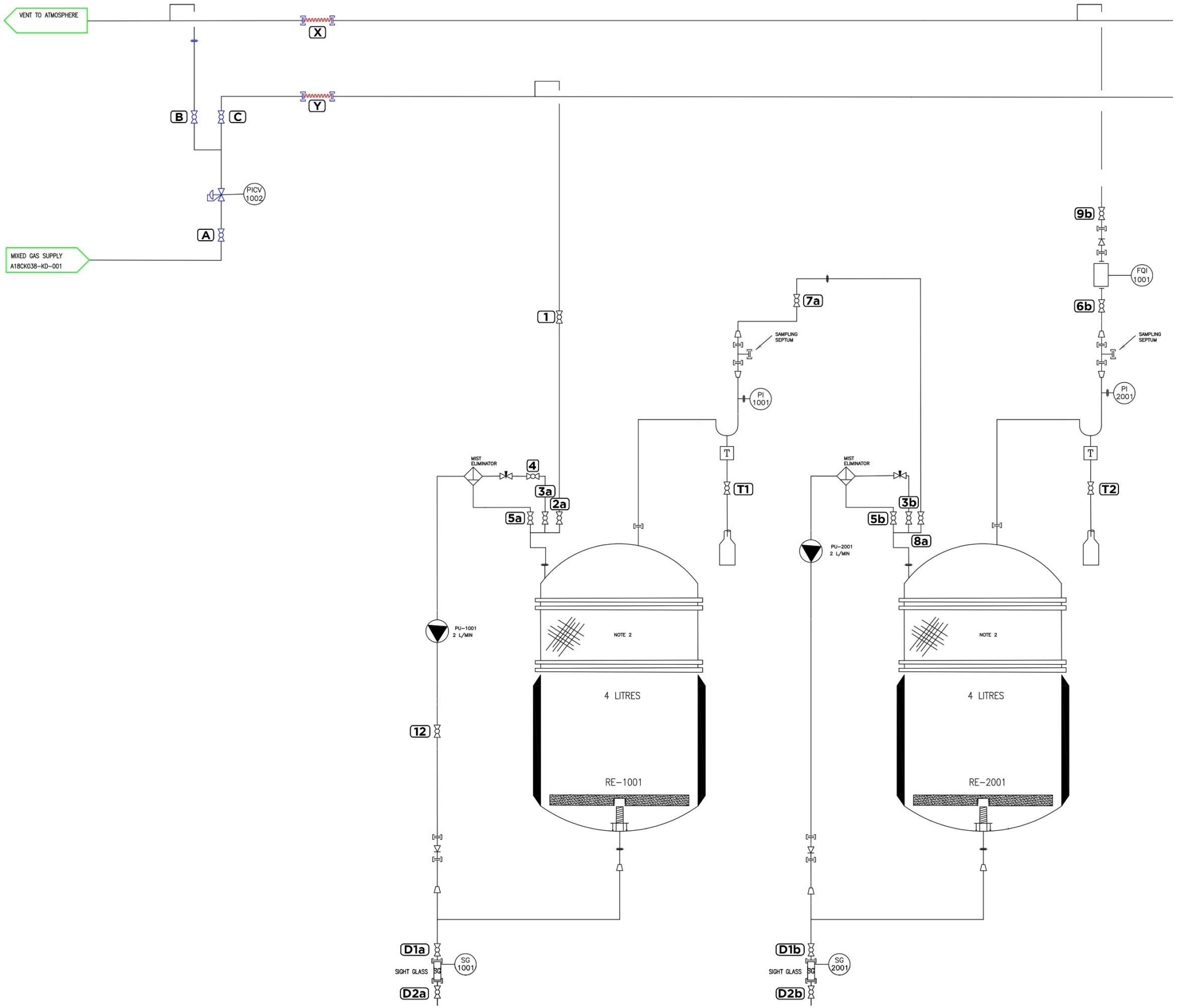


Figure 18: Final valve arrangement for R1 & 2 continuous in-series reactor system set-up (non-essential lines excluded).

7.2.15 R2 & R3 In-series

1. Ensure previous sections (7.2.1 to 7.2.10 inclusive, except 7.2.3 as the expansion vessel is not required for continuous operation.) are carried out before commencing continuous operation set-up.
2. Ensure the reactor system is in the '**safe state**'.
3. Ensure valves 2_b, $3_{b,c}$, $5_{b,c}$, 7_b, 8_b, 6_c, and 9_c are open for the working gases.
   Note: Valves 1, 4 and 12 are found on the Reactor 1 system.
4. Ensure valves $D1_{b,c}$ are open to allow for the capture of condensate in the gas lines. Check valves T2 and T3 for any condensate build-up in the lines leading away from the reactors. Caution must be taken in losing volumes of gas due to these checks.
5. Once confirmed, refer to section 7.2.9 to prepare the gas mixture for the system gas supply.
6. Once the working gas mixture has been prepared, close valve B and open valve C to let the mixture into the system. Monitor the reactor flushing for several minutes to ensure consistent gas flow (observe flow regulators).
7. At this stage, pumps PU-1002 and PU-1003 speeds should be set to the desired circulation rates*.
   ** The limit of the diffuser and the pump should be determined and restricted to the lower of the two to ensure the longevity of the equipment.*
8. Once the system has been purged and flushed, ensure valves C, A, MO, MC, MH and MM remain open (

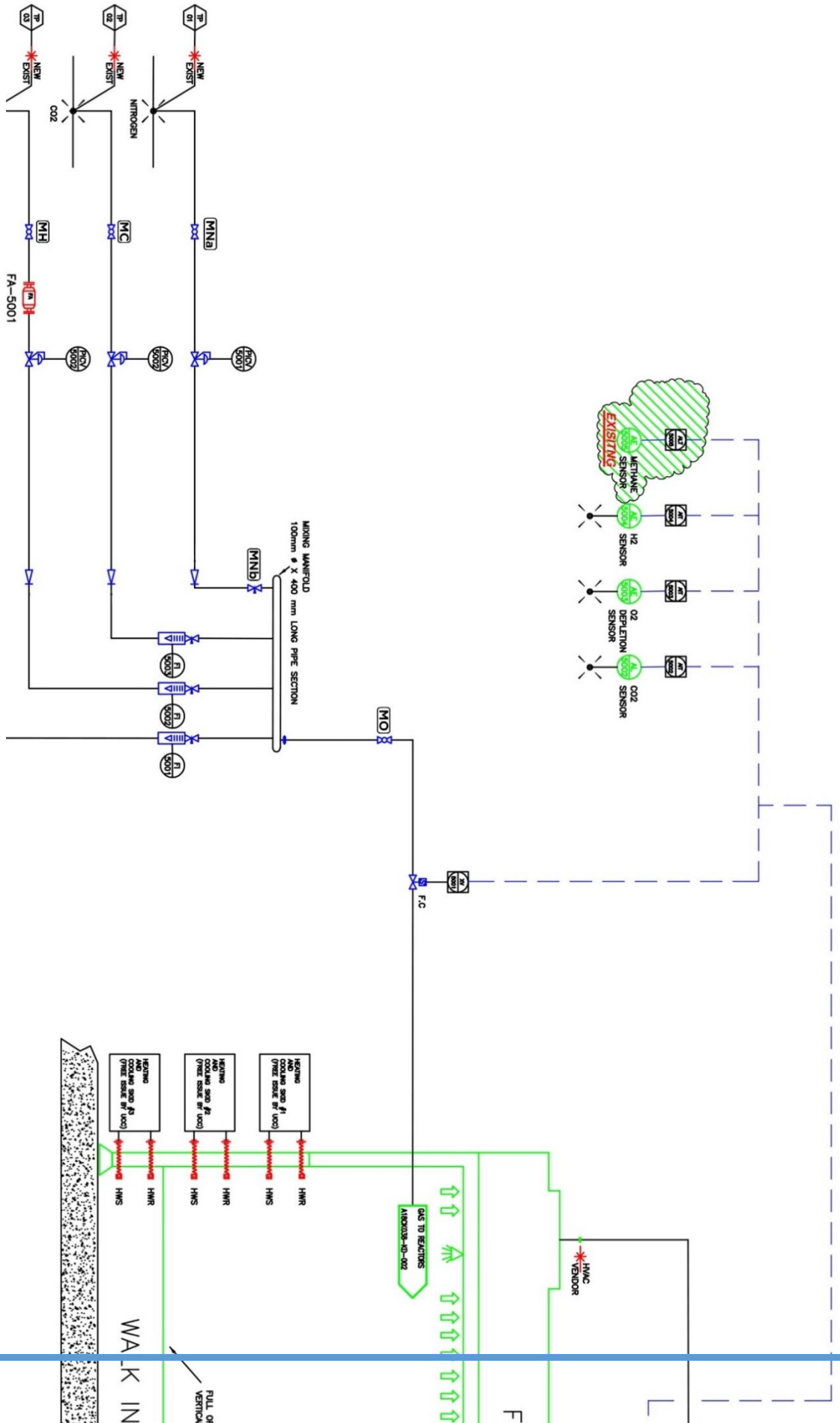


Figure 12: Gas supply and Manifold P&ID as per A18CK038-KD-001.

9.).

The R2 and R3, two-reactor continuous in-series system is now set up to operate until the operators decide to stop it. Figure 19 shows the final flow arrangement of the system.

Refer to the '7.2.14 - R2 & R3 In-series.xlsx' checklist when operating the system for verification.

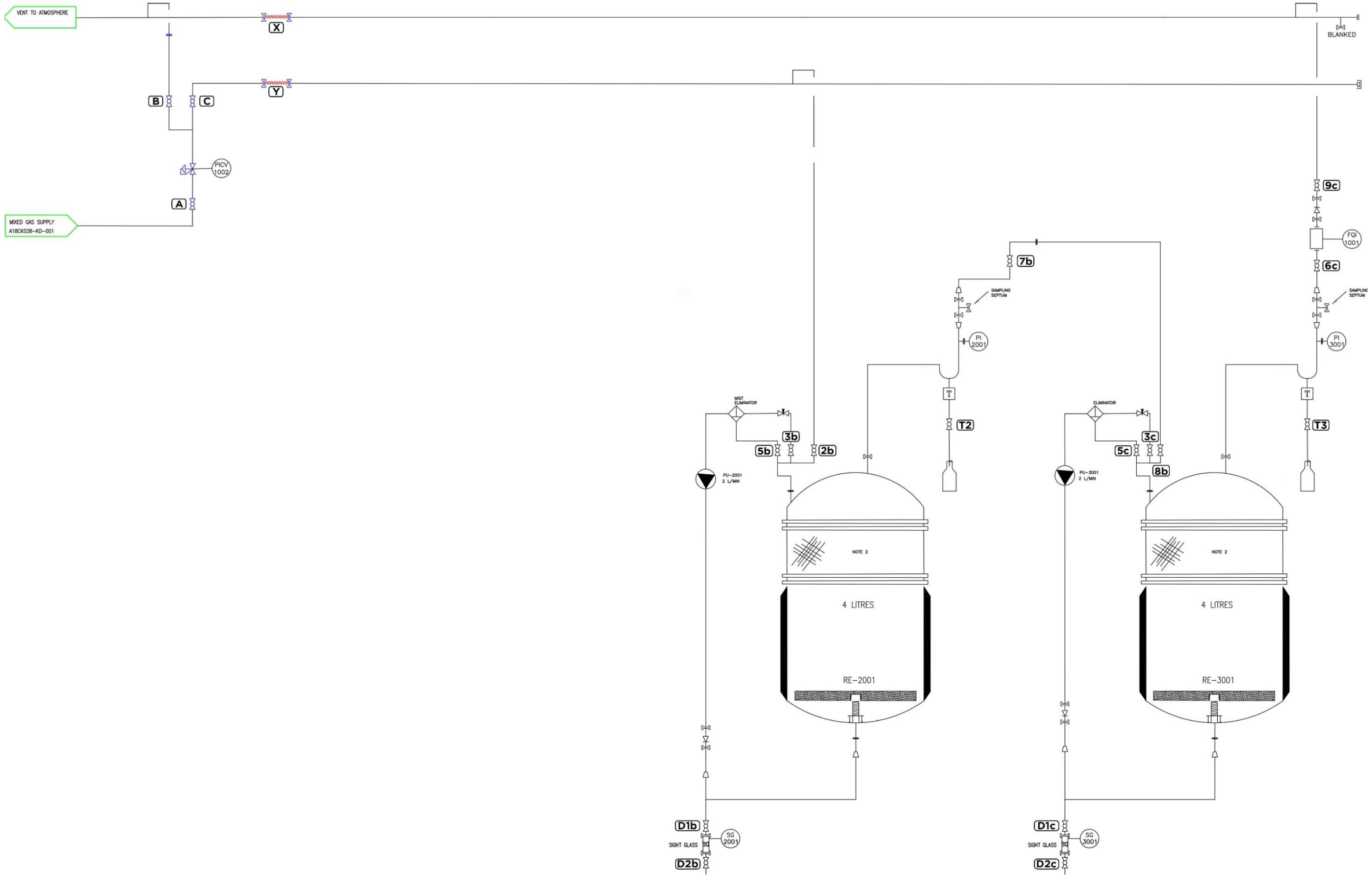


Figure 19: Final valve arrangement for R2 & 3 continuous in-series reactor system set-up (non-essential lines excluded).

7.2.16 R3 & R1 In-series

1. Ensure previous sections (7.2.1 to 7.2.10 inclusive, except 7.2.3 as the expansion vessel is not required for continuous operation.) have been carried out before commencing continuous operation set-up.
2. Ensure the reactor system is in the '**safe state**'.
3. Ensure valves 2_c, $3_{a,c}$, 4, $5_{a,c}$, 7_c, 8_c, 6_a, 9_a, 12 and 14 are open for the working gases.
   Note: Valves 1, 4 and 12 are only found on the Reactor 1 system.
4. Ensure valves $D1_{a,c}$ are open to allow for the capture of condensate in the gas lines. Check valves T1 and T3 for any condensate build-up in the lines leading away from the reactors. Caution must be taken in losing volumes of gas due to these checks.
5. Once confirmed, refer to section 7.2.9 to prepare the gas mixture for the system gas supply.
6. Once the working gas mixture has been prepared, close valve B and open valve C to let the mixture into the system. Monitor the reactor flushing for several minutes to ensure consistent gas flow (observe flow regulators).
7. At this stage, pumps PU-1001 and PU-1003 speeds should be set to the desired circulation rates*.
   ** The limit of the diffuser and the pump should be determined and restricted to the lower of the two to ensure the longevity of the equipment.*
8. Once the system has been purged and flushed, ensure valves C, A, MO, MC, MH and MM remain open (

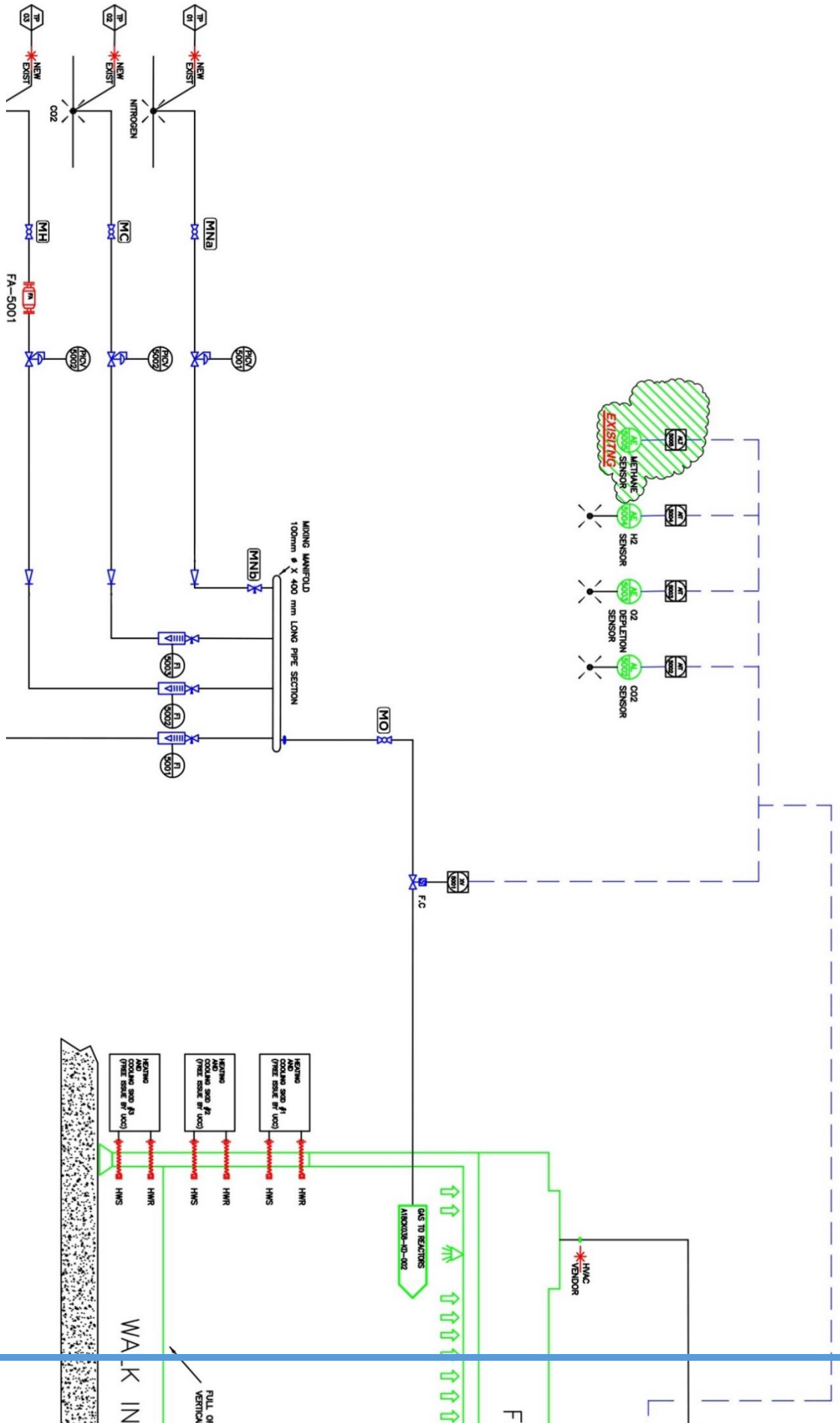


Figure 12: Gas supply and Manifold P&ID as per A18CK038-KD-001.

9.).

The R3 and R1, two-reactor continuous in-series system is now set up to operate until the operators decide to stop it. Figure 20 shows the final flow arrangement of the system.

Refer to the '7.2.15 - R3 & R1 In-series.xlsx' checklist when operating the system for verification.

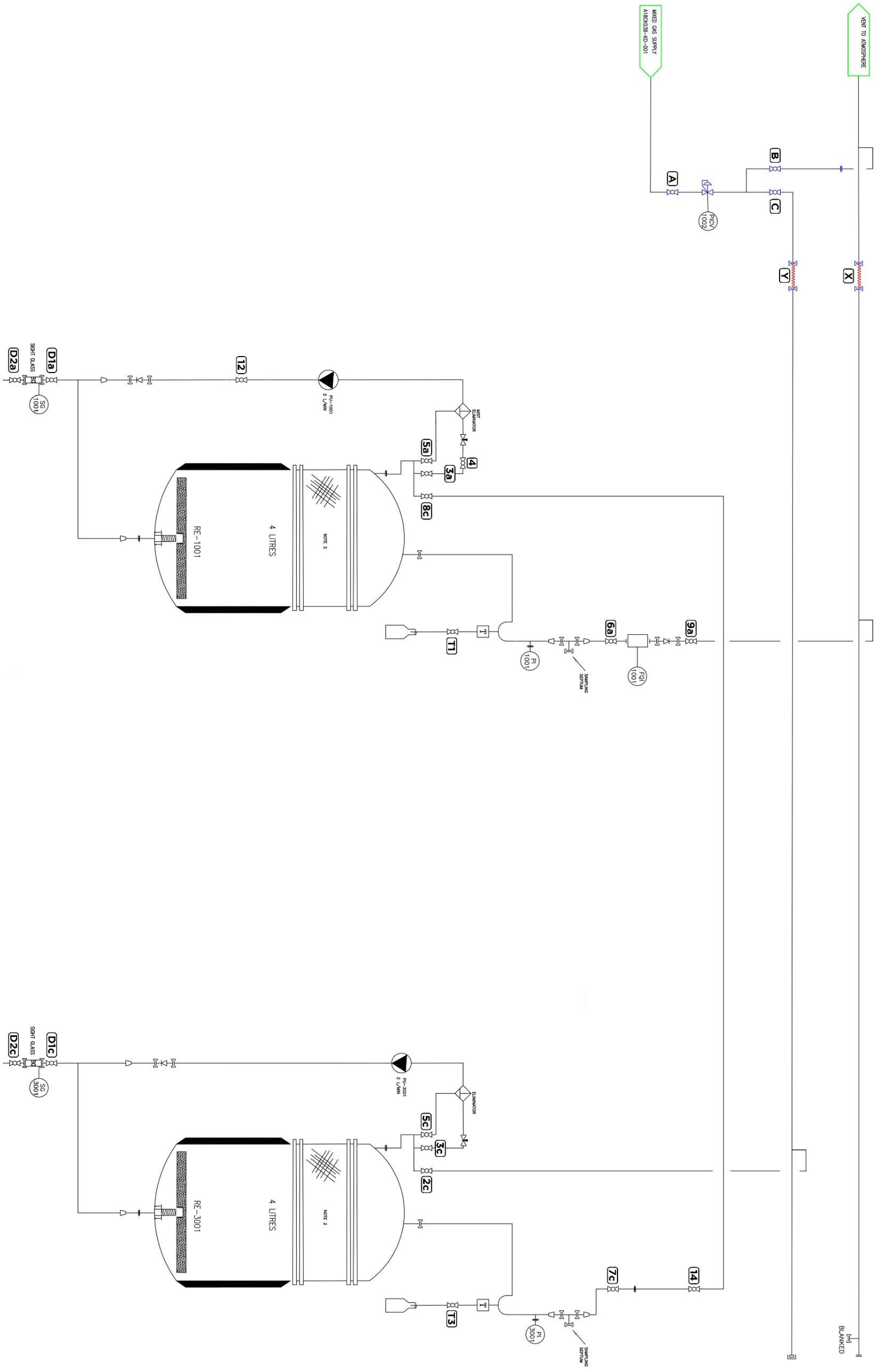


Figure 20: Final valve arrangement for R3 & 1 continuous in-series reactor system set-up (non-essential lines excluded).

7.2.17 R1, R2, R3 In-series

1. Ensure previous sections (7.2.1 to 7.2.10 inclusive, except 7.2.3 as the expansion vessel is not required for continuous operation.) have been carried out before commencing continuous operation set-up.

2. Ensure the reactor system is in the '**safe state**'.

3. Ensure valves 1, $2_{a,b,c}$, $3_{a,b,c}$, 4, $5_{a,b,c}$, $7_{a,b}$, $8_{a,b}$, 6_{c}, 9_{c}, and 12 are open for the working gases.
   Note: Valves 1, 4 and 12 are only found on the Reactor 1 system.

4. Ensure valves $D1_{a,b,c}$ are open to allow for the capture of condensate in the gas lines. Check valves T1, T2 and T3 for any condensate build-up in the lines leading away from the reactors. Caution must be taken in losing volumes of gas due to these checks.

5. Once confirmed, refer to section 7.2.9 to prepare the gas mixture for the system gas supply.

6. Once the working gas mixture has been prepared, close valve B and open valve C to let the mixture into the system. Monitor the reactor flushing for several minutes to ensure consistent gas flow (observe flow regulators).

7. At this stage, pumps PU-1001 PU-1002 and PU-1003 speeds should be set to the desired circulation rates*.
   ** The limit of the diffuser and the pump should be determined and restricted to the lower of the two to ensure the longevity of the equipment.*

8. Once the system has been purged and flushed, ensure valves C, A, MO, MC, MH and MM remain open (

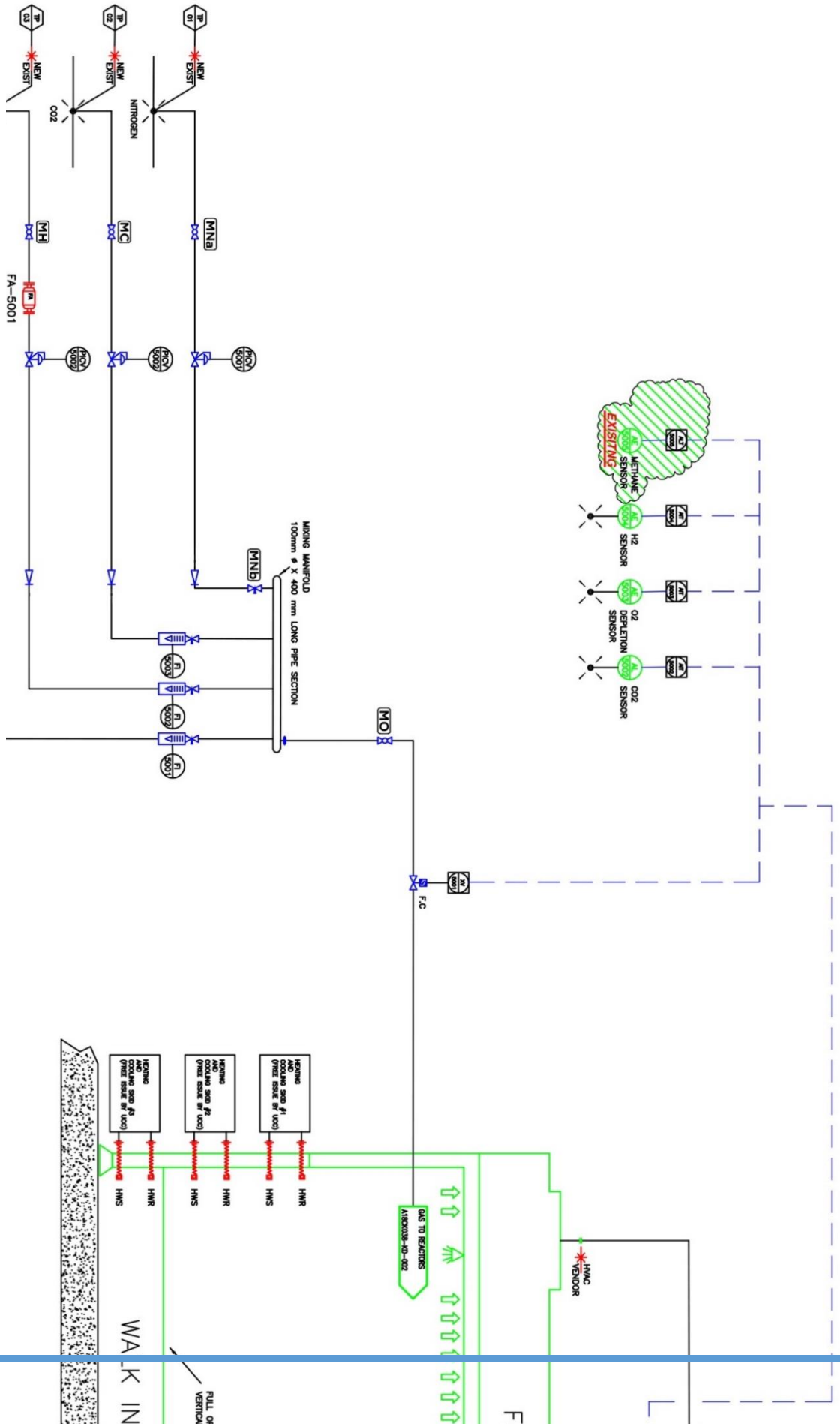


Figure 12: Gas supply and Manifold P&ID as per A18CK038-KD-001.

9.).

The three-reactor continuous in-series system is now set up to operate until the operators decide to stop it. Figure 21 shows the final flow arrangement of the system.

Refer to the '7.2.16 - R1, R2 & R3 In-series.xlsx' checklist when operating the system for verification.

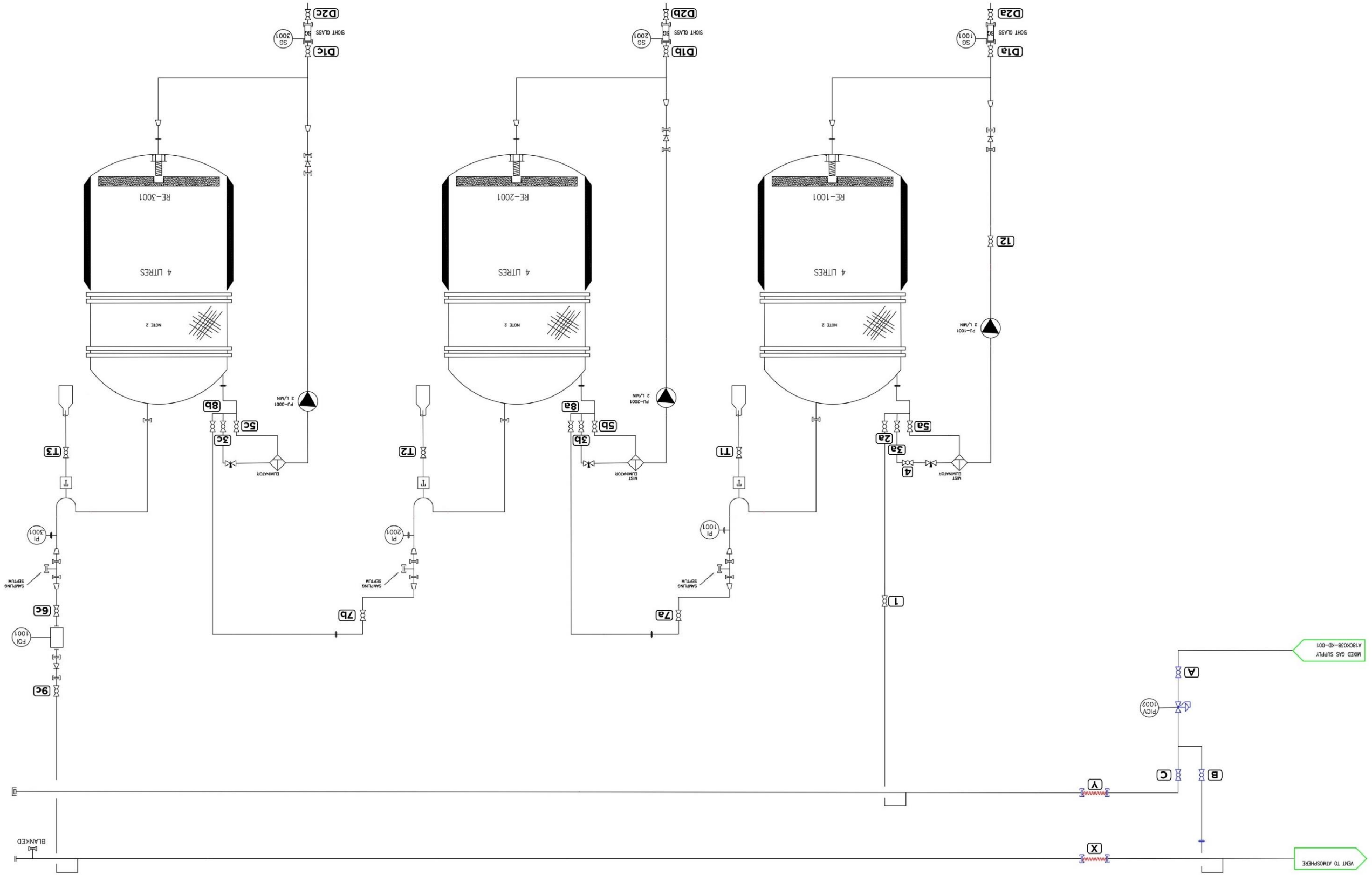


Figure 21: Final valve arrangement for continuous R1,2,3 in-series system set-up (non-essential lines excluded).

7.2.18 R1, R2, R3 Continuous Parallel

1. Ensure previous sections (7.2.1 to 7.2.10 inclusive, except 7.2.3 as the expansion vessel is not required for continuous operation.) have been carried out before commencing continuous operation set-up.

2. Ensure the reactor system is in the '**safe state**'.

3. Ensure valves 1, $2_{a,b,c}$, $3_{a,b,c}$, 4, $5_{a,b,c}$, $6_{a,b,c}$, $9_{a,b,c}$, and 12 are open for the working gases. *Note: Valves 1, 4 and 12 are found only on the Reactor 1 system.*

4. Ensure valves $D1_{a,b,c}$ are open to allow for the capture of condensate in the gas lines. Check valves T1, T2 and T3 for any condensate build-up in the lines leading away from the reactors. Caution must be taken in losing volumes of gas due to these checks.

5. Once confirmed, refer to section 7.2.9 to prepare the gas mixture for the system gas supply.

6. Once the working gas mixture has been prepared, close valve B and open valve C to let the mixture into the system. Monitor the reactor flushing for several minutes to ensure consistent gas flow (observe flow regulators).

7. At this stage, pumps PU-1001 PU-1002 and PU-1003 speeds should be set to the desired circulation rates*.
   ** The limit of the diffuser and the pump should be determined and restricted to the lower of the two to ensure the longevity of the equipment.*

8. Once the system has been purged and flushed, ensure valves C, A, MO, MC, MH and MM remain open (

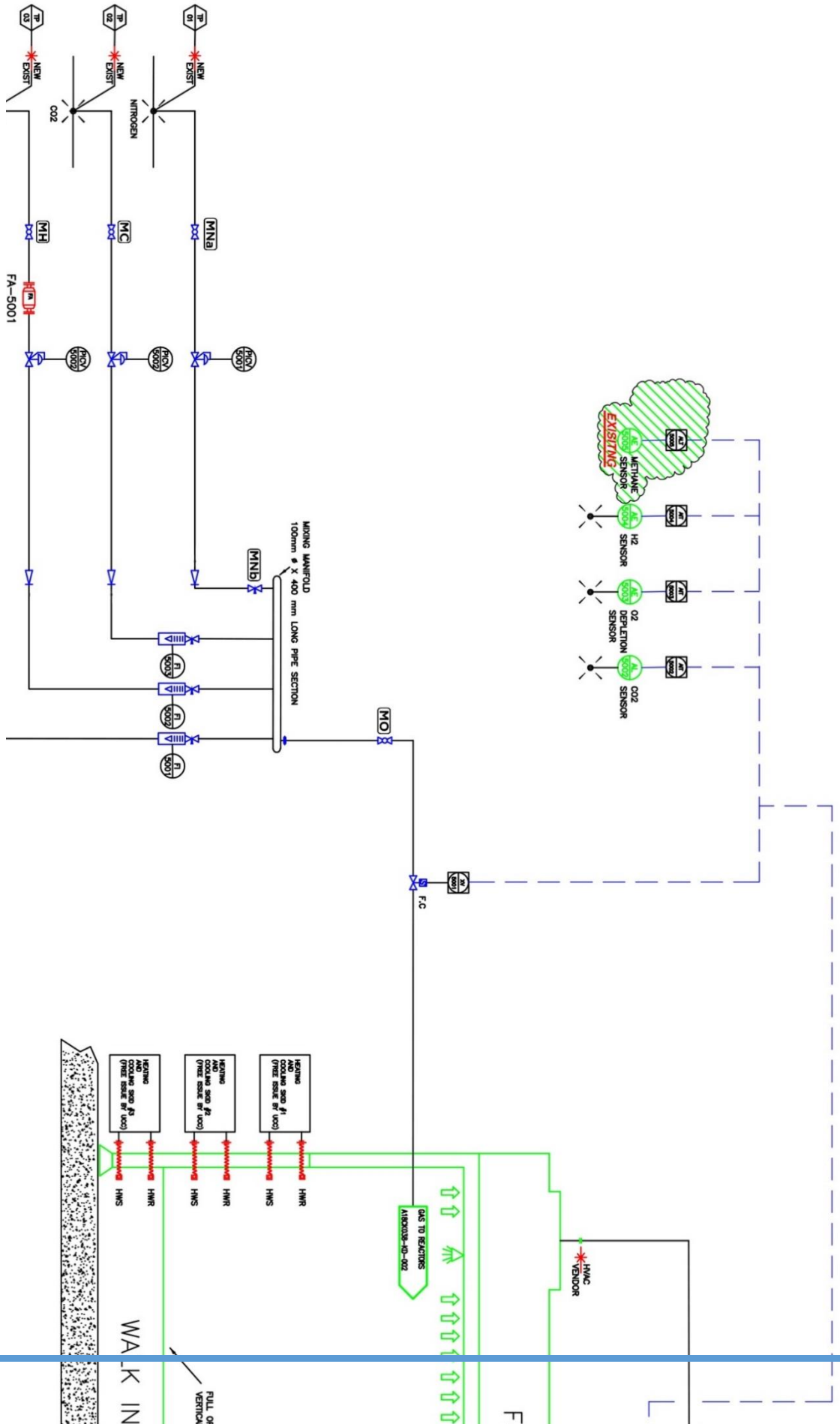
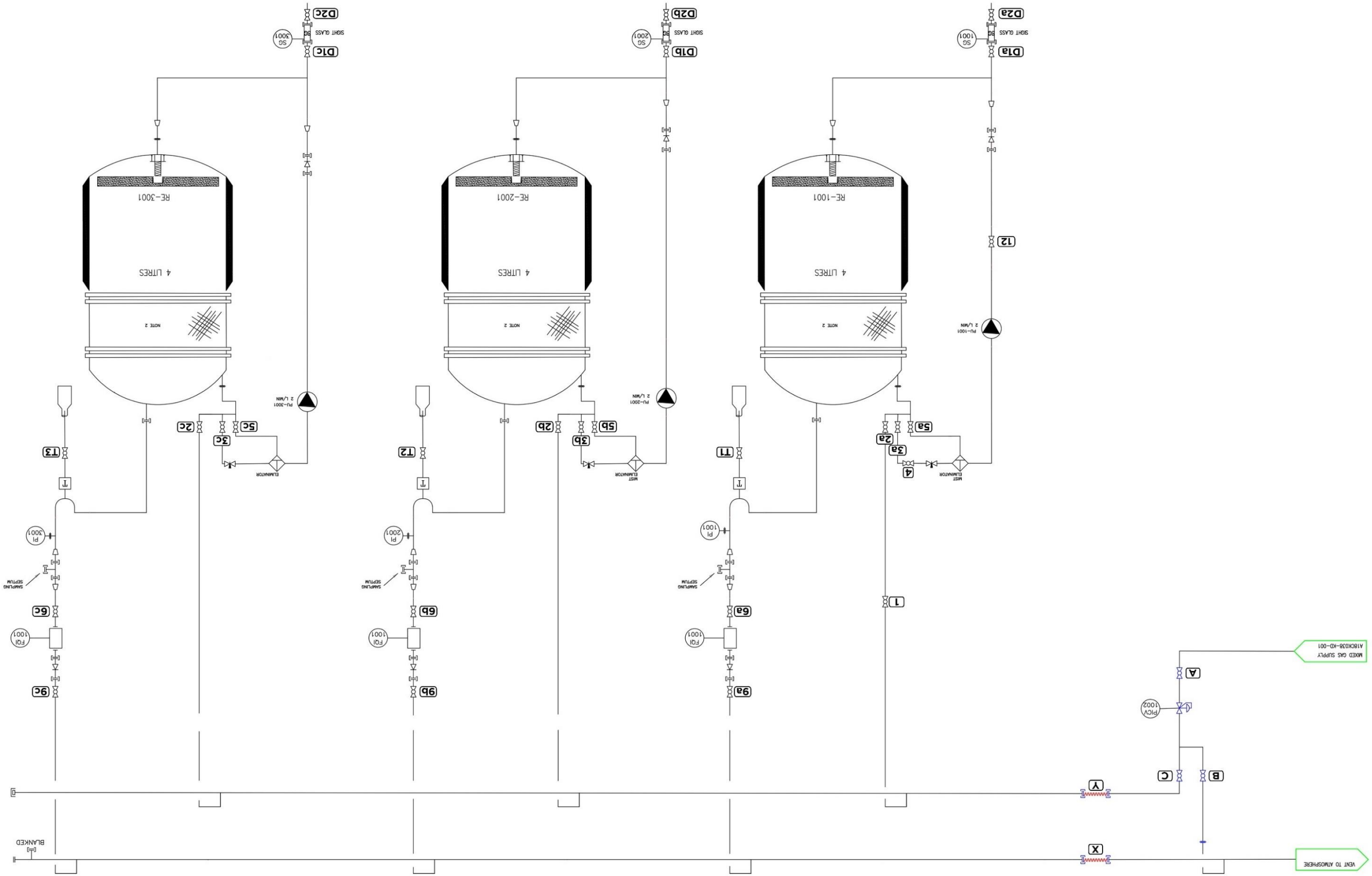


Figure 12: Gas supply and Manifold P&ID as per A18CK038-KD-001.

9.).

The three-reactor continuous parallel system is now set up to operate until the operators decide to stop it. Figure 22 shows the final flow arrangement of the system.
Refer to the '7.2.17 - R1, R2 & R3 Continuous Parallel.xlsx' checklist when operating the system for verification.

Figure 22: Final valve arrangement for continuous R1,2,3 parallel system set-up (non-essential lines excluded)



7.2.19 System reset

The gas supply can be turned off from the fume hood control panel by pressing the "Gas Off" button, or by turning off the fume hood extract fan by pressing the "Fan Off" button.
Additionally, the gas supply will be automatically shut off if any of the gas detectors within LG30 or within the fume hood detect a gas concentration of H_2, CH_4, O_2, or CO_2 outside of acceptable safe concentrations.
When the gas supply is shut off, either manually or automatically, the "MAP 50 Lock Out" button on the BHM rig control panel will illuminate. This will shut off the power supplied to the gas pumps on the BHM rig.

If the gas supply was shut off due to a deviation of gas concentration from safe levels, do not reset the system

1. Ensure that the fume hood fan is turned on
2. Ensure that the gas supply on the fume hood control panel is also turned off
3. Shut off the supply of H_2, CH_4, and CO_2 to LG30 from the gas bunkers external to the ERI.
4. Check the gas detection control panel outside of LG30 to assess which gas detector triggered the alarm.
5. If the gas detectors inside the fume hood triggered the alarm the probable cause is a leak of gas from the BHM rig.
6. If the gas detectors outside of the fume hood in LG30 triggered the alarm the probable cause is a leak of gas from the gas pipes.
7. As the fume hood extract fan is ventilating LG30 the gas concentration will eventually return to safe concentrations
8. The gas detection panel can now be reset.
9. Turn on the gas supply from the fume hood control panel
10. Reactivate the BHM rig control panel by pressing the "E Stop Activated / Reset" button.
11. Proceed to purge the manifold and BHM system with nitrogen gas to inert the system as per; *'Section 7.2.8 Manifold Purging'* and *'Section 7.2.10 Total System Purging and Flushing'.*
12. If the leak occurred along the gas pipes supplying the BHM rig contact buildings and estates to organise for an appropriate laboratory gas contractor to come to LG30 to repair the gas leak.
13. Once the system has been purged with nitrogen proceed to leak test the system using nitrogen gas as outlined in the section *"8.2.1 Leak Inspections: Nitrogen Leak"* and remedy any leaks found.
14. The supply of H_2, CH_4, and CO_2, can then be turned on in the gas bunker.
15. Ensure that the fume hood extract fan is turned on

Purge the gas manifold and BHM rig with nitrogen gas as per *'Section7.2.8 7.2.8 Manifold Purging'* and *'Section 7.2.10 Total System Purging and Flushing'*

16. Allow H_2 to flow into the BHM rig and allow the BHM rig to vent to the atmosphere

17. Proceed to leak test the BHM rig according to section '*8.2.2 Leak Inspections: Hydrogen and Methane Leaks'* and remedy any leaks found

7.2.19.1 System reset if fume hood fan was turned off

If the fume hood fan was turned off the following procedure must be followed to reactivate the gas supply and the BHM rig

1. Turn on the fume hood from the fume hood control panel. If the fume hood cannot be turned on stop immediately, open all windows in LG30 and contact buildings and estates immediately
2. If the fume hood can be turned on wait until the airflow on the fume hood control panel stabilises
3. The gas supply solenoids can then be opened by pressing the "Gas On" button on the fume hood control panel.
4. The BHM rig control panel can then be reset by pressing the "E Stop Activated / Reset" button
5. This will allow the user to turn on the gas pumps on the BHM rig again

7.2.19.2 System reset if gas supply was turned off via fume hood control panel

If the gas supply was shut off via the fume hood control panel by the operator, the following steps are to be followed to reactivate the gas supply and the BHM rig:

1. Turn on the fume hood extract fan
2. From the fume hood control panel, turn on the gas supply
3. There should be an audible "click" as the solenoid valves on the gas supply lines open
4. The BHM rig control panel can now be reset by pressing the "E Stop Activated / Reset" button.

7.2.20 Reactor output gas flow rate measurement

1. Ensure previous sections (7.2.1 to 7.2.10 inclusive and 7.2.17, except 7.2.3 as the expansion vessel is not required for continuous operation) have been carried out before measuring the reactor output gas flow rate.
2. Ensure the reactor system is in the '**safe state**'.
3. Ensure the three-reactor continuous in-series system is operated under the set sequence. For example, when the R1, R2 and R3 are running in series, the gas is flowing into R1 from the manifold, then from R1 into R2, then from R2 into R3, and then from R3 to the outlet.
4. Ensure valves $D1_{a,b,c}$ are open to allow for the capture of condensate in the gas lines. Check valves T1, T2 and T3 for any condensate build-up in the lines leading away from the reactors. Caution must be taken in losing volumes of gas due to these checks (7.5.2).

5. Ensure the gas flow rate is measured under reverse operating sequence. For example, the operating sequence is R1, R2 and R3, which means the gas is flowing into R1 from

the manifold, then from R1 into R2, then from R2 into R3, and then from R3 to the outlet. The gas flow rate of R3 must be measured first, then R2, and then R1.

6. At this stage, pumps PU-1001 PU-1002 and PU-1003 speeds should be set to the desired circulation rates*.
   ** The limit of the diffuser and the pump should be determined and restricted to the lower of the two to ensure the longevity of the equipment.*
7. Once all the above-mentioned steps are checked, the gas flow rate is ready to be measured. The measuring steps are shown as follows (the measuring sequence here is for R1, R2 or R3, with a,b,c corresponding to each reactor, respectively):

R1, 2 or 3 gas flow rate measurement

1. Raise the fume hood sash.
2. Check valve – T1, 2, or 3 (for R1, R2 or R3, respectively) and make sure the condensate has been discharged.
3. Connect T1, 2, or 3 (for R1, R2 or R3, respectively) with the extension tubing (silicon tubing; see Figure 23 and Figure 24 below).

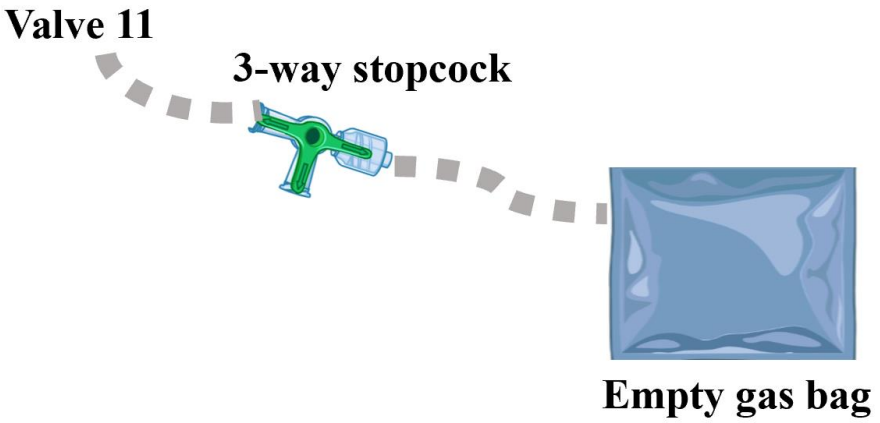


Figure 23: Gas flow measurement arrangement, comprising of an empty foil gas bag of approx. 2L volume (fully deflated), a 3-way stopcock valve and tubing. The empty gas bag is filled with the outflowing gas over a set time interval.

4. Connect an empty gas bag (2L in maximum) with the extension tubing using the 3-way stopcock which allows switching the flow direction (see the schematic diagram below).



Figure 24: Flexible silicon or tygon tubing and a simple timing device used during gas bag filling period.

5. Switch the 3-way stopcock to allow gas to flow into the fume hood.
6. Set the timer - 5 mins.
7. Close valve – $6_{a,b,c}$ (for R1, R2 or R3, respectively).
8. Close valve – $9_{a,b,c}$ (for R1, R2 or R3, respectively).
9. Open valve – T1, T2, or T3 (for R1, R2 or R3, respectively).
10. Switch the 3-way stopcock to allow gas to flow into the gas bag and click start of the timer simultaneously.
11. After 5 mins, switch the three-way stopcock valve to allow gas to flow into the fume hood.
12. Disconnect the full gas bag and reconnect a new empty gas bag (maximum 2L in volume) with the extension tubing.
13. Repeat steps 9 to 11 two additional times, you will have 3 gas bags filled in total.
14. Ensure the following when finished measuring the gas flow.
    a. Close valve – T1, T2, or T3 (for R1, R2 or R3, respectively).
    b. Open valve – $6_{a,b,c}$ (for R1, R2 or R3, respectively).
    c. Open valve - $9_{a,b,c}$ (for R1, R2 or R3, respectively).
15. Disconnect the extension tubing from the valve T1, T2, or T3 (for R1, R2 or R3, respectively).
16. Measure the gas volume in the three gas bags using a gastight syringe and record it in the data sheet (see the schematic diagram below) (Figure 25). Ensure that gas from the syringe is vented into the fume hood when emptying the syringe.
17. Close the fume hood sash.

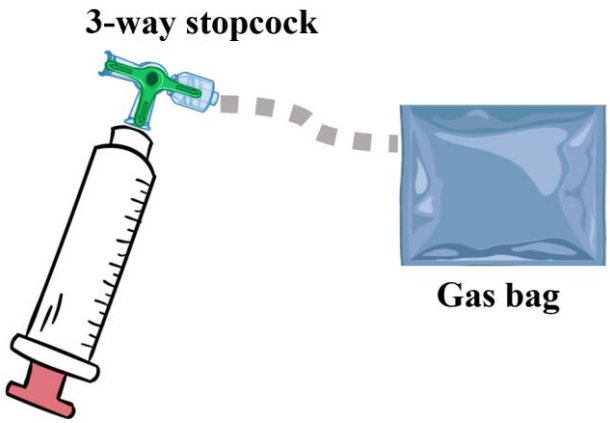


Figure 25: Connected gas tight syringe to the 3-way stopcock and filled gas bag. Syringe is filled and measured repeatedly until the gas bag is empty, giving an accurate volume over the timed period.

Resources & equipment required:

- 3 gas bags (2L in maximum)
- 1 300 mL syringe
- 1 3-way stopcock
- 1 timer

- 0.5 m silicon tubing
- PPE (lab coats, gloves, safety gloves and face masks).

Please note that the gas in the gas bag should be released in the fume hood during measurement!
Please be noted that the above-listed operating procedure is just for reactors run at atmosphere pressure (1atm)!
Refer to the '7.2.21 – Reactor output gas flow measurement.xlsx' checklist when measuring the flow rate for verification.

7.2.21 Input gas flow rate measurement

Ensure previous sections (7.2.1 to 7.2.9 inclusive and 7.2.17, except 7.2.3 as the expansion vessel is not required for continuous operation) have been carried out before measuring the input gas flow rate.

1. Ensure the reactor system is in the '**safe state**'.
2. Once confirmed, refer to "*Section 7.2.9 Mixed gas mixture*" for system gas preparation.
3. Once the working gas mixture has been prepared, close valve B and open valve C to allow the gas mixture to flow into the system. Monitor the reactor flushing for several minutes to ensure consistent gas flow (observe flow regulators FQI-XXXX).
4. Once a consistent gas flow has been achieved, the gas flow rate is ready to be measured. The measuring steps are shown as follows:
5. Raise the fume hood sash.
6. Connect the extension tubing to valve - 11(silicon tubing; see the picture below).
7. Connect the gas bag (2L in maximum) with the extension tubing using the 3-way stopcock which allows the flow direction to be switched (see the schematic diagram below).
8. Switch the 3-way stopcock to allow gas to flow into the fume hood.
9. Close valve - 2a.
10. Open valve – 11.
11. Set the timer to 2.5 mins.
12. Switch the 3-way stopcock to allow gas to flow into the gas bag and start the timer simultaneously.
13. Switch the three-way stopcock valve to allow gas to flow into the fume hood again.
14. Disconnect the full gas bag and reconnect a new empty gas bag (2L in maximum) with the tubing.
15. Repeat steps 5 to 7 two additional times. You will have a total of 3 full gas bags.
16. When finished measuring the gas flow ensure the following
    a. Close valve – 11.

b. Open valve – 2a.
c. Disconnect the extension tubing from the valve – 11.

17. Measure the gas volume in the three gas bags using the 300 mL syringe and record it in the data sheet (see the schematic diagram below). Ensure that gas from the syringe is vented into the fume hood when emptying the syringe.
18. Close the fume hood sash.

Resources and equipment required:

- 3 gas bags (2L in maximum)
- 1 300 mL syringe
- 1 3-way stopcock
- 1 timer
- 0.5 m silicon tubing
- PPE (lab coats, gloves, safety gloves and face masks).

Please note that the gas in the gas bag should be released in the fume hood during measurement!

Refer to the '7.2.19 - Input gas flow rate measurement.xlsx' checklist when measuring the flow rate for verification.

7.2.22 Intermittent gas supply

Intermittent gas supply is required when stimulating intermittent hydrogen supply. The periodic supply of H_2 and CO_2 to the BHM rig mimics intermittency in a variable renewable electricity scenario. The following steps need to be completed to arrange the system for intermittent gas supply.

1. Ensure previous sections (7.2.1 to 7.2.10 inclusive) have been carried out before commencing intermittent operation set-up.
2. Ensure the reactor system is in the '**safe state**'.
3. Once completed, turn off the gas pumps on the BHM rig control panel as per; "*Section 7.2.10 Fume hood operation and system start-up*".
4. Ensure that valves 1, $2_{a,b,c}$, $7_{a,b}$, $6_{a,b,c}$, $9_{a,b,c}$ are closed to isolate the BHM rig after total system purging and flushing.
5. After the standby period is assessed, the BHM rig is restarted according to the following steps:
6. Ensure that the condensate is emptied before restarting as per: "Section 7.5.2 Condensate traps".
7. Once completed, proceed to H_2 and CO_2 mixed gas preparation as per: "*Section 7.7.9 Mixed gas preparation*".
8. Proceed to purge the manifold and BHM system with the prepared gas mixture to inert the system as per; *'Section 7.2.8 Manifold Purging'* and *'Section 7.2.10 Total System Purging and Flushing'.*
9. Once completed, turn on the gas pumps on the BHM rig control panel as per: "*Section 7.2.10 Fume hood operation and system start-up*".
10. Proceed to set up and run R1, R2 and R3 In-series as per: "*Section 7.2.18 R1, R2 and R3 In-series*".

Refer to the '7.2.10 – Total System Purge & Flush.xlsx & 7.2.16 R1, R2 & R3 In-series.xlsx' checklist when purging and restarting the BHM rig.

7.3 Gas Sampling

When sampling gas, it is important to get a representative sample of the gases in the system. To get a gas sample, a 50ml gas syringe is required to take a sample.

To take a gas sample, the following steps need to be taken.

1. Use the gas syringe to pierce through one of the unused septa to insert the needle into the line and draw the required sample.
2. Draw and eject the contents of the syringe three times to ensure a good sample is taken.

3. Remove the needle once done so. Ensure the needle is capped to prevent any foreign gases from entering the syringe.
4. If the septum requires replacement, follow the sampling septum replacement section.



Figure 26: 50ml gas syringe and gas sampling port.

7.4 Gas chromatography

Refer to 'Agilent GC.docx' for a detailed step-by-step procedure on gas analysis.

7.5 General maintenance

7.5.1 Water bath

It is advised to regularly check for any leaks from the water baths and to also check the level of the water baths. If leaks are found, the water bath should be turned off and the leaks should immediately be fixed using an appropriate sealant (e.g. Tech 7).
Ensure that the water level of the water baths is always adequate. The water level can be topped up by removing the rubber cork from the reservoir and adding water to the reservoir. Check for any leaks along supply and return piping, weathering due to heat and mechanical wear.

7.5.2 Condensate traps

Condensate traps must be regularly checked and emptied. When emptying, it is necessary to close valve D1 ***FIRST***; otherwise, the pressure from the reactor will cause a discharge of the contents. When emptying, it is important to open the valves slowly to allow the chamber to depressurise slowly.

1. Make sure valve D1 is shut, place the condensate collection container at the outlet and slowly open valve D2.

2. Once the liquid has flowed into the container, shut valve D2.
3. Open valve D1.

7.5.3 Sampling septum replacement

The sampling septum (Figure 10) is comprised of seven small pores, allowing for seven uses before the sampling septum must be replaced.
To replace the sampling septum:

1. Shut off the pump circulation. Bring the reactor to the **'safe state'**.
2. Run section 7.2.10 to purge the system of working gases.
3. Bring the system to the **'safe state'**.
4. Unscrew the sampling port and remove the old sampling septum. (Label as spent)
5. Insert new septum. Ensure the port and septum are cleaned with an alcohol wipe and no residue is introduced to the reactor which may cause abrasions. Ensure the septum is fitted well and tightly in the port.
6. Screw back on the sampling port, checking to ensure a tight and correct seal is maintained.
7. Repeat section 7.2.8 for purging the reactor with N_2 to remove any possible oxygen that may have entered the system through the septum replacement process.
   Set the system to the appropriate operating set-up.



Figure 27: TruStream7, a seven-use sampling septum.

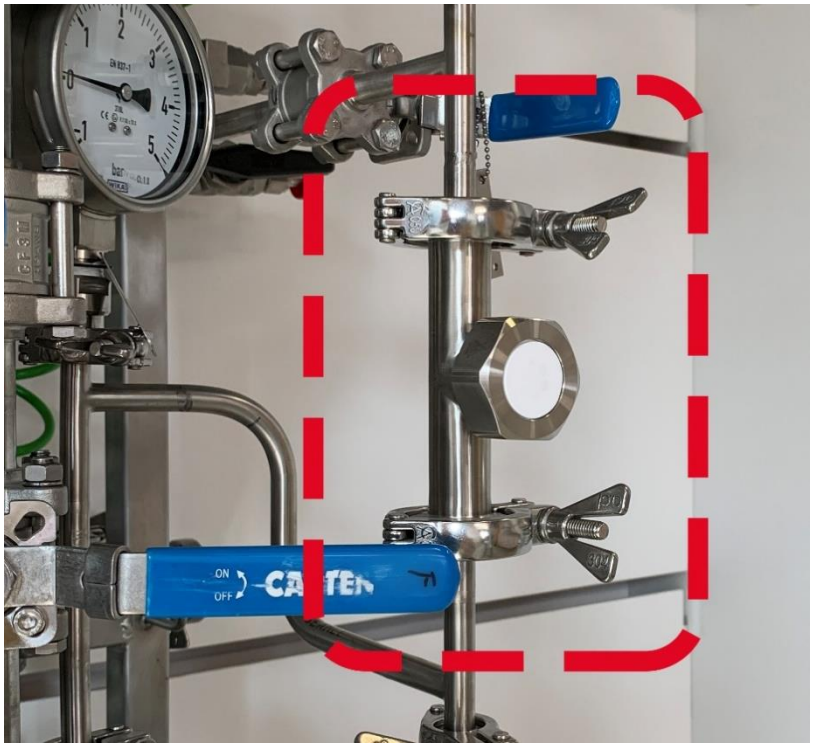


Figure 28: Gas Sampling port with sampling septum inserted located on the BHM rig. Above and below the sampling port are tri-clamps.

7.6 Liquid Substrate Sampling

To ensure a representative sample of the liquid substrate, a significant amount of liquor must be removed first. This is due to the clearance space below the diffuser, which creates a "dead" zone in the reactors for liquor to settle. This liquor, as a result, does not get the same interaction with the injected gas bubbles as the rest of the liquor in the reactor body.
As a result, the following steps need to be followed to allow for a representative sample to be acquired. Note that a,b,c refers to reactors 1,2 and 3, respectively.

1. Open valve $O1_{a,b,c}$. Allow the line between valves $O1_{a,b,c}$ and $O2_{a,b,c}$ to fill with reactor liquid contents.
2. Close valve $O1_{a,b,c}$.
3. Hold an adequately sized beaker to the outlet.
4. Slowly open valve $O2_{a,b,c}$, ensuring the chamber depressurises and slowly discharges the liquid into the sample beaker. The volume of the chamber is approximately (50 ml). Close valve $O2_{a,b,c}$.
5. Ensure both valves $F1_{a,b,c}$ and $F2_{a,b,c}$ are closed. Then slowly open valve $F1_{a,b,c}$.
6. Pour the liquid into the chamber and close valve F1.
7. Slowly open valve $F2_{a,b,c}$, allowing the chamber to pressurise and the liquid to drain into the reactor. Close valve $F2_{a,b,c}$.
8. Repeat steps 1-7 a total of four times to ensure that the reactor contents are well mixed.

9. To take a representative sample open valve $O1_{a,b,c}$. Allow the line between valves $O1_{a,b,c}$ and $O2_{a,b,c}$ to fill with reactor liquid contents.
10. Close valve $O1_{a,b,c}$.
11. Hold an adequately sized beaker to the outlet.
12. Slowly open valve $O2_{a,b,c}$, ensuring the chamber depressurises and slowly discharges the liquid into the sample beaker. The volume of the chamber is approximately (50 ml). Close valve $O2_{a,b,c}$.

7.7 Sample testing

Sample testing will vary across experiments. Tests for samples will depend on the researcher's data requirements. As tests are decided upon, the procedure should be described in this section under a separate heading.

7.7.1 pH

Testing for the pH is a simple process and can be carried out at the start of the sample testing.

1. Uncap the pH probe and rinse the probe down with distilled water over a wastewater beaker.
2. Gently pat down the probe with a clean tissue and place the probe in the substrate sample.
3. Gently stir the sample and press the "Record" button to take a reading of the sample, all while mixing the liquor, ensuring a homogeneous solution.
4. Keep stirring until the device lets out noise and the pH reading no longer changes.
5. Record pH.
6. Wash the probe once again and gently pat it down.
7. If using again, place the probe in the next sample and repeat the steps. Otherwise, replace the cap with the pH buffer (Fill up if required) and turn off the device.

7.8 Reactor feeding

Reactor feeding under pressurised conditions will be limited to low-viscosity nutrient solutions. This is due to the airlock system provided by valves $F1_{a,b,c}$ and $F2_{a,b,c}$ which prevent the addition of high-viscosity feedstock to be pushed into the reactor.
Additionally, feed which contains a high solids content should not be used as solid particles could settle below the diffuser and clog outlets.
The reactor feeding should be carried out in the following steps. Ensure that a representative substrate sample is taken before the feeding of nutrients.
Note that a,b,c refers to reactors 1,2 and 3, respectively.

1. Ensure both valves $F1_{a,b,c}$ and $F2_{a,b,c}$ are closed to prevent the reactor from depressurising. Open valve $F1_{a,b,c}$ slowly to release any possible pressure in the feed chamber.
2. Pour the liquid/nutrient medium into the chamber and close valve $F1_{a,b,c}$.

3. Slowly open valve $F2_{a,b,c}$, allowing the chamber to pressurise and allow the liquid to drain into the reactor.
4. Close valve $F2_{a,b,c}$. Repeat steps 1,2,3 until all the liquid is funnelled back into the reactor.

7.9 Sample to storage

A sample of reactor contents may also need to be put into cold storage. The sample must be clearly labelled, dated and necessary information to pinpoint its acquisition period, reactor indication and process taking place in the reactor e.g. Thermophilic/mesophilic methanation.

- Date
- Reactor
- Process

7.10 Reactor vessel dismantling

Ensure section 7.2.10 is carried out for a total system purge to eliminate the risk of volatile gases igniting. Ensure all components are being accurately tracked during the dismantling process and kept on clean nonabrasive surfaces.

1. Open valves $F1_{a,b,c}$, $F2_{a,b,c}$, $O1_{a,b,c}$ and $O2_{a,b,c}$ to drain the reactor of any liquid medium. Store the medium in an anaerobic environment to ensure the health of the microbial population.
2. Close valves $O1_{a,b,c}$ and $O2_{a,b,c}$.
3. Undo the Trilok clamps on the Feed inlets and set them aside.
4. Undo the Trilok clamps on the rest of the lines connecting the top flange of the reactor vessel.
5. Undo the outlet Trilok clamp on the vessel Pressure safety valve and set it aside.
6. Undo the Trilok clamp connecting the vessel to the sampling septum and set it aside.
7. Once done, use a socket wrench and a spanner to loosen the bolts connecting the top flange to the sight glass flange. Take care to loosen opposing bolts sequentially until all bolts are loosened.
8. Remove the bolts and keep track of bolts, washers, and nuts.
9. Remove the top flange and place it on a clean nonabrasive surface. Do the same for the PTFE gasket seal. Take care when lifting the top flange as the heavy weight can lead to physical injuries.
10. Using an Alan key of appropriate size, unscrew the sight glass sockets and place screws aside on a clean surface.
11. Remove the sight glass top flange and set it aside, along with the rubber O-ring gasket. Care must be taken as the glass sight glass will have a strong bond with the rubber gaskets sealing the vessel. As a result, the sight glass may lift with the top flange once lifted.
12. Carefully remove the glass sight glass so as not to chip or damage the glass. Afterwards, remove the acrylic protective cylinder. Set both aside.

13. Remove the lower rubber O-ring gasket.

The reactor vessel is now dismantled and available for maintenance checks. If removing the diffuser, ensure a fresh seal of PTFE thread sealing tape is applied on the threading to ensure a gastight seal.

8. Maintenance

The equipment must be subject to regular maintenance checks by the user per the manufacturers' SOPs with accounts being taken of any hazards encountered.

8.1 Making/Breaking connections

When the maintenance on the BHM rig is carried out, the operators may have to undertake a partial disassembly of the reactor system. This may include the breaking of connections of the gas lines along the system, (re)connection of the expansion vessel to the main reactor system or the disassembly of the reactor vessel.
In the event of any alterations to the connections, seals of the reactor vessel or threaded seals, refer to section 8.2.1 for the leak detection procedure.

8.2 Inspections

8.2.1 Leak Inspections: Nitrogen Leaks

Once connections have been (re)established, a gaseous leak detection procedure must be carried out to ensure a gas-tight connection is present at the affected connections. This can be first conducted using inert nitrogen gas and Teepol leak detection spray.



Figure 29 Teepol leak detection spray to detect nitrogen gas leaks

1. Ensure that nitrogen gas is flowing through the BHM rig
2. Spray Teepol leak detection spray on the joints/connections in question
3. If the solution forms bubbles, there is a nitrogen gas leak

4. Ensure leaks detected are recorded and addressed in the 'LG30 BHM Rig Leak Detection Log.xlsx'.
5. Once all leaks are detected, turn off the gas supply to the BHM rig.
6. Tighten all joints, flanges, or connections where leaks were found
7. Repeat steps 1 to 6 until all leaks have been remedied.

8.2.2 Leak Inspections: Hydrogen and Methane Leaks

Once connections have been (re)established, a gaseous leak detection procedure must be carried out to ensure a gas-tight connection is present at the affected connections. This is carried out using the EX-TEC® SNOOPER 4, calibrated for the detection of H_2 and CH_4 gases. The detector is equipped with an internal pump and an adjustable sensor probe to allow for the detection of the smallest leaks in confined spaces.
The detector is designed with a measuring range for semiconductor range of 0 – 22,000 ppm (2.2% vol. = 50% LEL)



Figure 30: EX-TEC Snooper 4

1. Ensure the device is charged and turned on.
2. Set the device detection to H_2 as this is the most likely to leak gas.
3. Manoeuvre the detector probe to near and around the connections to maximise the gas detection likelihood.
4. Ensure leaks detected are recorded and addressed in the 'LG30 BHM Rig Leak Detection Log.xlsx'.
5. Turn off the detector once the exercise has been completed.

8.3 Equipment maintenance checks

Fume hood:

Ensure the fume hood low-flow alarm system is functioning correctly. The fume hood sash must lift and lower properly, and the extraction system is operating at an adequate extraction level.

Pump:

A monthly inspection of the pump should be carried out to ensure smooth function. Particular attention must be paid to leaks and seals on the pump cover.

Heaters and gaskets:

It is recommended that monthly inspections of the heating system are carried out to check for leaks from heating hoses and heater supply.

Temperature Indicators:

Regular inspection of the thermocouples is necessary to ensure the probe is operating correctly and is responsive to the interface system.

Flow meter:

Ensure the flow meters are working properly and reacting accordingly with the variation of gas supply.

Pressure Indicators:

Ensure the pressure indicators are operating correctly and calibrated correctly.

Valves:

Ensure the valves are operating correctly and are oriented correctly, and ensure the seals are tight.

Ball Valves:

Ensure the valves are operating correctly and are oriented correctly, and ensure the seals are tight.

PSV:

Ensure the PSVs are operating correctly, are gas-tight and are calibrated correctly. Inspections of the PSVs will be conducted on an annual basis.

Gas Detection System:

Ensure that the gas detection system is operating correctly and that all gases are being displayed. Maintenance and inspection by a qualified technician will be conducted on an annual basis.

Safety Interlocks:

During the system, start to ensure that the safety interlock in place between the fume hood extract fan and slam-shut solenoids on the gas supply lines is operational. Gas should not flow unless the fume hood extract fan is operational. Inspection of this safety interlock will be conducted on an annual basis.

9. forms/Templates to be used

Checklists for each process in Excel format to be produced for:

- Commissioning process:
  - '7.2.1 - 7.2.8 - Reactor commission.xlsx'
  - '7.2.9 - Total System Purge & Flush.xlsx'
- Operating processes for respective sections:
  - '7.2.10 - R1 Batch Operation - Single Reactor Batch operation.xlsx'
  - '7.2.11 - R1 + R2 + R3 Batch Operation - Multiple Reactor Batch operation.xlsx'
  - '7.2.12 - R1, R2 or R3 Continuous Operation.xlsx'
  - '7.2.13 - R1 & R2 In-series.xlsx'
  - '7.2.14 - R2 & R3 In-series.xlsx'
  - '7.2.15 - R3 & R1 In-series.xlsx'
  - '7.2.16 - R1, R2 & R3 In-series.xlsx'
  - '7.2.17 - R1, R2 & R3 Continuous Parallel.xlsx'
- Checklists for maintenance checks to be carried out :
  - 'BHM Rig Leak Detection Log– 'LG30 BHM Rig Leak Detection Log.xlsx'
  - 'LG30 BHM Rig Leak Detection Log.xlsx'

10. internal and external references

This section is used to list all controlled internal references (e.g. SOPs) and external references referred to within the text of the SOP only.

10.1 Internal References

For relevant references and detailed information on the Biological Hydrogen Methanation Rig – refer to folders "LG30 EPD", "Component Documents" and "A18CK038-EPD-001"

10.2 External References

Insert relevant references as required, sufficient for the user to find the source document. Web references should be included where possible.

11. Risk Assessment

For a detailed Risk assessment outline, please refer to the LG30 Risk assessment documents for the relevant risk assessment for LG30 and the associated fume hood experiments relating to the Biological Hydrogen Methanation experiments.